GOLD AND SILVER COMPLEXES OF BIS(PHOSPHINO)HYDRAZINE LIGANDS AS POTENTIAL ANTI-TUMOUR AGENTS

by

Frederik Hermanus Kriel,

Thesis in fulfilment of the requirements of the degree of

Philosophiae Doctor Scientiae

in

Chemistry

at the

Faculty of Science

University of the Witwatersrand

Supervisor: Prof. Marcus Layh

Co-supervisor: Dr. Judy Caddy

Co-supervisor: Prof. Helder M. Marques

August 2007

Declaration

I declare that the work presented in this thesis was carried out exclusively by me under the supervision of Prof. Marcus Layh, Prof. Helder Marques and Dr. Judy Caddy. It is being submitted for the degree of Philosophiae Doctor of Science at University of the Witwatersrand, Johannesburg. It has not been submitted before for any degree or examination in any other University.

_____

Frederik Hermanus Kriel

_____day of _____, 2008

Acknowledgements

I would like to extend my sincere gratitude to the following people/institutions:

- *My supervisor: Prof. Marcus Layh for his patience and support;*
- *My Co-Supervisor: Dr. Judy Caddy for not only helping where possible but for also being a friend;*
- *My Co-Supervisor: Prof. Helder Marques for all his help;*
- *Prof. Connie Medlen and her team, Dr. Gisela Joone and Ms. Margo Nell for helping with biological studies at the Department of Pharmacology, University of Pretoria;*
- *Prof. Denver Hendricks, University of Cape Town, for kindly helping with the biological chapters;*
- *AuTEK Biomed (Mintek and Harmony Gold) for their financial support without which this project would not have been possible;*
- *My fellow students David Khanye and Mabel Coyanis;*
- *My friends for their moral support and always believing in me;*
- *My family, mom, dad, Wynand, Wouter, Marliza, Alexia and Xander for their love and support;*
- *My Lord, for showing the way;*

"Happiness is inward, and not outward; and so, it does not depend on what we have, but on what we are." – Henry van Dyke

Abstract

Cancer is presently responsible for about 25 % of all deaths in developed countries. It has a substantial impact on a patient's quality of life and many cancer treatments (such as chemotherapy) may have severe side-effects. New therapies that display a minimum of the drastic side-effects of current drugs are constantly sought after.

The first comprehensive studies of the anti-tumour potential of gold compounds, including gold drugs, were published in the mid-to-late 1980's. Gold(I) bisphosphine compounds of bis(diphenylphosphino)ethane (dppe) and related ligands with a tetrahedral coordination geometry turned out to be a particularly potent class of compounds. Clinical trials were, however, not pursued owing to the acute toxicity associated with them. The high toxicity of $[Au(dppe)_2]^+$ is attributable to the high lipophilicity of the cations which results in non-selective uptake into mitochondria in all cells. The tumour selectivity of tetrahedral gold(I) complexes was found to hinge on a fine balance between its lipophilic and hydrophilic character.

One way of introducing the more hydrophilic character to a ligand or complex, necessary for selectivity, is the addition of heteroatoms. To this end, one of the aims of this project was to synthesise a range of ligands where the lipophilic ethane bridge of dppe was replaced by a hydrazine bridge. It was hoped that the addition of the nitrogen heteroatoms would increase the hydrophilic character of the ligands, thus rendering more selective drug candidates. Further modifications identified included the initial phenyl substituents on the phosphorous centres could be enriched by replacing the phenyl with either *O*-methylanisol or *N*,*N*-dimethylaniline. In both cases four extra heteroatoms per ligand were added, oxygen in the case of anisol and nitrogen in the case of aniline. With dimethylhydrazine or diethylhydrazine as starting material six ligands were synthesised and characterised. Crystallisation efforts afforded a x-ray crystal structure of bis(diphenylphosphino)diethylhydrazine. In contrast to the stability of the diethylhydrazine ligands, the dimethylhydrazine ligands were found to be prone to decomposition, at times even under an inert atmosphere.

The aim of AuTEK Biomed is the inclusion of metals, in this case gold(I) and silver(I), to the above mentioned ligands (L) to enhance activity. To this effect, six phosphine-bridged gold complexes (ClAu-L-AuCl), six bischelated gold complexes (AuL_2Cl), six phosphine-bridged silver complexes (NO_3Ag-L-$AgNO_3$) and six bischelated silver complexes (AgL_2NO_3) were attempted.

It was found that the ClAu-L-AuCl complexes are very stable and readily crystallise from THF. Five of the six complexes could be characterised by x-ray crystallography. The sixth complex, that of bis(di(*N*,*N*-dimethylanaline)phosphino)dimethylhydrazine, could not be isolated due to the breakdown of the ligand upon addition of the metal starting material. Succesful preparation of five of the six AuL_2Cl complexes was accomplished. These complexes where found to be slightly hygroscopic and storage under an inert atmosphere was required. Efforts to crystallise these complexes led to the crystallisation of conglomerates of micro crystals, which could not be analysed crystallographicly due to the disordered nature of the micro crystals.

The synthesis of the bischelated gold complex of bis(di(*N*,*N*-dimethylanaline)-phosphino)diethylhydrazine led to an interesting phenomenon which was studied further. Upon complexation, the expected yellow complex spontaneously turned bright red even when the solvent was removed. Efforts to crystallise this complex was not successful until the counter ion (Cl^-) was replaced with that of NO_3^-. The crystal structure revealed that gold(I) had spontaneously oxidised to gold(III) and this crystal structure represents the first known complex to our knowledge of gold(III) chelated to four phosphorous centres.

NO_3Ag-L-$AgNO_3$ complexes were mostly unstable and regularly led to the formation of a silver mirror on the reaction vessel. Even with this inherent instability of these complexes, it was possible to characterise three of the complexes to some extent and to analyse the complex of bis(diphenylphosphino)diethylhydrazine by x-ray crystallography. The molecular structure showed intricate connectivity between the complexes leading to polymeric structures. The tetrahedral silver complexes were markedly more stable and five of the complexes could be isolated and characterised. The molecular structure of bis(bis(diphenylphosphino)diethylhydrazine)silver nitrate could be determined.

Thirteen of the complexes were found to be sufficiently stable to be investigated as potencial drug candidates and were subjected to *in vitro* anti-tumour screening. These thirteen complexes were firstly screened against three cell lines, namely the cancerous HeLa and Jurkat cell lines and Lymphocytes obtained from healthy human donors. These results were analysed and selectivity for toxicity towards cancerous cell-lines *vs* the healthy cell line was calculated.

Five complexes were identified as suitable for investigation on a further range of cell lines based on the specificity they displayed. Two of the complexes were of the type ClAu-L-AuCl, while the other three were of the type AgL_2NO_3. The five compounds were screened against A2780, A2780cis, Colo, MCF-7 and MCF-12 cell lines from which new selectivity profiles were calculated.

Due to the mechanism of activity of $[Au(dppe)_2]^+$ being described as apoptosis induced through the disruption of mitochondrial membrane potential, so leading to cell arrest, it was decided to test whether these analogues would work through the same mode of action. To this end, the best two complexes, namely ClAu(MeO-4-$Ph)_2$PN(Et)N(Et)P(Ph-4-$OMe)_2$AuCl and $[\{(MeO\text{-}4\text{-}Ph)_2PN(Me)N(Me)P(Ph\text{-}4\text{-}OMe)_2\}_2\ Ag]^+.NO_3^-$, selected through the analysing of selectivity calculations were subjected to the mitochondrial membrane potential and apoptosis assays. From the mitochondrial membrane potential assay it could be proven that these complexes do indeed affect the mitochondrial membrane potential by lowering the potential necessary to the cell for producing ATP. Results from the apoptosis assays were inconclusive and remain as future work.

The hypothesis of this theses is that it is possible to fine tune the lipophilic/hydrophilic balance of tetrahedral Group 11 complexes to improve selectivity towards cancerous cells above healthy cells. This has to a certain extent been proven through the increased selectivities of these complexes when compared to $[Au(dppe)_2]^+$. It has to be mentioned that even though increased selectivities are observed for these complexes, the selectivities are not profound enough to merit further investigation into the anti-tumour activity of these complexes.

Table of Contents

Abbreviations

Θ	Ligand cone angle
A2780	Human ovarian cancer
A2780cis	Human ovarian cancer (cisplatin resistant)
ATCC	American Type Culture Collection
ATP	Adenosine triphosphate
AIDS	Advanced ImmunoDeficiency Sindrome
CHO	Chinese Hamster Ovary
Colo 320 DM	Human colon cancer
damp	2-((dimethylamino)methyl)phenyl
DCM	Dichloromethane
DMARDS	Desease Modifying AntiRheumatic DrugS
DMEM	Dulbecco's Minimal Essential Medium
dmpe	1,2-bis(dimethylphosphino)ethane
DMSO	Dimethylsulphoxide
DNA	Dioxyribonucleic acid
dppe	1,2-bis(diphenylphosphino)ethane
dppen	1,2-bis(diphenylphosphino)ethene
EA	Elemental Analysis
EB	Ethidium Bromide
EDTA	Ethylenediaminetetraacetic acid
EMEM	Eagle's Minimal Essential Medium
EtOAc	Ethylacetate
EPA	Environmental Protection Agency
HeLa	Human adenocarcinoma of the cervix
HI FCS	Heat Inactivated Foetal Calf Serum
HIV	Human Immunodeficiency Virus
Hz	Hertz
IC_{50}	Amount of drug required to kill 50 % of cultured cells
J	Coupling Constant

JC-1	5,5',6,6'-tatrachloro-1,1',3,3'-tetraethylbenzimidazolyl-carbocyanine Iodide
Jurcat	Human T-cell cancer
L	Ligand
MCF-7	Human Breast cancer
MCF-12	Modified human non-cancerous breast cells
MP	Melting Point
MHC	Class II Major Histocompatiblity Complex
MRSA	Methicilin-Resistant *Staphyloccus Aurus*
MS	Mass Spectroscopy
MTT	3-(4,5-dimethylthiazol-2-yl)-2,5-diphenyltetrazolium Bromide
NIC	National Cancer Institute
NMR	Nuclear Magnetic Resonance
pdma	*o*-phenylene-bis(dimethylarsine)]
PBS	Phosphate Buffered Saline
PHA	Phytohaemaglutinide
PI	Propidium Iodide
PS	Phosphatidylserine
Quinala	*N*-(8-quinolyl)-L-alanine-carboxamide
Quingly	*N*-(8-quinolyl)glycine-carboxamide
Quinpy	*N*-(8-quinolyl)pyridine-2-carboxamide
RA	Rheumatoid Arthritis
rpm	revolutions per minute
RPMI	Roswell Park Memorial Institute (Medium)
TATG	1-thio-β-D-glucose tetraacetate
TB	Tuberculosis
TMEDA	*N,N,N'N'*-tetramethylethylenediamine
THF	Tetrahydrofuran
THT	Tetrahydrothiophene

Chapter 1

Group 11 Transition Metal Chemistry and Applications in the Medicinal Field

1.1 INTRODUCTION

In the USA and other developed countries, cancer is presently responsible for about 25% of all deaths.[1] On a yearly basis, 0.5% of the population is diagnosed with cancer. In the USA the most common male cancer type is prostate cancer (33%) and the most common occuring female cancer is breast cancer (32%). The cancer with the highest mortality rate for both females and males is however lung cancer (27% and 31%, respectively).[2] Figures for South Africa are as abysmal, with men dying from mainly lung cancer (21.9% in 2000) and woman mainly from cervical cancer (17.2% in 2000).[3]

Cancer has a substantial impact on a patient's quality of life and many cancer treatments (such as chemotherapy) may have severe negative side-effects. In the advanced stages of cancer, many patients need extensive care, affecting family members and friends. Once referred to as "the C-word", cancer has a reputation for being a deadly disease. While this certainly applies to certain particular cancer types, the truths behind the historical connotations of cancer are increasingly being overturned by advances in medical care. Some types of cancer have a prognosis that is substantially better than non-malignant diseases such as heart failures and strokes.[2]

---

[1] A. Jemal, T. Murray, E. Ward, A. Samuels, R.C. Tiwari, A. Ghafoor, E.J. Feuer, M.J. Thun, *CA Cancer J. Clin.*, **2005**, 55, 1, 10.
[2] en.wikipedia.org/wiki/Cancer
[3] www.mrc.ac.za

Cancer research is defined as the intense scientific effort to understand disease processes and discover possible therapies. While the understanding of cancer has greatly increased since the last decades of the 20th century, radical new therapies are only discovered and introduced gradually.[2] New therapies to curb cancer, while displaying a minimum of the drastic side-effects current drugs have, need to be constantly sought after.

1.2 COORDINATION COMPOUND CHEMISTRY

Phosphines are well known to chemists. Phosphine ligands are widely used in organic synthesis (*e.g.* Wittig reaction[4]) and transition metal phosphine complexes have been studied extensively, primarily in the context of their application as hydrogenation catalysts (*e.g.* Wilkinson's catalyst[5]).[6] Table 1.1 outlines some of the uses of phosphines as pertaining to biological systems.

Phosphine	**Application**	**Comment**
PH_3	Fumigant[7]	Generated *in situ*
$Et_3PAu(TATG)$	Auranofin[8]	Approved for clinical use
R_3P-Au-X	High toxicity[9]	Limited anti-tumour activity
Ph_2P-Y-PPh_2	Anti-tumour activity[10]	Activity related to structure (highest: Y = CH_2CH_2)
$XAu(Ph_2P(CH_2)_nPPh_2)AuX$	Cytotoxic, anti-tumour activity[6]	Activity related to structure (highest: n = 2)
$[M(Ph_2P(B)PPh_2)_2]X$	Cytotoxic, anti-tumour activity[6]	M = Au, Ag, Cu B = $(CH_2)_2$, $(CH_2)_3$ or CH=CH
trans-$[Tc(dmpe)_2Cl_2]^+$	Heart imaging agent[11]	Cationic lipophilic complex transports ^{99m}Tc into myocardial cells

Table 1.1: Phosphines and metal phosphine complexes of current interest in biology and chemistry.

[4] J. McMurry, *Organic Chemistry*, *4th Ed.*, **1995**, 743.
[5] J.A. Osborn, F.H. Jardine, J.F. Young, G. Wilkinson, *J. Chem. Soc. A,* **1966**, 1711ff.
[6] S.J. Berners-Price, P.J. Sadler, *Struc. and Bond.*, **1988**, 70, 27.
[7] E. Fluck, *The Chemistry of Phosphine*, *Topics in Current Chemistry*, **1973**, 35, 64.
[8] T.M. Simon, D.H. Kunishima, G.J. Vibert, A. Lorber, Cancer Philad., **1965**, 44.
[9] C.F. Shaw, A. Berry, G.C. Stocco, *Inorg. Chim. Acta*, **1986**, 123, 213.
[10] R.F. Struck, Y.F. Shealey, *J. Med. Chem.*, **1966**, 9, 414.
[11] E. Deutch, W. Bushong, K.A. Klavan, R.C. Elder, V.J. Sodd, D.L. Fortman, S.J. Lukes, *Science*, **1981**, 214, 85.

Over 150 different phosphines have been tested for anti-tumour activity by the National Cancer Institute.[12] None of the tested phosphines showed more than marginal anti-tumour activity. It was hypothesised that most of these phosphines are rapidly oxidised *in vivo* and that the coordination to transition metals might inhibit this oxidation to some extent.[6]

1.2.1 Phosphine Ligands

The fundamental characteristic of all phosphine compounds is the presence of a lone pair of electrons on the phosphorous atom.[7] This makes it possible for phosphorous to behave as both a nucleophile and a Lewis base. The greater size and lower electronegativity of phosphorous with respect to nitrogen leads to higher polarisability and hence, phosphorous compounds are better nucleophiles when compared to nitrogen compounds.[6]

Tertiary phosphines (PR_3) are among the most commonly found ligands in transition metal complexes. There are examples of phosphine complexes of virtually every transition metal.[13,14] This illustrates the versatility of these ligands and their ability to bind transition metals in both high and low oxidation states.[6]

Alteration of the substituents on PR_3 can cause substantial changes in the chemical and physical properties of the corresponding transition metal complexes and thus, the strength of the metal-phosphorous bond. Before 1970, almost all chemical behaviour was rationalised in terms of electronic effects of the phosphine substituents, but since then it has been recognised that steric effects are often as important and in many cases more important.[15,16] Tolman introduced the ligand cone angle (Θ) as a measure of steric bulk and subsequently many physical parameters have been correlated to it.[15] By studying and understanding the changes effected by varying the substituents it is

---

[12] www.cancer.gov
[13] K.K. Chow, W. Levason, C.A. McAuliffe, *Transition Metal Complexes of P, As, Sb and Bi ligands*, McMillan, London, **1973**.
[14] O. Stelzer, *Topics in Phosphorus Chemistry*, Wiley, New York, **1977**.
[15] C.A. Tolman, *Chem. Rev.*, **1977**, 77, 313.
[16] B.E. Mann, A. Musco, *J. Chem. Soc.*, **1975**, 1673.

possible to tailor these complexes to attain specific goals in reactivity (rational design).[6]

The discovery of new chelating bisphosphines continues to attract considerable attention because of their role in the development of catalytically useful transition metal complexes.[17,18] One of the simplest and most noteworthy of these bisphosphines is found in the group of alkane-bridged bisphosphines (*i.e.* $R_2P(CH_2)_nPR_2$, where R = phenyl and n = 2). This simple ligand system is abbreviated to dppe [bis(**di**p**h**enyl**p**hosphino)**e**thane] and is used as a simple chelating ligand for various transition metals (Figure 1.1).[17,18,19]

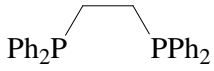

Figure 1.1: bis(diphenylphosphino)ethane (dppe).

Bis(di(alkyl or aryl)phosphino)ethanes have found numerous applications in the design of monometallic transition metal compounds and catalysts. The appropriate bite angle provided by the ethane backbone has been implicated as the main reason for the prevalence of stable five-membered mononuclear chelates that demonstrate catalytic properties.[19,20]

1.2.1.1 Nitrogen-Bridged Bisphosphines

The discovery of bis(dihalophosphino)amines (Figure 1.2) has led to extensive research in the main group and transition metal chemistry of this class of ligand systems.[21,22,23] Already in 1994, more than 300 published papers describe the rich

---

[17] G.W. Parshall, *Homogeneous Catalysis,* Wiley, New York **1980**.
[18] L.H. Pignolet (Ed.), *Homogeneous Catalysis with Metal Phosphine Complexes,* Plenum, New York, **1983**.
[19] V.S. Reddy, K.V. Katti, C.L. Barnes*, Inorg. Chem.*, **1995**, 34, 5483.
[20] K.G. Moloy, R.W. Wegman, *J. Chem. Soc., Chem. Commun.,* **1988**, 820.
[21] J.F. Nixon, *J. Chem. Soc. A*, **1968**, 2689.
[22] A.R. Davies, A.T. Dronsfield, R.N. Haszeldine, D.R. Taylor, *J. Chem. Soc., Perkin Trans. 1*, **1973**, 379.

coordination chemistry of $R_2PN(R')PR_2$-type ligands.[24] Varied bonding modes with transition metals have been observed. These include: i) monodentate ligation through P^{III} centre interaction; ii) bidentate chelation or bridging coordination; and iii) metal nitrogen σ-bond formation by means of the reaction at the nitrogen centre.[24] In sharp contrast, the corresponding studies of dinitrogen-bridged bisphosphines such as bis(dihalophosphino)dialkylhydrazine (Figure 1.2) have until recent work by Reddy and Katti,[19,25,26] been limited to only a few reports.[27,28,29]

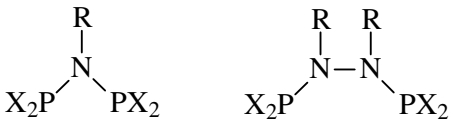

bis(dihalophosphino)amines bis(dihalophosphino)hydrazine

Figure 1.2: Nitrogen-bridged bisphosphines.

Metal complexes containing bisphosphine ligands with a P-C-P framework have been the subject of numerous investigations during the past decades,[30,31] while interest in analogous bis(phosphino)amine (also called diphosphazane) ligands, $RN(PX_2)_2$, has started to develop only more recently.[24] Bis(phosphino)amine ligands have proven very versatile since substituents on both the phosphorous and the nitrogen atoms can be varied independently, resulting in subsequent changes in the P-N-P bond angle and the conformation around the phosphorous centre.[32] Fairly small differences in these

---

[23] R. Jefferson, J.F. Nixon, T.M. Painter, R. Keat, L. Stubbs, *J. Chem. Soc., Dalton Trans.*, **1973**, 1414.
[24] M.S. Balakrishna, V.S. Reddy, S.S. Krishnamurthy, J.C.T.R. Burckett St. Laurent, J.F. Nixon, *Coord. Chem. Rev.*, **1994**, 129, 1.
[25] V.S. Reddy, K.V. Katti, *Inorg. Chem.*, **1994**, 33, 2695.
[26] V.S. Reddy, K.V. Katti, C.L. Barnes, *Chem. Ber.*, **1994**, 127, 1355.
[27] M.D. Havlicek, J.W. Gilje, *Inorg. Chem.*, **1972**, 11, 1624.
[28] H. Nöth, R. Ullmann, *Chem. Ber.*, **1976**, 109, 1942.
[29] A.M.Z. Slawin, M. Wainright, J.D. Woollins, *J. Chem. Soc., Dalton Trans.*, **2002**, 513.
[30] R.J. Puddaphatt, *Chem. Soc. Rev.*, **1983**, 99.
[31] B. Chaudret, B. Delavaux, R. Poilblanc, *Coord. Chem. Rev.*, **1988**, 86, 191.
[32] R. Keta, L.M.Muir, K.W. Muir, D.S. Rycroft, *J. Chem. Soc., Dalton Trans.*, **1987**, 2192.

ligands can cause significant changes in their coordination behaviour and the structural features of the resulting complexes.[24,33]

The synthesis of alkyl- or arylamino(bis(dichlorophosphines)) involves the reaction of alkyl or aryl substituted primary amines (Equation 1.1) or their hydrochlorides (Equation 1.2) with PCl_3.[21,22,23] Silylated amines, instead of primary amines, can be used in condensation reactions to form bis(dihalo- or diarylphosphino)amines (Equations 1.3 and 1.4).[24,34]

$$2\ PCl_3 + RNH_2 \rightarrow RN(PCl_2)_2 + 2\ HCl \qquad \textbf{Equation 1.1}$$

$$2\ PCl_3 + RNH_2.HCl \rightarrow RN(PCl_2)_2 + 3\ HCl \qquad \textbf{Equation 1.2}$$

$$2\ PCl_3 + MeN(SiMe_3)_2 \rightarrow MeN(PCl_2)_2 + 2\ Me_3SiCl \qquad \textbf{Equation 1.3}$$

$$2\ PPh_2Cl + HN(SiMe_3)_2 \rightarrow HN(PPh_2)_2 + 2\ Me_3SiCl \qquad \textbf{Equation 1.4}$$

The versatility of bis(phosphino)amines as ligands is illustrated by the fluoro diphosphazane derivative, $MeN(PF_2)_2$. Nixon *et al.*[35] and later King[36] showed that $MeN(PF_2)_2$ can bind to transition metals in a monodentate or bidentate binding mode, giving rise to mononuclear as well as dinuclear complexes. Cotton *et al.*[37] have found that the same ligand is capable of stabilising metal-metal triple bonds (Figure 1.3) and dubbed [$MeN(PF_2)_2$] the "Nixon" ligand in view of its versatility. Related ligands with P-O-P or P-C-P backbones fall short on account of lower flexibility in the case of P-O-P and lower thermal stability in the case of P-C-P.[24]

[33] J.S. Field, R.J. Haines, C.N. Sampson, *J. Chem. Soc., Dalton Trans.*, **1987**, 1933.
[34] I.G. Colquhoun, W. McFarlane, *J. Chem. Soc., Dalton Trans.*, **1977**, 1674.
[35] T.R. Johnson, J.F. Nixon, *J. Chem. Soc. A*, **1969**, 2518.
[36] R.B. King, *Acc. Chem. Res.*, **1980**, 13, 243.
[37] F.A. Cotton, W.H. Ilsley, W. Kaim, *J. Am. Chem. Soc.*, **1980**, 102, 1918.

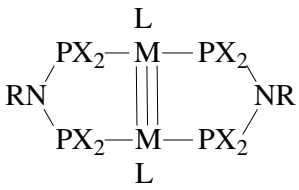

Figure 1.3: Stabilising effect of diphosphazane ligand on metal-metal triple bonds.

The fact that so little is known about hydrazine linked bisphosphines may, in part, be due to the lack of a simple synthetic route for such ligands. Gilje *et al.*[27] and Nöth *et al.*[28] have pioneered the synthesis of hydrazidophosphines. Their synthetic strategies involved: i) the condensation of PCl_3 with the highly unstable 1,2-dimethylhydrazine at -196 ^{o}C; and ii) the treatment of the heterocyclic cage compound $P[N(Me)N(Me)]_3P$ with PCl_3.[38] Aside from giving low yields of $Cl_2PN(Me)N(Me)PCl_2$ (15-20%), these methods suffer from the above mentioned practical disadvantages. Therefore, the development of a one-step, straightforward and high-yielding synthetic route to $Cl_2PN(Me)N(Me)PCl_2$ by Katti *et al.*,[25,26] had significant advantages in the long-term use of this ligand and its derivatives in the coordination chemistry of transition metals.[25]

1.2.1.2 Chelating Bisphosphine Ligands

The development of new bisphosphines that possess similar spacing between the P^{III} centres as in $R_2P(CH_2)_2PR_2$ presents the potential to expand the scope of the transition metal chemistry of chelating bisphosphines.[19,29] In connection with this, the ethylene-bridged bisphosphine $R_2PCH{=}CHPR_2$ has provided an example of a ligand with a similar chain length than that of dppe. The development of bisphosphines with main group centres *(e.g.* nitrogen) connecting the P^{III} centres offers new opportunities in tuning the electronic and steric characteristics of the interacting phosphines.[19,29]

The dinitrogen-bridged bisphosphine is a useful synthon since: i) it has a similar chain length to that of dppe, suggesting its utility in the formation of mononuclear five-

[38] H. Nöth, R. Ullmann, *Chem. Ber.*, **1974**, 107, 1019.

membered chelates;[25] and ii) the reactive chlorides may be used in the development of a wide spectrum of $R'_2PN(R)N(R)PR'_2$-type derivatives affording systematic tuning of nucleophilicity and π-acidity of the P^{III} centres.[24,25] It may be noted that the development of fundamental coordination chemistry of hydrazine-bridged bisphosphines may aid in furthering the chemistry of the related bis(phosphino)amines.[24]

The substitution of $X_2PN(R)N(R)PX_2$-type precursors to yield $R'_2PN(R)N(R)PR'_2$-type derivatives gives rise to a myriad of interesting ligands with varied properties that may be exploited. The variety of ligands accessible is shown in an exemplary fashion by the two reactions below (Scheme 1.1 and 1.2). Phosphinohydrazine ligands are easily produced with the addition of Grignard reagents or BuLi substitution (Scheme 1.1),[29] and phosphitohydrazine ligands can be synthesised by the condensation reaction of alcohols with the precursor $X_2PN(R)N(R)PX_2$, utilising a simple base like NEt_3 (Scheme 1.2).[19,26,29]

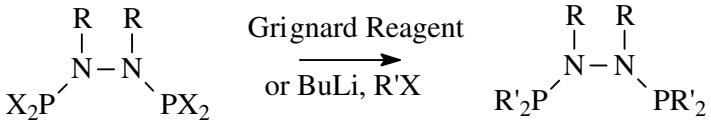

R = Me or Et, R' = Alkyl or Aryl

Grignard Reagent: (Alkyl or Aryl)MgX

Scheme 1.1: Synthesis of bisphosphine hydrazine ligands.

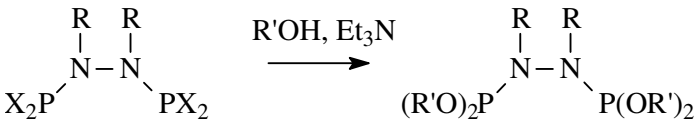

R = Me or Et, R' = Alkyl or Aryl

Scheme 1.2: Synthesis of bisphosphite hydrazine ligands.

Katti *et al.*[19,26] and Slawin *et al.*[29] illustrated the complexation ability of these ligands to form coordination complexes of palladium, platinum, tungsten and molybdenum by various alkyl-, aryl-, alkoxy- and aryloxy-substituted dimethyl- and diethylhydrazine

ligands. The precursor compound, $Cl_2PN(Me)N(Me)PCl_2$, was shown to be capable of forming complexes with platinum and palladium.[25]

1.2.2 The Chemistry of Gold

Gold has been known to all major cultures since before the beginning of recorded history. Gold mining and gold refining operations are portrayed in Egyptian carvings dating back to 2500 B.C. The word *gold* stems from the old Norse *gull* and the Gothic *gulth* and is thought to be derived ultimately from the Sanskrit verb *jval*, meaning "to shine". The symbol *Au*, on the other hand, comes from the Roman name for the element, *aurum*, which is related to *aurora* which means, "shining dawn". The name is thus derived from the distinctive shining appearance of the metal.[39,40,41]

Copper, silver and gold in their atomic state are all characterised by a single *s* valence electron configuration outside a completed *d* shell, but despite the similarities in electron structure and ionisation potentials there are few resemblances between gold, silver and copper. Gold is a soft, yellow metal with the highest ductility and malleability of any element. It is chemically inert and is not attacked by oxygen or sulphur, but reacts readily with halogens or with solutions containing or generating chlorine such as aqua regia. It dissolves in cyanide solutions in the presence of air or hydrogen peroxide to form $[Au(CN)_2]^-$. Addition of reducing agents to gold salts under suitable conditions give rise to colourful solutions containing colloidal gold or "purple of Cassius" as it is known.[39,41,42]

Gold chemistry is more diversified than that of silver in that gold is found in six oxidation states, from –I to III and V. Gold(-I) and gold(V) have no counterparts in silver chemistry. Gold(-I) can be formed and stabilised by solvated electrons in liquid ammonia. In the series of metal alloys of the alkaline metals with gold, CsAu is classified less as an alloy than an ionic compound better written as Cs^+Au^-. Gold(V) is

---

[39] M.C. Sneed, J.L. Maynard, R.C. Brasted, J.W. Laist, *Comp. Inorg. Chem., II*, D. van Nostrand Company Ltd., **1954**, 114.
[40] P.J. Sadler, *Gold Bull.*, **1976**, 9, 110.
[41] A.F. Holleman, E. Wiberg, *Inorg. Chem.*, Academic Press, **2001**, 1248.
[42] F.A. Cotton, G. Wilkinson, *Advanced Inorganic Chemistry 5th Ed.*,Wiley-interscience publication, **1988**, 937.

known in AuF_5 and $[AuF_6]^-$, in which it has a low-spin $[Xe]4f^{14}5d^6$ configuration.[40,41,43]

The other oxidation states of gold are more common with the most stable states being gold(I) and gold(III). Gold(I) (d^{10}) can be found in three common geometries namely, linear (most common), trigonal and tetrahedral (Figure 1.4). Gold(II) (d^9) can be found in square planar coordination compounds, while gold(III) (d^8) can be found in a square planar (most common), square pyramidal or octahedral coordination (Figure 1.5).[40,41]

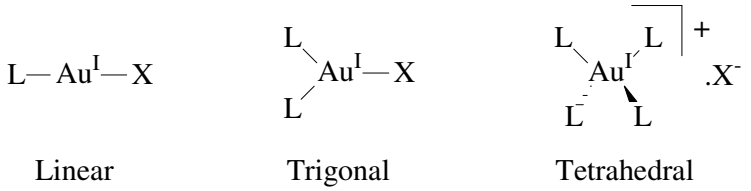

Figure 1.4: Possible geometries of gold(I) complexes.

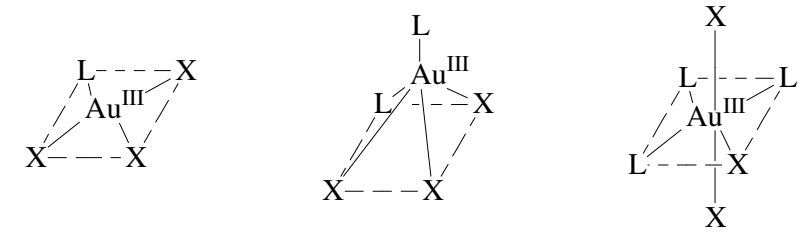

Figure 1.5: Possible geometries of gold(III) complexes.

Gold(III) is regarded as a "harder" acid than gold(I) and hence, is more likely to form stable compounds with donor atoms such as nitrogen and oxygen, whereas gold(I) exhibits a distinct preference for the "softer" sulphur and phosphorous donor atoms.[44]

[43] S. Patai, Z. Rappoport, *The Chemistry of Organic Derivatives of Gold and Silver*, Wiley Interscience Publications, **1999**.
[44] E.R.T. Tiekink, *Gold Bull.*, **2003**, 36, 117.

Gold has the curious tendency to bind to other gold atoms; this is called aurophilicity and has been known to lead to the formation of clusters.[45] If ligands are large, these gold-gold interactions tend to form dimers and if the ligands are small the interaction leads to polymeric chains, rings or even layered polymers. The Au–Au distances are usually about 3.0 Å, which is significantly less than the van der Waals contact. The distances generally observed are as follows: i) Au_2(g): 2.50 Å, ii) Au^{II}–Au^{II}: ~2.60 Å, iii) Au_x: 2.884 Å, iv) Au^{I}–Au^{I}: 2.75–3.40 Å; and v) sum of the van der Waals radii: 3.4 Å.[41]

1.2.2.1 Complexes of Gold(I)

The majority of gold(I) complexes are linear and tend to be of the LAuX type, where L is a neutral donor such as R_3P or R_2S and X is a halogen, pseudohalogen or RS. The phosphine complexes are particularly stable and easy to prepare. Those with thioether ligands, for example $(R_2S)AuCl$, are useful preparative intermediates, since R_2S is easily displaced by other ligands. With higher concentrations of R_3P ligands, higher coordination numbers are achieved, as in $(Ph_3P)_3AuCl$ and $[Au(PMePh_2)_4][PF_6]$, where tetrahedral coordination is found.[40,41,43]

Gold(I) thiolates, $[AuSR]_n$ have been extensively investigated in the context of chemotherapeutic agents for arthritis. They exist as linear, cyclic oligomeric or polymeric species (Figure 1.6).[40]

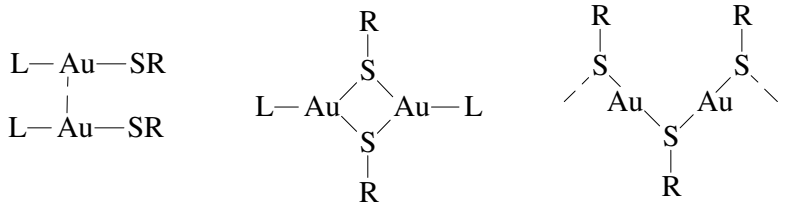

Figure 1.6: Possible conformations of $[AuSR]_n$ species.

[45] I.D. Salter, *Adv. Organomet. Chem.*, **1989**, 29, 249.

The overwhelming preference of gold(I) for linear two-coordination has made complexes of higher coordination more rare. A few three-coordinate complexes are known[46,47] and the existence of four-coordination has become more widespread,[48,49,50,51] including some monochelating ligand complexes with near tetrahedral symmetry, namely $[Au(PMePh_2)_4]^+$ and $[Au(SbPh_3)_4]^+$.[52,53] Reports of chelated gold(I) complexes were initially confined to bidentate ligands with rigid backbones: $[Au(pdma)_2]^+$ [pdma = *o*-phenylene-bis(dimethylarsine)] and $[Au(dppen)_2]^+$ [dppen = bis(diphenylphosphino)ethylene].[46] The latter ligand (L) readily formed the ring-opened complex [(ClAu-L-AuCI],[54] a type of species also formed by bis(diphenylphosphino)methane.[55] As a result of the discovery of $[Au(dppe)_2]^+$ the attention of researchers changed to the more flexible chelating ligands and has since led to many new tetrahedral complexes.[51,56,57]

1.2.2.2 Complexes of Gold(II)

The number of gold(II) complexes is very scarce if compared to the more common gold(I) and gold(III) derivatives.[58] Atomic ionisation potentials show that it is more difficult to obtain gold(II) than either copper(II) or silver(II), but easier to obtain gold(III) than either of the other two +3 ions. The only extensive series of genuine gold(II) compounds is found in dinuclear species exhibiting Au-Au bonds. These are

---

[46] P.G. Jones, *Gold Bull.*, **1981**, 14, 102.
[47] Z. Assefa, J.M. Forward, T.A. Grant, R.J. Staples, B.E. Hanson, A.A. Mohamed, J.P. Fackler, *Inorg. Chim. Acta*, **2003**, 352, 31.
[48] P.G. Jones, *J. Chem. Soc., Chem. Commun.*, **1980**, 1031.
[49] M.J. Mays, P.A. Vergnano, *J. Chem. Soc., Dalton Trans.*, **1979**, 1112.
[50] P. Byabartta, M. Laguna, *Inorg. Chem. Commun.*, **2007**, 10, 666.
[51] S.J. Berners-Price, R.J. Bowen, M.A. Fernandes, M. Layh, W.J. Lesueur, S. Mahepal, M.M. Mtotywa, R.E. Sue, C.E.J. van Rensburg, *Inorg. Chim. Acta*, **2005**, 358, 4237 and references therein.
[52] R.C. Elder, E.H.K. Zeiher, M. Onady, R.R. Whittle, *J. Chem. Soc., Chem. Commun.*, **1981**, 655.
[53] P.G. Jones, *Z. Naturforsch., Teil B,* **1982**, 37, 937.
[54] P.G. Jones, *Acra Crystallog., Sect. B,* **1980**, 36, 2775.
[55] H. Schmidbaur, A. Wohlleben, F. Wagner, O. Orama, G.Huttner, *Chem. Ber.,* **1977**, 110, 1748.
[56] S.J. Berners-Price, M.A. Mazid, P.J. Sadler, *J. Chem. Soc., Dalton Trans.*, **1984**, 969.
[57] S.J. Berners-Price, R.J. Bowen, P. Galettis, P.C. Healy, M.J. McKeage, *Coord. Chem. Rev.*, **1999**, 185, 823.
[58] A. Laguna, M. Laguna, *Coord. Chem. Rev.*, **1999**, 193, 837.

obtained by oxidative-addition of halogens to dinuclear gold(I) phosphine ylide complexes (Figure 1.7).[58,59] Related bridged dinuclear gold(I) complexes, like $Au_2(S_2CNR_2)_2$ and $Au_2Cl_2(Ph_2PCR_2PPh_2)$, can similarly be oxidised to give gold(II)–gold(II) bonds.[40,41,58]

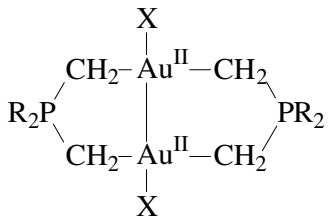

Figure 1.7: Dinulear gold(II) phosphine ylide complex.

1.2.2.3 Complexes of Gold(III)

Gold(III) is iso-electronic to platinum(II) and similarly displays predominantly square planar coordination. Complexes of the type $[AuX_4]^-$ were X is a halogen or pseudohalogen are well characterised. When gold is dissolved in aqua regia or Au_2Cl_6 is dissolved in HCl and the solution of $AuCl_4^-$ is evaporated, auric acid can be obtained as yellow crystals of $[H_3O]^+[AuCl_4]^-.3H_2O$. Other water-soluble salts such as $KAuCl_4$ and $NaAuCl_4$ are readily obtained. Neutral complexes of $AuCl_3$ in the form of $(R_3E)AuCl_3$, can be synthesised from simple adducts were E = P, As or Sb. Cationic complexes like $[Au(NH_3)_4]^{3+}$ are well characterised.[40,41,43]

1.2.2.4 Organogold Compounds

Alkyl derivatives of gold were among the first organometallic compounds of transition metals to be prepared. Both gold(I) and gold(III) compounds with σ bonds to carbon, as well as olefin complexes, are known. Gold(I) complexes are mainly complexes of the type RAuL, where L is a stabilising ligand. These complexes are prepared from the corresponding gold halides by reaction with LiR or RMgX. Gold(III) compounds are mainly complexes of the type R_3AuL, $[R_2AuL]^+$ or R_2AuXL.[40,41,43]

[59] H. Schmidbaur, K.C. Dash, *Adv. Inorg. Radiochem.*, **1982**, 25, 239.

Triphenylphosphine complexes of gold(I) and gold(III), such as $MeAuPPh_3$ and Me_3AuPPh_3, when reacted with methyllithium in ether, give the methylate ions $[AuMe_2]^-$ and $[AuMe_4]^-$, which can be isolated as lithium amine salts and are very stable organogold compounds.[40,41,43]

1.2.3 The Chemistry of Silver

Of the three noble metals of Group 11, silver was the last to be discovered, since it is not nearly as abundant in the native metallic state as copper or gold. Even so it was discovered very early and recognised as a metal of unusual merit. First recordings of the use of silver date back to 3500 B.C. in Egypt, where its value was established as two fifths the value of gold in the code of Menes.[39]

The Latin name for silver, *argentum* (from which the symbol *Ag* is derived), is in recognition of the brilliance of the metal, since *argentum* comes from the Greek name *argyros*, coming from a root for "bright' or "shining". Thus, as with gold, both the name and the symbol are tributes to the distinctive appearance of the metal.[39,41]

Silver is a white, lustrous, soft and malleable metal with the highest known electrical and thermal conductivities. It is chemically less reactive than copper, except towards sulphur and hydrogen sulphide, which rapidly blackens silver surfaces. The metal dissolves in oxidising acids and in cyanide solutions in the presence of oxygen or peroxide.[39,41]

Silver can be found in four oxidation states from 0 to III, with silver(I) being the most common. The most common geometries for silver(I) (d^{10}) are linear, trigonal and tetrahedral, while both silver(II) (d^9) and silver(III) (d^8) are known to form square planar compounds.[41,42]

1.2.3.1 Complexes of Silver(I)

Many nitrogen ligands readily form complexes with silver(I) in water, with NH_3 being the most important. The linear coordination of NH_3 as $[H_3N\text{-}Ag\text{-}NH_3]^+$ has been observed crystallographically, while with poly-amine ligands like bipyridine a more

complex behaviour is observed and tetrahedral cationic compounds may result.[39,41,42] Silver(I) has a relatively low affinity for oxygen donors, although compounds and complexes containing carboxylate ions are known. On the other hand, numerous complexes with the donor atoms sulphur, selenium, phosphorous and arsenic are known. Silver(I) is found to bind to peptides and proteins with a preference for the thioether sulphur atoms and imidazole nitrogen atoms.[42,43]

Monophosphines mainly form complexes of the type $(R_3P)_nAgX$, with n = 1 - 4. The 1:1 complexes are tetrameric, with either cubic or chair structures depending on steric requirements of both X and R_3P (Figure 1.8).[42]

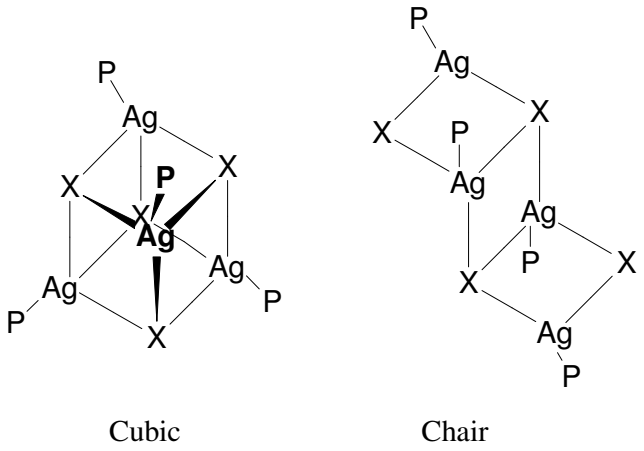

Figure 1.8: Cubic and chair structures of silver(I).

$(R_3P)_2AgX$ complexes are generally dimeric with bridging X ions, but in the case of very bulky phosphines, linear cations, $[R_3P\text{-}Ag\text{-}PR_3]^+$, can occur. Complexes with bridging bidentate phosphines tend to be dimers or tetramers (Figure 1.9), but with the addition of two ligands per silver(I), tetrahedral cationic species may form.[42,43]

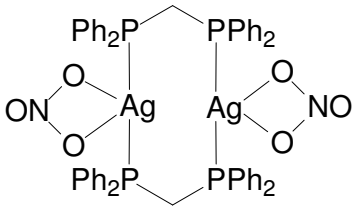

Figure 1.9: A dimeric silver(I) complex with bridging bidentate phosphine ligands.

1.2.3.2 Complexes of Silver(II)

Numerous complexes of silver(II) are known and they are normally prepared by peroxodisulphate oxidation of silver(I) solutions containing the complexing ligand. With neutral ligands, cationic silver(II) complexes form crystalline salts, whereas with a mono-anionic bidentate ligand, neutral silver(II) complexes are obtained (Figure 1.10).[39,42,43]

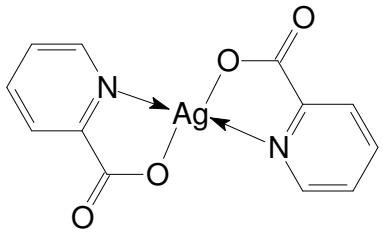

Figure 1.10: Neutral bis(picolinato)silver(II) complex.

1.2.3.3 Complexes of Silver(III)

Few simple silver(III) complexes are known due to the instability of the silver(III) ion. A silver(III) complex of remarkable stability is the one with ethylenedi(biguanide), which is obtained as a red sulphate when Ag_2SO_4 is treated with aqueous potassium peroxodisulphate in the presence of ethylenedi(biguanidium) sulphate (Figure 1.11). Silver(III) also form stable complexes with porphyrins.[42,41,43]

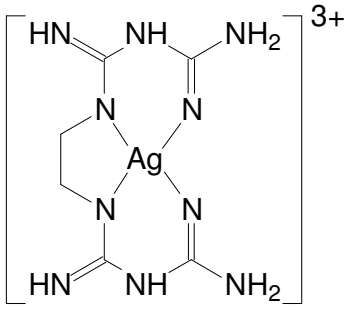

Figure 1.11: Ethylenedi(biguanide)silver(III).

1.3 ANTI-TUMOUR RESEARCH

Cancer is a class of diseases or disorders characterised by uncontrolled division of cells. These cells have the ability to invade other tissues, either by direct growth into adjacent tissue or by migration and implantation into other sites (*metastasis)*. Metastasis is the process by which cancer cells are transported through the bloodstream or lymphatic system and are spread to other tissues. Cancer may affect people of all ages, but older people have an increased risk as a result of DNA damage becoming more regular in aging DNA. Cancer is one of the leading causes of death in developed countries.[2,60,61]

There are numerous types of cancer. Severity of symptoms depends on the site and character of the malignancy and whether there is metastasis. Most cancers can be treated, and some cured, depending on the specific type, location and stage. Once diagnosed, cancer is usually treated with a combination of surgery, chemotherapy and radiotherapy. As research develops, treatments are becoming more specific for the type of cancer pathology. Drugs that target specific cancers already exist for several cancers.[2,60,61]

The unregulated cell growth that characterises cancer is caused by damage to DNA, resulting in mutations to genes that encode for proteins controlling cell division. Many mutation events may be required to transform a normal cell into a malignant cell. These mutations can be caused by chemicals or physical agents called carcinogens, by exposure to radioactive materials or by certain viruses that can insert their DNA into the human genome. Mutations mostly occur spontaneously, but some gene mutations are passed down from generation to generation.[2,60,61]

Hippocrates, the "Father of Medicine", described several kinds of cancers. He called benign tumours *oncos*, Greek for swelling, and malignant tumours *carcinos*, Greek for crab or crayfish. This strange choice of name probably comes from the appearance of the cut surface of a solid malignant tumour, with a roundish hard centre surrounded by pointy projections, vaguely resembling the silhouette of a crab. He later added the

[60] I.F. Tannock, R.P. Hill, *The Basic Science of Oncology 4th Ed.*, McGraw-Hill, **2005**.
[61] L.J. Kleinsmith, *Principles of Cancer Biology*, Pearson Benjamin Cummings, **2006**.

suffix *-oma*, Greek for swelling, giving the name *carcinoma*. Since it was against Greek tradition to open the body, Hippocrates only described and made drawings of outwardly visible tumours on the skin, nose and breasts. In the 16th and 17th centuries it became more acceptable for doctors to dissect bodies to discover the cause of death. Through the centuries it was thus discovered that cancer occured everywhere in the body. Treatment of cancers was initially based on the humor theory of four bodily fluids (black bile, yellow bile, blood and phlegm).[2,60,61]

With the widespread use of the microscope in the 18th century, it was discovered that cancer can spread from the primary tumour through the lymph nodes to other sites. The use of surgery to treat cancer was being employed, but had poor results due to problems with hygiene. When Pierre and Marie Curie discovered radiation at the end of the 19th century, they stumbled upon the first effective non-surgical cancer treatment. With radiation came the first signs of multi-disciplinary approaches to cancer treatment.[2,60,61]

Malignant tumour cells have distinct properties: i) evading apoptosis; ii) unlimited growth potential (immortalitisation) due to overabundance of telomerase; iii) self-sufficiency of growth factors; iv) insensitivity to anti-growth factors; v) increased cell division rate; vi) altered ability to differentiate; vii) no ability for contact inhibition; viii) ability to invade neighbouring tissues; ix) ability to build metastases at distant sites; and x) ability to promote blood vessel growth (angiogenesis).[2,60,61]

1.4 COORDINATION COMPOUNDS IN MEDICINE

Chemotherapy is the treatment of cancer with drugs that can destroy cancer cells. It interferes with cell division in various ways, *e.g.* interfering with the duplication of DNA or the separation of newly formed chromosomes. Most chemotherapeutic drugs work by impairing mitosis (cell division), effectively targeting fast-dividing cells. Most forms of chemotherapy target all rapidly dividing cells and are not specific for cancer cells. Hence, chemotherapy has the potential to harm healthy tissue, especially tissue with a high replacement rate (*e.g.* intestinal lining). These cells usually repair themselves after chemotherapy. As these drugs cause damage to cells, they are termed *cytotoxic*. Some drugs cause cells to undergo apoptosis (so-called "cell suicide").[2,60,61]

The beginnings of the modern era of cancer chemotherapy can be traced directly to the discovery of nitrogen mustard (Figure 1.12), a chemical warfare agent, as an effective treatment for cancer. Two pharmacists, Louis Goodman and Alfred Gilman,[62] were recruited by the United States Department of Defense to investigate potential therapeutic applications of chemical warfare agents. Autopsies of people exposed to mustard gas had revealed profound lymphoid and myeloid suppression. Goodman and Gilman reasoned that this agent could be used to treat lymphoma, since lymphoma is a tumour of lymphoid cells. They first set up an animal model by establishing lymphomas in mice and demonstrated they could treat them with mustard agents. Next, in collaboration with a thoracic surgeon, Gustav Linskog, they injected a related agent, mustine (the prototype nitrogen mustard anticancer chemotherapeutic drug), into a patient with non-Hodgkin's lymphoma. They observed a dramatic reduction in the patient's tumour masses. Although this effect lasted only a few weeks, this was the first step to the realisation that cancer could be treated by pharmacological agents. Cancer drug development since then has exploded into a multi-billion dollar industry.[2]

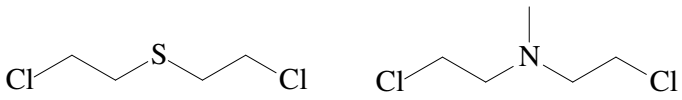

Mustard Gas Mustine

Figure 1.12: Mustard gas derivatives.

The majority of chemotherapeutic drugs can be divided into: i) alkylating agents; ii) anti-metabolites; iii) anthracyclines; iv) plant alkaloids; v) topoisomerase inhibitors; and vi) anti-tumour agents. All of these drugs affect cell division or DNA synthesis and function.[2,60,61]

Chemotherapeutic drugs of interest to this study are the group called alkylating agents. Currently, the most widely used anti-tumour drugs; cisplatin, carboplatin and

[62] L.S. Goodman, M.M. Wintrobe, W. Dameshek, M.J. Goodman, A. Gilman, M.T. McLennan, *J. Am. Med. Assoc.*, **1984**, 251, 2255.

oxaliplatin (Figure 1.13) are classified as alkylating agents due to a similar mode of action in their anti-tumour activity to alkylating agents (*i.e.* DNA crosslinking). Drugs containing transition metals, especially platinum-based drugs, have been shown to impede DNA replication and repair.[2]

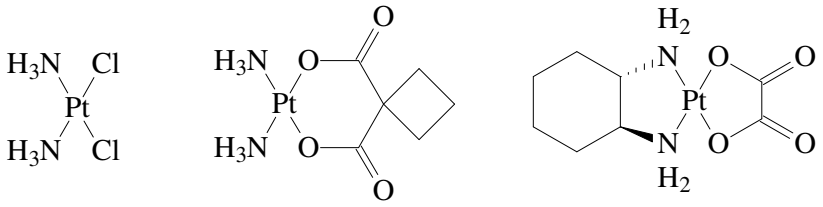

cisplatin carboplatin oxaliplatin

Figure 1.13: Commercially available platinum-based anti-tumour drugs.

Cisplatin was discovered by a Michigan State University researcher, Barnett Rosenberg,[63] working under an NCI contract. Rosenberg had initially wanted to explore the possible effects of an electric field on the growth of bacteria. He observed that the bacteria unexpectedly ceased to divide when placed in an electric field. The inhibition of bacterial division was pinpointed to an electrolysis product of the platinum electrode rather than the electrical field. This accidental discovery, soon initiated a series of investigations and studies into the effects of platinum compounds on cell division, culminating in the synthesis of cisplatin. Subsequently, Eve Wiltshaw *et al*. at the Institute of Cancer Research in the United Kingdom extended the clinical usefulness of platinum compounds with their development of carboplatin, a cisplatin derivative that combines broad anti-tumour activity and comparatively low nephrotoxicity.[2]

As can be seen from the three anti-tumour drugs above, the use of metal complexes compounds as anti-tumour drugs is well established. The transition metal group 11 compromises the diamagnetic metals copper (Cu), silver (Ag) and gold (Au). These elements are called noble metals or coinage metals due to having high resistance to corrosion and due to being used as coins since antiquity. The use of gold complexes as Rheumatoid Arthritic (RA) drugs is well established. The interest in the use of

[63] B. Rosenberg, L. van Camp, T. Krigas, *Patent no: US4339437*, **1982**.

Group 11 metals as anti-tumour drugs has recently increased and many new gold,[64,65,66] silver[67,68] and copper[69,70] compounds have been and are being tested as potential anti-tumour drugs.[6]

1.4.1 Gold Compounds in Medicine

Gold is normally present in human and animal tissues in minute concentrations. It has no natural biological function, although some algae are able to absorb considerable quantities of gold from solutions and there is one plant species known to concentrate the metal.[71] Many gold compounds are highly toxic to animals, especially chloro auric acid and its salts, largely due to their oxidising ability.[71]

1.4.1.1 History

The earliest application of gold as a therapeutic agent originated in China. Gold was, furthermore, widely used by ancient physicians and surgeons. Many ancient cultures, such as those in India and Egypt used gold-based medicinal preparations, but China was the earliest to cure sickness with it and this has been dated back as far as 2500 B.C.[72] Since the discovery of gold, people have thought of it as having an immortal nature (*e.g.* resistance to chemical corrosion) and associated it with longevity. Consequently, gold was used as a medicine to seek longevity. Pure gold was used to treat furuncles, smallpox and skin ulcers and to remove mercury from skin and flesh. Some ancient references noted that gold drugs can cure joint disease and disease in

---

[64] M.V. Baker, P.J. Barnard, S.J. Berners-Price, S.K. Brayshaw, J.L. Hickey, B.W. Skelton, A.H. White, *J. Chem. Soc., Dalton Trans.*, **2006**, 14, 30, 3708.
[65] J.S. Casas, E.E. Castellano, M.D. Couce, J. Ellena, A. Sanchez, J. Sordo, C. Taboada, *J. Inorg. Biochem.*, **2006**, 100, 11, 1858.
[66] C. Gabbiani, A. Casini, L. Messori, *Gold Bull.*, **2007**, 40, 73.
[67] B. Thati, A. Noble, B.S. Creaven, M. Walsh, M. McCann, K. Kavanagh, M. Devereux, D.A. Egan, *Cancer Lett.*, **2007**, 18, 250, 1, 128.
[68] H. Torigoe, K. Kawahashi, A. Takamori, A. Ono, *Nucleosides Nucleotides Nucleic Acids.*, **2005**, 24, 5, 915.
[69] K. Ahmad, *Lancet Oncol.*, **2007**, 8, 4, 289.
[70] G.D. Geromichalos, G.A.Katsoulos, A. Papageorgiou, D.T. Trafalis, C.C. Hadjikostas, S.H. Voyatzi, P. Stravoravdi, J BUON., **2004**, 9, 4, 433.
[71] R.V. Parish, S.M. Cottrill, *Gold Bull.*, **1987**, 20, 3.
[72] J.M. Needham, *Science and Civilization in China, Vol. 5*, Cambridge University Press, **1974**, 285.

lungs. There were prescriptions containing gold for curing measles and other diseases. Plant and animal medicines were used in ancient prescriptions and many of these contain gold as a trace element.[73, 44]

People in ancient times accumulated experience through trial and error and gradually developed useful gold drugs. Some of them had a reputation for having a good therapeutic effect. Ancient China had remarkable achievements in this field and some of these gold drugs have a relationship to their modern successors. In order to use pure gold for drugs, techniques were developed in the second century A.D. for refining gold and for separating gold–silver alloys. In order to use gold powder for drugs, techniques for making gold foil and powder were devised by alchemists.[73]

Arising from the fact that people had a thirst for gold treatments and that gold was linked to the mystery of life, alchemists devoted themselves to the manufacture of the elixir for immortal life and tried to produce man-made "gold". Though their objectives were absurd, they were successful in making a variety of imitation gold materials and had a deep understanding of the Au-Ag system, along with various other transition metal systems, *i.e.* Au-Cu, Cu-Zn, Cu-As, Cu-Hg, Sn-S, Hg-S, *etc.*[73]

Ancient alchemists in China found chemical species which help in the dissolution of gold (*i.e.* Fe^{3+} and Cl^-) and used cyanide-containing plants to dissolve gold. Potable gold referred to as "drinkable gold" and the earliest literature dealing with potable gold in China was "On Salt and Iron" written in 81 B.C. Since gold flakes or powder and medicinal gold are "heavy articles", which cannot stay long in the stomach, and were in some cases toxic, alchemists sought to solve the problem by making "drinkable gold" as an elixir. We now know that cyanide is present in over a thousand plants and some of the traditional Chinese herbs used for medicine are amongst these. Fresh raspberries contain cyanide and this is the key factor enabling dissolution of gold in the prescription "Baopuzi: The Internal Chapter" for potable gold. The above considerations indicate that potable gold was in fact likely to contain a very small amount of dissolved gold. Metallurgical and chemical achievements of these ancient alchemists in China were therefore considerable.[73]

---

[73] Z. Huaizhi, N. Yuantao, *Gold Bull.*, **2001**, 34, 24.

In 1890 Koch[74] discovered that $KAu(CN)_2$ was lethal to the micro-organism responsible for tuberculosis (mycobacterium tuberculosis) in a test tube study. This paved the way for a sounder basis for gold therapy. This compound was administered to tuberculosis (TB) sufferers, but although there were positive results there were serious toxic side effects. After intensive synthetic efforts in the 1920's several gold(I) thiol compounds were introduced for the treatment of tuberculosis. These compounds were later introduced as drugs against rheumatoid arthritis (RA) (see **1.4.1.2.1**), which lead to the mistaken postulation of a relationship between TB and RA. However, after 1935 the use of gold drugs for TB treatment was stopped due to serious side effects and a lack of clinical success.[40]

1.4.1.2 Recent Developments in the Medicinal Applications of Gold Compounds

Apart from the obvious use of gold alloys in dental restorations there are a number of direct applications of gold in medical devices. The excellent biocompatibility of gold led to its use in dental applications. Further applications include wires for pacemakers and gold plated stints used in the treatment of heart disease. Gold possesses a high degree of resistance to bacterial colonisation and because of this it is the material of choice for implants that are at risk of infection, such as the inner ear. Gold has a long tradition of use in these applications and is considered a very valuable metal in surgery.[75]

An interesting medical product now being marketed in Japan is a gold-titanium patch, based on the theory of ion adjustment in the human body. It is considered that fatigue and stiffness are generally caused by the increase of positive ions in the body, causing the interruption in the circulation of blood. The gold-titanium patch adjusts this imbalance of ions by inducing an electric stimulus (due to the galvanic effect between the gold and titanium metals). The induced warmth is said to alleviate the pain (Figure 1.14).[75]

[74] R. Koch, *Deutsche Med. Wochenschr.*, **1890**, 16, 756.
[75] http://www.gold.org.

Figure 1.14: Thermal image of patient before and after application of metallic patch, showing an increase in surface body temperature.

Recent interesting developments include the use of microscopic spheres of gold for the delivery of vaccines, pharmaceuticals or DNA portions into the human body. Gold has the required adsorptive characteristics and biocompatibility for such applications. It has been used in the detection of deadly poisons such as anthrax, the development of gold-coated lasers to aid in skin rejuvenation and the testing of vaccines. Nano-scale gold particles are being investigated for use in biomedical diagnostic kits.[75]

Gold is the perfect raw material for certain rapid tests. A rapid test is an inexpensive, disposable, membrane-based technique that provides visual evidence of the presence of an analyte in a liquid sample.[75] Applications for rapid tests include clinical uses (fertility tests, tumour markers, toxicology, allergies, viral infection),[76,77,78] agricultural uses (food safety, plant and crop diseases)[78] and environmental uses (biological and environmental contamination).[78]

Early rapid tests used coloured latex to produce the visual signal. Gold labels were first introduced into membrane-based rapid tests in the late 1980's because of their greater potential stability and an ever-increasing demand for ultra sensitivity. These labels are based on gold colloids, a suspension of nanometre sized gold particles individually surrounded by a negative charge layer.[79,80] This charge layer provides the

[76] http://www.atfirstdiagnostic.com.
[77] J.L. Greenwald, G.R. Burstein, J. Pincus, B. Branson, *Curr. Infec. Dis. Rep.,* **2006**, 8, 125.
[78] J.A. Chandler, *Patent no: ZA9600802*, **1996**.
[79] J.L. Brennan, N.S. Hatzakis, T.R. Tshikhudo, N. Dirvianskyte, V. Razumas, S. Patkar, J. Vind, A. Svendsen, R.J. Nolte, A.E. Rowan, M. Brust, *Bioconjug. Chem.*, **2006**, 17, 6, 1373.

means for the gold particles to repel each other and remain in suspensed form indefinitely. Gold is essentially inert and forms almost perfect spherical particles when properly manufactured. Proteins bind to the surfaces of these gold particles with enormous strength when correctly coupled, thus providing a high degree of long-term stability, both in the solid and solvent-free state. If manufacturing processes ensure that gold particles of any accurately defined diameter can be manufactured reproducibly, there will be minimal batch-to-batch variation. What's more, different sizes of gold may be used for different applications, thus making it a very flexible raw material for both manufacture and development. Overall, the superior stability, sensitivity and reproducibility of manufacture, makes gold a first class raw material component for a wide range of rapid test applications.[75,78,81]

One of the connections between the chemistry and the biology of gold is the use of gold for the solving of crystal structures of proteins. Gold, due to its high scattering factor for x-rays, is used as a label on crystalline proteins to solve the phasing problem experienced in these large structures. In these endeavours both gold(I) as $[Au(CN)_2]^-$ and gold(III) as $[AuCl_4]^-$ or $[AuI_4]^-$ have been used. What was commonly observed in these structures was the binding of gold to mostly histidine (free nitrogen containing amino acid)[82] or cysteine (free sulphur containing amino acid)[83] moieties in protein molecules. It is now known that many proteins depend on a free cysteine for activity and the loss of this free site due to gold binding will lead to inactivity of the protein.[40]

1.4.1.2.1 Gold(I) in Rheumatoid Arthritis Treatment

Gold and gold-containing compounds have historically been used in drugs for the treatment of a wide range of ailments. The use of gold compounds in medicine is called chrysotherapy (from the Greek word for gold, *chrysos*). The Frenchman

---

[80] T.R. Tshikhudo, D. Demuru, Z. Wang, M. Brust, A. Secchi, A. Arduini, A. Pochini, *Angew. Chem. Int. Ed. Engl.*, **2005**, 44, 19, 2913.
[81] http://www.bb-international.com
[82] F.R. Salemme, S.T. Freer, N.H. Xuong, R.A. Alden, J. Kraut, *J. Biol. Chem.*, **1973**, 248, 11, 3910.
[83] G.E. Schulz, K. Biedermann, W. Kabsch, R.H. Schirmer, *J. Mol. Biol.*, **1973**, 80, 4, 857.

Jacques Forestier reported in 1929 that the use of gold complexes was beneficial in the treatment of arthritis.[84] Later work, after World War II, demonstrated conclusively that gold drugs are effective in treating RA patients.[6,75,85]

RA is an inflammatory disease characterised by a progressive erosion of the joints resulting in deformities, immobility and a great deal of pain. It is an autoimmune disease in which the body's immune system mounts a response against itself. This results in a malign growth of the synovial cells (the cells lining the joint) called a pannus and permeation of the joint space by cells of the immune system, primarily macrophages, and associated production of immunoglobulin proteins called rheumatoid factors. Phagocytic cells release degradative enzymes such as collagenase and generate the reactive oxygen species, hydroxyl radical ($^{\cdot}OH$) and superoxide (O_2^-), all of which contribute to the resulting tissue damage. This progressive inflammatory response is promoted by raised levels of chemical mediators such as prostaglandins, leukotrienes and cytokines.[85]

The class of RA drugs that include gold compounds are termed Disease-Modifying Anti-Rheumatic Drugs, the DMARDS. As the name suggests, DMARDS, act to impede or even stop the progression of RA. These are appropriately employed for newly diagnosed patients so as to manage the disease by halting progression. Gold-based compounds fall within the DMARDS class, as there is experimental evidence to indicate that chrysotherapy is disease modifying. Unfortunately, as with all chemotherapies, chrysotherapy is associated with various negative side effects. This leaves scope for improvement of therapies.[6,40,71,44,85]

There are two classes of gold compounds used in the treatment of RA. Membership of each class relates to the inherent chemistry of the compound and dictates their mode of administration and therefore bio-distribution. The first class of compounds is generally polymeric, charged and water-soluble. By contrast, the second class of compound is monomeric, neutral and lipophilic. Class I (Figure 1.15) comprises: i) sodium aurothiomalate (*e.g.* Miocrin, Myochrysine, Myocrisin, Shiosol and Tauredon); ii) sodium aurothiopropanol sulphonate (*e.g.* Allochrysine Limière); iii)

[84] P. De Marchin, *Acta Rhumatologica Belgica*, **1978**, 2, 97.
[85] S.P. Fricker, *Gold Bull.*, **1996**, 29, 2, 53.

aurothioglucose (*e.g.* Aureotan, Auromyose and Solganol); and iv) sodium aurothiosulphate (*e.g.* Fosfocrisolo and Sanocrysin). The Class II drugs have but one member, which is: triethylphosphinegold(I) tetra-acetylated thioglucose, commonly known as auranofin (*e.g.* Aktil, Crisinor, Crisofin and Ridaura). All of these drugs are registered trademarks and commercially available.[71,44,85]

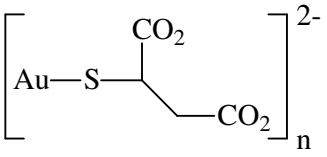

Sodium aurothiomalate

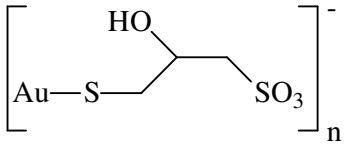

Sodium aurothiopropanol sulphonate

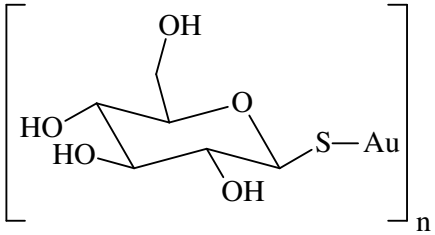

Aurothioglucose

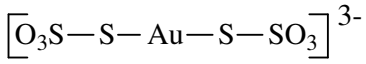

Sodium aurothiosulphate

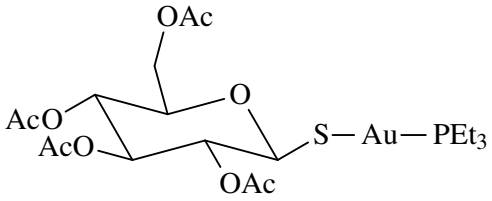

Auranofin

Figure 1.15: Commercially available gold-based Rheumatoid Arthritis drugs.

RA is not a well understood disease. RA can be treated by a variety of drugs, including gold-based drugs, but not cured. Similarly, the mechanism of action of gold-drugs is also not well understood. The mode of administration of the Class I drugs *via* intramuscular injections of suspensions indicates that the drugs are delivered to the vascular system. This is rich in the blood protein albumin and it is thought that the gold drug undergoes a substitution reaction so that an albumin molecule replaces one of the thiomalate ligands. Subsequent metabolism may involve the substitution of the

second thiolate ligand of the drug by another albumin molecule resulting in the original gold atom existing within a ball of protein that is presumably carried to the site of inflammation. Once at the target site, the gold may be extracted by cyanide (a metabolite of thiocyanate generated at sites of inflammation) to form a small anionic species, $[Au(CN)_2]^-$, that is known to have a very high stability constant. It was thus postulated that this may be the active species. A similar mechanism of action is envisaged for auranofin. The conclusion of what is known about the metabolic pathways of both Class I and II drugs is that the administered drugs rapidly undergo substitution reactions of one sort or another and therefore can be regarded as prodrugs.[40,44,71,85]

There is evidence to suggest that auranofin inhibits the production of reactive oxygen species such as $^{\cdot}OH$ and O_2^- produced during the oxidative burst of activated polymorphonuclear cells (a phagocytic cell of the immune system). In this case the active metabolite may be aurocyanide. One suggestion is that gold complexes may react with the cyanide released during phagocytosis forming aurocyanide. This can readily enter cells and has been shown to inhibit the oxidative burst.[85]

Recently de Wall *et al.*[86] have put forward another theory, which postulates that gold(I) is oxidised to gold(III) *in vitro* and *in vivo.* They have shown that platinum(II) and their iso-electronic gold(III) complexes led to the inhibition of the immune response by the blocking of the Class II major histocompatibility complex (MHC) proteins. MHC proteins are responsible for many of the autoimmune responses associated with RA and their inhibition would prevent the symptoms seen in typical RA patients.

1.4.1.2.2 Gold in HIV and Asthma Treatment

In the desperate quest to seek a cure for AIDS, some gold drugs have been evaluated for activity against human immunodeficiency virus (HIV).[87,88] Early results suggest

[86] S.L. de Wall, C. Painter, J.D. Stone, R. Bandaranayake, D.C. Wiley, T.M. Mitchison, L.J. Stern, B.S. de Decker, *Nat. Chem. Biol.*, **2006**, 2, 4, 197.
[87] E. de Clercq, *Expert Opin. Emerg. Drugs*, **2005**, 10, 2, 241.
[88] T. Okada, B.K. Patterson, S.Q. Ye, M.E. Gurney, *Virology*, **1993**, 192, 631.

that there might be some inhibition of HIV exhibited by gold compounds such as sodium aurothiomalate and aurothioglucose. Some gold compounds used in the treatment of RA have demonstrated effectiveness against severe bronchial asthma owing to their immuno-suppressant properties.[89,90] Recent reviews describing new agents for treating asthmatics suggest that gold-therapy might be limited to severe cases such as chronic corticosteroid-dependent asthma, *i.e.* as second-line agent as for the treatment of RA by DMARDS. Phosphine gold(I) thiolates have been evaluated for their activity against parasitic diseases such as malaria[91] and Chagas disease. However, in terms of drug development, to date most attention has been devoted to the investigation of the anti-tumour potential of gold compounds (see *1.4.1.2.4*).[6,44,92]

1.4.1.2.3 Gold in Anti-Microbial Treatment

The implication of microbial infection as a causative agent in arthritis was the stimulus for the investigation of the anti-microbial properties of gold complexes. The early work by Robert Koch[74] demonstrated that gold compounds were active against the *Tubercle bacillus*. Subsequent extensive work in the 1930's and 1940's demonstrated that a variety of gold compounds were active against a broad spectrum of micro-organisms.[93] Activity in *in vitro* test systems was demonstrated against both gram negative and gram positive bacteria, a number of strains of mycoplasma and the protozoan *Leishmania*. Gold complexes were able to modify the course of a number of *in vivo* infections in a variety of animal hosts. Many of these early studies were flawed and the lack of evidence for the role of an infectious agent in RA resulted in this work not being pursued.[85]

Today there is a growing need for new clinical anti-microbial agents. The therapeutic efficacy of drugs currently available for the treatment of a class of bacteria known as "problem Gram positive cocci" is limited by the emergence of multiple-resistant strains such as methicillin-resistant *Staphylococus aureus* (MRSA) and enterococci

---

[89] G.W. Canonica, *Chest*, **2006**,130, 21S.
[90] M. Muranaka, T. Miyamoto, T. Shida, J. Kabe, S. Makino, H. Okumura, K. Takeda, S. Suzuki, Y. Horiuchi, *Ann. Allergy*, **1978**, 40, 132.
[91] M. Navarro, H. Pérez, R.A. Sánchez-Delgado, *J. Med. Chem.*, **1997**, 40, 1937.
[92] E.R.T. Tiekink, *Crit. Rev. Oncol. Hematol.*, **2002**, 42, 225.
[93] J.H. Liebarth, R.H. Persellin, *Agents and Actions*, **1981**, 11, 458.

e.g. Enterococcus faecalis.[94] Vancomycin (Figure 1.16) is the drug of choice for these organisms but it too has limitations as it must be administered by intravenous infusion and there are problems with resistance.[85]

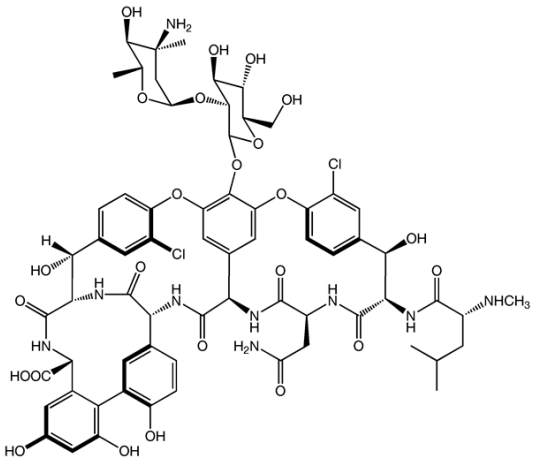

Figure 1.16: Structure of Vancomycin.

In recent studies a number of different metal complexes have been tested for anti-microbial activity.[95] The compounds were tested against a number of bacterial strains including clinical isolates of MRSA, methicillin-sensitive *S. aureus*, enterococci, coagulase-negative staphylococci and streptococci. A gold(I) thiocyanate complex, $Au(SCN)(PMe_3)$ demonstrated activity against Gram positive bacteria including MRSA. Comparative toxicity against mammalian cells was evaluated *in vitro* against the CHO (Chinese Hamster Ovary) cell line. The gold complex demonstrated good selectivity for bacteria over mammalian cells with an IC_{50} of 0.33 against *Staphylococcus aureus* and 0.77 against *Enterococcus faecalis*, and with lethal doses of at least 10x higher necessary to kill CHO cells.[85]

Further investigation of gold complexes led to the identification of a series of gold(I) phosphonium dithiocarboxylate complexes which have activity against Gram positive bacteria including "problem Gram positive cocci". The anti-microbial activity of the gold(III) compounds $AuCl_2$(damp) and $Au(OAc)_2$(damp) (Figure 1.17) have been

[94] W. Brumfitt, J.M.T. Hamilton-Miller, *Drugs Exptl. Clin. Res.*, **1990**, 16, 205.
[95] A.M. Elsome, J.M.T. Hamilton-Miller, W. Brumfitt, W.C. Noble, *J. Antimicrob. Chemother.*, **1996**, 37, 5, 911.

investigated. Both exhibit broad spectrum activity against a range of organisms with a small degree of specificity against the Gram positive organisms *S. aureus* and *E. faecalis* with the more water soluble diacetate derivative being the most potent. Both complexes show similar toxicity against mammalian CHO cells indicating that the diacetate complex is the more selective of the two complexes for bacteria over mammalian cells.[85]

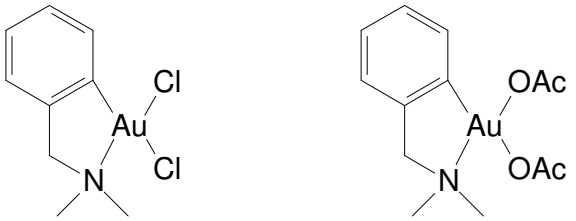

$AuCl_2$(damp) $Au(OAc)_2$(damp)

Figure 1.17: Anti-microbial gold(III) compounds.

1.4.1.2.4 Gold(I) in Anti-Tumour Treatment

The first comprehensive studies of the anti-tumour potential of gold compounds, including gold drugs, were published in the mid-to-late 1980's and these studies still have relevance today.[96] A key outcome of this early work was the conclusion that gold was essential for elevated potency. These studies showed that the most promising class of gold(I) compounds were the phosphine gold(I) thiolates, *i.e.* related to the structure of auranofin (Figure 1.15). Active compounds featuring P-Au-S as structural element displayed the first structure activity relationship. This principle proved fruitful in screening for anti-tumour activity where thiols such as 6-mercaptopurine and 6-thioguanine were utilised.[97,98] The potency of phosphine gold(I) thiolates was found to be higher in a range of human cancer cell lines when compared with the free thiols.[44]

[96] C.K. Mirabelli, R.K. Johnson, D.T. Hill, L.F. Faucette, G.R. Girard, G.Y. Kuo, C.M. Sung, S.T. Crooke, *J. Med. Chem.*, **1986**, 29, 218.
[97] P.D. Cookson, E.R.T. Tiekink, M.W. Whitehouse, *Aust. J. Chem.*, **1994**, 47, 577.
[98] M.W. Whitehouse, P.D. Cookson, G. Siasios , E.R.T. Tiekink, *Metal-Based Drugs*, **1998**, 5, 245.

A large number of phosphine complexes (R_3PAuX) have been evaluated and all exhibit *in vitro* potent cytotoxicity against tumour cells.[96] Variations of the phosphine substituents (R_3P) modulate the anti-tumour activity *in vivo* as do changes in the counter ion X. Anti-tumour activity is lowest for the complexes that contain a good leaving group (*e.g.* Cl^-, NO_3^-), although cytotoxic potency is unaffected. These complexes are very reactive towards thiols and it may be predicted that the ligand is rapidly exchanged by –SH groups *in vivo*. Potent *in vitro* cytotoxic activity and *in vivo* anti-tumour activity have been observed only for gold(I) complexes with coordinated phosphine ligands, while complexes with ligands R_2S, pyridine, or cyclo-octadiene show low cytotoxicity and marginal anti-tumour activity. Activity of phosphines is mostly attributed to the lipophilic nature of these compounds. The lipophilic phosphines are believed to aid in the uptake of the complex into the cell, while polymeric gold(I) thiolates do not readily enter cells.[6]

Another avenue of investigation has been to synthesise gold complexes containing ligands with known anti-tumour activity.[99] Examples of this are a series of $Ph_3PAu(I)$-nucleotide complexes containing ligands such as 5-fluorouracil and 6-mercaptopurine, phosphinogold(I) ferrocene complexes such as [μ-1,1-bis(bis(diphenylphosphino))-ferrocene] di(gold choride), more recently a series of novel nitrogen containing phosphino gold(I) ferrocenes,[100] and a gold(III) complex of streptonigrin, a substituted 7-amino-quinoline-5,8,-dione.[85,99]

Gold(I) bisphosphine compounds of dppe and related ligands with a tetrahedral coordination geometry turned out to be a particularly potent class of compounds but clinical trials were not pursued owing to the acute toxicity associated with them.[6] However, subsequent studies have focused on chemically modifying the aromatic substituents, such as to form *n*-pyridyl analogues, so as to moderate the lipophilicity of the compounds and to emphasise their apparent anti-mitochondrial activity.[44,85] The physiological action of tetrahedral complexes will be discussed further in Chapter 3.

---

[99] C.P. Shaw, *Metal Compounds in Cancer Therapy*, ed. S.P. Fricker, Chapman and Hall, London, **1994**, 46.
[100] M. Viotte, B. Gautheron, M.M. Kubicki, I.E. Nifant'ev, S.P. Fricker, *Metal-Based Drugs*, **1995**, 2, 31.

1.4.1.2.5 Gold(III) in Anti-Tumour Treatment

Factors, that suggest a study of the anti-tumour potential of gold compounds might be worthwhile, relate to the fact that gold in the +3 oxidation state has the same electronic configuration and structural characteristics as platinum(II), a component of the world's most widely-used anticancer drug, cisplatin [$(NH_3)_2PtCl_2$]. The major drawback of cisplatin is the exhibition of serious side effects.[44,71,85,101,102]

The gold(III) compounds investigated for potential anti-tumour activity are inevitably four-coordinate and feature square planar geometries, as found for cisplatin. A similar mechanism of action, *i.e.* interaction with DNA and disruption of normal cellular processes, was initially assumed for these compounds. In connection with this, evidence has been provided that some species bind to DNA.[44,71,101]

One of the key problems that hampered the development of gold(III) complexes is their low stability under physiological conditions. Gold(III) compounds are strong oxidation agents and are able to oxidise a series of biomolecules such as methionine and glycine. In recent years, owing to the contributions of a few research groups, new gold(III) compounds have been synthesised and characterised that show sufficient stability under physiologically relevant conditions. The stability of gold(III) compounds can be enhanced by introducing chelating ligands. Gold(III) complexes should ideally be coordinated by at least two chelating nitrogen donors which lowers the redox potential of the metal centre and thereby stabilises the complexes.[71,101,102]

There are basically three classes of gold(III) compounds receiving serious attention at present. The three classes are: i) those incorporating biologically active species such as streptonigrin;[64,103] ii) compounds with imine (pyridine-type nitrogen) donor atoms;[64,104] and iii) organogold compounds, *i.e.* containing Au-C bonds.[64,,105]

---

[101] L. Messori, G. Marcon and P. Orioli, *Bioinorg. Chem. Appl.*, **2003**, l, 2, 177.
[102] T. Yang, C. Tu, J. Zhang, L. Lin, X. Zhang, Q. Liu, J. Ding, Q. Xu, Z. Guo, *J. Chem. Soc., Dalton Trans.*, **2003**, 3419.
[103] A. Moustatih, A. Garnier-Suillerot, *J. Med. Chem.,* **1989**, 32, 1426.
[104] L. Messori, F. Abbate, G. Marcon, P. Orioli, M. Fontani, E. Mini, T. Mazzei, S. Carotti, T. O'Connell, P. Zanello, *J. Med. Chem.*, **2000**, 43, 3541.
[105] R.V. Parish, *Metal-Based Drugs*, **1999**, 6, 271.

Whereas, the overwhelming majority of gold(III) compounds investigated thus far, contain ligands containing some combination of chloride, nitrogen, oxygen and carbon as donor atoms, perhaps it is significant that arguably the compound showing the most promise contains a sulphur donor atom and is a complex of 2-mercaptobenzoate.[44,106]

The chelating binding mode of the thiosalicylate ligand in this gold(III) complex, {*p*-$MeOC_6H_3CH_2NMe_2$} Au($SC_6H_4CO_2$-2) (Figure 1.18), is very different to the previously characterised gold(I) thiolate complexes. These complexes might display different biological activities, which could be of interest given the medical importance of gold-thiolate complexes.[85,106] Further analogues of (damp)$AuC1_2$ have been evaluated in this way. Biochemical studies indicate that these compounds have a mechanism of action significantly different to that of cisplatin suggesting that this is a potentially important novel class of metal-containing anti-tumour agents.[85]

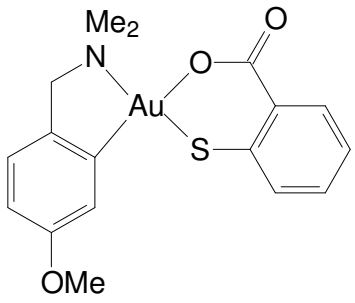

Figure 1.18: The chemical structure of the 2-mercaptobenzoate gold(III) compound, {*p*-$MeOC_6H_3CH_2NMe_2$} Au($SC_6H_4CO_2$-2).

Other gold(III) compounds receiving attention are those patented by Leung *et al.*[107] and compounds being studied by Guo *et al.*,[102] Messori *et. al.*[101] and Yang *et al.*[108] An Associate Professor at the National University of Singapore, Pak Hing Leung and his team have discovered that phosphine supported gold complexes have excellent anti-tumour activity and clinical trials are likely to begin in the near future.[75]

---

[106] M.B. Dinger,W. Henderson, *J. Organomet. Chem.*, **1998**, 560, 233.
[107] P.H. Leung, S.H.Chan, Y. Song, *Patent no: US 6,774,254*.
[108] D. Fan, C.T. Yang, J.D. Ranford, J.J. Vittal, *J. Chem. Soc., Dalton Trans.*, **2003**, 4749.

The Research group of Zijan Guo[102] at Ninjang University, China, has studied a series of gold(III) compounds that show potential anti-tumour activity. The three gold(III) complexes studied are: i) [Au(Quinpy)Cl]Cl; ii) [Au(Quingly)Cl]Cl; and iii) [Au(Quinala)Cl]Cl (Figure 1.19). The ligands coordinate to gold(III) in a tridentate mode forming two five-membered chelate rings. The gold(III) in these complexes shows a slightly distorted square planar coordination formed by three nitrogen atoms of the ligand and one chloride atom. All the complexes have shown considerable cytotoxic activity against several tumour cell lines. The complexes are able to replace the DNA stain, ethidium bromide (EB), from the DNA-EB system, suggesting that they may intercalate into DNA. It is not clear whether such an interaction is responsible for the observed cytotoxicity.[102]

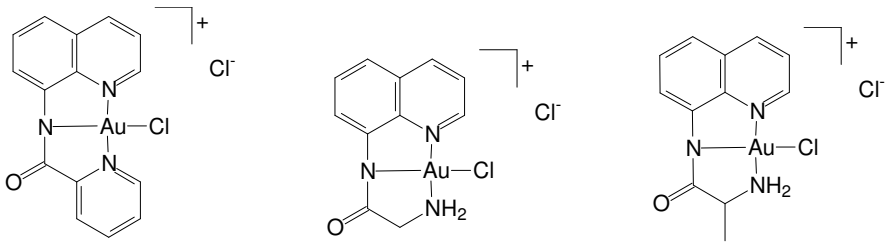

[Au(Quinpy)Cl]Cl [Au(Quingly)Cl]Cl [Au(Quinala)Cl]Cl

Figure 1.19: Gold(III) coordination compounds showing potential anti-tumour activity.

Chang-Tong Yang[108,109,110] and his group at the University of Singapore have studied 2-phenylpyridine gold(III) complexes (Figure 1.20) with, among others, a dithiolate ligand. These thiolate gold(III) complexes were found to be more stable than the similar dicarboxylate complexes. Their research included gold(III) complexes with chelated mono-anionic N–N$^-$ ligands (Figure 1.20). These compounds have shown some cytotoxicity.[108,109,110]

[109] D. Fan, C.T. Yang, J.D. Ranford, J.J. Vittal, P.F. Lee, *J. Chem. Soc., Dalton Trans.*, **2003**, 3376.
[110] D. Fan, C.T. Yang, J.D. Ranford, P.F. Lee, J.J. Vittal, *J. Chem. Soc., Dalton Trans.*, **2003**, 2680.

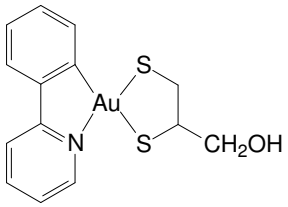

2-phenylpyridine gold(III) complex

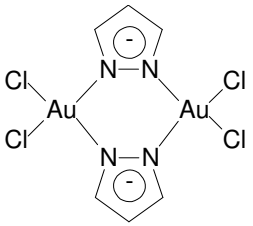

pyrozolide gold(III) complex

Figure 1.20: Compounds investigated by the group of Chang-Tong Yang.

In an attempt to find the physiological mode of action of gold(III) complexes, Messori[101] and his group at the University of Florence have taken representative gold(III) complexes and subjected them to numerous experiments to find the elusive mechanism of cytotoxicity. What they found was that the interactions of gold(III) complexes with the DNA double helix were generally weak, reversible and predominantly electrostatic in nature, suggesting that DNA is not the primary target for the cytotoxic effects of these complexes. Later experiments with bovine serum albumin as a general model for plasma proteins revealed different patterns of reactivity for the various compounds in relation to the specific chemical properties of the gold(III) complexes. In some cases close adducts were formed in which the bound gold(III) centres are probably coordinated to histidine residues at the surface of the protein. It was hypothesised that the ability of selected gold(III) complexes to tag either cysteine or histidine residues may result in specific damaging of crucial intracellular proteins, thus accounting for the relevant cytotoxic effects of these compounds.[101,111]

1.4.2 Silver Compounds in Medicine

Silver is neither toxic nor essential for human beings either as an element or in its complexed form and the human body normally contains no silver. However, for micro-organisms it is highly toxic, since silver(I) ions block the activity of thio-enzymes. Even traces of colloidal silver kill any germs present in water. Chronic ingestion of soluble silver compounds over long periods of time produces black

[111] G. Marcon, L. Messori, P. Orioli, M.A. Cinellu, G. Minghetti, *Eur. J. Biochem.*, **2003**, 270, 4655.

coloration of the skin, liver, kidneys, *etc.* as insoluble silver sulphide precipitates. The condition is known as *argyria*. When silver nitrate solution is dropped on the skin, it causes the skin to turn black.[41]

1.4.2.1 History

For thousands of years silver has been highly regarded as a versatile healing tool. In ancient Greece, Rome, Phoenicia and Macedonia silver was used extensively to control infections and spoilage. Hippocrates taught that silver healed wounds and controlled disease. Around 400 B.C. he listed as a singular treatment for ulcers "the flowers of silver alone, in the finest powder". Herodotus, a Dorian Greek historian, describes how the King of Persia carried with him boiled water in silver flagons to prevent sickness. In 69 B.C. silver nitrate was described in the contemporary Roman pharmacopoeia. Pliny the Elder, an ancient Roman nobleman, in his survey of the world's knowledge, states in Natural History (78 A.D.), Book XXXIII, Section XXXV, that the slag of silver "... has healing properties as an ingredient in plasters, being extremely effective in causing wounds to close up...".[112,113]

The popularity of medicinal silver developed from 702 A.D. to 980 A.D. throughout the Middle East where it was widely used and esteemed for blood purification, heart conditions and controlling halitosis. Paracelsus, an alchemist, physician, astrologer and general occultist (circa 1520), extensively incorporated silver in medical applications. Angelus Sala used silver nitrate to successfully treat chorea, *Tabes dorsalis* (syphilis), and "doubtably epilepsy". These silver salts were reported by Sala to occasionally cause the bluish hue of skin discoloration due to overuse (*Argyria*). It is widely thought that during the Middle Ages silver utensils and goblets contributed a bluish hue to the skin tone of the upper class, resulting in the term “royal blue bloods”. Plausibly the term “born with a silver spoon in his mouth” was coined during that time for the same reason as an attribute for describing the good fortune of health more than having wealth. These blue bloods were noted to have obtained a measure of protection from the rampant plagues common to Europe in those centuries. The use of silver to provide bacteria-free tableware, pacifiers and storage vessels has been

[112] http://www.oligodynamic.com/history.html
[113] http://www.silverlon.com/history.html

practiced throughout history. Today it is known that metallic silver will dissolve in water to the level of 5-10 mg/L and this water will therefore be toxic to *Escherichia coli* and *Bacillus typhosus*.[112,113]

Pioneers of the American West would often put a silver dollar into a jar or container of milk to help keep it fresh without refrigeration. They would drop silver and copper coins in their barrels of drinking water to combat bacteria and algae. During the wars with Napoleon the armies of Tsar Alexander used water casks lined with silver to clean drinking water from rivers and streams. This practice by the Imperial Russian army was common through World War I and continued to be incorporated by some units in the Soviet Army during World War II. Raulin recorded the first clinical description of the water-cleansing effect by silver in 1869. He observed that *Aspergillus niger* could not grow in silver vessels.[112]

The Swiss botanist von Nageli recorded one of the remarkable discoveries of the 19th Century in 1869. Von Nageli coined the term "oligodynamic" to describe the microbiocidal properties of a metal hydrosol (*e.g.* copper, silver and tin) at minute concentrations. Recent studies confirm that silver ions are active against bacteria at concentrations as low as one part per billion in pure water. Silver ions react rapidly with the walls of prokaryotic cells typical of micro-organisms, whereas the membranes of eukaryotic cells of mammals strongly resist any effect by silver.[112,113,114]

In 1884 the German obstetrician C.S.F. Crede[115] observed that there was a 79% relationship between blind children and maternal venereal disease. He subsequently introduced a prophylactic 1% silver nitrate eye solution for newborns for the prevention of ophthalmia neonatorum. Following its introduction the incidence of eye disease in newborns dropped to about 0.2%. His treatment was a milestone in clinical prophylaxis and became a government regulation throughout most of the world. By 1897 silver nitrate began to be used in America to prevent blindness in newborns and is still used today. By 1910 Henry Crookes had documented that certain metals, when

[114] N.R. Thompson, *Comprehensive Inorganic Chemistry*, Vol. 5, 28, Elmsford, N.Y.: Pergamon Press, **1973**.
[115] C.S.F. Crede, *Die Verhütung der Augenentzündung der Neugeborenen.*, Archiv für Gynäkologie, München, **1881**, 17, 50.

in a colloidal state, had strong germicidal action, but were harmless to human beings. The oligodynamic concept motivated the development of many anti-microbial processes and products.[112, 113]

1.4.2.2 Recent Developments in the Medicinal Applications of Silver Compounds

1.4.2.2.1 Silver in Anti-Microbial Treatment

During World War II Charles L. Fox,[116] a surgeon, observed that many soldiers died of uncontrolled bacterial infection in open wounds. He had long used silver nitrate as part of his medical practice, but it was far too aggressive with protein structures - limiting its clinical uses. His research at the Department of Surgery and Microbiology, College of Physicians and Surgeons, Columbia University, New York, led to the discovery of silver sulphadiazine (Figure 1.21).[117] This combination provided controlled release of silver ions in a wound along with an active antibiotic drug. Silver sulphadiazine provided a steady, long-term delivery of silver ions onto or into a wound. It is a dual antagonist: silver has the primary activity against pathogens but should an organism be sensitive to sulphonamids the sulphadiazine component will also be active. This dual function has been studied extensively and its effectiveness against a wide range of bacteria, fungi, extracellular viruses and protozoa has been proven.[112]

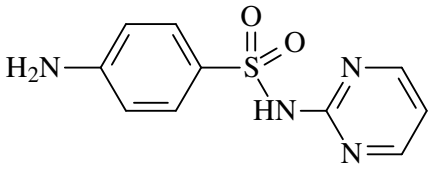

Figure 1.21: Sulphadiazine.

In the early 1970's, Drs. Becker, Marino and Spadaro[118] of the Veterans Administration Hospital in Syracuse, New York, pioneered the study of silver-coated

[116] C.L. Fox, *Patent no: EP0287204*, **1988**.
[117] N. Grier, *Disinfection, Sterilization and Preservation*, ed. Lea & Febiger, Philadelphia, **1983**, 380.
[118] R.O. Becker, J.A. Spadaro, A.A. Marino, *Clin. Orthop. Relat. Res.*, **1977**, 124, 75.

fabrics for the treatment of complex bone infections. Having studied with Dr. Becker, Dr. A.B. Flick began developing broader clinical applications for silver nylon fabrics in partnership with Dr. Becker during his Orthopaedic Surgery residency training at the University of Vermont.[119,120] Dr. Flick subsequently entered private practice and continued his research independently.[113]

During roughly the same time three other university centred research teams investigated the wound healing properties of silver plated fabrics after the application of an electrical potential. Dr. Alvarez,[121] at the Department of Dermatology, University of Miami, in 1985, studied the effect of electrically activated silver-coated fabrics on an animal model of skin wounds in pigs. Dr. Marino and Dr. Albright,[122] at the Department of Orthopedic Surgery, Louisiana State University, 1983 - 1986, studied the effect of electrically activated silver plated fabrics on chronic bone infections in humans. Dr. Chu and Dr. McManus,[123] at the Army Surgical Research Centre, Fort Sam, Houston, 1989 - 1996, studied the effect of electrically activated and non-electrically activated silver-coated fabrics on several animal burn wound models.[112,113]

Research initiated in the 1990's by the Chinese government through the Department of Materials Science and Engineering, Tsinghua University, Beijing, studied the reaction between bacteria and silver ions. Their goal was to develop an effective antiseptic that would sanitise almost any surface. They developed a silver/zircon phosphate complex that proved to be an excellent disinfectant with stable, long-term sterilisation effects. This silver complex maintained perfect safety with no toxicity to humans. The Science and Technology Ministry of China certified the new anti-microbial as a "National Key New Product". It is marketed as Concal PAg-40™.[112]

---

[119] R.O. Becker, A.B. Flick, *Patent no: US5814094*, **1998**.
[120] A.B. Flick, *Patent no: US6087549*, **2000**.
[121] O.M. Alvarez, P.M. Mertz, R.V. Smerbeck, W.H. Eaglstein, *J. Invest. Dermatol.*, **1983**, 81, 2,144.
[122] E.A. Deitch, A.A. Marino, V. Malakanok, J.A. Albright, *J. Trauma*, **1987**, 27, 301.
[123] C.S. Chu, N.P. Matylevitch, A.T. McManus, C.W. Goodwin, B.A. Pruitt Jr., *J. Trauma*, **2000**, 49, 115.

In the U.S., silver is being used as a broad-spectrum antiseptic in several commercial areas. For example, silver dihydrogen citrate (Axenohl) is an electrolytically generated compound that works well in combination with other compounds used as hard surface disinfectant for food contact surfaces, clinical work surfaces, medical disinfectant wipes and water treatment systems. The black polyvalent silver oxide, Ag_40_4, is a compound with two single-charged and two triple-charged silver atoms. It is a microbacidal compound effective against bacteria, yeast and mold. It is a safe, EPA (Environmental Protection Agency) approved, antiseptic compound. Tetrasil is an example of this oxide used in a bactericidal topical ointment. It is the best choice of silver compound currently available for sanitising acrylic hot tubs.[106,112]

1.4.2.2.2 Silver in Anti-Tumour Treatment

The use of silver compounds in pharmaceuticals has been hampered by their unfavourable chemical properties. Many silver(I) complexes are light sensitive and the insolubility of AgCl always presents a problem when silver compounds come into contact with physiological fluids. Over 100 silver compounds have been evaluated for anti-tumour activity by the National Cancer Institute (NCI) and only five have shown marginal activity.[6]

By slowing down the rapid-ligand exchange reactions common in silver(I) chemistry it seems likely that a silver complex could be designed that would not be precipitated by Cl^-. This might lead to *in vivo* anti-microbial and anti-tumour activity. Tetrahedral bisphosphine silver(I) complexes might be a good candidate to withstand physiological conditions.[6] This will be discussed further in Chapter 2 and 3.

1.5 CONCLUSION

As can be seen from the literature, silver and gold both have long histories as metals of worth, either as decoration or as bartering tool. Due to the interest in the properties of these metals, the rich chemistry of Group 11 transition metals and indirectly also the chemistry of related metals has been explored extensively.

The use of ligands to manipulate the properties of metal compounds and more specifically those of the transition metals is well known and documented. These ligands contain more often than not phosphorous and bidentate phosphine ligands have become common in metal complexation. The versatility of dppe, for example, to bind metal ions is enormous. Due to recent synthetic advances the incorporation of a hydrazine bridge instead of an ethane bridge has become possible. This small alteration gives new opportunities to manipulate the steric and electronic properties of these phosphines.

Gold and silver have long histories as medicinal tools, both in metaphysical and genuine medical applications. The research into the physical and biological properties of these two metals has yielded important medicinal drugs. The application of gold-based auranofin in the treatment of RA is well documented and recently gold-based anti-tumour drugs are becoming as effective as platinum-based anti-tumour drugs at treating cancer.[44] Silver is still seen to be superior in its use as anti-microbial agent. Silver complexes, however, are said to be physiologically too unstable to be used as anti-tumour drugs, but tetrahedral silver might hold the break-through required to stabilise the complexes sufficiently to enable them to reach the target site.

The anti-tumour properties of these two metals have recently come into the spotlight with the exploration of $[Au(dppe)_2]^+$ and $[Ag(dppe)_2]^+$ as potential anti-tumour agents. The cytotoxicity of these tetrahedral gold(I) and silver(I) compounds was found to directly relate to their lipophilic cationic nature. The lipophilic/hydrophilic balance was found to modulate cytotoxicity, bioavailability and cell uptake of the drugs. In this thesis the chemistry and anti-tumour properties of gold(I) and silver(I) complexes were investigated. To this effect the incorporation of hydrazine-bridged bisphosphines to further fine-tune the hydrophilic/lipophilic balance of tetrahedral gold(I) and silver(I) complexes was employed.

Chapter 2

Synthesis of Hydrazine-Bridged Ligands and Related Group 11 Transition Metal Complexes

2.1 INTRODUCTION

In this chapter the synthesis of bidentate phosphine ligands with a flexible backbone and the subsequent gold and silver complexes of these ligands will be discussed. The flexible backbone was provided by dimethyl or diethyl hydrazine. The addition of varied phosphine moieties served to introduce small variations in the electronic and steric properties of the ligand. The complexation of gold(I) and silver(I) to these ligands was aimed at providing a range of complexes with varied, yet related properties. The complexes were earmarked for anti-tumour activity tests and the results were expected to give insight into the structure/toxicity and structure/selectivity relationship of these complexes.

2.2 LIGAND SYNTHESIS

2.2.1. Ligand Precursor Synthesis

The synthetic route pioneered by Katti *et al.*[25] to produce bis(dichlorophosphino)-dimethylhydrazine (**2**) involved the treatment of 1,2-dimethylhydrazine dihydro-chloride with phosphorous trichloride (PCl_3) (Scheme 2.1). PCl_3 was used as both solvent and reactant and the mixture was refluxed for 36 hours to give $Cl_2PN(Me)N(Me)PCl_2$ (**2**) in 92% yield.[25]

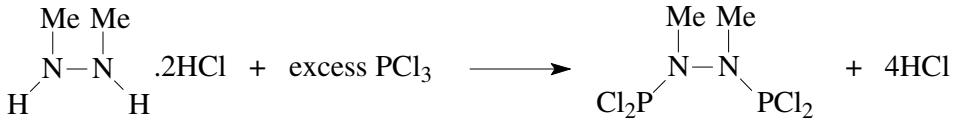

1 **2**

Scheme 2.1: Synthesis of bis(dichlorophosphino)dimethylhydrazine.

The ^{31}P NMR spectrum of the product (**2**) was in agreement with literature and consisted of a single peak at 160.2 ppm. The ^{1}H NMR spectrum of **2** consisted of a deceptively simple triplet centred at 3.15 ppm (J = 3.7 Hz), presumably due to virtual coupling of the methyl groups to the two phosphorous atoms. Katti *et al.*[25] had found that the high yield and the purity of **2** remained unchanged even when the reaction was carried out at a scale of up to 50 – 100 g, suggesting the feasibility of this reaction in large scale. The presence of two trivalent phosphorous centres in **2** presents the possibility of using this ligand as a electron donor toward transition metals. To prove this theory, Katti *et al.*[25] reacted **2** with (PhCN)2PdCl$_2$ and (COD)PtCl$_2$to produce the new metallocyclic compounds [(Cl$_2$PN(Me)N(Me)PCl$_2$)MCl$_2$] containing M = Pd(II) (**3**) or Pt(II) (**4**) centres. The determination of the molar mass of **3** and **4** in solution indicated them to be monomeric in solution. The ^{31}P NMR spectra of **3** and **4** in CDCl$_3$ revealed sharp singlets at 151.9 and 121.4 ppm, respectively. The downfield ^{31}P chemical shift of the free ligand **2** (160.2 ppm) as compared to the Pd(II), **3**, (151.9 ppm) and Pt(II), **4**, (121.4 ppm), complex has been noted earlier for a number of Pd(II)/Pt(II) complexes of R$_2$PN(R')PR$_2$.[24,25,36]

Employing a similar technique to that of Katti *et al.*,[25] Slawin *et al.*[29] were able to synthesise the analogous diphosphine, Cl$_2$PN(Et)N(Et)PCl$_2$ (Scheme 2.2), from the reaction of 1,2-diethylhydrazine dihydrochloride and phosphorous trichloride.

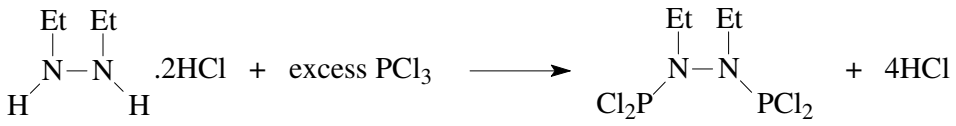

5 **6**

Scheme 2.2: Synthesis of bis(dichlorophosphino)diethylhydrazine.

This method employed the dropwise addition of PCl_3 to a finely ground sample of 1,2-diethylhydrazine dihydrochloride resulted in the formation of a viscous orange suspension. The reaction mixture was heated under reflux for 96 hours and excess PCl_3 was removed *in vacuo* to leave a viscous orange oil. Kugelrohr distillation of the crude product yielded **6** as a colourless oil in good yield (72%). The ^{31}P NMR spectrum of **6** showed a singlet at 156 ppm, an upfield shift of approximately 4 ppm compared to the value reported for $Cl_2PN(Me)N(Me)PCl_2$ by Katti *et al.*[25] Having successfully synthesised $Cl_2PN(Et)N(Et)PCl_2$, Slawin *et al.*[29] were able to use this compound as a precursor in nucleophilic substitution reactions and reactions with Grignard reagents to produce a range of aryloxy- and aryl-substituted phosphorous(III)hydrazides.[29]

Synthesis of ligand precursors (**2** and **6**) in our group was done in a similar manner to the synthetic routes pioneered by Katti *et al.*[25] and Slawin *et al.*[29] 1,2-dimethyl hydrazine dihydrochloride (**1**) or 1,2-diethylhydrazine dihydrochloride (**5**) were suspended in an excess of PCl_3. The reaction mixture was heated to reflux under argon and monitored by visual inspection until most of the starting material had been consumed, while formation of yellow oxidic side products was still minimal (between 8 and 48 hours). The excess PCl_3 was removed *in vacuo* and recycled. The resulting suspension of chlorophosphine and phosphorous oxides was treated with oxygen-free, dry ether. This led to the precipitation of all unreacted starting material and oxides. The ether was decanted from the solids and concentrated *in vacuo* to yield the products (**2** and **6**) in >95% yield as colourless to slightly yellow oils.

Katti *et al.*[25] also reported the synthesis of various metal complexes in which diphosphine derivatives of $Cl_2PN(Me)N(Me)PCl_2$ act as P, P' chelates.[19,25] Slawin *et al.*[29] later described the synthesis of metal complexes containing derivatives of $Cl_2PN(Et)N(Et)PCl_2$ acting as P, P' chelates as well as further examples involving derivatives of $Cl_2PN(Me)N(Me)PCl_2$.

2.2.2. Synthesis of Aryl-Substituted Bisphosphine Ligands

To demonstrate the versatility of $Cl_2PN(Et)N(Et)PCl_2$ (**6**) as a ligand precursor Slawin *et al.*[29] reacted **6** with four equivalents of RMgBr (R = Ph or CH_2Ph) in diethylether to

synthesise the diphosphines $Ph_2PN(Et)N(Et)PPh_2$ (**7**) and $(PhCH_2)_2PN(Et)N(Et)$-$P(CH_2Ph)_2$ (**8**) as colourless to pale yellow solids in good yields (70% and 74%, respectively) (Scheme 2.3).[29] This method had first been used by Katti *et al.*[25] to convert $Cl_2PN(Me)N(Me)PCl_2$ (**2**) to $Ph_2PN(Me)N(Me)PPh_2$ (**9**).

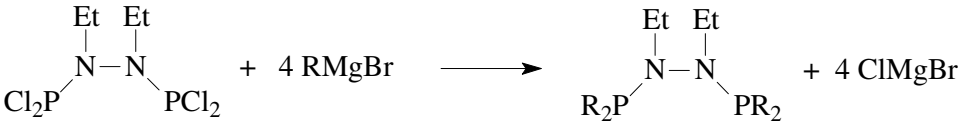

R = Ph (**7**), R = CH_2Ph (**8**)

Scheme 2.3: Synthesis of bis(phosphino)hydrazine ligands.

The ^{31}P NMR spectra of compounds **7** and **8** showed singlets at 64.2 ppm and 64.8 ppm, respectively.[29] This was in agreement with what Katti *et al.*[19] had found for the related compound **9** (^{31}P NMR 62.5 ppm).

Slawin *et al.*[29] also successfully synthesised a series of ligands containing phenyl groups with substituents in the *ortho* position (Scheme 2.4). Reaction of $Cl_2PN(Me)N(Me)PCl_2$ (**2**) with the Grignard reagent *o*-tolylmagnesium chloride, (2-Me)PhMgCl, or *o*-anisylmagnesium bromide, (2-MeO)PhMgBr, yielded $((2\text{-}Me)Ph)_2PN(Me)N(Me)P(Ph(2\text{-}Me))_2$ (**10**), and $((2\text{-}MeO)Ph)_2PN(Me)N(Me)P(Ph(2\text{-}OMe))_2$ (**11**), respectively, while the reaction of $Cl_2PN(Et)N(Et)PCl_2$ (**6**) with *o*-anisylmagnesium bromide generated $((2\text{-}MeO)Ph)_2PN(Et)N(Et)P(Ph(2\text{-}OMe))_2$ (**12**).

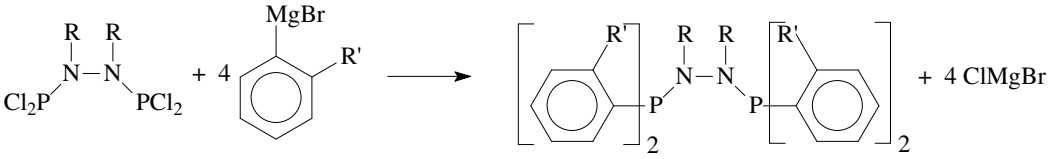

R = Me, R' = CH_3 (**10**);

R = Me, R' = OCH_3 (**11**);

R = Et, R' = OCH_3 (**12**);

Scheme 2.4: Synthesis of *ortho* substituted bis(phenylphosphino)hydrazines.

The ^{31}P NMR spectra of **10**, **11** and **12** showed singlets at 47.2, 42.6 ppm and 40.5 ppm, respectively. The $R_2PN(R')N(R')PR_2$ ligands described were all air-stable solids although the starting materials, **2** and **6**, hydrolysed rapidly in air.[29]

Six ligands were synthesised for our purposes. Three derivatives of each of the chloro-precursors $Cl_2PN(Me)N(Me)PCl_2$ (**2**) and $Cl_2PN(Et)N(Et)PCl_2$ (**6**) were synthesised. The addition of phenyl-, *p*-methoxyphenyl- or *N,N*-dimethyl-*p*-aminophenyl-groups to the phosphorous centres was hoped to yield a range of ligands characterised by small variations in their steric properties. The resulting ligands: i) bis(diphenylphosphino)dimethylhydrazine (**13**); ii) bis(diphenylphosphino)diethyl-hydrazine (**14**); iii) bis(di(*p*-methoxyphenyl)phosphino)dimethylhydrazine (**15**); iv) bis(di(*p*-methoxyphenyl)phosphino)diethylhydrazine (**16**); v) bis(di(*N,N*-dimetyl-*p*-aminophenyl)phosphino)dimethylhydrazine (**17**) and vi) bis(di(*N,N*-dimetyl-*p*-aminophenyl)phosphino)dimethylhydrazine (**18**) (Scheme 2.5) were conveniently synthesised using the corresponding bis(chlorophosphino)hydrazine and the appropriate Grignard reagent.

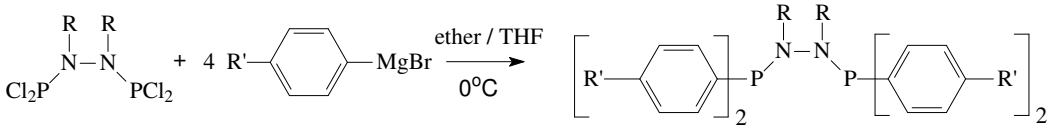

R = Me, R' = H (**13**); R = Et, R' = H (**14**);
R = Me, R' = OMe (**15**); R = Et, R' = OMe (**16**);
R = Me, R' = NMe_2 (**17**); R = Et, R' = NMe_2 (**18**);

Scheme 2.5: Syntheses of bisphosphine hydrazine ligands.

The reaction of the ligand precursors with the Grignard reagents in either diethylether, in the case of the phenyl Grignard reagent, or in THF, in the case of the remaining two Grignard reagents proceeded without any problems. The reactions were carried out by adding Grignard reagent drop-wise at 0 °C and stirring at 0 °C for a period of 4 hours, after which the reaction was left to reach room temperature overnight. The consecutive rapid addition of brine to the reaction mixture under argon led to two layers. The organic layer was subsequently removed by means of a separating funnel,

dried over anhydrous magnesium sulphate and removed *in vacuo* to yield the products **13** - **18** as sticky yellow semi-liquids in yields of 70 – 90%.

The ligands were found to be almost pure after work-up (>95% based on the ^{31}P NMR spectrum) and were shown to be sufficiently pure for further reactions. It was possible to further purify **14** through crystallisation from ether at –20 ^{o}C, while attempts to purify and crystallise the other 5 ligands were unsuccessful.

A comparison of the compounds in Table 2.1 shows that electron donor substituents in *ortho* position result in significant upfield shift (compounds **11** and **12**; ^{31}P NMR signals 42.6 ppm and 40.5 ppm, respectively) of the adjacent phosphorous atom, while substituents in the *para* position (compounds **15** and **16**; ^{31}P NMR signals 61.4 ppm and 61.0 ppm, respectively) hardly influence the ^{31}P-NMR spectroscopic shifts if compared to the unsubstituted derivatives **13** and **14** (^{31}P NMR signals 63.3 ppm and 63.4 ppm, respectively). This overall upfield shift of *ortho* substituted aryls at a phosphorous centre compared to other substituents has been described by Grim *et al.*[124] and is said to be attributable to a γ effect, described as an upfield contribution to the chemical shift caused by a substituents in the position γ to the nucleus in question.

[124] S.O. Grim, A.W. Yankowsky, *Phos. Sulf.*, **1977**, 3, 191.

No.	Methylhydrazine Compound	^{31}P NMR	No.	Ethylhydrazine Compound	^{31}P NMR
2	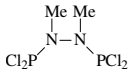	160.9 160.2[19]	**6**	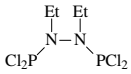	156.3 156.3[29]
13	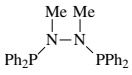	63.3 62.5[19]	**14**	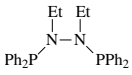	63.4 64.8[29]
10	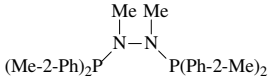	47.1[29]	**8**	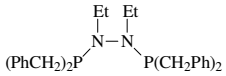	64.8[29]
11	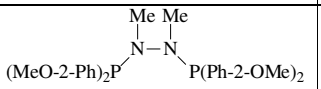	42.6[29]	**12**	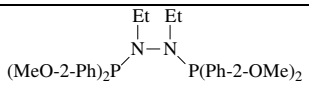	40.5[29]
15	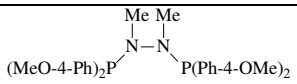	61.4	**16**	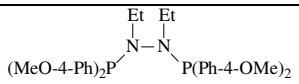	61.0
17	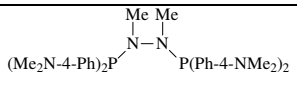	61.5	**18**	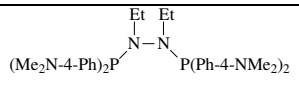	60.4

Table 2.1: ^{31}P NMR spectroscopic shifts of bisphosphine hydrazine ligands.

The functionality of the hydrazine bridge proved to have a profound impact on the stability of the ligand. The methylated hydrazine-bridged was markedly less stable when compared to the ethylated hydrazine bridge. While all three of the ethylated ligands were stable when kept under argon, two of the methylated ligands showed slow degradation even when kept under argon. Ligand **13** has been previously described as hygroscopic and was found to easily decompose unless the utmost care was taken.[19] Ligand **15** was more stable, but still showed degradation after prolonged periods of storage. Ligand **17** proved to be stable when stored under argon, but showed signs of decomposition in the presence of metal salts during complexation reactions. In sharp contrast to this behaviour ligand **14** in crystalline form showed prolonged stability even when kept in moist air.

2.2.3. Synthesis of Pyridyl-Substituted Bisphosphinohydrazine Ligands

The chemistry of water-soluble coordination compounds has received significant interest in the past few years, particularly in the area of biphasic catalysis.[125,126,127] Even though there is currently a large interest in this field, the lack of suitable water-soluble ligands is a serious bottleneck. The ligands synthesised for catalytic purposes may, however, be exploited for the use in the biochemical field where water solubility is a huge advantage in delivering biologically active metal centres to the desired site of activity. Bisphosphines containing a hydrazine bridge have also been reported to add solubility to these ligands as compared to their carbon analogues. When a hydrazine backbone is coupled with tertiary bisphosphines containing 2-, 3- and 4-pyridyl substituents the water solubility can be greatly enhanced. A small amount of pyridyl substituted phosphines are known and methods for their preparation, have more often than not, failed in the past.[125,128] Recent methods described by Berners-Price *et al.*[125] have been successful in synthesising a range of these ligands and thereby opening up the study of these kinds of ligands for applications not only in industry, but also in the biomedical field.

The synthesis of pyridyl-substitututed bisphosphines as developed by Berners-Price *et al.*[125] calls for the slow addition of 2-, 3- or 4-bromopyridine to a solution of butyl lithium and TMEDA (*N,N,N',N'*-tetramethylethylenediamine) in diethylether at –115 ^{o}C, followed by quenching with $Cl_2P(CH_2)_2PCl_2$. We applied the same method for the attempted synthesis of the analogous hydrazine-bridged pyridyl phosphine ligands with the only difference being that the quenching was carried out with $Cl_2PN(Et)N(Et)PCl_2$ instead of $Cl_2P(CH_2)_2PCl_2$. The reaction mixture was then stirred for 2 hours, allowed to warm to –80 ^{o}C over an 11 hour period, followed by warming to ambient temperature over a 3-4 hour period. Berners-Price *et al.*[125] found that the addition of TMEDA increased the reactivity of pyridyllithium towards the chlorophosphine precursor and low temperatures suppressed competitive addition or coupling reactions.[125]

---

[125] R.J. Bowen, A.C. Garner, S.J. Berners-Price, I.D. Jenkins, R.E. Sue, *J. Organomet. Chem.*, **1998**, 554, 181.
[126] W.A. Hermann, C.W. Kohlpainter, *Angew. Chem. Int. Ed.,* **1993**, 32, 1524.
[127] B.E. Hanson, *Coord. Chem. Rev.*, **1999**, 185, 795.
[128] G.R. Newkome, *Chem. Rev.*, **1993**, 93, 2067.

The synthesis of 2-, 3- and 4-pyridyl substituted diethylhydrazine-bridged bisphosphine ligands proved to be straightforward (Scheme 2.6). The ^{31}P NMR spectra of the crude reaction mixtures showed only one distinct phosphorous signal for bis(di(3-pyridyl-phosphino))-1,2-diethylhydrazine (**20**) and bis(di(4-pyridylphosphino))-1,2-diethyl hydrazine (**21**) ligands, respectively (Table 2.2). Bis(di(2-pyridylphosphino))-1,2-diethylhydrazine (**19**) seemed to produce moderate amounts of two other phosphorous containing side products. This could be circumvented by cooling the reaction mixture below –115 ^{o}C with liquid N_2 and thereby minimising the production of these side products.

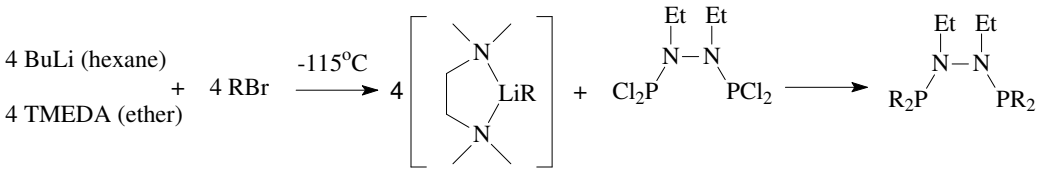

R = 2-pyridine (**19**), R = 3-pyridine (**20**), R = 4-pyridine (**21**)

Scheme 2.6: Synthesis of 2-, 3- and 4-pyridylphosphines.

Ligand	Nr.	^{31}P NMR
Bis(di(2-pyridylphosphino))-1,2-diethylhydrazine	**19**	60.1
Bis(di(3-pyridylphosphino))-1,2-diethylhydrazine	**20**	54.2
Bis(di(4-pyridylphosphino))-1,2-diethylhydrazine	**21**	53.6

Table 2.2: ^{31}P NMR spectroscopic shifts of pyridyl substituted diethylhydrazine bisphosphines.

The purification of the three ligands, however, proved to be problematic. ^{1}H-NMR spectroscopic investigation of the products after an aqueous work-up with brine (to remove Li-salts and polar side products) showed numerous signals in the ^{1}H-NMR spectrum indicative of a large number of impurities. Purification of the resulting organic phase by precipitation or crystallisation failed due to the similar solubilities of the product and the impurities. Various solvent extraction methods also lead to the decomposition of the ligands. Due to the instability of the ethylhydrazine bisphosphine ligands the methylhydrazine bisphosphine ligands were not attempted.

Unpurified ethylhydrazine bisphosphine ligands were therefore used in complexation reactions in the hope that the resulting complexes might be easier to purify. Broad ^{31}P NMR signals were observed for the complexes, accompanied by signals arising from the ligand and from various other phosphorous containing products. In most cases the complexation led to the formation of colloidal gold or silver. Efforts to try to precipitate the complexes led to the breakdown of the complexes into characteristic ligand fragments.

2.3 Gold Complexes

In the vast majority of its complexes gold(I) exhibits linear two coordination. As a consequence ligand exchange reactions occur rapidly *via* an associative mechanism and a three-coordinate transition state (Scheme 2.7). Facile ligand exchange reactions with thiols have been reported to play an important role in the anti-arthritic activity of many gold(I) compounds, but they may also bring about reduction in the cytotoxic potency of gold(I) phosphine complexes. It seems likely that tetrahedral gold(I) complexes containing chelated bisphosphine ligands are more stable with respect to ligand-exchange as this would require a dissociative mechanism (five-coordinated gold(I) species are unknown) (Scheme 2.8).[6]

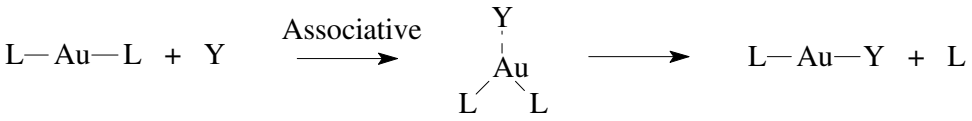

Scheme 2.7: Associative ligand exchange of linear gold(I).

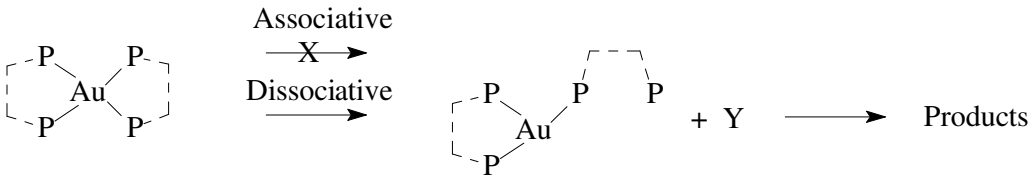

Scheme 2.8: Dissociative ligand exchange of tetrahedral gold(I).

The study of four-coordination and chelation have until recently been neglected in gold(I) chemistry. Early investigations describe examples of bisphosphine ligands as chelating ligands for gold(I), but even as recent as 1988, studies involving more

flexible bidentate phosphines did not report four-coordinate gold(I) complexes. In general the characteristic products were reported to have bridged digold or annular structures in which gold(I) was coordinated in a linear fashion. Complexes of the type $XAuPh_2P(CH_2)_nPPh_2AuX$ have been characterised for n = 1 to 12.[6]

In the early 1980's the existence of tetrakis(monophosphine)gold(I) complexes was established. ^{31}P NMR solution studies of monophosphine gold(I) complexes in the presence of free PR_3 demonstrated that complexes with different Au:P ratios underwent rapid ligand exchange. ^{31}P NMR studies of the bisphosphine-bridged digold complex $ClAuPh_2P(CH_2)_2PPh_2AuCl$ in the presence of free dppe demonstrated that the bischelated complex $[Au(dppe)_2]^+$ was present in solution at Au:P ratios as low as 1:1.5. Furthermore, the four-coordinated complex exhibited remarkably high kinetic stability.[6]

The complexation of gold(I) to the above bisphosphinohydrazine ligands to give bridged or tetrahedral complexes was straightforward. The use of either dimethylsulphidegold(I) chloride ($(Me_2S)AuCl$) or tetrahydrothiophenegold(I) chloride ((THT)AuCl) made no difference to the formation of the complexes as both sulphur containing ligands were easily displaced by the incoming phosphorous centres and both sulphur ligands could be removed *in vacuo*.

The synthesis of $ClAuPh_2PN(Me)N(Me)PPh_2AuCl$ (Figure 2.9, **22**) was achieved by suspending the gold(I) precursor in THF and adding the ligand (**13**) dissolved in dichloromethane (DCM). Preparing a solution of **13** in THF before adding it to the gold(I) precursor led, however, to the breakdown of the ligand. As soon as the two reagents were mixed a micro-crystalline precipitate formed, which could be separated by filtration. This micro-crystalline powder proved insoluble in a range of organic solvents including highly polar solvents like DMSO and DMF. The stability of the new gold(I) complex is in stark contrast to the lability of the ligand, that was discussed above. To slow down the formation of crystals, the reaction was carried out in DCM. This made it possible to analyse the complex by NMR spectroscopy before insoluble crystals could form. To grow crystals suitable for single crystal X-Ray analysis one or two drops of THF were added to the DCM solution, which over a period of five hours led to the formation of crystals.

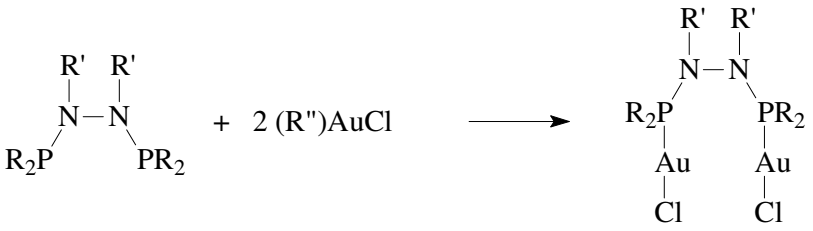

R = Ph; R' = Me; R" = THT or SMe_2 (**22**)

R = Ph; R' = Et; R" = THT or SMe_2 (**23**)

R = 4-PhOMe; R' = Me; R" = THT or SMe_2 (**24**)

R = 4-PhOMe; R' = Et; R" = THT or SMe_2 (**25**)

R = 4-PhNMe$_2$; R' = Me; R" = THT or SMe_2 (**26**)

R = 4-PhNMe$_2$; R' = Et; R" = THT or SMe_2 (**27**)

Scheme 2.9: Phosphine-bridged digold complexes.

Compound ClAuPh_2PN(Et)N(Et)PPh_2AuCl (Figure 2.9, **23**) was synthesised from the gold(I) precursor and ligand in THF. As soon as the reaction turned clear, stirring was halted and crystals big enough for single crystal X-Ray analysis formed overnight. Unlike crystals of complex **22**, crystals of complex **23** are soluble in both $CDCl_3$ and *d*-DMSO.

Complexes ClAu((4-MeO)Ph)$_2$PN(Me)N(Me)P(Ph(4-OMe))$_2$AuCl (Figure 2.9, **24**) and ClAu((4-MeO)Ph)$_2$PN(Et)N(Et)P(Ph(4-OMe)$_2$AuCl (Figure 2.9, **25**) were both synthesised by dissolving the gold(I) precursor in DCM and adding the corresponding ligand. The addition of a few drops of THF led to the growth of crystals suitable for use in single crystal X-Ray analysis. The presence of THF during the initial complexation led to undesirable side products as a result of breakdown of the ligand.

The synthesis of complex ClAu((4-Me_2N)Ph)$_2$PN(Me)N(Me)P(Ph(4-NMe_2))$_2$AuCl (Figure 2.9, **26**) was not successful due to breakdown of the ligand during complexation. Various combinations of solvents were tried in an attempt to facilitate the formation of the complex. The addition of the ligand to the gold(I) starting material consistently led to a change in colour from colourless to dark blue-purple. The dark blue-purple mixture was analysed by NMR for the presence of **26**, but due to

the complexity of the mixture, no positive identification could be made. It is interesting to note that the ligand itself is stable under argon, but the addition of any gold or silver compound led to the immediate breakdown of the ligand.

Complex ClAu(Me_2N-4-Ph)$_2$PN(Et)N(Et)P(Ph-4-NMe_2)$_2$AuCl (Figure 2.9, **27**), in contrast to its analogous methylhydrazine derivative, was formed in DCM as solvent with minimal breakdown of ligand. The reaction was done in the absence of THF, as this led to significant breakdown of ligand.

The four complexes i) [(Ph_2PN(Me)N(Me)PPh_2)$_2$ Au]$^+$.Cl$^-$ (Scheme 2.10, **28**); ii) [(Ph_2PN(Et)N(Et)PPh_2)$_2$ Au]$^+$.Cl$^-$ (Figure 2.10, **29**); iii) [((MeO-4-Ph)$_2$PN(Me)N(Me)P(Ph-4-OMe)$_2$)$_2$ Au]$^+$.Cl$^-$ (Figure 2.10, **30**) and iv) [((MeO-4-Ph)$_2$PN(Et)N(Et)P(Ph-4-OMe)$_2$)$_2$ Au]$^+$.Cl$^-$ (Figure 2.10, **31**) were synthesised in a similar manner. Two equivalents of ligand were dissolved in DCM and one equivalent of solid gold(I) precursor was then added. The rapid formation (within seconds) of the complex was accompanied by a slight darkening of the light yellow solution. All efforts to grow single crystals of these complexes failed. It was possible to obtain crystalline deposits of some of the complexes, but these turned out to be disordered lumps of crystalline material, which could not be analysed by single crystal X-Ray analysis.

R = Ph; R' = Me; R" = THT or SMe_2 (**28**)

R = Ph; R' = Et; R" = THT or SMe_2 (**29**)

R = 4-PhOMe; R' = Me; R" = THT or SMe_2 (**30**)

R = 4-PhOMe; R' = Et; R" = THT or SMe_2 (**31**)

R = 4-$PhNMe_2$; R' = Me; R" = THT or SMe_2 (**32**)

R = 4-$PhNMe_2$; R' = Et; R" = THT or SMe_2 (**33**)

Scheme 2.10: Bisphosphine gold complexes.

The synthesis of the complexes $[(((4\text{-}Me_2N)Ph)_2PN(Me)N(Me)P(Ph(4\text{-}NMe_2)_2)_2Au]^+.Cl^-$ (Scheme 2.10, **32**) and $[((Me_2N\text{-}4\text{-}Ph)_2PN(Et)N(Et)P(Ph\text{-}4\text{-}NMe_2)_2)_2Au]^+.Cl^-$ (Scheme 2.10, **33**) was accompanied by an unexpected phenomenon. Initially the reaction mixture of the complexes in THF after the addition of gold(I) precursor showed the characteristic yellow colour associated with complexes of this type, but upon stirring for prolonged periods the solution darkened and turned red. The same colour change was observed when the solvent was removed *in vacuo*. The yellow solid changed from yellow to red in the absence of any solvent while standing under an argon atmosphere. When doing the same reaction in DCM as solvent the colour change was observed to be markedly faster. Due to the breakdown of the methylhydrazine ligand upon complexation this effect could, however, not be studied. The ethylhydrazine ligand showed, as discussed above, greater stability and ^{31}P NMR studies showed that the colour change was accompanied by a shift in the phosphorous signal from 85.9 ppm to 96.5 ppm. These two signals seemed to reach an equilibrium when the signal intensities had reached a ratio of 1:2. This equilibrium ratio was reached after about 15 min in DCM or 40 min in THF and then remained constant for several days.

Efforts to crystallise complex (**33**) led to the crystallisation of a small amount of the corresponding bridged complex (**27**) as long colourless needles together with a crystalline precipitate showing a powder diffraction pattern. To facilitate the crystallisation of the bischelated complex, **33** was redissolved in DCM and the anion was exchanged from chloride to nitrate *via* a metathesis reaction with silver nitrate. This resulted in a dark brown solution from which red crystals suitable for X-ray crystallographic analysis could be grown.

The determination of the crystal structure revealed that the gold(I) centre in **33** had been oxidised to gold(III) (**34**) (Scheme 2.11). It is not clear whether the oxidation took place during the normal course of the reaction or during the metathesis reaction. However, the slow change of colour from yellow to red during the reaction and the subsequent downfield shift in the ^{31}P NMR spectrum from 84.9 ppm to 96.5 ppm, indicating further deshielding of phosphorous centres due to higher oxidation of gold ion, led us to believe that the slow oxidation of the gold centre from gold(I) to gold(III) took place during complex formation and not during methatesis. A small downfield shift has also been observed for $Ph_3PAu^{III}Me_3$ and $(Ph_3P)_2Au^{III}Me$ relative to $Ph_3PAu^{I}Me$, with ^{31}P NMR shifts of 1.11, 1.18 and 0.53, repectively.[43] This slow oxidation would thus also correspond to the colour change from yellow to red.

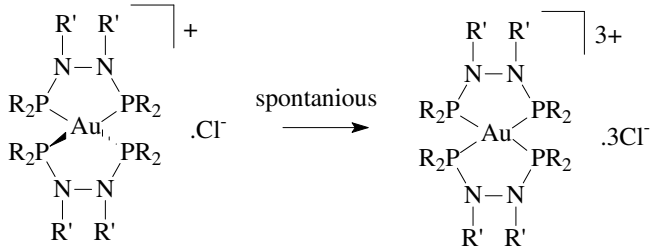

33 **34**

R = Ph-4-NMe_2; R' = Et

Scheme 2.11: Oxidation of gold(I) to gold(III).

The unexpected behaviour is not yet fully understood but may have to do with the fact that the bulky amino groups favour π-stacking in the square planar arrangement (Figure 2.1). The molecular structure of the trinitrate complex (**35**) was unfortunately

obtained at a late stage of the project, disallowing further investigations into the formation and the properties of the complex.

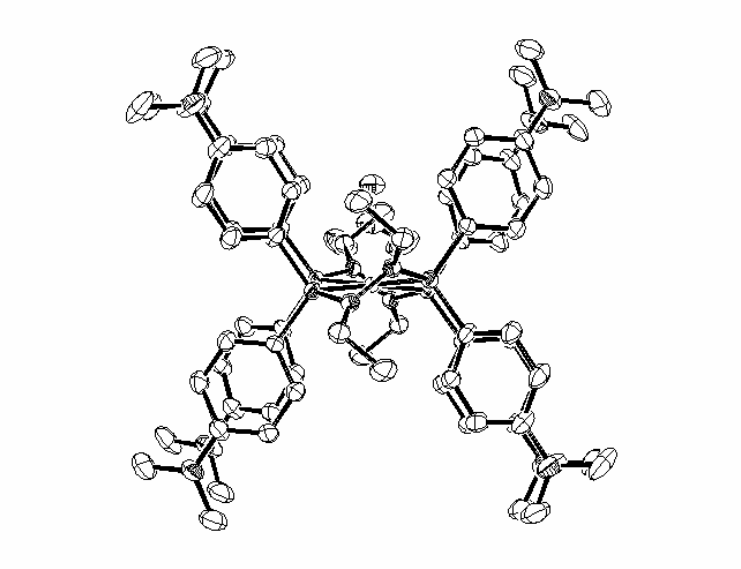

Figure 2.1: Crystal structure of **35** showing the distinct square planar configuration and π-stacking of phenyl rings.

Analysis of the ^{31}P NMR spectra of the gold complexes (Table 2.3) inidicates a general downfield shift of about 25 ppm for the metal complexes in comparison to the free ligands (Table 2.1). This can be rationalised if one takes into account the deshielding experienced by the phosphorous atoms due to the electron withdrawing nature of the metal cation. Generally the bridged gold(I) complexes show a marginal downfield shift compared to the bischelated derivatives. A similar effect is also observed (although more pronounced) in the analogous dppe gold complexes ClAu(dppe)AuCl (**36**, 27.1 ppm) and $[Au(dppe)_2]^+$ (**37**, 20.7 ppm).[129]

[129] S.J. Berners-Price, P.S. Jarrett, P.J. Sadler, *Inorg. Chem.*, **1987**, 26, 3074.

No.	Complex	^{31}P NMR	No.	Complex	^{31}P NMR
22	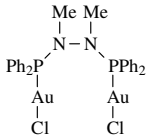	87.1	**28**	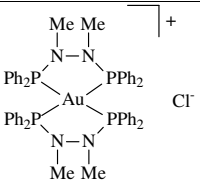	83.9
23	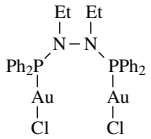	87.6	**29**	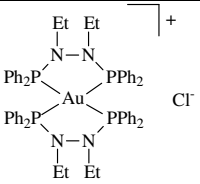	86.5
24	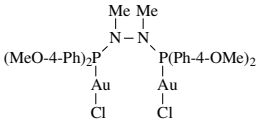	85.1	**30**	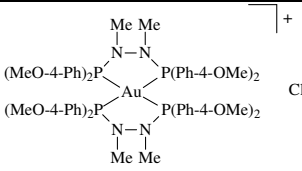	81.9
25	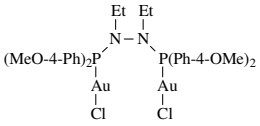	84.7	**31**	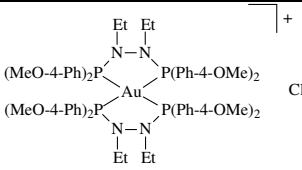	83.9
26	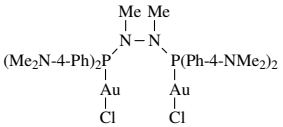	Unstable	**32**	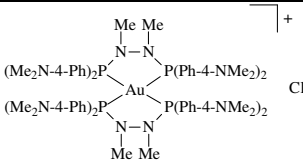	Unstable
27	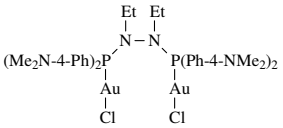	83.5	**33**	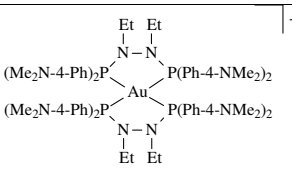	84.9

Table 2.3: ^{31}P NMR spectroscopic shifts of gold(I) complexes.

An exemplary titration of (THT)AuCl with ligand **14** indicated the stability of the bischelated gold(I) complexes (Figure 2.2) as previously shown for related gold(I) complexes. From bottom to top 0.5 equivalents of ligand **14** were added to (THT)AuCl. At a ratio of 0.5:1 the bridged complex **23** is formed as indicated by the broad singlet at 87.7 ppm together with a small amount of bischelated complex **29** as indicated by a singlet at 86.5 ppm. The broadening of the bridged gold complex signal is indicative of phosphorous ligand exchange on the NMR time scale, while **29** shows a sharp signal (no exchange at NMR time scale), implying that the bischelated complex is kinetically more stable. An unknown complex not found under normal reaction conditions is observed (triplet at 88.8 ppm, J = 68 Hz). This unknown complex is possibly attributable to the reverse addition of the gold precursor to the ligand in the NMR tube, making the [(P-P)Au(μ-(P-P)$_2$)Au(P-P)] complex formation possible (Figure 2.2). Already at a ligand:Au ratio of 1:1 bis-chelated complex becomes the predominat species. The unknown species once formed does not seem to dissappear, while at a ratio of 1.5:1 excess ligand is indicated by a peak at 63.3 ppm. The premature appearance of the residual ligand and bischelated species signals might be due to the removal of gold(I) centres by the unknown species formed in the first addition of ligand.

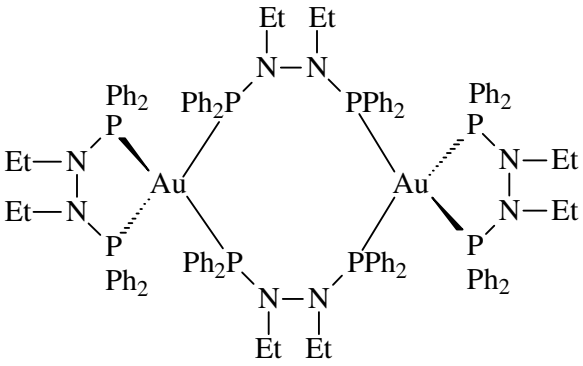

Figure 2.2: [(P-P)Au(μ-(P-P)$_2$)Au(P-P)] complex

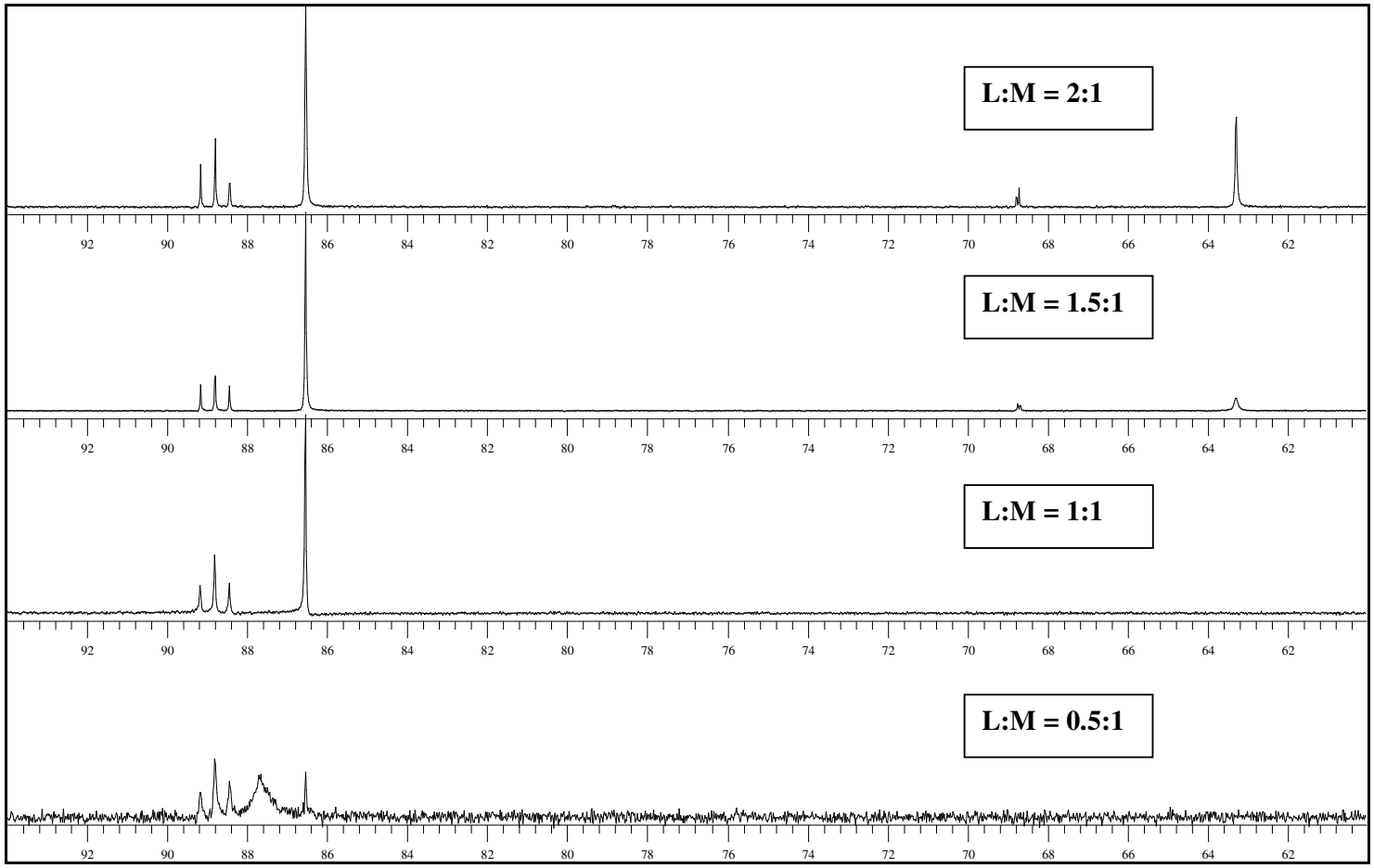

Figure 2.3: Titration of (THT)AuCl with ligand **14** (from top to bottom: 2:1; 1.5:1; 1:1; 0.5:1; ratios of ligand **14**:(THT)AuCl.

2.4 Silver Complexes

In contrast to the chemistry of gold(I), four-coordination is common for silver(I) phosphine complexes. This is often achieved by Ag-X-Ag bridges such as in Et_3PAgX which has a tetrameric cubane structure.[130] Linear coordination is generally only found with very bulky ligands and non-coordinating anions. Tetrakis monophosphine complexes can usually only be isolated with large non-coordinating anions. Halides generally bind to the metal with the exclusion of the fourth phosphine ligand. ^{31}P NMR studies have demonstrated the high kinetic lability of phosphines in $[Ag(PR_3)_4]^+$ complexes.[6]

Investigations of silver(I) complexes with bidentate phosphine ligands have been far less extensive. ^{31}P NMR studies have shown that the bridged dinuclear complex $(AcO)AgPh_2P(CH_2)_2PPh_2Ag(OAc)$ exists in $CDCl_3$ solution at a Ag(OAc):dppe ratio of 2:1, and the silver-phosphorous spin coupling is resolved only at low temperatures (<221 K). In contrast to this, at a ratio of 1:2 for Ag(OAc):dppe, two overlapping doublets (attributable to the unequal ^{31}P-^{107}Ag and ^{31}P-^{109}Ag coupling constants) are resolved at 300 K. The addition of excess dppe caused only slight broadening of the multiplet resonance and the appearance of a slightly broadened peak for free dppe, indicating a relatively slow exchange between free and bound ligand on the NMR time scale.[6]

It was found that many bischelated silver(I) phosphines showed enhanced kinetic and thermodynamic stability compared to monodentate phosphine complexes. $[Ag(dppe)_2]NO_3$ was reported to be stable in the presence of Cl^- and showed no light-mediated decomposition. Ligand exchange reactions with thiols appeared to be more thermodynamically favourable for $[Ag(dppe)_2]NO_3$ compared to the gold(I) analogue.[6]

The complexation of silver(I) to the hydrazine bisphosphine ligands proved to be more difficult than in the case of gold(I). Formation of the phosphine-bridged silver complex $(NO_3)AgPh_2PN(Me)N(Me)PPh_2Ag(NO_3)$ (**38**) could not be achieved due to

[130] M.R. Churchill, J. Donahue, F. Rotella, *Inorg Chem.*, **1976**, 15, 2752.

the breakdown of the ligand and the deposition of a silver mirror on the side of the reaction vessel. Various solvent systems were tried, yet all led to decomposition. The phosphorous signal of the complex could be identified in the ^{31}P NMR spectrum at 66.6 (dd, *J*=246.4 Hz, *J*=284.2 Hz) ppm but the product could not be isolated.

The complexes $(NO_3)AgPh_2PN(Et)N(Et)PPh_2Ag(NO_3)$ (**39**), $(NO_3)Ag((4\text{-}MeOPh)_2P\text{-}N(Me)N(Me)P(Ph(4\text{-}OMe))_2Ag(NO_3)$ (**40**) and $(NO_3)Ag((4\text{-}MeO)Ph)_2PN(Et)N(Et)\text{-}P(Ph(4\text{-}OMe))_2Ag(NO_3)$ (**41**) were synthesised by dissolving $AgNO_3$ in a few drops of acetonitrile and addition of a solution of the corresponding ligand in DCM. Care was taken to stop the reaction and remove solvent before the solution started turning brown and complex decomposition took place. We were fortunate to be able to crystallise complex **39** from a mixture of acetonitrile, EtOAc and hexane.

It was not possible to synthesise complex $(NO_3)Ag((4\text{-}Me_2N)Ph)_2PN(Me)N(Me)\text{-}P(Ph(4\text{-}NMe_2))_2Ag(NO_3)$ (**42**) due to the breakdown of ligand during complexation reminiscent of similar observations for the analogous gold complex. The complexation of $(NO_3)Ag((4\text{-}Me_2N)Ph)_2PN(Et)N(Et)P(Ph(4\text{-}NMe_2))_2Ag(NO_3)$ (**43**) was once again possible and was done according to the method described for **39** – **41**. The formation of the complex was accompanied by a colour change from colourless to dark blue.

The four complexes: i) $[(Ph_2PN(Me)N(Me)PPh_2)_2\ Ag]^+.NO_3^-$ (**44**); ii) $[(Ph_2PN(Et)\text{-}N(Et)PPh_2)_2\ Ag]^+.NO_3^-$ (**45**); iii) $[(((4\text{-}MeO)Ph)_2PN(Me)N(Me)P(Ph(4\text{-}OMe))_2)_2\ Ag]^+.NO_3^-$ (**46**) and iv) $[(((4\text{-}MeO)Ph)_2PN(Et)N(Et)P(Ph(4\text{-}OMe))_2)_2\ Ag]^+.NO_3^-$ (**47**) were synthesised in a similar manner. One equivalent of silver(I) nitrate was dissolved in a drop of acetonitrile, to which was added two equivalents of the corresponding ligand dissolved in DCM. The addition of the ligand in DCM led to the precipitation of finely divided $AgNO_3$. The complexation was complete within 30 minutes, *i.e.* after all solid silver nitrate was dissolved. All of the reaction mixtures turned colourless with progression of the reaction. While complex **44** proved to be unstable over time, it was stable enough to do some characterisation of the complex. It was possible to obtain crystals of complex **44** by performing the reaction in THF, reducing the volume and leaving the solution standing overnight.

It was not possible to fully characterise the complex [(((4-Me_2N)Ph)$_2$PN(Me)N(Me)P(Ph(4-NMe_2)$_2$)$_2$ Ag]$^+$.NO_3^- (**48**), due to the breakdown of ligand and deposition of a silver mirror during complexation. In contrast, the complexation of the related [(((4-Me_2N)Ph)$_2$PN(Et)N(Et)P(Ph(4-NMe_2)$_2$)$_2$ Ag]$^+$.NO_3^- (**49**) went smoothly and was done according to the method described for **44 - 47**. The formation of the complex was accompanied by a colour change from colourless to light brown.

Complexes of silver(I) showed similar trends than the gold(I) complexes with respect to their ^{31}P NMR data (Table 2.4). The upfield shifts of the silver complexes as compared to the ligand precursor is not as pronounced as that of gold, with a shift of only about 10 ppm for the bridged silver complex *vs* almost 25 ppm for the bridged gold analogues (*c.f.* Tables 2.3 and 2.4). A more noticeable difference can be seen between the bridged and bischelates, when compared to the similar effect observed for gold. A characteristic feature of these complexes was the interaction of the spin active isotopes ^{107}Ag and ^{109}Ag with ^{31}P resulting in a doublet for the bridged complex and a doublet of doublets for the bischelates (Figure 2.4). Studies by Berners-Price *et al.*[131,132] have shown a similar trend as evident by ^{31}P-NMR-signals for (AcO)Ag(dppe)Ag(OAc) (**50**) at 3.3 ppm and [Ag(dppe)$_2$]$^+$ (**51**) at 4.4 ppm *vs* the free ligand signal at -12.3 ppm. Berners-Price *et al.*[131] have found that the broad signals in **50** resolved into a complex multiplet upon cooling to 221 K, indicating the three combinations of ^{107}Ag and ^{109}Ag in the bridged species. Coupling constants of $^1J(^{109}Ag\text{-}^{31}P)$ = 757 Hz, $^1J(^{109}Ag\text{-}^{31}P)$ = 657 Hz and various smaller couplings were found for **50**. The bischelated silver(I) complex (**51**) showed well-resolved couplings with coupling constants of $^1J(^{109}Ag\text{-}^{31}P)$ = 266 Hz and $^1J(^{109}Ag\text{-}^{31}P)$ = 231 Hz. With the addition of excess ligand, a slight broadening was observed which is indicative of relatively slow exchange on the NMR time scale (>400s^{-1}) of free and bound dppe ligand.

[131] S.J. Berners-Price, C. Brevard, A. Pagelot, P.J. Sadler, *Inorg. Chem.*, **1985**, 24, 4278.
[132] S.J. Berners-Price, R.K. Johnson, A.J. Giovenella, L.F. Faucette, C.K. Mirabelli, P.J. Sadler, *J. Inorg. Biochem.*, **1988**, 33, 285.

No	Complex	^{31}P NMR	No	Complex	^{31}P NMR
38	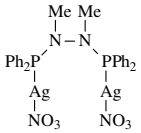	75.3 d *J*=764.2	**44**	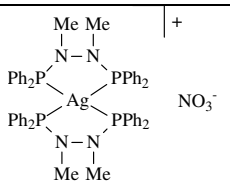	68.4 dd *J*=245.7 *J*=283.5
39	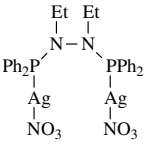	77.1 d *J*=782.9	**45**	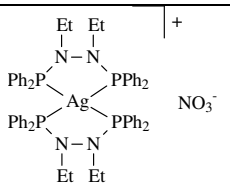	69.1 dd *J*=248.1 *J*=285.3
40	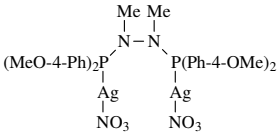	Unstable	**46**	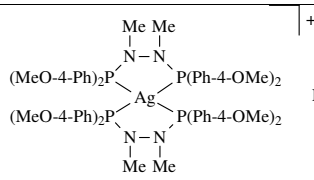	66.2 dd *J*=246.9 *J*=284.9
41	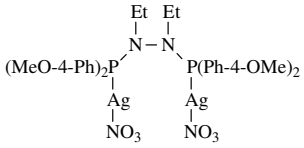	74.2 d *J*=834.2	**47**	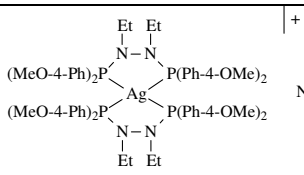	67.5 dd *J*=249.9 *J*=285.3
42	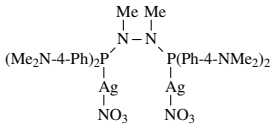	Unstable	**48**	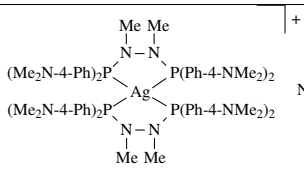	66.6 dd *J*=246.4 *J*=284.2
43	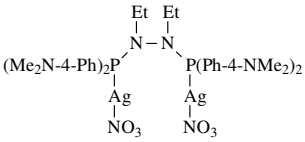	74.5 d *J*=819.6	**49**	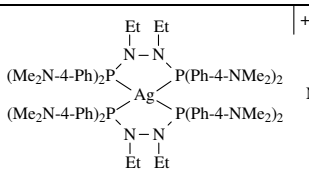	67.6 dd *J*=248.3 *J*=286.1

Table 2.4: ^{31}P NMR spectroscopic shifts of silver(I) complexes

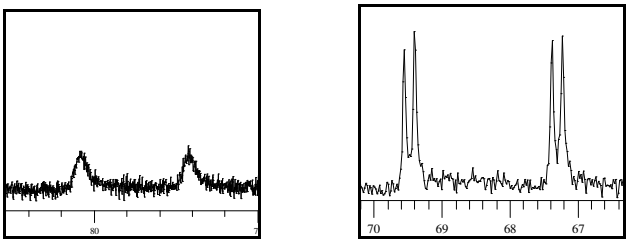

a **b**

Figure 2.4: ^{31}P NMR showing typical $^{107/109}$Ag–^{31}P interactions of bridged complex **39** (**a**) and bischelated complex **45** (**b**).

2.5 MOLECULAR STRUCTURES

2.5.1 Bis(diphenylphosphino)diethylhydrazine (14)

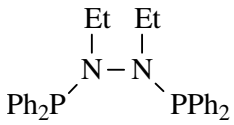

The molecular structure of bis(diphenylphosphino)diethylhydrazine (**14**) with the atom numbering scheme is shown below in Figure 2.7 and selected bond distances are in Table 2.5. Full data tables can be found in Appendix A.

14 was obtained as light yellow single crystalline flakes from the worked-up diethylether layer. The diethylether layer was concentrated and kept at –20 ^{o}C for 1-3 days. The supernatant was removed from the crystalline flakes and placed back in the freezer for further crystallisation.

The crystals of **14** (Figure 2.7) are found to be monoclinic, crystallising in the space group $P2_1/c$. Crystals of the dppe analogue show similar characteristics with it being monoclinic and crystallising in the space group $P2_1/n$.[133] Dppe has, however, an extra plane of symmetry in the centre of the compound and has two molecules per unit cell *vs* **14** having four per unit cell.

Dppe is seen to adopt a staggered conformation while **14**, in contrast, shows a *gauche* conformation. This *gauche* conformation adopted by hydrazine has been well documented and studied both experimentally and by *ab anitio* molecular modelling.[134] It was found that the ground-state geometry of hydrazine is *gauce* with a dihedral angle close to 90^{o}. *Ab initio* theoretical estimates of the *gauche-anti* and *gauche-syn* barrier heights fall in the ranges 1.6-6.2 and 9.7-13.7 kcal/mol, respectively. In hydrazine, the relative stability of the conformations are *gauche* > *anti* > *syn*.[134] The

[133] C. Perizzi, G Perizzi, *Acta Cryst.*, **1979**, B35, 1785.
[134] A.H. Cowley, D.J. Mitchell, M.H Whangbo, S. Wolfe, *J. Am. Chem. Soc.*, **1979**, 101, 18, 5224.

planar conformation of dppe also allows it to form stacks of molecules (Figure 2.5), that is not possible in **14** (Figure 2.6).

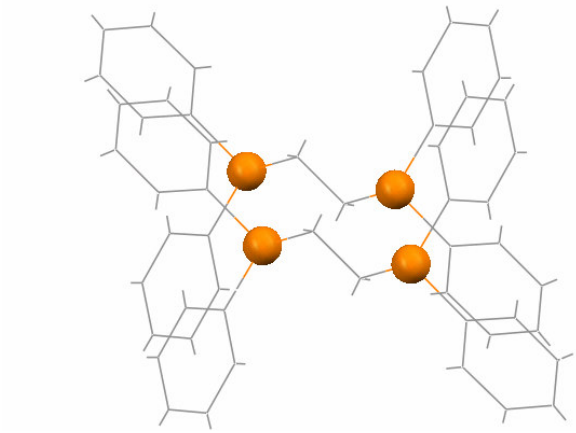

Figure 2.5: Mercury representation of dppe[135] showing parallel molecule packing.

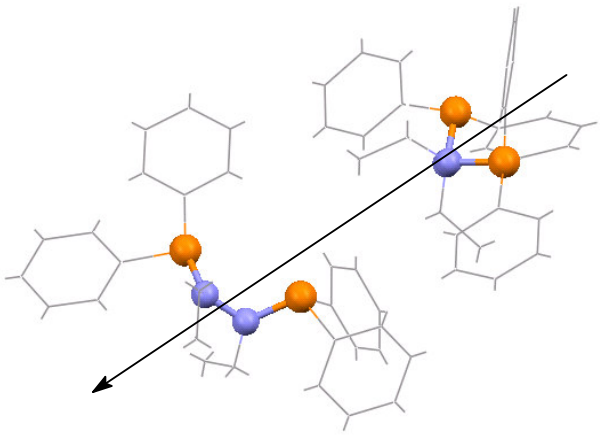

Figure 2.6: Mercury representation of **14** showing the perpendicular N-N bridges and head to tail packing (arrow).

Bond lengths and angles (Table 2.5) are in the typical range expected for P-N and P-C bonds.[26] A normal hydrazine N-N bond length of 1.427 Å is observed.

[135] DPPETH.cif file obtained from Cambridge Crystallographic Database.

Bond lengths [Å]		**Angles [°]**	
N(1)-N(2)	1.427(3)	N(2)-N(1)-P(1)	116.4(2)
N(1)-P(1)	1.710(2)	N(1)-N(2)-P(2)	118.4(2)
N(2)-P(2)	1.692(2)	**Torsion angle [°]**	
		P(1)-N(1)-N(2)-P(2)	-79.7(2)

Table 2.5: Selected bond lengths, angles and torsion angles for **14**.

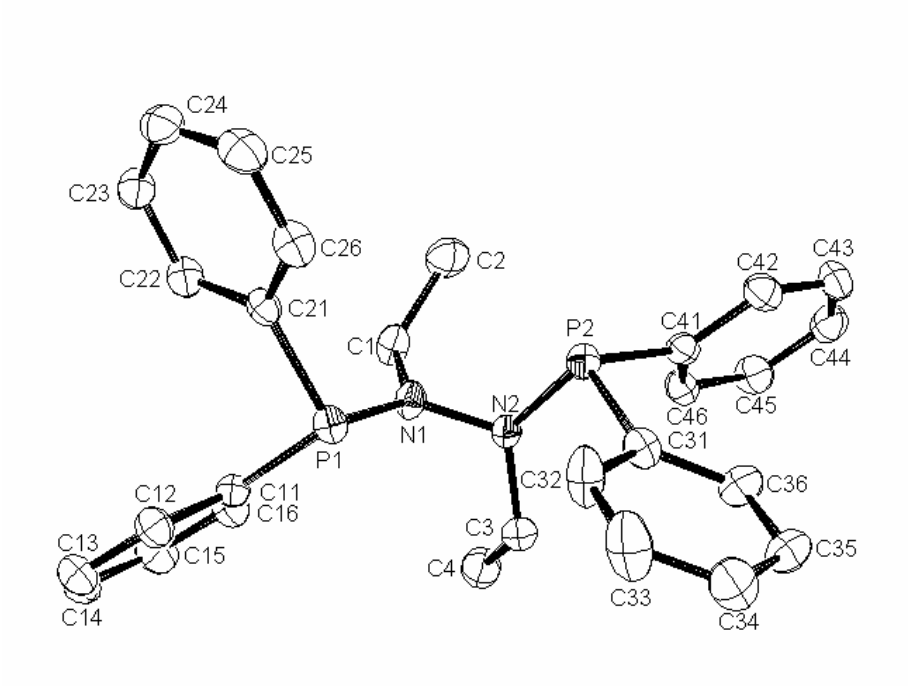

Figure 2.7: ORTEP diagram of **14** drawn at the 50 % probability level. Hydrogen atoms have been omitted for clarity.

2.5.2 Bis(phenylphosphino)cyclo-tetramethyldihydrazine (52)

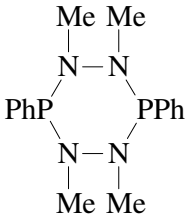

The molecular structure of bis(phenylphosphino)cyclo-tetramethyldihydrazine (**52**) with the atom numbering scheme is shown below in Figure 2.8 and selected bond distances are in Table 2.6. Full data tables can be found in Appendix A.

In an attempt to crystallise ligand **13**, bis(diphenylphosphino)dimethylhydrazine, the worked-up diethylether reaction mixture was concentrated and kept at –20 ^{o}C for two days. Two small crystals were formed and on analysis of one of the crystals, **52** was identified as the formed product. Analysis of the ^{31}P NMR of ligand **13** showed product **52** being present in less than 5 % in the sample. Further analysis of **52** was not attempted due to the small amount of this side product.

The compound crystallises in the orthorhombic crystal system, space group *Pbca*. The molecule has a centre of symmetry and the six-membered ring adopts a chair conformation with the phenyl groups on the phosphorous atoms being *trans* to each other (Figure 2.8). Katti *et al.*[26] have observed in related compounds (*e.g.* $[HNP(Et)N(Me)]_2$ and $[HNP(Ph)N(Me)]_2$), that the chair conformation was favoured over the boat conformation and was seen to readily crystallise. $[HNP(Ph)N(Me)]_2$ is found to also crystallise in space group *Pbca*, while $[HNP(Et)N(Me)]_2$, with the ethane substituent on the phosphorous, crystallises in a monoclinic crystal system, space group $P2_1/c$. Bond lengths and angles of **52** are, with values for N-N of 1.432 Å, P-N of 1.695 Å and P-C_{arom} of 1.841 Å (Table 2.6), in the range observed in related structures.

Bond lengths [Å]		**Angles [°]**	
N(1)-N(2)$^{\#}$1	1.432(2)	N(2)$^{\#}$1-N(1)-P(1)	120.94(9)
N(1)-P(1)	1.695(1)	N(1)$^{\#}$1-N(2)-P(1)	120.04(9)
Torsion angle [°]		N(1)-P(1)-N(2)	106.49(6)
P(1)-N(1)-N(2)$^{\#}$1-P(1)$^{\#}$1	-43.20	$^{\#}$*1 = -x, -y, -z*	

Table 2.6: Selected bond lengths, angles and torsion angles for **52**.

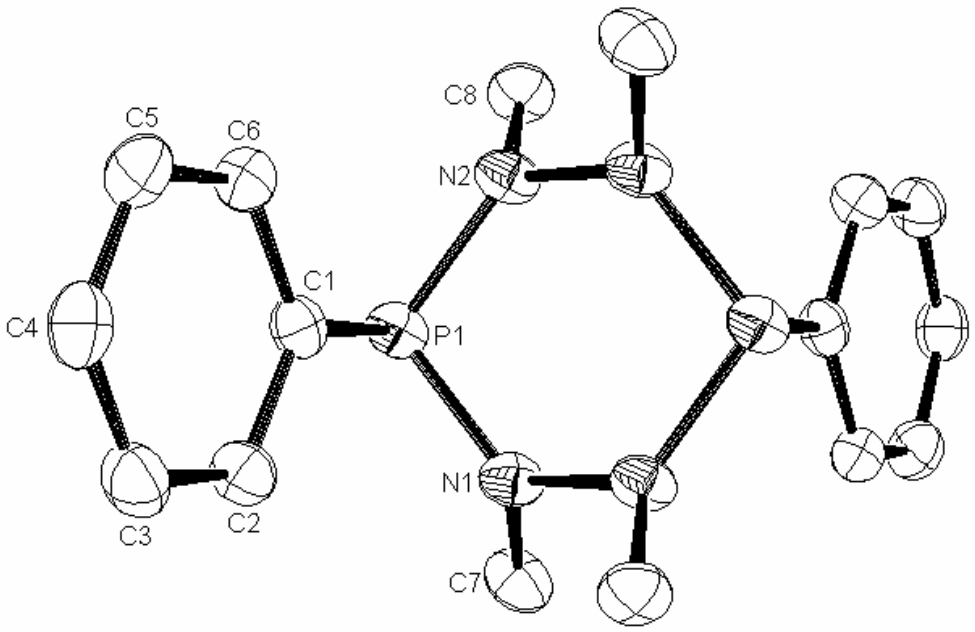

Figure 2.8: ORTEP diagram of **52** drawn at the 50 % probability level as viewed approx. perpendicular to N1-N2-N2$^{\#1}$-N1$^{\#1}$. Hydrogen atoms have been omitted for clarity.

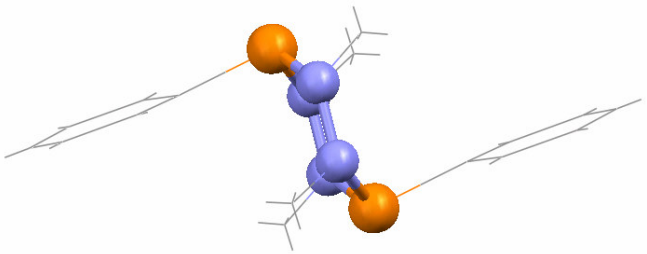

Figure 2.9: Mercury representation of **52** showing chair conformation.

2.5.3 Bisphosphine-Bridged Gold Complexes

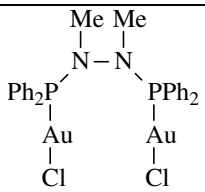	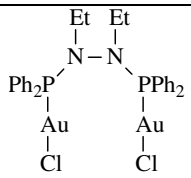
Bis(diphenylphosphino)dimethylhydrazine di(gold chloride) (**25**)	Bis(diphenylphosphino)diethylhydrazine di(gold chloride) (**26**)
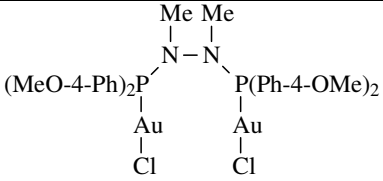	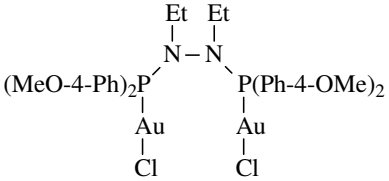
Bis(di(4-methoxyphenyl)phosphino)-dimethylhydrazine di(gold chloride) (**27**)	Bis(di(4-methoxyphenyl)phosphino)-diethylhydrazine di(gold chloride) (**28**)
Crystal structure was not obtained	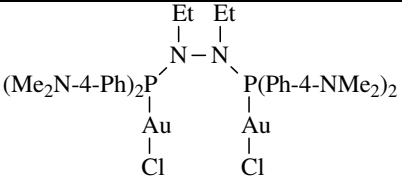
Bis(di(*N,N*-dimetyl-4-aminophenyl)-phosphino)dimethylhydrazine di(gold chloride) (**29**)	Bis(di(*N,N*-dimetyl-4-aminophenyl)-phosphino)diethylhydrazine di(gold chloride) (**30**)

Table 2.7: Crystal structures of bisphosphine-bridged gold complexes.

The molecular structures of bis(diphenylphosphino)dimethylhydrazine di(gold chloride) (**22**), bis(diphenylphosphino)diethylhydrazine di(gold chloride) (**23**), bis(di(4-methoxyphenyl)phosphino)dimethylhydrazine di(gold chloride) (**24**), bis(di(4-methoxyphenyl)phosphino)diethylhydrazine di(gold chloride) (**25**) and bis(di(*N,N*-dimetyl-4-aminophenyl)phosphino)diethylhydrazine di(gold chloride) (**27**) with the atom numbering schemes are shown below in Figures 2.10 – 2.14 and selected bond distances are compared in Table 2.8. Full data tables can be found in Appendix A.

Micro-crystals of **22** were obtaines when 0.5 equivalents of **13** dissolved in DCM was added to 1 equivalent of the gold(I) precursor suspended in THF. To slow down crystal formation and grow crystals of suitable size the reaction was done in DCM and, to initiate crystallisation, a drop of THF was added and the solution left overnight. On the other hand, crystals suitable for analysis of **23** spontaneously grew upon mixing 1 equivalent of gold(I) precursor and 0.5 equivalents of **14** in THF.

Complexes **24** and **25** were obtained in a similar manner to complex **22**. 0.5 equivalents of the corresponding ligand, **15** or **16**, dissolved in DCM were added to 1 equivalent of gold(I) precursor dissolved in DCM. Crystal formation was initiated by the addition of a drop of THF after which the solution was left for 2 days at room temperature.

Needle-like colourless crystals of **27** were isolated from the attempted crystallisation of the red coloured **33** (see below). Attempts at crystallising complex **27** by any other means were not successful due to the breakdown of the complex and ligand.

Even though the five complexes crystallise in different space groups, all the complexes, with the exception of complex **27**, exhibit a two-fold rotation axis. Complex **22** crystallises in the tetragonal crystal system, space group $P4_12_12$, complex **23** in the orthorhombic space group *Pccn*. Complexes **24** and **25** both crystallise in the monoclinic crystal system, space group *C*2/*c*, and **27** crystallises in the monoclinic system with space group $P2_1/c$. The crystal structures of complexes **23**, **24** and **25** all include a THF molecule. This inclusion might be the key to the ease of crystallisation of these crystals as these complexes spontaneously crystallise in THF. While complex

22 also spontaneously crystallises from THF it does not include THF in the crystal. Complex **27** includes one disordered molecule of DCM into the structure.

The term 'aurophilicity' was introduced in 1989 to describe phenomena in the structural chemistry of gold which could not be readily rationalised by conventional concepts of chemical bonding. Gold shows a clear preference not only for short and strong bonds, suggesting a small atomic/ionic radius and a high electronegativity, but also for small coordination numbers.[46,136,137]

The most striking phenomenon in the structural chemistry of gold is the tendency of the low-coordinate compounds of gold(I) to associate into dimers, oligomers or even uni- and multi-dimensional polymers *via* direct gold-gold contacts.[46,138] The metal atoms approach each other to an equilibrium distance of between 2.7 and 3.4 Å. This range includes the distance between gold atoms in gold metal.[59,136]

The Au-Au distances of complexes **23**, **24**, **25** and **27** (Figures 2.11, 2.12, 2.13 and 2.14) are 3.131 Å, 3.122 Å, 3.141 Å and 3.186 Å, respectively and are clearly in the range of aurophilic interactions while the Au-Au distance of 3.482 Å in complex **22** (Figure 2.10) is slightly too long for a true aurophilic interaction (normally 2.7 – 3.4 Å).[41]

A direct comparison of these complexes and the analogous dppe complex; ClAu(dppe)AuCl (**36**) shows that the preference for the *gauche* conformation of the hydrazine backbone (as discussed for **14**) may explain the observed intramolecular Au-Au interactions as compared to the intermolecular Au-Au interactions observed in the two polymorphs of **36**. The formation of intermolecular Au-Au interactions between dimers of **36** may be attributed to the different conformation of the ethyl backbone as illustrated by the torsion angles of the two polymorphs (-18.6 ^{o} and

[136] H. Schmidbaur (ed.), *Gold: Progress in Chemistry, Biochemistry and Technology*, J. Wiley & Sons, Chichester, **1999**.
[137] H. Schmidbaur, *Gold Bull.,* **2000**, 33, 3.
[138] (a) H. Schmidbaur, *Gold Bull.*, **1990**, 23, 11; (b) H. Schmidbaur, *Chem. Soc. Rev.*, **1995**, 24, 391.

50.7 °).[139] Intermolecular Au-Au contacts are also observed for the analogous ClAu(dppen)AuCl complex (dppen = bis(diphenylphosphino)ethene), where the ethene bridge is constrained to a *cis* conformation by the double bond. This observation supports the argument that the geometry of the ligands may at least partially determine the geometry of the complex.

In all complexes gold(I) forms almost linear complexes with P-Au-Cl angles of between 175.68 ° and 179.22 ° (Table 2.9). N-N bond lengths between 1.405 Å and 1.43 Å, similar to compounds **14** and **52**, are observed as well as P-N bond lengths between 1.67 - 1.710 Å and P-C_{arom} lengths of 1.76 Å - 1.84 Å. The Au-P and Au-Cl bonds are similar to those reported for other phosphinogold(I) chloride complexes with slightly shorter Au-P bond lengths (2.224 Å - 2.239 Å) than Au-Cl bond lengths (2.291 Å - 2.313 Å).[139,140]

[139] D.S. Eggleston, D.F. Chodosh, G.R. Girard, D.T. Hill, *Inorg. Chim. Acta*, **1985**, 108, 221.
[140] P.A. Bates, J.M. Waters, *Inorg. Chim. Acta*, **1985**, 98, 125.

Compound	14	22	23	24	25	27
Bond lengths [Å]						
Au-Au		3.487	3.131(5)	3.122(7)	3.141(7)	3.19(1)
Au-P		2.232(2)	2.233(1)	2.224(1)	2.227(1)	2.238(5) 2.239(6)
Au-Cl		2.298(2)	2.302(1)	2.291(1)	2.294(1)	2.313(5) 2.313(7)
P-N	1.710(2) 1.692(2)	1.702(5)	1.679(3)	1.678(2)	1.685(3)	1.68(2) 1.67(2)
N-N	1.427(3)	1.43(1)	1.416(6)	1.417(4)	1.405(6)	1.43(2)
Angles [°]						
P-Au-Cl		176.34(6)	179.22(4)	175.68(3)	175.99(4)	176.6(2) 175.9(3)
N-N-P	116.4(2) 118.4(2)	113.3(5)	118.4(3)	115.7(2)	117.5(2)	119(1) 118(1)
Torsion angle [°]						
P-N-N-P	-79.7(2)	-114.13	98.61	105.97	-101.14	-96.4
Symmetry operator		-x + 1, -y + 1, -z + 1/2	-x + 3/2, -y + 1/2, z	-x + 1, y, -z + 1/2	-x + 1, y, -z + 3/2	

Table 2.8: Selected bond lengths, angles and torsion angles for free ligand **14** and complexes **22**, **23**, **24**, **25** and **27**.

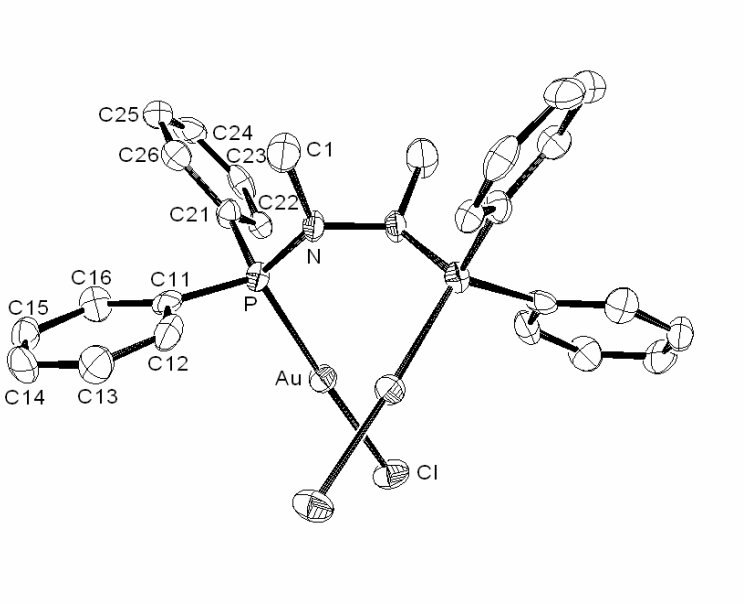

Figure 2.10: ORTEP diagram of **22** drawn at the 50 % probability level as viewed down the c-axis. Hydrogen atoms have been omitted for clarity.

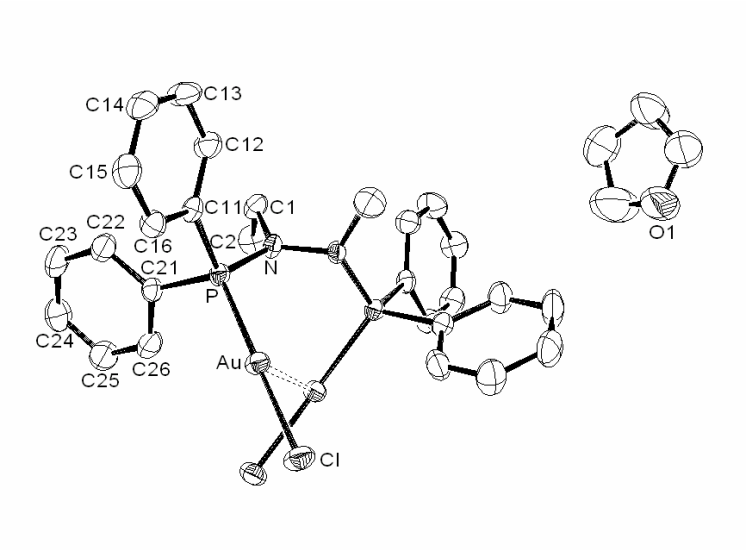

Figure 2.11: ORTEP diagram of **23** drawn at the 50 % probability level as viewed down the b-axis. Hydrogen atoms have been omitted for clarity.

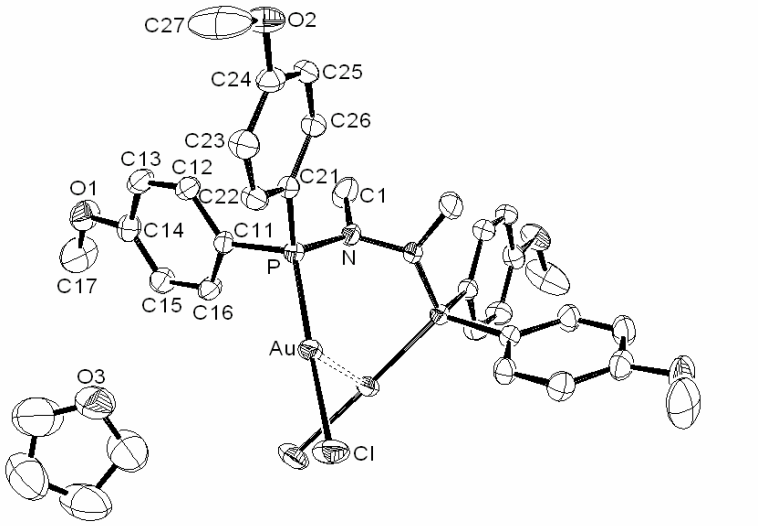

Figure 2.12: ORTEP diagram of **24** drawn at the 50 % probability level. Hydrogen atoms have been omitted for clarity.

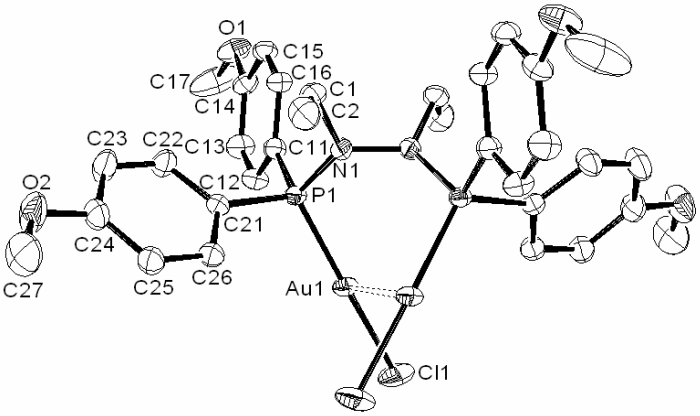

Figure 2.13: ORTEP diagram of **25** drawn at the 50 % probability level. Hydrogen atoms and a molecule of THF have been omitted for clarity.

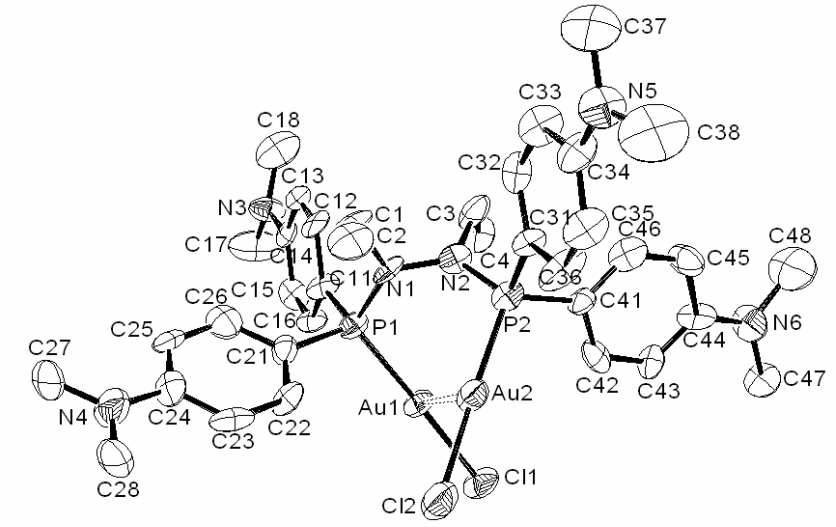

Figure 2.14: ORTEP diagram of **27** drawn at the 50 % probability level. Hydrogen atoms and a disordered molecule of DCM have been omitted for clarity.

The insolubility of complex **22** in both non polar and highly polar solvents once crystallised may be a result of the tightly packed parallel helixes, that are formed in the solid state (Figure 2.15). While the complex readily crystallises from THF it does not include THF in the structure as complexes **23**, **24** and **25** do. This structure exhibits a left-handed α-helical packing down the c-axis. This unique packing results in parallel helixes that have no voids large enough to include solvent (Figure 2.16) and leads to a stabilising short contact distance of 2.899 Å between Cl and H(15).

Complex **23** exhibits columns of head-to-tail complexes forming channels filled with THF. Intermolecular short contacts of 2.822 Å and 2.835 Å are displayed between Cl and H(1a) and Cl and H(14), respectively. The Cl-H(1a) interaction can be seen on the head-to-tail arranged complexes in a column between chlorides and adjacent hydrogen atoms situated on the ethyl substituted hydrazine bridge (Figure 2.17). The Cl-H(14) interaction occurs between chlorides and hydrogens situated on a phenyl ring in close proximity. Hydrogen bonding distances between the THF O(1) atom and H(1b) and H(22) are observed to be 2.553 Å and 2.698 Å, respectively.

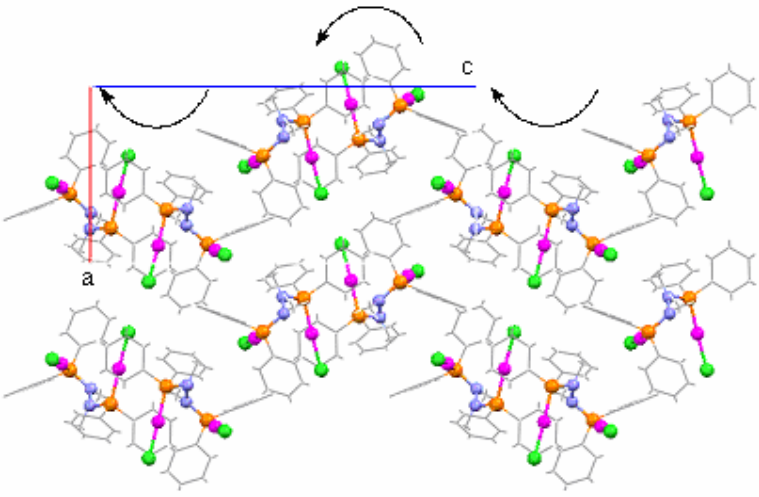

Figure 2.15: Mercury representation of **22** packing viewed along the b-axis showing left handed α-helical packing (arrows).

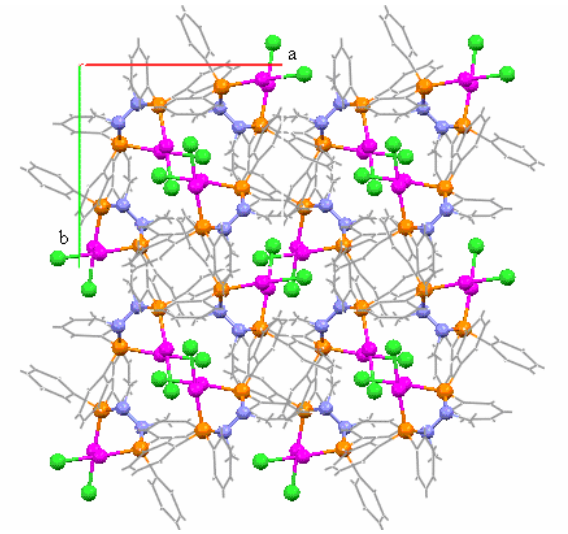

Figure 2.16: Mercury representation of **22** viewed along the c-axis showing tightly packed α-helices.

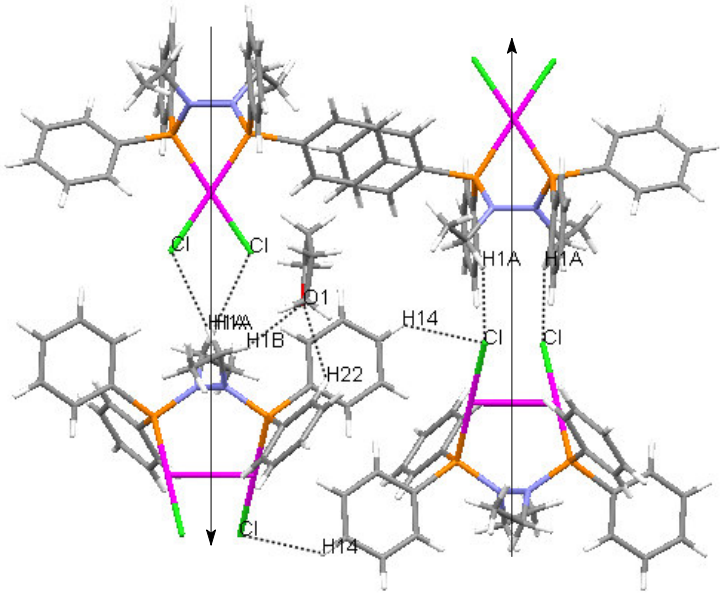

Figure 2.17: Mercury representation of **23** showing head-to-tail arrangement (arrow), H-Cl and H-O interactions (dotted line).

Complexes **24** and **25**, like **23**, show intermolecular short contacts of 2.892 Å between Cl and H(1c) for **24** and 2.817 Å between Cl and H(1b) for **25**. This interaction can be seen in the head to tail arranged compounds in a column down the b-axis between chlorides and adjacent hydrogen atoms situated on the methyl and α-carbon of ethyl substituted hydrazine bridge, respectively (Figure 2.18). Hydrogen bonding distances between THF (O(3)) and **24** (H(15) and H(17b)) are observed to be 2.608 Å and 2.557 Å, respectively and 2.667 Å and 2.555 Å for O(3) to H(15) and H(17b) in **25**. Other intermolecular hydrogen bond lengths of 2.629 Å and 2.637 Å are observed between O(1) and H(13) in **24** and O(1) and H(13) in **25**, respectively.

While ligand **14** and complex **23** showed alternating N-N bridges in a head-to-tail arrangement, complexes **24** and **25** show parallel N-N bridges. The complexes also showed corrugated sheets of complexes with inter-dispersed THF molecules (Figure 2.19).

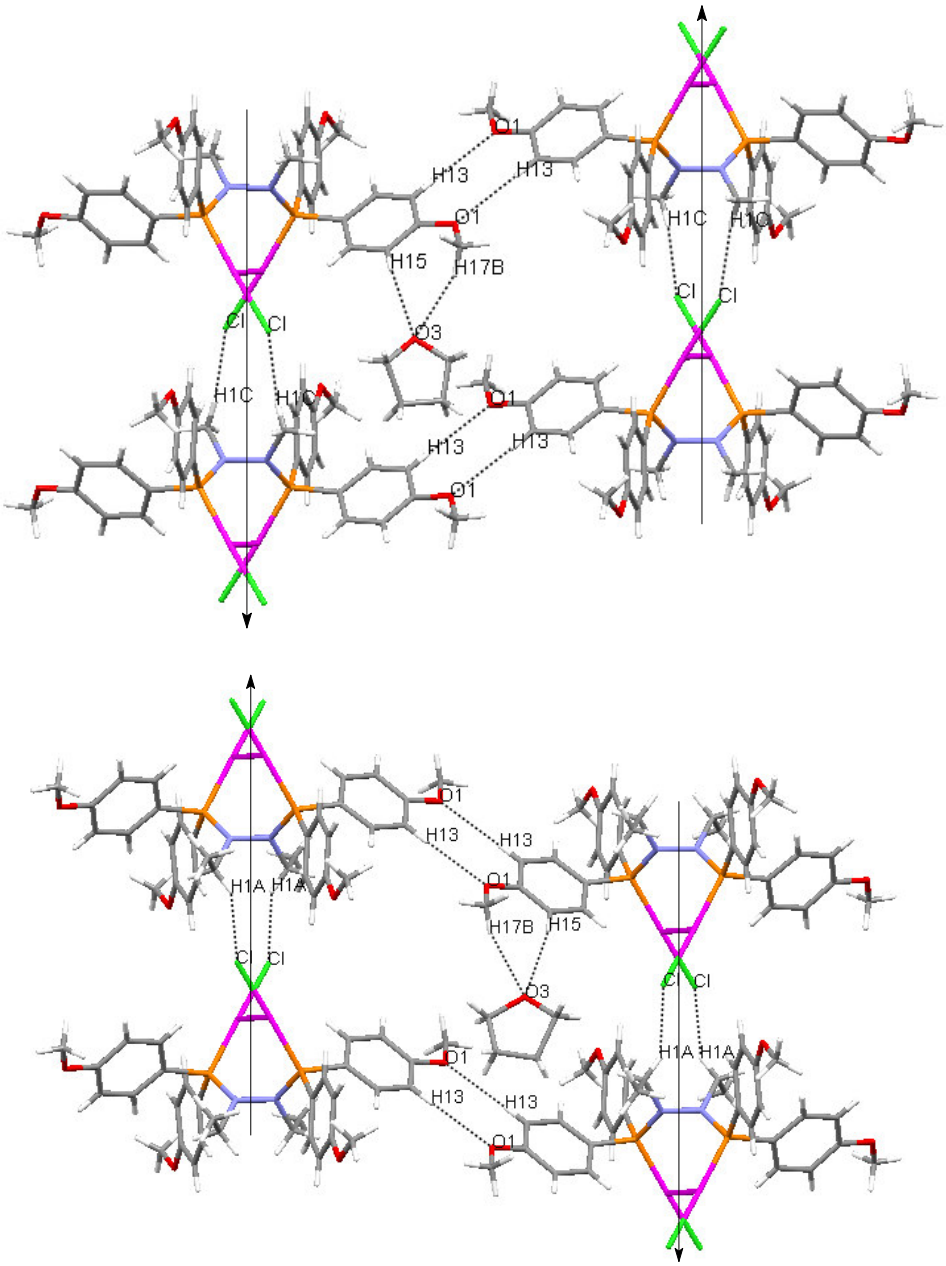

Figure 2.18: Mercury representation of **24** (above) and **25** (below) showing head-to-tail arrangement (arrows), H-Cl and H-O interactions (dotted lines).

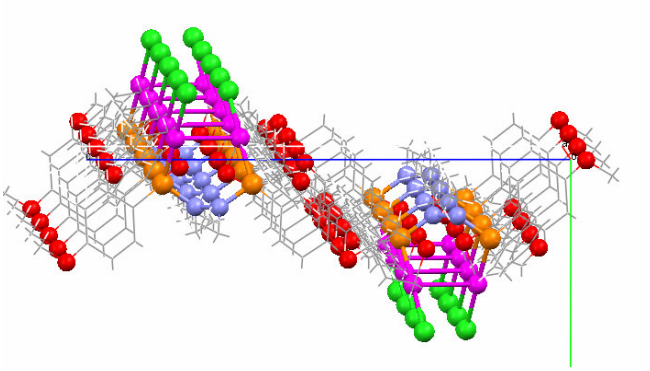

Figure 2.19: Mercury representation of corrugated sheets present in complexes **24** and **25**.

Complex **27** is seen to have intermolecular short contacts of 2.888 Å and 2.844 Å between Cl(2) and H(48c) and Cl(2) and H(38a), respectively (Figure 2.20). An interesting observation to note is that only one of the chloride atoms (Cl(2)) shows any H-Cl interaction.

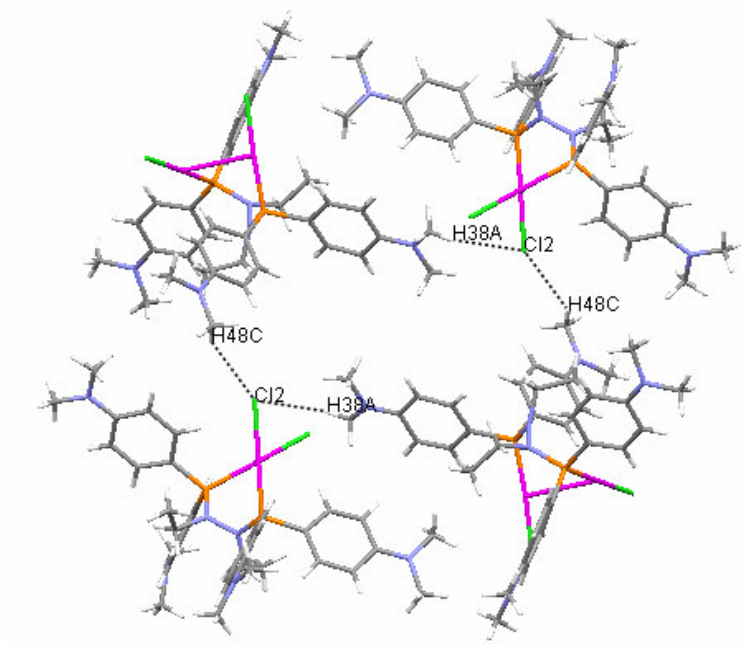

Figure 2.20: Mercury representation of **27** showing H-Cl interactions (dotted lines).

2.5.8 Bis(bis(di(*N,N*-dimetyl-4-aminophenyl)phosphino)diethylhydrazine)gold trinitrate (35)

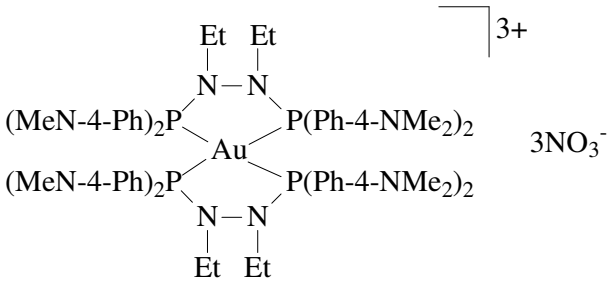

The molecular structure of bis(bis(di(*N,N*-dimetyl-4-aminophenyl)phosphino)-diethylhydrazine)gold trinitrate (**35**) with the atom numbering scheme is shown below in Figure 2.23 and selected bond distances are found in Table 2.9. Full data tables can be found in Appendix A.

Efforts to crystallise the complex bis(bis(di(*N,N*-dimetyl-4-aminophenyl)phosphino)-diethylhydrazine) gold(I) chloride (**33**) failed. When the anion of the complex was changed from chloride to nitrate *via* a metathesis reaction with silver nitrate it was possible to crystallise **35** from DCM and hexane as bright red crystal flakes.

Complex **35** crystallises in the orthorhombic space group *Pban*. The molecule shows two-fold rotation and an inversion centre coinsiding with the Au centre. The Au centre shows a slightly distorted square planar geometry with two phosphorous atoms 7.45° above and below the plane (gray line) formed by the remaning two phosphorous atoms and the gold atom (Figure 2.21).

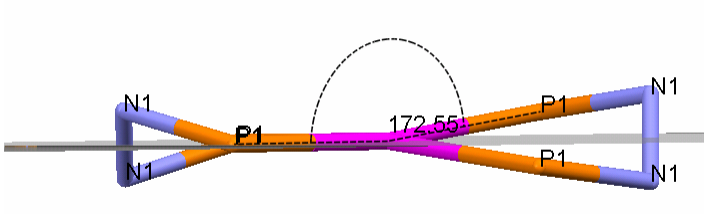

Figure 2.21: Mercury representation of distorted square planar geometry around the Au centre in complex **35**.

The molecules are packed in such a way as to accommodate three nitrate ions, two being ordered and one being disordered. Cavities also showed the inclusion of a

disordered hexane. Due to the Au-P bond lengths and square planar conformation of this complex and most importantly the presence of 3 NO_3^- counterions per complex a formal charge of 3+ was assigned to the Au centre. The observed Au-P bond length of 2.387 Å is only slightly shorter than that in the tetrahedral gold(I) dppe analogue which has Au-P bond lengths of 2.389 Å and 2.416 Å.[56] Two distinct P-Au-P angles are formed, an endocyclic angle of 83.50° forms between the gold and the phosphorous centres on the same ligands and a larger exocyclic angle of 96.99 ° between gold and phosphorous centres on opposite chelating ligands (Figure 2.22). This is to be expected as this is the indication of the bite angle of the ligand in question.

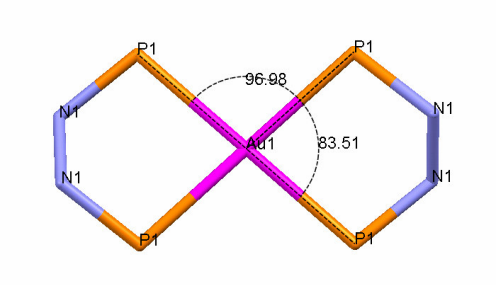

Figure 2.22: Mercury representation of endocylic and exocyclic angles displayed by complex **35**.

A π-π interaction or aromatic interaction is a noncovalent interaction between organic compounds containing aromatic moieties. π-π interactions are caused by intermolecular overlapping of p-orbitals in π-conjugated systems, so they become stronger as the number of π-electrons increases.[141]

The intermolecular interaction of aromatic systems has been studied extensively, especially in the last two decades.[142,143] The importance of the attraction between π systems has been stressed repeatedly in many fields of chemistry from molecular biology to material design. The π-π interaction influences the three-dimensional structures of biological systems such as protein and DNA[144] and is important for the crystal packing of organic molecules containing aromatic rings such as nonlinear

[141] http://en.wikipedia.org/wiki/Pi-pi_interaction.
[142] V. Spirko, O. Engkvist, P. Soldan, H.L. Selzle, E.W. Schlag, P. Hobza, *J. Chem. Phys.*, **1999**, 111, 572.
[143] K.S. Kim, P. Tarakeshwar, J.Y. Lee, *Chem. Rev.*, **2000**, 100, 4145.
[144] K.M. Guckian, T.R. Krugh, E.T. Kool, *J. Am. Chem. Soc.*, **2000**, 122, 6841.

optical materials.[145] This is also important for molecular recognition processes in biological and artificial systems.[146147]

A stabilising effect observed in this complex is the occurrence of π-π interactions between the various phenyl rings (Figure 2.24). A phenyl centroid to centroid distance of 3.819 Å is observed between the respective four pairs of phenyl rings.

A search through the literature and the Cambridge Crystallographic Database revealed this complex to be the first example of a discrete cationic gold(III) atom coordinated to four chelating phosphorous centres in a square planar fashion. Traditionally gold(I) is seen as a "soft" metal centre mostly forming complexes with "soft" ligands like phosphorous and sulphur while gold(III) is seen as a "hard" metal centre mostly coordinating to "hard" ligands like nitrogen and oxygen. The occurance of P-N ("soft"-"hard") mixed ligand complexed to gold(III) is not uncommon. The striking feature of this complex is its unusual combination of a "hard" metal centre and four "soft" chelating phosphous centres.

Bond lengths [Å]		**Angles [°]**	
P(1)-Au(1)	2.387(8)	N(1)$^{\#}$1-N(1)-P(1)	111.0(2)
N(1)-P(1)	1.683(3)	P(1)$^{\#}$2-Au(1)-P(1)$^{\#}$1	172.54(4)
N(1)-N(1)$^{\#}$1	1.429(6)	P(1)$^{\#}$2-Au(1)-P(1)$^{\#}$3	83.50(4)
Torsion angle [°]		P(1)$^{\#}$1-Au(1)-P(1)$^{\#}$3	96.99(4)
P(1)-N(1)-N(1)$^{\#}$3-P(1)$^{\#}$3	-68.81	$^{\#}$1 -x + 1/2, y, -z + 1	
$^{\#}$2 -x + 1/2, -y + 3/2, z		$^{\#}$3 x, -y + 3/2, -z + 1	

Table 2.9: Selected bond lengths, angles and torsion angles for **35**.

[145] R. Vallee, P. Damman, M. Dosiere, E. Toussaere, J. Zyss, *J. Am. Chem. Soc.*, **2000**, 122, 6701.
[146] F.M. Raymo, K.N. Houk, J.F. Stoddart, *J. Org. Chem.*, **1998**, 63, 6523.
[147] S. Tsuzuki, K. Honda, T. Uchimaru, M. Mikami, K. Tanabe, *J. Am. Chem. Soc.*, **2002**, 124, 1, 104.

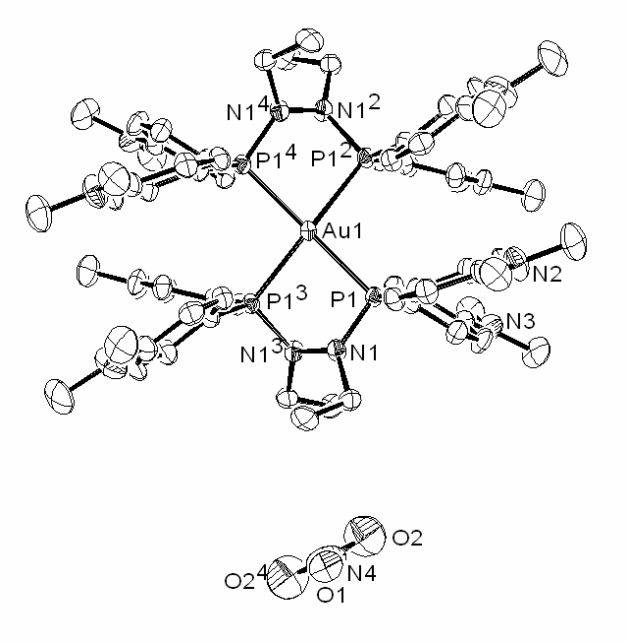

Figure 2.23: ORTEP diagram of **35** drawn at the 50 % probability level as viewed down the a-axis. Hydrogen atoms and two disordered molecules of NO_3^- and hexane were left out for clarity. Superscripts 2 – 4 indicate symmetry operator created atoms: No. 2 = -x + 1/2, y, -z + 1; No. 3 = -x + 1/2, -y + 3/2, z and No. 4 = x, -y + 3/2, -z + 1.

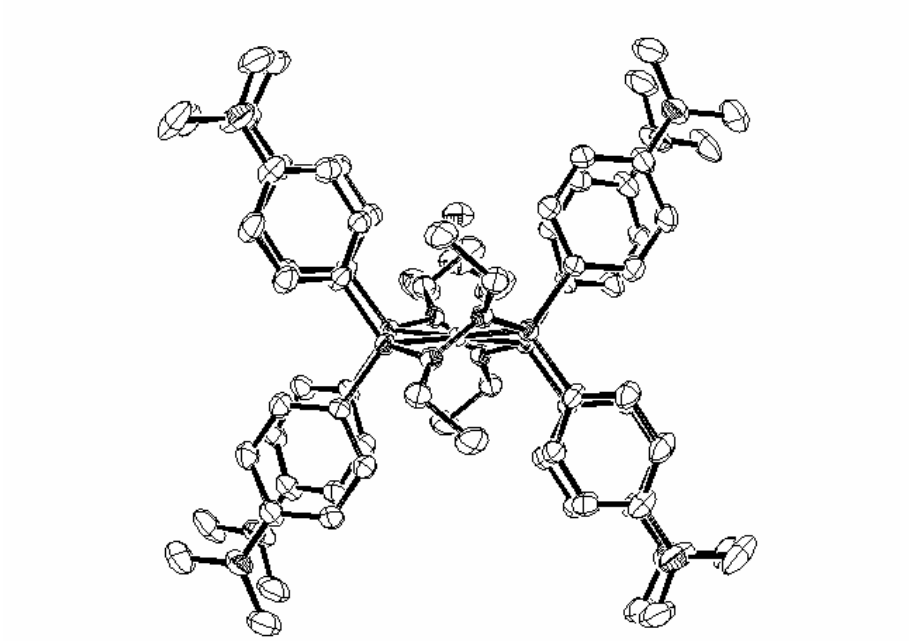

Figure 2.24: ORTEP diagram of **35** drawn at the 50 % probability level as viewed down the b-axis. Hydrogen atoms and molecules of NO_3^- and hexane were left out for clarity.

2.5.9 Bis(diphenylphosphino)diethylhydrazine di(silver nitrate) (39)

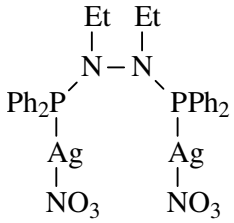

The molecular structure of bis(diphenylphosphino)diethylhydrazine di(silver nitrate) (**39**) with the atom numbering scheme is shown in Figures 2.26 and selected bond distances are in Table 2.10. Full data tables can be found in Appendix A.

Complex **39** crystal-lised from a mixture of acetonitrile, EtOAc and hexane after being left at –20 °C for two weeks.

39 crystallises in the orthorhombic space group *Pna*2_1. The centre of a polymeric α-helix produced by complex **39** is filled by nitrate counter ions. Three oxygen atoms from three different nitrate ions occupy the equatorial positions of a trigonal bipyramid and two silver atoms are situated at the axial positions (Figure 2.25). This complex arrangement connects each silver atom of one complex to a silver atom in a neighbouring complex. The resulting α-helices (Figure 2.27) are packed parallel to each other and run down the c-axis of the crystal (Figure 2.28).

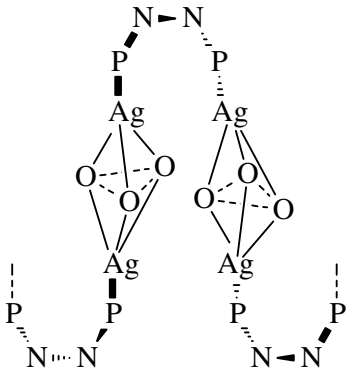

Figure 2.25: Representation of helix formed by complex **39**.

Polymerisation in silver nitrate complexes analogous to **39** is common as seen for example in the case of (NO_3)Ag(dppe)Ag(NO_3) (**50**), that forms long chains with P-

Ag-P units as the connecting entity.[148] These long chains are also periodically connected by short chains of Ag-O-Ag bonds, giving rise to sheets of connected complexes.

The Ag-P bond distances of 2.334 Å and 2.349 Å in **39** are considerably shorter than those of **50** (2.414 Å and 2.436 Å). The trigonal bipyramidal structure of **39** consists of four long Ag-O bonds in the range of 2.5 Å and two short Ag-O bonds in the range of 2.3 Å. Two longer bonds are to the same NO_3^-, while two sets of a short and long bond are connected to the other two nitrates, respectively. This compares to Ag-O bond lengths between 2.68 Å and 2.17 Å in **50**. Complex **39** exhibits Ag-O-Ag angles in the range of 93 ^{o} and 99 ^{o} and O-Ag-O angles in the range of 66 ^{o} to 75 ^{o}.

[148] S-Z Hu, *Jiegou Huaxue* (Chin.) (*Chinese J. Struct. Chem.*), **2000**, 19, 153 (cif file obtained from the *Cambridge Crystallographic Database*).

Bond lengths [Å]		**Angles [°]**	
P(1)-Ag(1)	2.334(2)	N(1)-N(2)-P(2)	116.9(4)
P(2)-Ag(2)	2.349(2)	N(2)-N(1)-P(1)	117.7(4)
O(1)-Ag(1)	2.302(5)	Ag(1)-O(1)-Ag(2)$^{\#}$1	97.9(2)
O(2)-Ag(1)$^{\#}$1	2.553(5)	Ag(2)$^{\#}$2-O(2)-Ag(1)$^{\#}$1	98.7(2)
O(4)-Ag(1)$^{\#}$3	2.506(5)	Ag(1)$^{\#}$3-O(4)-Ag(2)	94.0(2)
O(1)-Ag(2)$^{\#}$1	2.592(5)	O(1)-Ag(1)-P(1)	164.7(1)
O(2)-Ag(2)$^{\#}$2	2.314(5)	O(2)$^{\#}$4-Ag(2)-P(2)	154.2(1)
O(4)-Ag(2)	2.548(5)	P(1)-Ag(1)-O(4)$^{\#}$1	116.3(1)
N(1)-P(1)	1.699(6)	P(1)-Ag(1)-O(2)$^{\#}$3	126.8(1)
N(2)-P(2)	1.705(6)	P(2)-Ag(2)-O(4)	118.8(1)
N(1)-N(2)	1.406(8)	P(2)-Ag(2)-O(1)$^{\#}$3	137.7(1)
Torsion angle [°]		O(1)-Ag(1)-O(4)$^{\#}$1	71.7(2)
P(1)-N(1)-N(2)-P(2)	99.5(5)	O(1)-Ag(1)-O(2)$^{\#}$3	67.3(2)
		O(4)$^{\#}$1-Ag(1)-O(2)$^{\#}$3	72.7(2)
		O(2)$^{\#}$4-Ag(2)-O(4)	75.9(2)
		O(2)$^{\#}$4-Ag(2)-O(1)$^{\#}$3	66.4(2)
		O(4)-Ag(2)-O(1)$^{\#}$3	66.6(2)
		N(3)-O(1)-Ag(1)	114.6(4)
		N(3)-O(1)-Ag(2)$^{\#}$1	132.6(4)
$^{\#}$1 -x, -y, z + 1/2		N(3)-O(2)-Ag(2)$^{\#}$2	116.2(4)
$^{\#}$2 x, y, z + 1		N(3)-O(2)-Ag(1)#1	143.5(4)
$^{\#}$3 -x, -y, z - 1/2		N(4)-O(4)-Ag(1)$^{\#}$3	116.8(5)
$^{\#}$4 x, y, z - 1		N(4)-O(4)-Ag(2)	101.5(4)

Table 2.10: Selected bond lengths, angles and torsion angles for **39**.

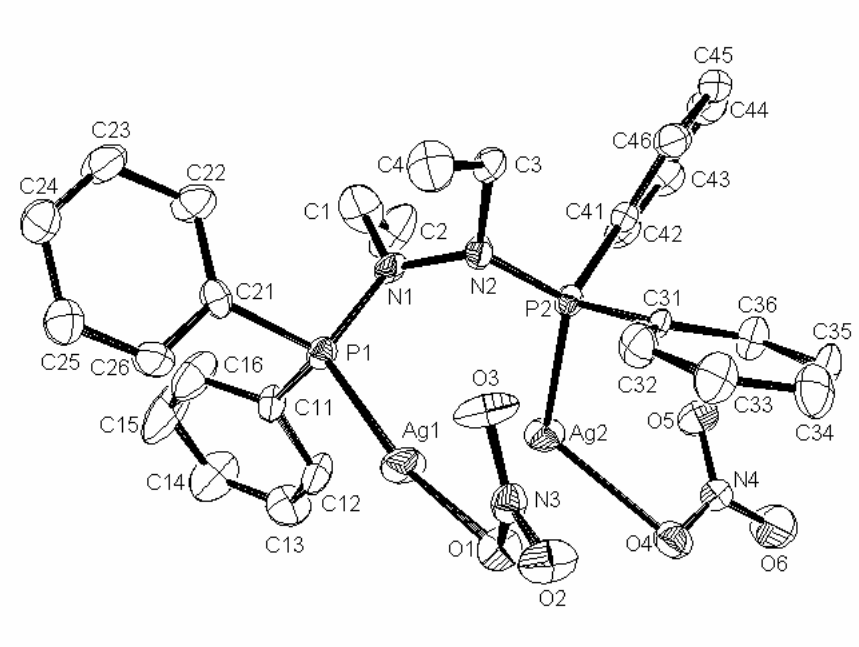

Figure 2.26: ORTEP diagram of **39** drawn at 50 % probability level. Hydrogen atoms have been omitted for clarity.

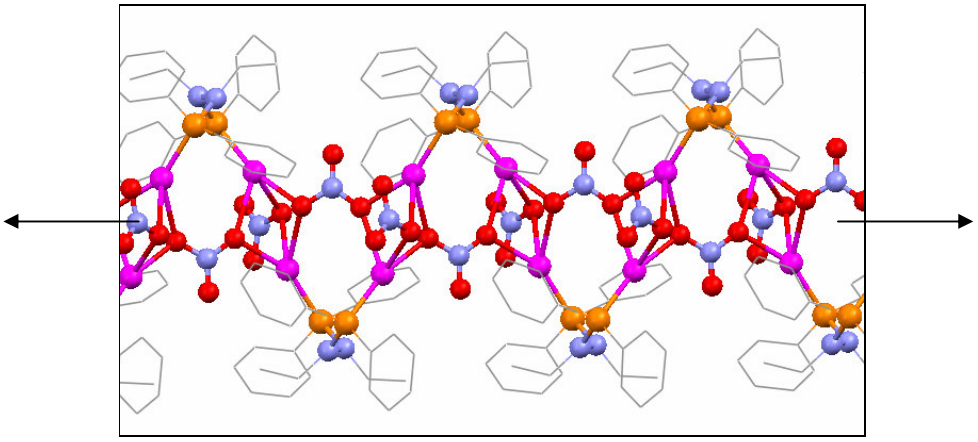

Figure 2.27: Mercury representation of **39** showing the polymeric helix. Hydrogen atoms have been omitted for clarity.

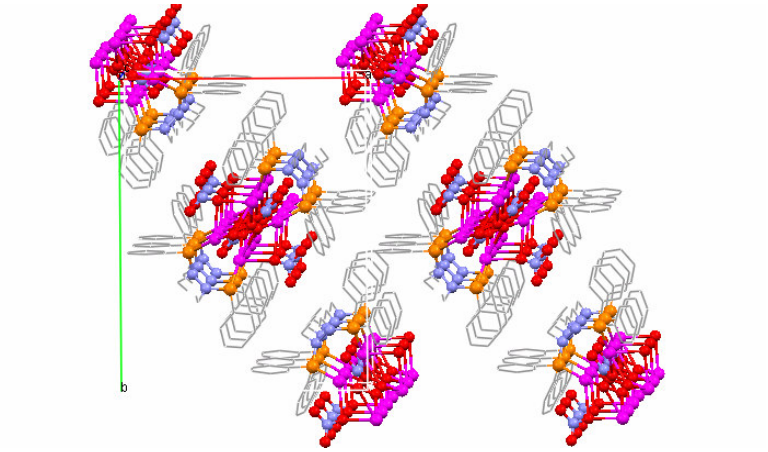

Figure 2.28: Mercury representation of **39** packing viewed along the c-axis. Hydrogen atoms have been omitted for clarity.

2.5.10 Bis(bis(diphenylphosphino)diethylhydrazine)silver nitrate (45)

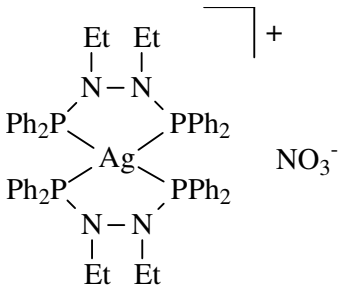

The molecular structure of bis(bis(diphenylphosphino)diethylhydrazine)silver nitrate (**45**) with the atom numbering scheme is shown below in Figure 2.29 and selected bond distances are in Table 2.11. Full data tables can be found in Appendix A.

Compex **45** was synthesised by adding 2 equivalents of **14** dissolved in THF to 1 equivalent of silver(I) nitrate suspended in THF. The solvent was reduced *in vacuo* and the reaction mixture left overnight to form colourless crystal plates. Various crystals tested were found to be twinned and subsequently could not be analysed. A crystal suitable for X-ray analysis was finally found and analysed.

45 crystallises in the triclinic space group $P\bar{1}$. Complex **45** shows an arrangement where nitrate counter ions and THF molecules occupy cavities between the metal cations. The silver(I) atom shows a tetrahedral coordination with Ag-P bond lengths between 2.513 Å and 2.531 Å and endocyclic P-Ag-P angles of 79.2 ^{o} and 79.3 ^{o}. The

related $[Ag(dppe)_2]^+.NO_3^-$ (**51**) complex shows similar Ag-P bond lengths of about 2.52 Å and endocyclic P-Ag-P angles of about 84 °.[149] The difference in P-Ag-P angles of 79 ° and 84 ° shows the difference in chelating bite angle between these two ligands, with **51** having a larger bite angle than ligand **14**. This difference in bite angle may be attributed to the difference in the bisphosphine bridge and more specifically the shorter distance between N-N *vs* C-C, bringing the two phosphorous atoms closer to each other in the case of N-N and hereby presumably causing a smaller bite angle. Other bond lengths and angles where within the expected range.

Bond lengths [Å]		**Angles [°]**	
N(1)-P(1)	1.73(2)	N(2)-N(1)-P(1)	107(1)
N(2)-P(2)	1.68(1)	N(1)-N(2)-P(2)	120.1(9)
N(3)-P(3)	1.70(1)	N(4)-N(3)-P(3)	120(1)
N(4)-P(4)	1.74(2)	N(3)-N(4)-P(4)	108(1)
P(1)-Ag(1)	2.531(5)	P(3)-Ag(1)-P(2)	129.0(2)
P(2)-Ag(1)	2.526(4)	P(3)-Ag(1)-P(4)	79.3(1)
P(3)-Ag(1)	2.513(4)	P(2)-Ag(1)-P(4)	128.8(2)
P(4)-Ag(1)	2.528(4)	P(3)-Ag(1)-P(1)	125.9(2)
N(1)-N(2)	1.47(2)	P(2)-Ag(1)-P(1)	79.2(1)
N(3)-N(4)	1.42(2)	P(4)-Ag(1)-P(1)	121.3(2)
Torsion angle [°]			
P(1)-N(1)-N(2)-P(2)	-60(1)		
P(3)-N(3)-N(4)-P(4)	-60(1)		

Table 2.11: Selected bond lengths, angles and torsion angles for **45**.

[149] C.S.W. Harker, E.R.T. Tiekink, *J. Coord. Chem.*, **1990**, 21, 287.

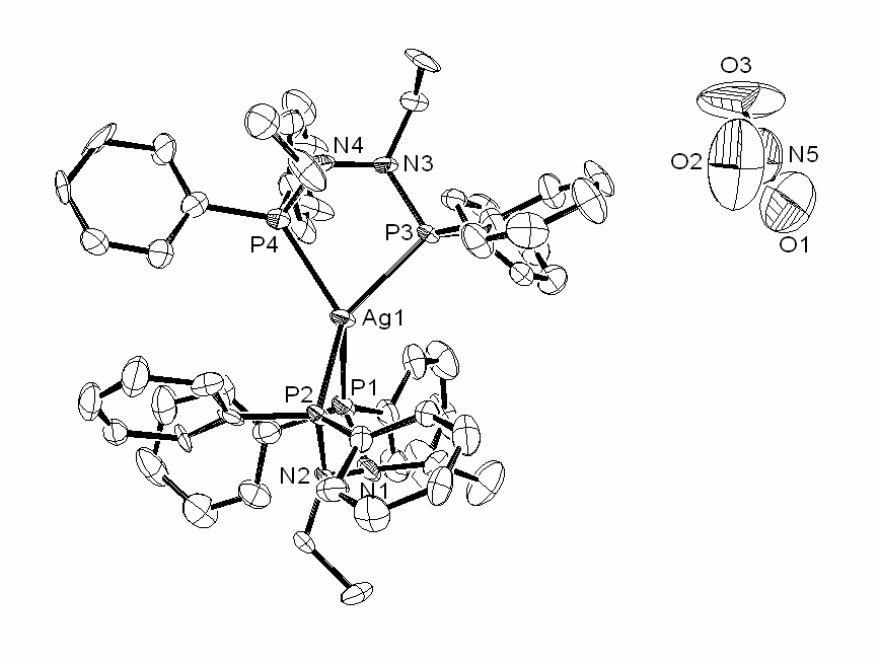

Figure 2.29: ORTEP diagram of **45** drawn at 50 % probability. Hydrogen atoms and a molecule of THF have been omitted for clarity.

2.6 Conclusion

A series of hydrazine-bridged phosphine ligands including the previously reported compounds $Ph_2PN(Me)N(Me)PPh_2$ and $Ph_2PN(Et)N(Et)PPh_2$ as well as the new derivatives $((4\text{-}MeO)Ph)_2PN(Me)N(Me)P(Ph(4\text{-}OMe))_2$, $((4\text{-}MeO)Ph)_2PN(Et)N(Et)$-$P(Ph(4\text{-}OMe))_2$, $((4\text{-}Me_2N)Ph)_2PN(Me)N(Me)P(Ph(4\text{-}NMe_2))_2$, $((4\text{-}Me_2N)Ph)_2PN(Et)$-$N(Et)P(Ph(4\text{-}NMe_2))_2$ was successfully synthesised by adopting and modifying existing methods. A total of six ligands were prepared in this manner. Three of these ligands have methyl substituted hydrazine bridges and three have ethyl substituted hydrazine bridges. Other differences include the use of phenyl, methoxyphenyl and dimethylaminophenyl substitutents on the free phosphorous sites. Attempts to extend these efforts to the synthesis of the analogous 2-, 3- and 4-pyridal ligands were not successful due to problems in separating the products from various side products.

The synthesis of gold(I) and silver(I) complexes of the aforementioned ligands was attempted. The synthesis of bisphosphine-bridged digold species was mostly successful and crystal structures of five of these complexes could be obtained:

$ClAuPh_2PN(Me)N(Me)PPh_2AuCl$; $ClAuPh_2PN(Et)N(Et)PPh_2AuCl$; $ClAu((4\text{-}MeO)Ph)_2PN(Me)N(Me)P(Ph(4\text{-}OMe))_2AuCl$; $ClAu((4\text{-}MeO)Ph)_2PN(Et)N(Et)\text{-}P(Ph(4\text{-}OMe))_2AuCl$ and $ClAu((4\text{-}Me_2N)Ph)_2PN(Et)N(Et)P(Ph(4\text{-}NMe_2))_2AuCl$. These crystal structures show large similarities in the paddle like arrangement of the P-Au-Cl moieties and other structural features. The complexes were found to be stable in crystalline form in moist air. The synthesis of the tetrahedral gold(I) species was in most cases also successful. These compounds were found to range in colour from light yellow to bright orange and in the case of complex **34** and **35**, red. The complexes were also found to be hygroscopic. Attempts to crystallise these complexes led to disordered crystals giving powder diffraction patterns when analysed. The crystallisation of complex **35** revealed the spontaneous oxidisation of gold(I) to gold(III) with a change from tetrahedral to square planar coordination.

The synthesis of bisphosphine-bridged disilver species was more problematic when compared to the analogous gold species. Attempts regularly led to the formation of a silver mirror on the reaction vessels. We were able to crystallise one of the complexes of this type, namely $NO_3AgPh_2PN(Et)N(Et)PPh_2AgNO_3$. This structure showed long helical columns of interconnected silver complexes. The synthesis of the bischelated silver(I) species was easier than that of the disilver species and the crystal structure of $[(Ph_2PN(Et)N(Et)PPh_2)_2Ag]^+.NO_3^-$ showing distinct tetrahedral coordination was successfully determined.

Chapter 3

Biological Activity of Complexes

3.1 INTRODUCTION

The anti-tumour potential of gold(I) phosphine complexes was first identified at the time when auranofin was shown to kill tumour cells in culture. This sparked the interest of Berners-Price *et al.*[6,150] and led to the development of the bischelated gold(I) phosphine anti-tumour compound $[Au(dppe)_2]Cl$ (**37**), whose active entity was found to be the cationic ion $[Au(dppe)_2]^+$. Whereas auranofin exhibited only modest anti-tumour activity in one animal tumour model, $[Au(dppe)_2]^+$ exhibited significant *in vivo* anti-tumour activity in a range of tumour models in mice. It was selected for pre-clinical trials, but was unfortunately abandoned after the identification of severe hepatoxicity in dogs.[6,150]

The high toxicity of $[Au(dppe)_2]^+$ is attributable to the high lipophilicity of the cation which results in non-selective uptake into mitochondria in all cells. Delocalised lipophilic cations (*e.g.* Rhodamine 123) have a long history as potential anti-tumour drugs and have been shown to preferentially concentrate within tumour cell mitochondria in response to elevated mitochondrial membrane potentials, which are characteristic features of carcinoma cells.[151] Clinical development of compounds of this type has been hindered by severe toxicity, but several classes of delocalised lipophilic cations have demonstrated a relationship between anti-tumour selectivity and lipophilic-hydrophilic balance.[6,150]

[150] S.J. Berners-Price, *Chem. Aust.*, **2004**, 71, 10.
[151] J.S. Modica-Napolitano, J.R. Aprille, *Advan. Drug Deliv. Rev.*, **2001**, 49, 63.

Inhibition of tumour colony formation by $[Au(dppe)_2]Cl$ has been associated with preferred inhibition of protein synthesis, DNA protein cross-links and DNA strand breaks. The *in vitro* activity of $[Au(dppe)_2]Cl$ was seen to be less inhibited than that of auranofin by the presence of serum proteins in the tissue culture medium due to better stablity in the presence of serum proteins, thiols and disulphides. These findings provided evidence for a mechanism of anti-tumour activity for $[Au(dppe)_2]Cl$ that differed from that of auranofin.[152]

Berners-Price *et al.*[152] set out to determine whether $[Au(dppe)_2]Cl$ induced cytotoxicity was related to changes in mitochondria. Studies were carried out on intact isolated rat hepatocytes. They found that within 30 minutes of exposure, $[Au(dppe)_2]Cl$ had been taken up by isolated hepatocytes and distributed to mitochondria, nucleus, cytoplasm and cellular membranes. The isolated rat hepatocytes were found to lose cellular viability as indicated by the release of lactate dehydrogenase. $[Au(dppe)_2]Cl$ also induced a rapid dissipation of the inner mitochondrial membrane potential, efflux of calcium, increased mitochondrial respiration, mitochondrial swelling and increased permeability of the inner membrane to cations and protons in isolated mitochondria.[153] Cytotoxic effects to isolated hepatocytes appeared to be a result of the inhibition or uncoupling of oxidative phosphorylation by gold(I) phosphine complexes. These results suggested that mitochondria were a possible target organelle for $[Au(dppe)_2]Cl$ cytotoxicity in intact isolated rat hepatocytes.[152]

Further studies done by Berners-Price *et. al.*[154] found that the anti-tumour activity of $[Au(dppe)_2]Cl$ and tetrahedral bis(dipyridylphosphino)gold(I) complexes *in vivo* showed a dependence on lipophilicity in subcutaneous colon 38 tumours. The most lipophilic and hydrophilic compounds showed no significant tumour growth delay. However, a compound of intermediate lipophilicity showed significant anti-tumour

[152] M.J. McKeage, L. Maharaj, S.J. Berners-Price, *Coord. Chem. Rev.*, **2002**, 232, 127.
[153] P.F. Smith, G.D. Hoke, D.W. Alberts, P.J. Bugelski, S. Lupo, C.K. Mirabelli, G.F. Rush, *J. Pharmacol. Exp. Therap.*, **1989**, 249, 944.
[154] M.J. McKeage, S.J. Berners-Price, P. Galettis, R.J. Bowen, W. Brouwer, L. Ding, L. Zhuang, B.C. Baguley, *Cancer Chemother. Pharmacol.*, **2000**, 46, 343.

activity, less dose-limiting toxicity and higher gold concentration in plasma and tumours compared with the more lipophilic or hydrophilic analogues.[152]

Following on the work done by Berners-Price *et al*.,[6] a range of gold(I) and silver(I) complexes designed to have varying degrees of lipophilicities was described in the previous chapter (see Chapter 2). The testing for biological activity of these lipophilic cationic complexes is described here in.

3.2 BIOLOGICAL SCREENING

3.2.1 *In Vitro* Screening

A range of thirteen compounds was found to be suitably chemically stable for biological screening (Table 3.1). Complexes with different aromatic substituents at the phosphorous centres of the chelating ligands were synthesised. The variations were generated to indroduce a range of different lipophilicities to allow for a structure/anti-tumour activity relationship to be formulated. Biological screening was carried out at the Department of Pharmacology at the University of Pretoria under the guidance of Prof. Connie Medlen, Dr. Gisella Joone and Mrs. Margo Nell. Further advice and guidance was also received from Prof. Denver Hendricks at the University of Cape Town.

The screening assays allowed for the identification of the most selective compounds (*i.e.* the compounds most toxic to cancer cells and least toxic to normal cells). Furthermore, pharmacokinetic studies were undertaken to provide a broader understanding of the factors determining activity and selectivity.

The range of compounds was screened against three cell lines, namely HeLa (Human cervix adenocarcinoma), Jurkat (Human T-cell carcinoma) and healthy lymphocytes from human blood. The HeLa cell line was selected due to it being the cancerous cell line most readily available and generally used in initial screening for activity. The cancerous Jurkat cell line was used to determine the toxicity of drugs to cancerous human T-cells, while normal lymphocytes, harvested from healthy human blood donors, were used to determine the toxicity of drugs to normal human T-cells.

A standard MTT (3-(4,5-dimethylthiazol-2-yl)-2,5-diphenyl tetrazolium bromide) assay was performed to determine IC_{50} values for the selected compounds. HeLa cells were examined under an inversion microscope to determine satisfactory growth and to check for possible infection. The cells were trypsinated to remove the adherent cells from the growth vessel. After trypsination the free floating cells were centrifuged to form an easily manageable pellet and to remove supernatant growth medium and trypsin.

The cells were resuspended in 1 ml of growth medium and counted by suspending 50 µl of the resuspended cells in white cell counting fluid. This was used to count cells utilising a Haemocytometer and a Reichert-Jung Microstar 110 microscope. Cells were diluted to a concentration of $2.5x10^4$ cells/mL. A further 1:4 dilution was made and 100 µl of these cells loaded on 96 well plates preloaded with 80 µl growth medium and warmed to physiological temperature. The plates were left for 1 hour in the incubation oven to settle to the bottom of the plates and start adhering.

After 1 hour the plates were loaded with 20 µl of drug dissolved in the growth medium. Drug solutions were made up by dissolving the compound of interest in 1 ml of DMSO to make up a 10 mM solution. This solution was dispensed into Eppendorf tubes in 50 µl portions and kept frozen until used. The drug-growth medium solution was made up just before administration by diluting the contents of one Eppendorf tube using the appropriate growth medium. Eight subsequent 1:1 dilutions of this solution were made up and added to the wells to give a final range of eight drug concentrations. Each drug concentration was administered to three wells to obtain triplicate results.

The plates were placed in a covered (not closed) container with paper towels soaked with distilled water at the bottom to minimise evaporation of the growth medium in the wells. Containers were left for 7 days to incubate at 37 ^oC in a 5 % CO_2 atmosphere.

After the 7 day incubation period the plates were removed from the incubator and 20 µl of MTT solution were added to each well. The plates were placed back in the incubator for another 3 to 4 hours.

The plates were centrifuged and the supernatant in every well was removed separately and discarded. The cells were repeatedly washed with PBS (phosphate buffered saline) and left to dry completely overnight in a dark cupboard (due to the light sensitivity of the reagent). The next morning the purple crystals were dissolved in DMSO and an absorption intensity reading taken on a plate reader. IC_{50} values were calculated from the intensities as compared to the triple column of control cells (cells with no drug added) on each plate.

A similar procedure was carried out for Jurkat cells, except that due to Jurkat cells being floating cells it was not necessary to trypsinate them. Jurkat cells were diluted to $3x10^4$ cells/ml after counting compared to $2.5x10^4$ cells/ml in the case of HeLa cells.

For the isolation of normal lymphocytes, 30 ml of heparinised blood from a human donor was loaded onto 15 ml of Histopaque 1077. The suspension was centrifuged and the monolayer of plasma was removed and the layer of lymphocytes and monocytes was collected. The tube was filled with RPMI (Roswell Park Memorial Institute) growth medium and centrifuged to remove platelets. Sterile cold ammonium chloride was added and left on ice for 10 minutes to lyse remaining red cells. After centrifuging, the remaining pellet was resuspended in RPMI followed by centrifuging.

The pellet was resuspended in 1 ml RPMI and subsequently counted, diluted to $2x10^6$ cells/ml and 100 µl of that solution was loaded onto the 96 well plates (preloaded with 60 µl medium). 20 µl of PHA (Phytohaemaglutinine) were added to the stimulated lymphocyte assay while 20 µl RPMI were added to the resting lymphocyte assay. PHA was added to stimulate the lymphocytes in the same manner as an *in vivo* immune response. A procedure similar to the drug administration described for HeLa cells was followed for both resting and stimulated lymphocytes and the plates were incubated for 3 days after which MTT was added and readings were taken.

	Compound		Compound
37 Reference compound	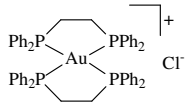	**30**	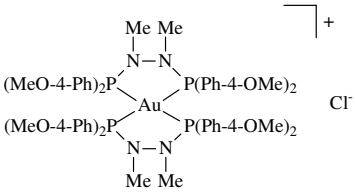
23	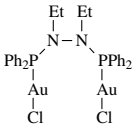	**31**	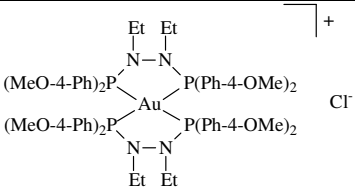
24	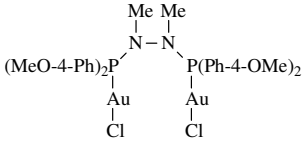	**43**	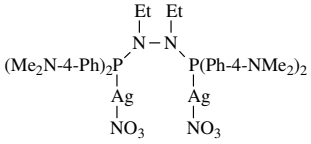
25	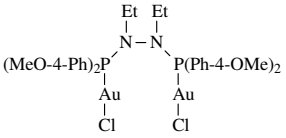	**45**	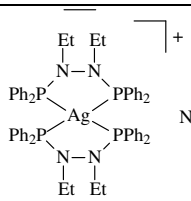
27	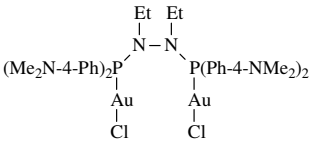	**46**	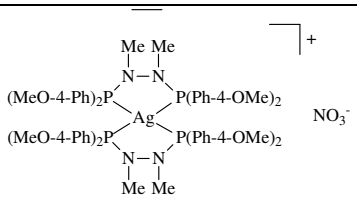
28	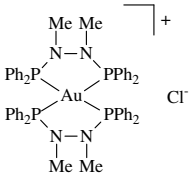	**47**	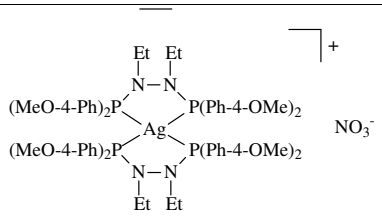
29	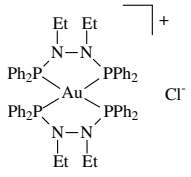	**49**	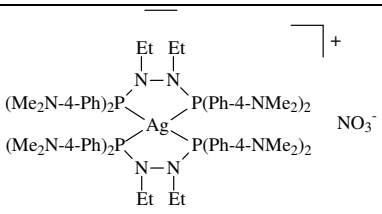

Table 3.1: Compounds selected for biological screening.

3.2.2 Results from Activity Screening and Selectivity Determination

IC_{50} values (*i.e.* the amount of drug delivered to cause 50% mortality to viable cells) were determined by performing the standard MTT assay on the following cell lines; i) HeLa cells; ii) Jurkat cells; iii) resting lymphocytes; and iv) stimulated lymphocytes. A series of results were obtained and the toxicology profile of each compound as pertaining to the tested cell lines is represented graphically (Appendix B, Graphs 3.1 – 3.56). Each point on these graphs is the result of three repetitions of the experiment. One experimental value is derived from the mean of three wells (per plate) containing the same concentration incubated under the same conditions.

A summary of the IC_{50} values obtained from the cytotoxicity profiles is given in Table 3.2 reported as the mean value of three experimental results and given in μM concentrations of administered drug.

Compound	HeLa	Jurkat	Resting Lymphocyte	Stimulated Lymphocyte
37 (Ref)	0.747 ±0.273	0.030 ±0.049	0.325 ±0.324	0.131 ±0.101
23	0.858 ±0.149	0.735 ±0.433	4.299 ±0.593	0.938 ±0.901
24	1.009 ±0.330	1.014 ±.003	7.258 ±0.072	5.730 ±1.266
25	5.470 ±2.499	0.440 ±1.416	7.522 ±4.031	12.805 ±0.298
27	39.375 ±8.570	18.030 ±2.954	32.285 ±0.703	25.296 ±2.390
28	4.570 ±0.336	2.500 ±1.542	1.536 ±0.584	1.098 ±0.318
29	1.264 ±0.588	0.440 ±0.305	1.363 ±0.215	0.841 ±0.266
30	0.736 ±0.662	0.305 ±0.175	0.776 ±0.255	0.646 ±0.127
31	2.451 ±0.508	1.911 ±0.112	3.175 ±0.677	4.489 ±0.953
43	0.563 ±0.051	1.822 ±0.285	3.240 ±0.257	2.911 ±0.103
45	1.087 ±0.167	0.649 ±0.234	3.746 ±0.605	3.097 ±0.554
46	0.705 ±0.595	0.380 ±0.157	1.954 ±0.126	6.516 ±0.298
47	0.913 ±0.467	1.144 ±0.349	4.209 ±0.585	3.355 ±0.837
49	1.738 ±0.528	3.126 ±0.580	10.246 ±0.905	4.892 ±1.043

Table 3.2: IC_{50} (μM) of cells following treatment with experimental compounds (mean of three experiments).

From the results obtained from the screening, specificity of the compounds was calculated (Table 3.3). Specificity was calculated as follows: the sum of the IC_{50} values from normal cells (resting and stimulated lymphocytes in this case) divided by the sum of the IC_{50} values of the cancerous cells (HeLa and Jurkat cells in this case). The higher the specificity, the better the selectivity of the compound towards inhibiting the growth of cancerous cells, while not impeding the growth of normal cells. It has to be mentioned that this calculation is only a guide toward the effectiveness of these compounds.

Compound	Specificity	Compound	Specificity
37 (Ref)	0.587	**30**	1.366
23	3.288	**31**	1.757
24	6.420	**43**	2.579
25	3.439	**45**	3.942
27	1.003	**46**	7.806
28	0.373	**47**	3.677
29	1.293	**49**	3.112

Table 3.3: Specificity of compounds tested
(lymphocytes IC_{50}'s/Jurkat, HeLa IC_{50}'s).

Compounds **23**, **24**, **28**, **31**, **47** and **49** all showed a distinct exponential toxicity profile in the HeLa cell line with a dramatic increase in toxicity being observed with an increase in compound concentration. These compounds mostly showed acute toxicity for drug concentrations of 6 µM. Compounds **37**, **29**, **30**, **43**, **45** and **46**, even though having more tapered graphical profiles had sharp increases in toxicity reaching acute toxicity at 3 µM. Compounds **25** and **27** had more moderate toxicity profiles with acute toxicity only setting in after 20 µM concentrations of the compound.

Compounds **37**, **24**, **28**, **43** and **49** showed exponential toxicity profiles in Jurkat cells with acute toxicity for about 3 µM concentrations with the exception of **37** being extremely potent with acute toxicity at less than 0.5 µM. Compound **27** displayed a more moderate profile with acute toxicity only after 20 µM

concentrations. The rest of the compounds showed more linear toxicity profiles with extreme toxicity, sometimes of less than 0.5 μM.

The toxicity of these compounds in lymphocytes is of great importance. The selectivity of these compounds hinges on their ability to not eradicate healthy cells. A high IC_{50} value in resting and stimulated lymphocytes is thus preferable. Compounds **37** and **30** had very low IC_{50} values making them very toxic to the healthy cells and thus unsuitable as a potential drug. Compound **27** showed a very high IC_{50} making it less toxic but since this compound was also non-toxic to cancer cells it seemed ineffective. Compound **28** exhibited a low IC_{50} in lymphocytes and a higher IC_{50} in cancer cell lines, making it selectively toxic for healthy cells which is undesirable. Compounds **29** and **30** had low IC_{50} values and **31** and **43** had slightly higher IC_{50} values. These four compounds are not very selective with specificities close to 1. Compounds **23**, **25**, **45**, **47** and **49** all had specificities of about 3, making them 3 times more potent against cancer cells than healthy lymphocytes. Compounds **24** and **46** had good specificities of 6.4 and 7.8, respectively, making them roughly 7 times more selective for cancer cells.

3.3 MORE IN DEPTH *IN VITRO* EVALUATIONS

Based on the specificity displayed by the compounds (Table 3.3), five potential inhibitors were chosen for further evaluation against other cancerous cell lines. The compounds displaying some of the highest specificity included:

i) two bridged gold compounds;

- $ClAu((4\text{-}MeO)Ph)_2PN(Me)N(Me)P(Ph(4\text{-}OMe))_2AuCl$ (**24**)
- $ClAu((4\text{-}MeO)Ph)_2PN(Et)N(Et)P(Ph(4\text{-}OMe))_2AuCl$ (**25**)

ii) three bischelated silver compounds;

- $[(Ph_2PN(Et)N(Et)PPh_2)_2\ Ag]^+.NO_3^-$ (**45**)
- $[(((4\text{-}MeO)Ph)_2PN(Me)N(Me)P(Ph(4\text{-}OMe))_2)_2\ Ag]^+.NO_3^-$ (**46**)
- $[(((4\text{-}Me_2N)Ph)_2PN(Et)N(Et)P(Ph(NMe_2))_2)_2\ Ag]^+.NO_3^-$ (**49**)

It can already be noted that compounds **24** and **46** show a ten fold higher specificity compared to the standard $[Au(dppe)_2]Cl$ (**37**). Both these complexes have the same

ligand, *i.e.* $((4\text{-MeO})Ph)_2PN(Me)N(Me)P(Ph(4\text{-OMe}))_2$, but different metal centres, the bridged complex being a gold and the bischelated complex being a silver complex.

Even though the bridged gold(I) compounds **24** and **25** showed high selectivity it is believed that the active agent is the corresponding bischelated complex. Studies by Berners-Price *et al.*[71,129] have shown the bridged gold(I) compound, ClAu(dppe)AuCl, in blood was rapidly converted into the cationic species $[Au(dppe)_2]^+$. Similarly, the bridged gold complexes **24** and **25** are excpected to be converted to the bischelated species.

It is known that bischelated silver(I) compounds similar to **45**, **46** and **49** do not readily react with halides or other possible ligands that occur in biological fluids and thus may reach the intended target site without decomposition/metabolisation.[6]

3.3.1 Activity Screening and Specificity Determination

The five selected compounds were further tested on A2780 (Human ovarian cancer), A2780cis (Human ovarian cancer - cisplatin resistant), Colo 320 DM (Human colon cancer), MCF-7 (Human breast cancer) and MCF-12A (Immortalised human non-cancerous breast cells) cell lines. A series of results were obtained and toxicity profiles are represented graphically (Appendix B, Graphs 3.57 – 3.85) and a summary of IC_{50} values obtained is given in Table 3.4.

Compound	A2780	A2780cis	Colo 320 DM	MCF-7	MCF-12A
37 (Ref)	0.017 ±0.068	0.234 ±0.143	0.461 ±0.037	0.196 ±0.092	0.443 ±0.166
24	0.284 ±0.408	1.877 ±0.323	1.344 ±0.024	0.786 ±0.361	1.596 ±0.254
25	0.923 ±0.190	1.995 ±0.637	0.327 ±0.8016	1.120 ±0.068	0.762 ±0.221
45	0.341 ±0.107	0.957 ±0.568	0.236 ±0.810	0.625 ±0.424	0.884 ±0.368
46	0.028 ±0.190	5.541 ±0.637	0.507 ±0.245	0.962 ±0.068	12.665 ±0.221
49	0.499 ±0.075	2.030 ±0.672	2.985 ±0.784	0.578 ±0.299	4.547 ±0.855

Table 3.4. IC_{50} (μM) of cells following treatment with experimental compounds (mean of three experiments).

All five compounds showed low IC_{50} values for the three cancer cell lines A2780, Colo 320 DM and MCF-7. These complexes showed higher IC_{50} values in the cisplatin resistant A2780cis cell line. This might imply an overlap of mode of action of cell death or more likely show the vigorous growth of the cisplatin resistant cells. Only compounds **46** and **49** showed good selectivity for the cancerous MCF-7 cell line over the "healthy" MCF-12A cell line. MCF-12A is a cell line derived from normal breast epithelial cells.[155] In order to keep this cell line viable *in vitro* it had to be immortalised, which is the key trademark of cancerous cells. It can thus be seen as a benign cancerous cell line.

From the further assays done on these five compounds a broader selectivity profile was determined (Table 3.5). The broader specificity was calculated by taking the sum of the IC_{50} values from healthy cells (MCF-12A, resting and stimulated lymphocytes) divided by the sum of the IC_{50} values of the cancerous cells (HeLa, Jurkat, A2780, A2780cis, CoLo 320 DM and MCF-7).

Compound	Specificity	Compound	Specificity
37 (Ref)	1.067	**45**	2.800
24	4.305	**46**	5.767
25	5.096	**49**	3.593

Table 3.5: Specificity of compounds tested (lymphocytes, MCF-12A IC_{50}'s/Jurkat, HeLa, Colo 320 DM, A2780, A2780cis, MCF-7 IC_{50}'s).

From these specificities it can be seen that the overall specificity of these five compounds is not ideal. The two compounds with the highest specificities (**25** and **46**) showed a five times higher specificity if compared to the reference (**37**). Even though this is an improvement on the activity of the reference an even higher specificity is necessary for a good potential anti-tumour drug.

[155] H.G.R. Thompson, J.W. Harris, B.J. Wold, F. Lin, J.P. Brody, *Oncogene*, **2003**, 22, 2322.

From the assay results in Tables 3.4 and 3.5, two compounds were chosen for further studies. The selected compounds, **25** and **46**, were subjected to pharmacokinetic studies. Full discussion on the pharmacokinetic studies (mitochondrial membrane potential and apoptosis assay) follows.

3.4 PHARMACOKINETIC STUDIES

Recently it has become clear that mitochondria play a central role in both apoptotic and necrotic cell death.[156] Cells can be considered to die by either necrotic or apoptotic pathways. Necrotic cell death occurs in response to acute damage and results in rapid, uncontrolled death with subsequent cell lysis and a damaging inflammatory response.[157] Necrotic cell death follows ATP depletion and cellular calcium overloading, consequently extensive mitochondrial damage leads to necrotic cell death in situations such as heart attack and stroke.[158] In contrast, during apoptotic cell death an endogenous cell death programme is activated that causes the ordered self-destruction of the cell, ending with its phagocytosis by surrounding cells without leakage of damaging contents and thus no inflammatory response.[157] Apoptosis occurs during development to remove superfluous cells and also in response to cell damage, viral infection or transformation.[157] The distinction between apoptotic and necrotic cell death in response to cell damage is somewhat arbitrary as completion of the apoptotic programme requires ATP, and if the ATP level falls below a critical threshold after initiation of apoptosis the apoptotic programme is aborted and the cell dies by necrosis.[159,160]

The understanding of the role of mitochondria in apoptosis is still developing, but it is clear that mitochondria are critically involved in deciding whether a cell undergoes apoptosis.[156] By activation of caspases, cells irreversibly initiate

---

[156] P.E. Bernardi, *Biochim. Biophys. Acta*, **1998**, 1366, 1.
[157] A.J. Hale, C.A. Smith, L.C. Sutherland, V.E.A. Stoneman, V.L. Longthorne, A.C. Culhane, G.T. Williams, *Eur. J. Biochem.,* **1996**, 236, 1.
[158] P. Nicotera, G. Bellomo, S. Orrenius, *Annu. Rev. Pharmacol. Toxicol.,* **1992**, 32**,** 449.
[159] M. Leist, P. Nicotera, *Exp. Cell Res.,* **1998**, 239, 183.
[160] M.P. Murphy, R.A.J. Smith, *Adv. Drug Del. Rev.*, **2000**, 41, 2, 235.

apoptosis.[161] Caspases are cysteine proteases present in an inactive pro-form in the cytoplasm, that are activated by auto-proteolysis and then further proteolyse other pro-caspases leading to a self-amplifying caspase cascade and cell death.[160,161]

The membrane potential of mitochondria *in vitro* has an inside negative value not larger than 180–200 mV. This is about the maximum a lipid bilayer can sustain without breaking down.[162] Within living cells and organisms this potential is lower, usually about 130–150 mV, as a result of ATP synthesis and ion translocation.[163] As the mitochondrial membrane potential is far larger than that of others areas of the cells, lipophilic cations accumulate selectively within mitochondria. Lipophilic cations can easily pass through the hydrophobic barrier of the lipid bilayer since their positive charge is shielded or delocalised over a large surface area.[164]

The mitochondrial accumulation of lipophilic cations was first demonstrated by Skulachev *et al*.[165] and lipophilic cations such as triphenylmethylphosphonium or tetraphenylphosphonium are now used routinely to measure the membrane potential of mitochondria within living cells.[163] In addition, fluorescent lipophilic cations such as rhodamine and JC-1 are used to visualise mitochondria by fluorescence microscopy or to estimate mitochondrial energisation by flow cytometry.[164]

Mitochondria accumulate most lipophilic cations to a greater or lesser extent depending on the degree of charge screening or delocalisation in these ions. The plasma membrane potential (typically 30–60 mV, negative inside) also drives cation accumulation in the cell and the cations are then further accumulated in the mitochondria. This process is so effective that 90–95% of the cations become localised in the mitochondria.[160,166]

---

[161] G.S. Salvesen, V.M. Dixit, *Cell,* **1997**, 91, 443.
[162] M.P. Murphy, *Biochim. Biophys. Acta,* **1989**, 977, 123.
[163] G.F. Azzone, D. Pietrobon, M. Zoratti, *Curr. Top. Bioenerg.,* **198**4, 13, 1.
[164] L.B. Chen, *Annu. Rev. Cell Biol.,* **1988**, 4, 155.
[165] E.A. Liberman, V.P. Topali, L.M. Tsofina, A.A. Jasaitis, V.P. Skulachev, *Nature,* **1969**, 222, 1076.
[166] R.J. Burns, M.P. Murphy, *Arch. Biochem. Biophys.,* **1997**, 339, 33.

The ability of mitochondria to accumulate lipophilic cations has been researched as a potential therapy.[164,167] The most widespread approach has been to use lipophilic cations to selectively kill cancer cells.[167] This is possible because many cancer cells have an elevated mitochondrial membrane potential that leads to the accumulation of lipophilic cations in the cancer cells and thereby causes cell death by non-specific disruption of mitochondrial function.[160,167]

If mitochondria targeting drugs derived from lipophilic cations are to be of use *in vivo* then their uptake and pharmacokinetics must be understood. Most lipophilic cations enter cells through the lipid bilayer of the plasma membrane and their uptake does not require specific carriers. This has been demonstrated for triphenylalkyl-phosphonium cations, which are rapidly taken up into mitochondria of the isolated perfused heart and liver and are retained within the organs for several hours.[168] Similar rapid uptake and mitochondria localisation has been found for many other fluorescent lipophilic cations in perfused organs and intraventricular injection of lipophilic cations leads to their accumulation in neuronal mitochondria.[169] Furthermore, intraperitoneal or intravenous injection of triphenylalkylphosphonium cations leads to their rapid uptake into the heart and other organs.[170] Most lipophilic cations are not rapidly metabolised. However, cells that acquire multi-drug resistance due to expression of P-glycoprotein, the MDR-1 gene product, can export lipophilic cations across the plasma membrane and this mechanism may be a problem for the use of lipophilic cations in cancer therapy.[160,171]

3.4.1 Mitochondrial Membrane Potential Assay

A mitochondrial membrane potential assay is used to determine whether the application of a drug lowers or increases the mitochondria membrane potential. This was done using the fluorescent probe JC-1 after a 24 hour incubation of the cells. There is a direct correlation between the fluorescent absorption of JC-1 and the membrane potential.

---

[167] M.P. Murphy, *Trends Biotechnol.,* **1997**, 15, 326.
[168] R. Kauppinen, *Biochim. Biophys. Acta,* **1983**, 725, 131.
[169] J.C. Smith, *Biochim. Biophys. Acta,* **1990**, 1016, 1.
[170] P.C. Srivastava, H.G. Hay, F.F. Knapp, *J. Med. Chem.,* **1985**, 28, 901.
[171] M.M. Gottesman, I. Pastan, *Annu. Rev. Biochem.,* **1993**, 62, 385.

Mitochondria are seen as targets for discrete lipophilic cations and thus the depolarisation (lowering) of the mitochondrial membrane potential would indicate that the complexes under investigation cause cell death *via* a mitochondrial mode of action. Results of the assay on normal lymphocyte cells are displayed in Table 3.6. Valinomycin is used as positive control of the method as this is known to reduce the membrane potential of mitochondria. Concentrations used were taken at 1x, 2x, 5x and 10x the IC_{50} value previously obtained from cytotoxicity studies. Percentage of normal membrane activity is given as an easy comparison.

	Concentration	**Absorption Ratio**	**Absorption/Control x 100%**
Control		760 ±245	100%
Valinomycin	10µM	355 ±26	50%
	0.1µM	390 ±25	55%
37 (Ref)	1.0µM	464 ±110	62%
	0.5µM	517 ±173	68%
	0.2µM	606 ±240	79%
	0.1µM	658 ±237	86%
25	50.0µM	388 ±34	53%
	25.0µM	466 ±44	64%
	10.0µM	617 ±168	82%
	5.0µM	701 ±228	92%
46	66.0µM	315 ±89	42%
	33.0µM	316 ±138	41%
	13.2µM	271 ±38	38%
	6.6µM	301 ±34	41%

Table 3.6: Lymphocytes mitochondrial membrane potential at 1x, 2x, 5x and 10x IC_{50} value. (mean of three experiments).

A clear trend is evident from the lymphocyte mitochondria membrane potential assay (Table 3.6). Complex **25** compares to the $[Au(dppe)_2]Cl$ reference compound (**37**) in that a decrease of the membrane potential is correlated to an increase in the

concentration of the drug. It was seen to be more effective than **37** in reducing membrane potential and therefore comparable to the known membrane potential reduction agent valinomycin. Compound **46** on the other hand showed a huge decrease in membrane potential independant of the concentration of the administered drug. This reduction (about 60%) of membrane potential was more than that observed for valinomycin (about 50%). The concentration dependence of compounds **37** and **25** implies a reversible interaction with the membrane while the concentration independence of compound **46** may imply a less labile or permanent interaction and disruption.

The assay was repeated on the cancerous Jurkat cell line and the results are displayed in Table 3.7

	Concentration	**Absorbtion Ratio**	**Absorbtion/Control x 100%**
Control		486 ±76	100%
Valinomycin	10µM	365 ±23	75%
	0.1µM	373 ±21	77%
37 (Ref)	1.0µM	417 ±67	86%
	0.5µM	440 ±54	90%
	0.2µM	423 ±22	87%
	0.1µM	416 ±7	85%
25	10.0µM	482 ±127	99%
	5.0µM	451 ±52	93%
	2.0µM	459 ±86	94%
	1.0µM	457 ±78	94%
46	4.0µM	450 ±132	93%
	2.0µM	474 ±145	98%
	0.8µM	426 ±139	88%
	0.4µM	484 ±140	99%

Table 3.7: Jurkat mitochondrial membrane potential at 1x, 2x, 5x and 10x IC_{50} value. (mean of four experiments).

The results obtained for the mitochondrial membrane potential of Jurkat cells allows no meaningful interpretation. No significant decrease in membrane potential could be observed for any of the drugs at a range of concentrations while the valinomycin control still showed a reasonable decrease in membrane potential (about 25%), although not as pronounced as in the healthy cells.

3.4.2 Apoptosis and Necrosis Assay

The apoptosis assay was carried out on the Jurkat cell line to determine whether cell death occurred *via* apoptosis or necrosis. The absorption of Annexin V and propidium iodide (PI) is measured and is directly indicative of apoptosis or necrosis. In the early phase of apoptosis, the integrity of cell membrane is maintained but the cells lose membrane phospholipid asymmetry. Phosphatidylserine (PS), a negatively charged phospholipid located in the inner leaflet of the plasma membrane, is then exposed at the cell surface. Annexin V, which is a calcium and phospholipid binding protein, binds preferentially to PS.[172] Annexin V can, in the case of an apoptotic cell, bind to PS exposed on the outer cell membrane and gives an indication of cell death before cell lysing, while PI can only interact with cell DNA once the cell membranes are breached, making it possible for PI to move into cell (see also Table 3.8). Measurements were taken after 6, 24 and 48 hours, respectively. In order to clarify the apoptosis assay results, Figures 3.1, 3.2 and Table 3.8 have been constructed.

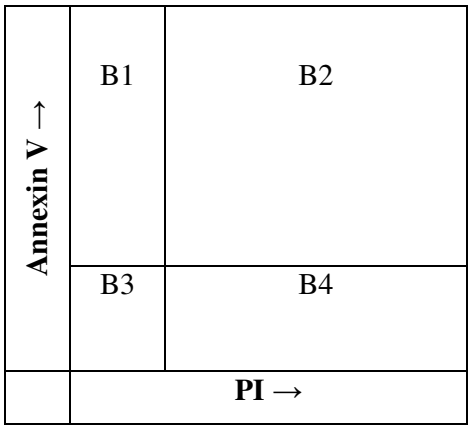

Figure 3.1: Legit of areas of distribution.

[172] www.beckmancoulter.com/eCatalog/CatalogItemDetails.do?productId=4745.

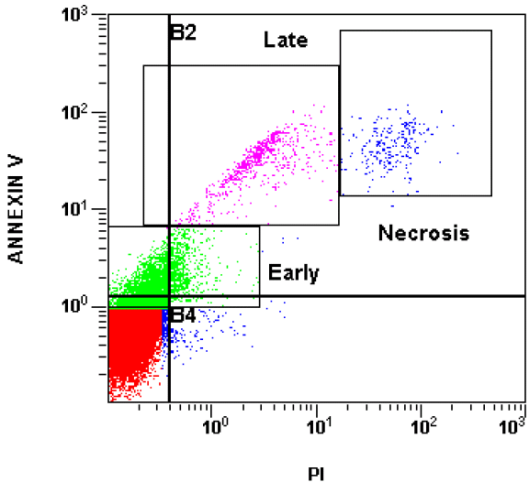

Figure 3.2: Example of a typical assay.

Block	Expression	Indication
B1	High Annexin V, Low PI	Early apoptosis
B2	High Annexin V, High PI	Late apoptosis, Early necrosis
B3	Low Annexin V, Low PI	Viable or healthy cells
B4	Low Annexin V, High PI	Late necrosis (*i.e.* cell fragments)
Early		Early Apoptosis
Late		Late Apoptosis
Necrosis		Early Necrosis

Table 3.8: Apoptosis or necrosis indication.

Results were obtained after 6, 24 and 48 hours incubation after drug administration (Appendix C) and a summary of results obtained is given in Tables 3.9, 3.10 and 3.11.

	Apoptosis Assay after 6 Hours							
	1 x IC_{50}				2 x IC_{50}			
	Control	**37** (Ref)	**25**	**46**	**Control**	**37** (Ref)	**25**	**46**
B1	23.47 ±15.82	28.59 ±20.19	31.31 ±12.65	19.13 ±14.90	20.04 ±5.84	34.14 ±8.98	34.72 ±9.35	26.54 ±7.35
B2	11.51 ±8.93	14.12 ±10.51	16.48 ±10.87	8.84 ±6.03	10.41 ±4.99	18.17 ±7.83	18.26 ±8.41	14.35 ±6.49
B3	64.55 ±23.63	56.44 ±29.08	52.04 ±21.68	69.26 ±15.87	69.13 ±9.17	47.56 ±15.86	46.83 ±15.53	58.87 ±13.66
B4	0.47 ±0.60	0.85 ±1.55	0.17 ±0.04	2.77 ±5.08	0.43 ±0.25	0.13 ±0.08	0.20 ±0.08	0.26 ±0.14
Early	37.71 ±25.55	39.68 ±26.90	48.78 ±14.74	32.01 ±22.59	36.47 ±9.60	51.74 ±10.07	53.51 ±8.91	44.93 ±8.21
Late	5.89 ±4.04	9.59 ±7.07	8.49 ±6.21	4.10 ±3.22	3.70 ±0.90	10.56 ±3.84	9.07 ±4.79	6.18 ±3.51
Necrosis	0.82 ±1.00	1.79 ±2.61	2.11 ±1.75	1.23 ±1.53	1.46 ±1.56	1.97 ±1.67	2.33 ±1.69	2.00 ±1.65

Table 3.9: Apoptosis results after a 6 hour incubation period

(mean of four experiments).

	Apoptosis Assay after 24 Hours							
	1 x IC_{50}				2 x IC_{50}			
	Control	**37** (Ref)	**25**	**46**	**Control**	**37** (Ref)	**25**	**46**
B1	14.11 ±4.37	14.02 ±4.73	12.06 ±9.67	10.21 ±4.68	12.85 ±13.27	13.73 ±2.12	12.98 ±6.98	12.58 ±9.79
B2	6.62 ±1.82	7.22 ±2.94	5.44 ±3.69	5.81 ±2.71	6.47 ±5.02	7.17 ±2.04	8.21 ±2.79	6.47 ±4.70
B3	78.57 ±3.33	77.90 ±2.62	81.28 ±11.24	83.15 ±7.29	80.11 ±18.19	78.44 ±2.72	78.10 ±9.11	79.36 ±13.09
B4	0.71 ±0.47	0.87 ±0.82	1.22 ±1.03	0.83 ±0.41	0.57 ±0.42	0.66 ±0.49	0.71 ±0.42	1.59 ±1.48
Early	27.83 ±6.18	27.55 ±7.11	22.95 ±16.47	21.61 ±8.89	23.82 ±21.45	26.78 ±3.24	25.43 ±11.81	25.36 ±18.99
Late	2.24 ±.046	2.66 ±1.00	1.74 ±1.17	1.72 ±0.44	2.45 ±1.83	2.84 ±0.67	3.55 ±1.50	1.48 ±0.98
Necrosis	0.87 ±0.42	0.97 ±0.64	0.83 ±0.76	0.88 ±0.38	0.64 ±0.55	1.27 ±0.68	1.12 ±0.46	0.83 ±0.68

Table 3.10: Apoptosis results after a 24 hour incubation period

(mean of four experiments).

	Apoptosis Assay after 48 Hours							
	1 x IC_{50}				2 x IC_{50}			
	Control	**37** (Ref)	**25**	**46**	**Control**	**37** (Ref)	**25**	**46**
B1	10.06 ±4.80	5.81 ±4.89	6.39 ±3.70	5.12 ±5.31	5.01 ±6.07	7.37 ±1.67	6.52 ±4.48	8.96 ±5.89
B2	7.84 ±3.27	5.33 ±3.47	7.54 ±3.36	5.85 ±5.27	5.93 ±5.34	8.83 ±4.05	6.41 ±1.65	5.85 ±3.41
B3	81.14 ±7.61	87.15 ±5.91	84.89 ±6.98	87.04 ±9.94	87.16 ±10.39	82.14 ±4.64	85.01 ±3.25	84.03 ±8.64
B4	0.97 ±0.42	1.71 ±1.44	1.19 ±0.26	1.99 ±1.08	1.91 ±1.54	1.67 ±0.75	2.06 ±2.78	1.16 ±0.42
Early	24.85 ±9.33	15.25 ±10.08	18.24 ±8.87	15.29 ±13.27	13.87 ±14.70	20.47 ±5.98	16.38 ±7.29	20.96 ±11.49
Late	1.94 ±0.41	1.61 ±1.19	2.03 ±0.58	1.18 ±0.85	1.31 ±1.45	2.65 ±1.03	2.75 ±2.40	1.44 ±1.01
Necrosis	0.64 ±0.09	0.71 ±0.74	0.62 ±.032	0.42 ±0.37	0.39 ±0.46	0.98 ±0.35	0.53 ±0.40	0.48 ±0.33

Table 3.11: Apoptosis results after a 48 hour incubation period (mean of four experiments).

No meaningful difference between treated cells and the untreated control could be established from the data obtained from the apoptosis assays. More work is needed to better understand the mode of cell death displayed by these compounds.

3.5. CONCLUSION

Toxicity studies were carried out on thirteen metal complexes of silver(I) and gold(I) and related to results of the known anti-tumour agent $[Au(dppe)_2]Cl$ (**37**). The most active complexes were found to be bridged gold and tetrahedral silver complexes. Five complexes were tested against various other cell lines to obtain a better toxicology profile. The bisphosphine-bridged gold complexes $ClAu((4\text{-}MeO)Ph)_2PN(Et)N(Et)P(Ph(4\text{-}OMe))_2AuCl$ (**25**) and the bischelated silver complex $[(((4\text{-}MeO)Ph)_2PN(Me)N(Me)P(Ph(4\text{-}OMe))_2)_2\ Ag]^+.NO_3^-$ **46** were seen to exhibit the best specificities and subsequently were used in mitochondria membrane potential and apoptosis assays. These two assays, unfortunately, did not yield conclusive results. Although proving to be more selective than the reference

compound (**37**) the complexes tested did not exhibit profound selectivity and thus did not warrant further investigation.

Chapter 4

Chemical Experimental Procedures

4.1 GENERAL

4.1.1 Solvents

All solvents used were chemically pure or pre-purified. Solvents were distilled from drying agents and degassed. Solvents were stored under argon or nitrogen over molecular sieves. All other reagents were purchased analytically pure or synthetically pure.

4.1.2 Group 11 Transition Metals

Gold metal was obtained from Harmony Gold and further synthesis of gold precursors was done as described later in this chapter. Silver nitrate was obtained from Sigma Aldrich.

4.1.3 Instrumentation

4.1.3.1 Nuclear Magnetic Resonance Spectroscopy (NMR)

NMR spectra were recorded on either a Bruker Avance 300MHz or a Bruker Avance DRX 400MHz spectrometer. All NMR spectra were obtained from solutions in deuterochloroform ($CDCl_3$) or deutero dimethyl sulphoxide (*d*-DMSO). The peak multiplicity of the signals are abbreviated as follows: bs - broad singlet, d - doublet, dd - doublet of doublets, dt - doublet of triplets, t - triplet, td - triplet of doublets, p - pentet, q - quartet, m – multiplet, s - singlet. The coupling constants (*J*) is calculated

in Hertz and reported to the nearest 0.1 Hz.

^{1}H-NMR data are listed in order: Chemical shift (δ, reported in ppm and referenced to the residual solvent peak of $CDCl_3$ [δ = 7.26 ppm] or *d*-DMSO [δ = 2.54 ppm][173]), multiplicity, coupling constants, related compound proton assignment. Proton decoupled ^{13}C-NMR data are reported in the order: Chemical shift (δ, reported in ppm and referenced to the residual solvent peak of $CDCl_3$ [δ = 77.00 ppm] or *d*-DMSO [δ = 40.45 ppm][173]), multiplicity (due to C-P spin coupling), coupling constants, related compound carbon assignment. ^{31}P-NMR data are listed as chemical shift (δ, reported in ppm and referenced to phosphoric acid [δ = 0.00 ppm]).

4.1.3.2 Single Crystal X-Ray Diffraction

Intensity data were collected on a Bruker SMART 1K CCD area detector diffractometer with graphite monochromated Mo K_α radiation (40kV, 40mA). The collection method involved ω-scans of width 0.3°. Data reduction was carried out using the program *SAINT+*[174] and absorption corrections were made using the program *SADABS*.[174]

The crystal structures were solved by direct methods using *SHELXTL*.[175] Non-hydrogen atoms were first refined isotropically followed by anisotropic refinement by full matrix least-squares calculations based on F^2 using *SHELXTL*. Hydrogen atoms were first located in the difference map then positioned geometrically and allowed to ride on their respective parent atoms. Diagrams and publication materials were generated using *SHELXTL, PLATON,*[176] *MERCURY*[177] and *ORTEP*[178].

---

[173] H.E.Gottlieb, V. Kotlyar, A. Nudelman, *J. Org. Chem.*, **1997**, 62, 7512.
[174] Bruker, *SAINT-Plus*, Version 6.02 (includes *XPREP* and *SADABS*), Bruker AXS Inc., Madison, Wisconsin, USA, **1999**.
[175] G.M. Sheldrick, *SHELXL-97* release 97-2, University of Göttingen, Germany, **1997**.
[176] A.L. Spek, *Platon* version 200905, Utrecht University, Padualaan 8, 3584 CH Utrecht, The Netherlands, Copyright © **1980-2006**.
[177] *Mercury 1.4*, The Cambridge Crystallographic Data Centre, 12 Union Road, Cambridge, CB2 1EZ, UK Copyright © **2004**.

4.1.3.3 Mass Spectroscopy

EI and FAB-MS spectra were collected using a VG70-SEQ mass spectrometer in positive ion mode.

4.1.3.4 Elemental Analysis

Elemental analyses were determined on either a Thermo Flash EA1112 CHNS-O elemental analyser by the University of Cape Town or by the Institute for Soil, Climate and Water, Pretoria, South Africa on a Carlo Erba NA1500 Nitrogen/Carbon/Sulphur Analyser which has been modified to allow CHN analysis.

4.2 LIGAND SYNTHESIS

4.2.1 Ligand Precursor Synthesis

Bis(dichlorophosphino)dimethylhydrazine (**2**)[19,25] and bis(dichlorophosphino)-diethylhydrazine (**6**)[29] were synthesised by heating under reflux, 2g of dimethylhydrazine dihydrochloride or diethylhydrazine dihydrochloride in 25ml phosphorous trichloride. Heating under reflux conditions was discontinued when most of the starting material (white solid) had dissolved, but only small amounts of phosphorous oxides (orange solids) had formed. Reflux heating was carried out for periods between 8 to 48 hours. Excess phosphorous trichloride was removed by vacuum distillation and recycled. Dry ether was added to the liquid products and phosphorous oxides and the mixture left for 15 minutes to allow complete precipitation of all solids. The liquid phase was decanted and the ether removed *in vacuo* to afford the pure products as colourless liquids in >90% yield. The products were stored under argon.

---

[178] L.J. Farrugia, *ORTEP-3* for Windows version 1.08, Department of Chemistry, Joseph Black Building, University of Glasgow, Glasgow G12 8QQ, Copyright © **1997-2005**.

4.2.1.1 Bis(dichlorophosphino)dimethylhydrazine (2)

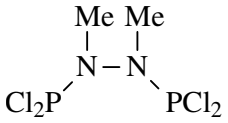

Properties:

- Slightly milky, colourless or yellow liquid
- Air sensitive with slow degradation
- Stored under argon in a Schlenk tube

Characterisation:

^{1}H NMR: ($CDCl_3$, 300 MHz) δ_H 3.13 (t, $\underline{CH_3}$, ^{3}J (H^{1}-P^{31}) = 3.7 Hz, 6H)

^{13}C NMR: ($CDCl_3$, 75 MHz) δ_C 33.4 (d, $\underline{CH_3}$, ^{2}J (C^{13}-P^{31}) = 1.8 Hz)

^{31}P NMR: ($CDCl_3$, 162 MHz) δ_P 160.9

4.2.1.2 Bis(dichlorophosphino)diethylhydrazine (6)

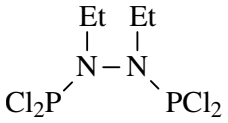

Properties:

- Colourless or slightly yellow liquid
- Air sensitive with slow degradation
- Stored under argon in a Schlenk tube

Characterisation:

^{1}H NMR: ($CDCl_3$, 300 MHz) δ_H 3.75 and 3.23 (m, $\underline{CH_2}CH_3$, 4H), 1.27 (t, $CH_2\underline{CH_3}$, ^{3}J (^{1}H-^{1}H) = 7.1 Hz, 6H)

^{13}C NMR: ($CDCl_3$, 75 MHz) δ_C 42.2 (s, $\underline{CH_2}CH_3$), 14.0 (s, $CH_2\underline{CH_3}$),

^{31}P NMR: ($CDCl_3$, 162 MHz) δ_P 156.3

4.2.2 Grignard Reagents

Magnesium shavings were activated by washing with diluted hydrochloric acid, followed by washing with ethanol and acetone and drying *in vacuo.* Activated magnesium was stored under argon.

5 g of activated magnesium shavings were stirred in 75 ml dry ether or dry THF and an iodine crystal was added. 1 equivalent of either bromobenzene, 4-bromoanisole or 4-bromo-*N,N*-dimethyl aniline dissolved in 25 ml was added drop-wise at a rate to keep the solution under constant reflux.[179] The solution was left to stir overnight. The resulting Grignard reagent was stored under argon in the fridge without further filtration.

4.2.2.1 Phenylmagnesium Bromide (53)

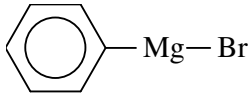

Properties:

- 2M solution in ether
- Brown liquid
- Air sensitive, pyrophoric
- Stored in a Schlenk tube under argon in the fridge

[179] J. March, *Advanced Organic Chemistry*, 4th Ed., Wiley-Interscience Publication, **1992**, 622.

4.2.2.2 4-Anisolmagnesium Bromide (54)

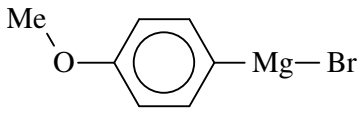

Properties:

- 2M solution in THF
- Brown liquid
- Air sensitive, pyrophoric
- Stored in a Schlenk tube under argon in the fridge

4.2.2.3 N,N-dimethyl-4-anilinemagnesium Bromide (55)

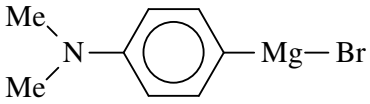

Properties:

- 2M solution in THF
- Brown liquid
- Air sensitive, pyrophoric
- Stored in a Schlenk tube under argon in the fridge

4.2.3 Ligand Synthesis

Ligands **13** - **18** were all synthesised in a similar manner to published methods.[19,29] 1 equivalent of bis(dichlorophosphino)dimethylhydrazine (**2**) or bis(dichloro-phosphino)diethylhydrazine (**6**) was dissolved in dry ether for **13** and **14,** or dry THF for **15** - **18**. The solution was cooled to 0 ^{o}C in an ice bath and 4.1 equivalents of the corresponding cold Grignard reagent were slowly added while stirring vigorously. The reaction mixture was left to warm to room temperature overnight. The reaction mixture was added to cold brine while stirring vigorously. The two phases were separated by means of a separation funnel and the organic phase was dried with

anhydrous magnesium sulphate, filtered and reduced *in vacuo* to yield the desired product. The product was stored under argon.

4.2.3.1 Bis(diphenylphosphino)dimethylhydrazine (13)

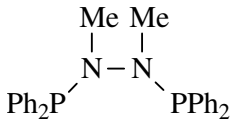

Reaction:

- **2**: 3.480 g (13.3 mmol)
- **54**: 27.2 ml (54,5 mmol)
- Diethylether: 100 ml
- Yield: 72 %

Properties:

- Sticky yellow liquid
- Air sensitive with slow degradation
- Stored under argon in a Schlenk tube

Characterisation:

^{1}H NMR: ($CDCl_3$, 300 MHz) δ_H 7.39 (bs, Arom, 8H), 7.23 (bs, Arom, 12H), 2.66 (bs, $\underline{CH}_3$, 6H)

^{13}C NMR: Due to sample breakdown ^{13}C could not be done

^{31}P NMR: ($CDCl_3$, 162 MHz) δ_P 63.3

MS: 429 (10%, M + H), 214 (43%, $MeNPPh_2$), 185 (100%, PPh_2)

4.2.3.2 Bis(diphenylphosphino)diethylhydrazine (14)

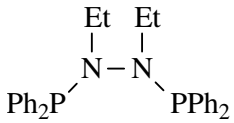

Reaction:

- **6**: 2.957 g (10.2 mmol)
- **54**: 20.9 ml (41.8 mmol)
- Diethyl ether: 100 ml
- Yield: 86 %

Properties:

- Yellow sticky solid or crystalline flakes
- Decomposes slowly in air
- Stored under argon in a Schlenk tube

Characterisation:

^{1}H NMR: ($CDCl_3$, 300 MHz) δ_H 7.54 (bs, Arom, 4H), 7.36 (bs, Arom, 4H), 7.26 (m, Arom, 12H), 3.23 (m, $\underline{CH_2}CH_3$, 4H), 0.79 (t, $CH_2\underline{CH_3}$, ^{3}J (^{1}H-^{1}H) = 7.0 Hz, 6H)

^{13}C NMR: ($CDCl_3$, 75 MHz) δ_C 140.2 (m, Arom), 133.4 (m, *o*-Ph), 131.4 (s, Arom), 128.7 (s, Arom), 48.7 (t, $\underline{CH_2}CH_3$, ^{2}J (^{13}C-^{31}P) = 2.5 Hz), 14.3 (d, $CH_2\underline{CH_3}$, ^{3}J (^{13}C-^{31}P) = 4.1 Hz)

^{31}P NMR: ($CDCl_3$, 162 MHz) δ_P 63.4

MS: 427 (9%, M – H), 214 (81%, $MeNPPh_2$), 185 (100%, PPh_2)

MP: 95-96 ^{o}C

4.2.3.3 Bis(di(4-methoxyphenyl))dimethylhydrazine (15)

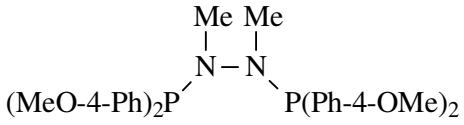

Reaction:

- **2**: 1.567 g (6.0 mmol)
- **55**: 12.3 ml (24.5 mmol)
- THF: 75 ml
- Yield: 74 %

Properties:

- Yellow sticky liquid
- Air sensitive with slow degradation
- Stored under argon in a Schlenk tube

Characterisation:

^{1}H NMR: ($CDCl_3$, 300 MHz) δ_H 7.32 (bs, Arom, 8H), 6.81 (d, Arom, ^{3}J (^{1}H-^{1}H) = 8.4 Hz, 8H), 3.73 (s, O$\underline{CH_3}$, 12H), 2.60 (s, N$\underline{CH_3}$, 6H)

^{13}C NMR: ($CDCl_3$, 75 MHz) δ_C 160.3 (s, Arom), 134.2 (m higher order, Arom), 131.1 (bs, Arom), 114.2, (m, Arom), 55.5 (s, O$\underline{CH_3}$), 38.1 (m, N$\underline{CH_3}$)

^{31}P NMR: ($CDCl_3$, 121 MHz) δ_P 61.4

MS: No useful information could be obtained

4.2.3.4 Bis(di(4-methoxyphenyl))diethylhydrazine (16)

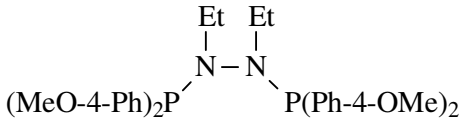

Reaction:

- **6**: 2.341 g (8.1 mmol)
- **55**: 16.6 ml (33.1 mmol)
- THF: 100 ml
- Yield: 75 %

Properties:

- Yellow sticky liquid
- Air sensitive
- Stored under argon in a Schlenrok tube

Characterisation:

^{1}H NMR: ($CDCl_3$, 300 MHz) δ_H 7.44 (m, Arom, 4H), 7.26 (m, Arom, 4H), 6.80 (m, Arom, 8H), 3.71 (s, O$\underline{CH_3}$, 12H), 2.99 (m, $CH_2\underline{CH_3}$, 6H), 0.88 (t, $CH_2\underline{CH_3}$, ^{3}J (^{1}H-^{1}H) = 5.4 Hz, 4H)

^{13}C NMR: Due to sample break down ^{13}C could not be done

^{31}P NMR: ($CDCl_3$, 121 MHz) δ_P 61.0

MS: No useful information could be obtained

4.2.3.5 Bis(di(N,N-dimetyl-4-aminophenyl))dimethylhydrazine (17)

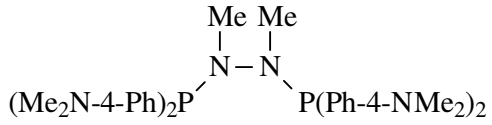

Reaction:

- **2**: 2.556 g (9.8 mmol)
- **56**: 20 ml (40.0 mmol)
- THF: 100 ml
- Yield: 82 %

Properties:

- Yellow sticky liquid
- Air sensitive
- Stored under argon in a Schlenk tube

Characterisation:

^{1}H NMR: ($CDCl_3$, 400 MHz) δ_H 7.44 (bs, Arom, 8H), 6.79 (d, Arom, ^{3}J (^{1}H-^{1}H) = 8.3 Hz, ^{3}J (^{1}H-^{31}P) = 17.5 Hz, 8H), 3.01 (s, N($\underline{CH_3}$)$_2$, 24H), 2.74 (bs, N$\underline{CH_3}$, 6H)

^{13}C NMR: Due to sample break down ^{13}C could not be done

^{31}P NMR: ($CDCl_3$, 162 MHz) δ_P 61.5

MS: 271 (58%, P($PhNMe_2$)$_2$), 120 (100%, $PhNMe_2$)

4.2.3.6 Bis(di(N,N-dimetyl-4-aminophenyl))diethylhydrazine (18)

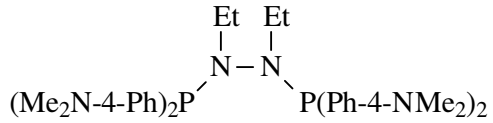

Reaction:

- **6**: 3.158 g (10.9 mmol)
- **56**: 20 ml (44.7 mmol)
- THF: 100 ml
- Yield: 90 %

Properties:

- Yellow sticky liquid
- Air sensitive
- Stored under argon in a Schlenk tube

Characterisation:

^{1}H NMR: ($CDCl_3$, 400 MHz) δ_H 7.52 (bs, Arom, 4H), 7.31 (bs, Arom, 4H), 6.70 (t, J (^{1}H-^{31}P) = 6.0 Hz, Arom, 8H), 2.96 (m, N($\underline{CH_3}$)$_2$, 24H), 3.1 (m, $\underline{CH_2}CH_3$, 4H), 0.92 (t, ^{3}J (^{1}H-^{1}H) = 7.0 Hz, $CH_2\underline{CH_3}$, 6H)

^{13}C NMR: ($CDCl_3$, 75 MHz) δ_C 149.23 (m, Arom), 133.67 (m, Arom), 131.65 (m Arom), 111,01 (m, Arom), 46.9 (s, $\underline{CH_2}CH_3$), 38.97 (m, N($\underline{CH_3}$)$_2$), 13.41 (s, $CH_2\underline{CH_3}$)

^{31}P NMR: ($CDCl_3$, 162 MHz) δ_P 60.4

MS: 271 (42%, P(PhNMe$_2$)$_2$), 120 (100%, PhNMe$_2$)

4.3 GOLD PRECURSOR SYNTHESIS

4.3.1 Auric acid hydrate (56)

Gold pellets were dissolved in *aqua regia* overnight. The resulting solution was dried *in vacuo*, washed with HCl and dried again until bright yellow crystals of $HAuCl_4.4H_2O$ remained.[180,181]

4.3.2 Dimethylsuphidegold(I) chloride (57)

Auric acid hydrate (**56**) (approx. 5 g) was dissolved in water and zinc powder was added until very finely divided gold particles precipitated. The excess zinc was dissolved with HCl. The solid gold particles were isolated by filtration and placed in a 200 ml round bottomed flask. 50 ml of DMSO and 25 ml HCl were added and the mixture was stirred under reflux for 1 – 2 days. The mixture was cooled down to –20 ^oC and the resulting white precipitate and the gold particles were removed by filtration. The white precipitate was dissolved in DCM and the solid gold particles filtered out. Hexane was added to the DCM solution to precipitate $(SMe_2)AuCl$ as a white micro-crystalline powder.[180,182,183]

4.3.2 Tetrahydrothiophenegold(I) chloride (58)

Auric acid hydrate (**56**) (approx. 2 g) was dissolved in ethanol. Tetrahydrothiophene (THT) was added dropwise to the stirred solution, until the yellow colour disappeared and only a white precipitate remained. The precipitate was left to settle and the ethanol-THT mixture was decanted. The complex was washed with ethanol and the precipitate was dried *in vacuo* to yield (THT)AuCl as a white powder.[180,184]

---

[180] In-house publication, Project AuTEK Biomed, Mintek.
[181] A. Haas, J. Helmbrecht, U. Niemann, in *Handbuch der Präparativen Anorganischen Chemie*, Ed. G Brauer, Verlag Stuttgart, Stuttgart **1978**, 1014.
[182] T.E. Müller, J.C. Green, D.M.P. Mingos, C.M. McPartlin, C. Wittingham, D.J. Williams, T.M. Woodroffe, *J. Organomet. Chem.*, **1998**, 551, 313.
[183] K.C. Dash, H. Schmidbaur, *Chem. Ber.*, **1973**, 106, 1221.
[184] R. Uson, A. Laguna, J. Vicente, *J. Organomet. Chem.*, **1977**, 131, 471.

4.4 COMPLEX SYNTHESIS

4.4.1 Synthesis of Bridged-Gold Complexes

Tetrahydrothiophenegold(I) chloride [(THT)AuCl] (**57**) or dimethylsulphide(I)gold chloride [(Me_2S)AuCl] (**58**) (1 equivalent) was suspended in THF. 0.5 equivalents of ligand **13** or **14** dissolved in DCM was added to the stirred suspension. The suspension turned yellow and after a short time micro crystals started to form. The solvent was removed *in vacuo* to afford the products **22** and **23** as micro-crystalline powders, respectively. For ligands **15**, **16** and **18** the reaction was carried out in DCM and afforded complexes **24**, **25** and **27**. By addition of a few drops of THF it was possible to grow crystals overnight. Complexation of gold to ligand **17** failed in both DCM and THF due to the breakdown of the ligand upon mixing with the gold precursor.

4.4.1.1 Bis(diphenylphosphino)dimethylhydrazine di(gold chloride) (22)

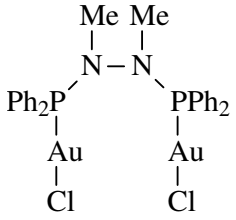

Reaction:

- **13**: 146 mg (0.34 mmol)
- **58**: 200 mg (0.68 mmol)
- THF: 2 ml
- DCM: 5 ml
- Yield: 89 %

Properties:

- Grey crystals or white precipitate
- Stable in air
- Crystals are insoluble in organic and highly polar solvents

Characterisation:

^{1}H NMR: ($CDCl_3$, 300 MHz) δ_H 7.85 (dd, Arom, *J* (^{1}H-^{31}P) = 13.2, *J* (^{1}H-^{1}H) = 8.1), 7.52 (t, Arom, *J* (^{1}H-^{1}H) = 9.40 Hz), 7.40 (dd, Arom, *J* (^{1}H-^{31}P) = 17.7, *J* (^{1}H-^{1}H) = 7.4), 2.76 (d, $\underline{CH}_3$, ^{3}J = 7.8 Hz)

^{13}C NMR: Compound too insoluble in NMR solvents

^{31}P NMR: ($CDCl_3$, 121 MHz) δ_P 87.1

MS: No useful information could be obtained

EA: Calc: ($Au_2Cl_2P_2N_2C_{26}H_{26}$) C 34.96 %, H 2.93 %, N 3.14 %

Found: C 35.29 %, H 2.93 %, N 3.13 %

MP: 228 - 230 °C

4.4.1.2 Bis(diphenylphosphino)diethylhydrazine di(gold chloride) (23)

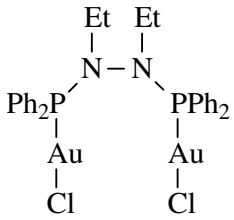

Reaction:

- **14**: 155 mg (0.34 mmol)
- **58**: 200 mg (0.68 mmol)
- THF: 5 ml
- Yield: 86 %

Properties:

- Colourless to grey crystals
- Stable in air

Characterisation:

^{1}H NMR: (*d*-DMSO, 300 MHz) 7.90 (dq, Arom, *J* (^{1}H-^{31}P) = 28.9, *J* (^{1}H-^{1}H) = 7.1 Hz), 7.71 (d, Arom, *J* = 7.0 Hz), 7.60 (d, Arom, *J* = 7.1 Hz), 7.55 (d, Arom, *J* (^{1}H-^{1}H) = 7.0 Hz), 3.33 (bs, $\underline{CH_2}CH_3$), 0.43 (t, $CH_2\underline{CH_3}$, ^{3}J (^{1}H-^{1}H) = 6.6 Hz)

^{13}C NMR: (*d*-DMSO, 75 MHz) δ_C 132.3 (bs, Arom), 130.6 (m, Arom), 129.0 (s, Arom), 128.0 (bs, Arom), 43.6 (bs, $\underline{CH_2}CH_3$), 14.1 (d, $CH_2\underline{CH_3}$, ^{3}J (^{13}C-^{31}P) = 16.1 Hz)

^{31}P NMR: (*d*-DMSO, 121 MHz) δ_P 87.7

MS: 920 (2%, M), 885 (14%, M - Cl)

EA: Calc: ($Au_2Cl_2P_2N_2C_{28}H_{30}$) C 36.50 %, H 3.28 %, N 3.04 %

Found: C 35.42 %, H 3.44 %, N 2.64 %

MP: 202 - 204 °C

4.4.1.3 Bis(di(4-methoxyphenyl)phosphino)dimethylhydrazine di(gold chloride) (24)

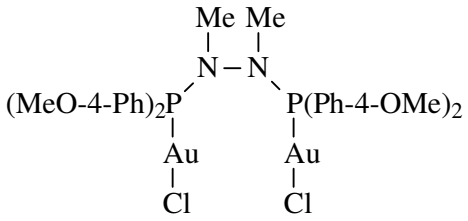

Reaction:

- **15**: 167 mg (0.29 mmol)
- **59**: 200 mg (0.57 mmol)
- DCM: 5 ml
- THF: few drops
- Yield: 75 %

Properties:

- Colourless to grey crystals
- Stable in air

Characterisation:

^{1}H NMR: ($CDCl_3$, 300 MHz) δ_H 7.79 (t, Arom, *J* = 8.2 Hz, 4H) 7.41 (t, Arom, *J* = 8.2 Hz, 4H), 6.97 (d, Arom, *J* = 7.6 Hz, 4H), 6.81 (d, Arom, *J* = 7.6 Hz, 4H), 3.86 (s, OMe, 6H), 3.81 (s, OMe, 6H), 2.69 (d, N$\underline{CH_3}$, ^{3}J (^{1}H-^{31}P) = 5.8 Hz, 6H)

^{13}C NMR: ($CDCl_3$, 75 MHz) δ_C 163.5 (d, Arom, *J* = 33.4 Hz), 135.9 (m, Arom), 115.3 (m, Arom), 55.52 and 55.45 (s, O$\underline{CH_3}$), 35.1 (s, N$\underline{CH_3}$)

^{31}P NMR: ($CDCl_3$, 121 MHz) δ_P 85.1

MS: 977 (83 %, M - Cl), 245 (80%, $P(PhOMe)_2$)

EA: Calc: ($Au_2Cl_2P_2O_4N_2C_{30}H_{34}$) C 35.56 %, H 3.38 %, N 2.76 %

Found: C 36.78 %, H 3.79 %, N 2.47 %

MP: 166 – 170 ^{o}C

4.4.1.4 Bis(di(4-methoxyphenyl)phosphino)diethylhydrazine di(gold chloride) (25)

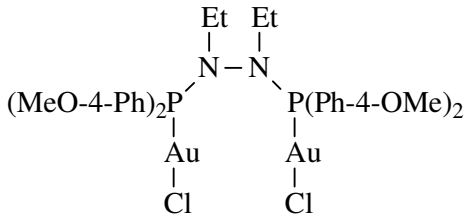

Reaction:

- **16**: 159 mg (0.29 mmol)
- **59**: 200 mg (0.57 mmol)
- DCM: 5 ml
- THF: few drops
- Yield: 80 %

Properties:

- Grey crystals or purple precipitate
- Stable in air

Characterisation:

^{1}H NMR: ($CDCl_3$, 400 MHz) δ_H 7.16 (m, Arom), 6.64 (m, Arom), 3.73 (s, OCH_3), 2.58 (bs, $\underline{CH_2}CH_3$, 4H), 1.78 (m, $CH_2\underline{CH_3}$, 6H)

^{13}C NMR: Due to sample breakdown ^{13}C could not be done

^{31}P NMR: ($CDCl_3$, 121 MHz) δ_P 84.7

MS: 1004 (100%, M - Cl)

EA: Calc: ($Au_2Cl_2P_2O_4N_2C_{32}H_{38}$) C 36.91 %, H 3.68 %, N 2.69 %

Found: C 37.02 %, H 3.91 %, N 1.94 %

MP: 96 – 97 ^{o}C

4.4.1.5 Bis(di(N,N-dimetyl-4-aminophenyl)phosphino)dimethylhydrazine di(gold chloride) (26)

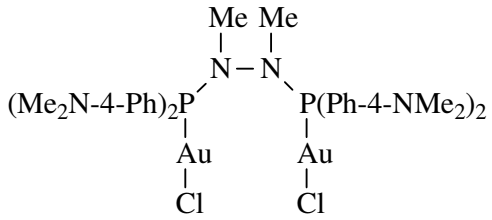

The complex could not be prepared due to the breakdown of the ligand during complexation.

4.4.1.6 Bis(di(N,N-dimetyl-4-aminophenyl)phosphino)diethylhydrazine di(gold chloride) (27)

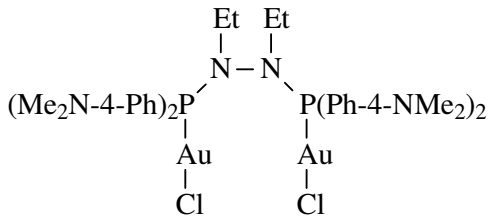

Reaction:

- **18**: 182 mg (0.29 mmol)
- **59**: 200 mg (0.57 mmol)
- DCM: 5 ml
- Yield: 86 %

Properties:

- Purple-blue in reaction solution
- Green powder after solvent removal, becomes black over time
- Stored under argon in a Schlenk tube

Characterisation:

^{1}H NMR: (*d*-DMSO, 400 MHz) δ_H 7.61 (m, Arom, 8H), 6.87 (d, ^{3}J (^{1}H-^{1}H) = 7.6 Hz, Arom, 4H), 6.72 (d, ^{3}J (^{1}H-^{1}H) = 7.6 Hz, Arom, 4H), 3.16 (bs, $\underline{CH_2}CH_3$, 4H), 3.01 and 2.96 (s, $N(CH_3)_2$, 24 H), 0.85 (t, ^{3}J (^{1}H-^{1}H) = 6.8 Hz, $CH_2\underline{CH_3}$, 6H)

^{13}C NMR: Due to sample breakdown ^{13}C could not be done

^{31}P NMR: (*d*-DMSO, 162 MHz) δ_P 83.5

MS: 1057 (M - Cl), 271 (100%, $P(PhNMe_2)_2$)

EA: Calc: ($Au_2Cl_2P_2N_6C_{36}H_{50}$) C 39.54 %, H 4.61 %, N 7.68 %
Found: Large deviations from calculated where observed

MP: 170 – 172 ^{o}C

4.4.2 Synthesis of Bischelated Gold Complexes

Tetrahydrothiophenegold(I) chloride [(THT)AuCl] (**57**) or dimethylsulphidegold(I) chloride [(Me_2S)AuCl] (**58**) (1 equivalent) was suspended in THF. To the stirred suspension was added 2 equivalents of ligand (**13** - **18**) in THF or DCM. The suspension turned yellow (except for complexes **32** and **34**, which turned bright red over time). The solvent was removed *in vacuo* to afford the products as solids.

4.4.2.1 Bis(bis(diphenylphosphino)dimethylhydrazine) gold chloride (28)

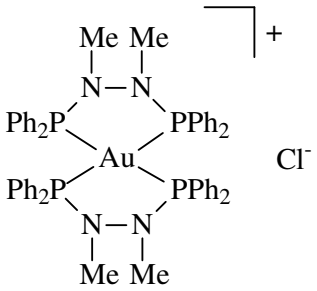

Reaction:

- **13**: 291 mg (0.68 mmol)
- **58**: 100 mg (0.34 mmol)
- THF: 2 ml
- DCM: 5 ml
- Yield: 86 %

Properties:

- Yellow solid
- Decomposes slowly in air
- Hygroscopic
- Stored under argon in a Schlenk tube

Characterisation:

^{1}H NMR: ($CDCl_3$, 300 MHz) δ_H 7.33 (t, Arom, ^{3}J (^{1}H-^{1}H) = 7.6 Hz, 8H), 7.21 (t, Arom, coupling not resolved, 16H), 7.12 (t, Arom, J (^{1}H-^{1}H) = 7.6 Hz, 16H), 2.69 (t, coupling not resolved, N$\underline{CH_3}$, 12H)

^{13}C NMR: Due to sample break down, ^{13}C could not be done

^{31}P NMR: ($CDCl_3$, 121 MHz) δ_P 83.9

MS: 1053 (100 %, M - Cl)

EA: Calc: ($AuClP_4N_4C_{52}H_{52}$) C 57.34 %, H 4.81 %, N 5.14 %
Found: Large deviations from calculated where observed

MP: 84 - 86 ^{o}C

4.4.2.2 Bis(bis(diphenylphosphino)diethylhydrazine) gold chloride (29)

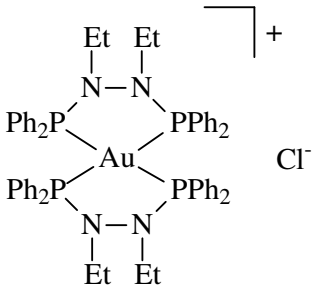

Reaction:

- **14**: 310 mg (0.68 mmol)
- **58**: 100 mg (0.34 mmol)
- THF: 5 ml
- Yield: 92 %

Properties:

- Yellow Solid
- Decomposes slowly in air
- Hygroscopic
- Stored under argon in a Schlenk tube

Characterisation:

^{1}H NMR: (*d*-DMSO, 300 MHz) δ_H 7.84 (m, Arom, 16H), 7.36 (m, Arom, 24H), 2.94 (m, $\underline{CH_2}CH_3$, 8H), 0.96 (t, $CH_2\underline{CH_3}$, ^{3}J (^{1}H-^{1}H) = 6.9 Hz, 12H)

^{13}C NMR: (*d*-DMSO, 100.6 MHz) δ_C 132.5 (m, Arom), 131.9 (m, Arom), 130.5 (m, Arom), 128.7 (m, Arom), 46.3 (d, $\underline{CH_2}CH_3$, ^{2}J (^{13}C-^{31}P)= 22.5 Hz), 14.1 (m, $CH_2\underline{CH_3}$)

^{31}P NMR: (*d*-DMSO, 121 MHz) δ_P 86.5

MS: 1109 (75 %, M - Cl)

EA: Calc: ($AuClP_4N_4C_{52}H_{52}$) C 58.72 %, H 5.28 %, N 4.89 %
Found: Large deviations from calculated where observed

MP: 109 - 110 ^{o}C

4.4.2.3 Bis(bis(di(4-methoxyphenyl)phosphino)dimethylhydrazine) gold chloride (30)

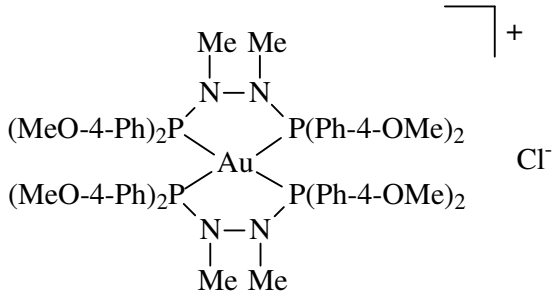

Reaction:

- **15**: 310 mg (0.57 mmol)
- **59**: 100 mg (0.29 mmol)
- THF: 5 ml
- Yield: 83 %

Properties:

- Bright yellow solid
- Decomposes slowly in air
- Slightly Hygroscopic
- Stored under argon in a Schlenk tube

Characterisation:

^{1}H NMR: ($CDCl_3$, 300 MHz) δ_H 7.16 (d, ^{3}J (^{1}H-^{1}H) = 7.6 Hz, Arom, 16H), 6.64 (d, ^{3}J (^{1}H-^{1}H) = 8.5 Hz, Arom, 16H), 3.73 (s, O$\underline{CH_3}$, 24H), 2.58 (bs, N$\underline{CH_3}$, 12H)

^{13}C NMR: ($CDCl_3$, 75 MHz) δ_C 161.9 (BS, Arom), 134.2 (m, Arom), 126.0 (m, Arom), 114.6 (s, Arom), 55.6 (bs, O$\underline{CH_3}$), 37.4 (s, N$\underline{CH_3}$)

^{31}P NMR: ($CDCl_3$, 121 MHz) δ_P 81.9

MS: 1293 (85 %, M - Cl), 274 (54 %, MeNP(PhOMe)$_2$), 245 (98 %, P(PhOMe)$_2$), 138 (100 %, P(PhOMe))

EA: Calc: ($AuClP_4O_8N_4C_{60}H_{68}$) C 54.20 %, H 5.16 %, N 4.21 %
Found: C 51.10 %, H 4.96 %, N 3.72 %

MP: 96 - 97 ^{o}C

4.4.2.4 Bis(bis(di(4-methoxyphenyl)phosphino)diethylhydrazine) gold chloride (31)

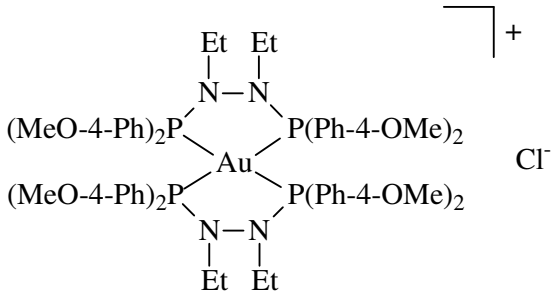

Reaction:

- **16**: 312 mg (0.57 mmol)
- **59**: 100 mg (0.29 mmol)
- THF: 5 ml
- Yield: 90 %

Properties:

- Bright orange solid
- Decomposes slowly in air
- Slightly Hygroscopic
- Stored under argon in a Schlenk tube

Characterisation:

^{1}H NMR: ($CDCl_3$, 300 MHz) δ_H 7.73 (Arom, 4H), 6.95 (Arom, 4H); 3.84 and 3.86 (s, O$\underline{CH_3}$, 6H), 3.46 (m, $\underline{CH_2}CH_3$, 1H), 3.27 (m, $\underline{CH_2}CH_3$, 1H) 0.79 (t, CH_3, 3H, J = 2.1 Hz)

^{13}C NMR: Due to sample breakdown ^{13}C could not be done

^{31}P NMR: ($CDCl_3$, 121 MHz) δ_P 83.9

MS: 1349 (25 %, M - Cl), 138 (100 %, P(PhOMe))

EA: Calc: ($AuClP_4O_8N_4C_{62}H_{72}$) C 55.48 %, H 5.53 %, N 4.04 %
Found: Large deviations from calculated where observed

MP: 89 – 92 ^{o}C

4.4.2.5 Bis(bis(di(N,N-dimethyl-4-aminophenyl)phosphino)dimethylhydrazine) gold chloride (32)

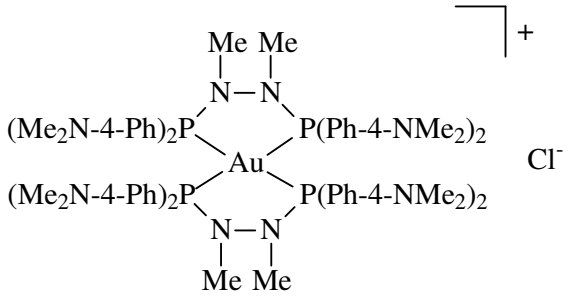

The complex could not be prepared due to the breakdown of ligand during complexation.

4.4.2.6 Bis(bis(di(N,N-dimethyl-4-aminophenyl)phosphino)diethylhydrazine) gold chloride (33)

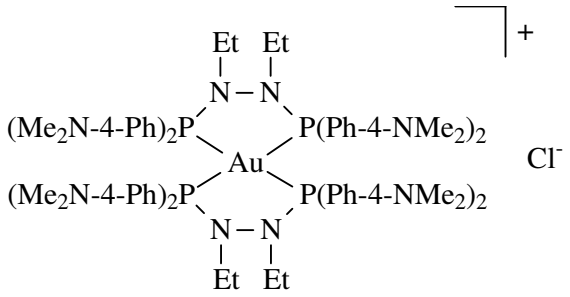

Reaction:

- **18**: 358 mg (0.57 mmol)
- **59**: 100 mg (0.29 mmol)
- THF: 5 ml
- Yield: 90 %

Properties:

- Yellow solid, turns red overtime
- Decomposes slowly in air
- Stored under argon in a Schlenk tube

Characterisation:

Yellow compound

^{31}P NMR: ($CDCl_3$, 161.98 MHz) δ_P 84.9

Red compound

^{31}P NMR: ($CDCl_3$, 161.98 MHz) δ_P 96.5

MS: 1491 (9%, M + 2), 825 (100%, L + Au)

MP: 142 – 143 ^{o}C

4.4.3 Synthesis of Bridged-Silver Complexes

Silver nitrate (1 equivalent) was suspended in THF or dissolved in acetonitrile. To the stirred suspension were added 0.5 equivalents of ligand (**13** - **18**) in DCM. The suspension turned colourless or light brown except for **41** and **42**, in which case a blue-green colour was observed. The solvent was removed *in vacuo* to afford the product as a solid.

4.4.3.1 Bis(diphenylphosphino)dimethylhydrazine di(silver nitrate) (38)

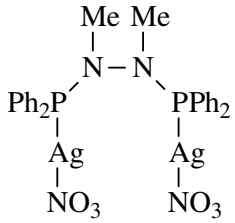

Reaction:

- **13**: 124 mg (0.29 mmol)
- **$AgNO_3$**: 100 mg (0.59 mmol)
- THF: 2 ml
- DCM: 2 ml

Properties:

- Unstable

Characterisation:

Too unstable to obtain pure sample.

^{31}P NMR: (*d*-DMSO, 121 MHz) δ_P 75.28 (d, ^1J ($^{107/109}Ag$-^{31}P) = 764.2 Hz)

4.4.3.2 Bis (diphenylphosphino)diethylhydrazine di(silver nitrate)(39)

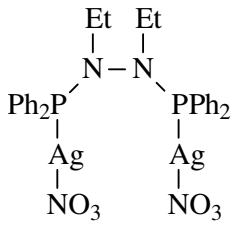

Reaction:

- **14**: 132 mg (0.29 mmol)
- **$AgNO_3$**: 100 mg (0.59 mmol)
- THF: 2 ml
- DCM: 2 ml
- Yield: 65 %

Properties:

- Colourless crystals or light brown powder
- Decomposes slowly in air
- Stored under argon in a Schlenk tube
- Possibly light sensitive leading to decomposition

Characterisation:

^{1}H NMR: (*d*-DMSO, 300 MHz) δ_H 7.79 (bs, Arom), 7.64 (bs, Arom), 7.54 (bs, Arom), 3.19 (m, $\underline{CH_2}CH_3$), 0.57 (t, ^{3}J (^{1}H-^{1}H) = 6.6 Hz, $CH_2\underline{CH_3}$)

^{13}C NMR: ($CDCl_3$, 100.6 MHz) δ_C 135.8 (s, Arom), 134.0 (Arom), 131.2 (m, Arom), 128.2 (s, Arom), ^{13}C ethyl signals could not be seen

^{31}P NMR: (*d*-DMSO, 121 MHz) δ_P 77.14 (d, ^{1}J ($^{107/109}$Ag-^{31}P) = 782.9 Hz)

MS: 733 (M - NO_3), 653 (L + Ag), 455 (L)

EA: Calc: ($Ag_2P_2N_4O_6C_{28}H_{30}$) C 42.24% H 3.80% N 7.04%

Found: C 41.48% H 3.95% N 6.77%

MP: 182 – 183 ^{o}C

4.4.3.3 Bis(di(4-methoxyphenyl)phosphino)dimethylhydrazine di(silver nitrate) (40)

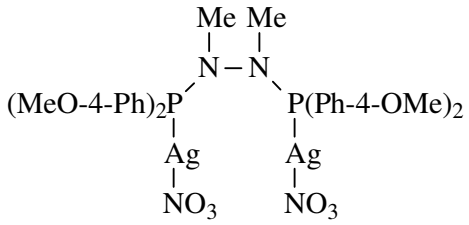

The complex could not be prepared due to the breakdown of ligand during complexation.

4.4.3.4 Bis(di(4-methoxyphenyl)phosphino)diethylhydrazine di(silver nitrate) (41)

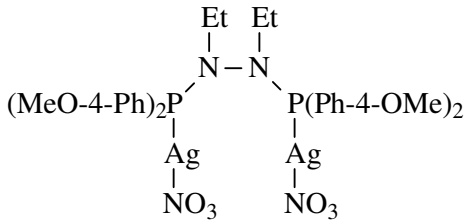

Reaction:

- **16**: 167 mg (0.29 mmol)
- **$AgNO_3$**: 100 mg (0.59 mmol)
- Acetonitrile: 2 ml
- DCM: 2 ml
- Yield: 70 %

Properties:

- White-grey powder
- Decomposes slowly in air

Characterisation:

^{1}H NMR: ($CDCl_3$, 400 MHz) δ_H 7.54 (m, Arom, 8H), 7.00 (m, Arom, 8H), 3.85 (s, O$\underline{CH_3}$, 12H), 3.41 and 3.18 (bs, $\underline{CH_2}CH_3$, 4H), 1.02 (bs, $CH_2\underline{CH_3}$, 6H)

^{13}C NMR: Due to sample breakdown ^{13}C could not be done

^{31}P NMR: ($CDCl_3$, 162 MHz) δ_P 74.19 (d, ^1J ($^{107/109}$Ag-^{31}P) = 834.2 Hz)

MS: 826 (12 %, M – NO_3), 138 (100 %, P(PhOMe))

EA: Calc: ($Ag_2P_2N_4O_{10}C_{32}H_{38}$) C 43.60 % H 4.15 % N 6.78 %
Found: Large deviations from calculated where observed

MP: 91 – 92 ^oC

4.4.3.5 Bis(di(N,N-dimetyl-4-aminophenyl)phosphino)dimethylhydrazine di(silver nitrate) (42)

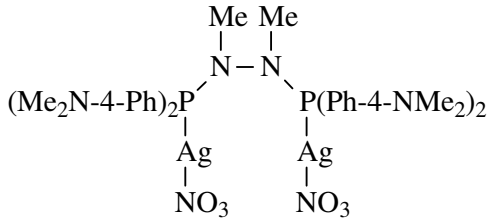

The complex could not be prepared due to the breakdown of ligand during complexation.

4.4.3.6 Bis(di(N,N-dimetyl-4-aminophenyl)phosphino)diethylhydrazine di(silver nitrate) (43)

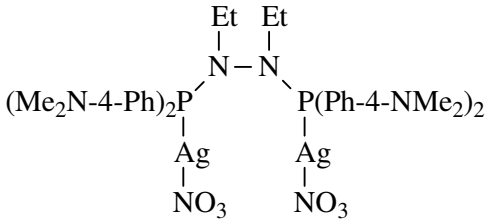

Reaction:

- **18**: 182 mg (0.29 mmol)
- **$AgNO_3$**: 100 mg (0.59 mmol)
- Acetonitrile: 2 ml
- DCM: 2 ml
- Yield: 74 %

Properties:

- Initial purple-blue colour in reaction solution
- Green solid, turns black over time
- Decomposes slowly in air
- Stored under argon in a Schlenk tube

Characterisation:

^{1}H NMR: (*d*-DMSO, 400 MHz) δ_H 7.43 (m, Arom), 6.78 (m, Arom), 3.11 (m, $\underline{CH_2}CH_3$, 4H), 2.97 and 2.99 (s, N($\underline{CH_3}$)$_2$, 24H), 0.66 (t, ^{3}J (^{1}H-^{1}H) = 6.8 Hz, $CH_2\underline{CH_3}$, 6H)

^{13}C NMR: Due to sample breakdown ^{13}C could not be done

^{31}P NMR: (*d*-DMSO, 162 MHz) δ_P 74.46 (d, ^{1}J ($^{107/109}$Ag-^{31}P) = 819.6 Hz)

MS: 951 (10%, M – CH_3, 10%), 751 (100 %, L + Ag + CH_3/N)

EA: Calc: ($Ag_2P_2N_8O_6C_{36}H_{50}$) C 44.64 %, H 5.20 %, N 11.57 %
Found: C 44.14 %, H 5.23 %, N 10.60 %

MP: 118 - 120 ^{o}C

4.4.4 Synthesis of Bischelated Silver Complexes

Silver nitrate (1 equivalent) was suspended in THF. To the stirred suspension were added 2 equivalents of ligand (**13** - **18**) in THF or DCM. The suspension turned colourless (unless otherwise stated). THF was removed *in vacuo* to afford the product as a white solid (unless otherwise stated).

4.4.4.1 Bis(bis(diphenylphosphino)dimethylhydrazine)silver nitrate (44)

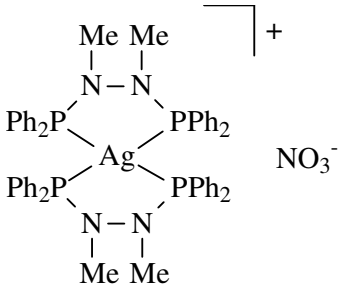

Reaction:

- **13**: 252 mg (0.59 mmol)
- **$AgNO_3$**: 50 mg (0.29 mmol)
- THF: 2 ml
- DCM: 2 ml
- Yield: 76 %

Properties:

- White solid
- Unstable

Characterisation:

Complex was too unstable to obtain pure sample. The following characterisation was possible:

^{1}H NMR: (*d*-DMSO, 300 MHz) δ_H 7.51 (bs, Arom), 7.34 (bs, Arom), 2.73 (bs, CH_3)

^{31}P NMR: (*d*-DMSO, 121 MHz) δ_P 68.42 (dd, ^{1}J (^{107}Ag-^{31}P) = 245.7 Hz, ^{1}J (^{109}Ag-^{31}P) = 283.5 Hz)

MS: 963 (38%, M - NO_3), 535 (58 %, Ligand + Ag), 214 (100 %, PPh)

MP: 96 - 98 ^{o}C

4.4.4.2 Bis(bis(diphenylphosphino)diethylhydrazine)silver nitrate (45)

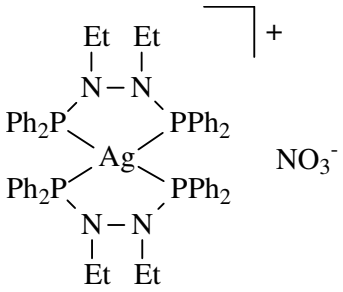

Reaction:

- **14**: 269 mg (0.59 mmol)
- **$AgNO_3$**: 50 mg (0.29 mmol)
- THF: 5 ml
- Yield: 84 %

Properties:

- White or grey solid
- Decomposes slowly in air
- Hygroscopic
- Stored under argon in a Schlenk tube
- Possibly light sensitive leading to decomposition

Characterisation:

^{1}H NMR:	($CDCl_3$, 300 MHz) δ_H 7.39 (bs, Arom, 16H), 7.19 (bs, Arom, 24H), 2.94 (unresolved q, $\underline{CH_2}CH_3$, 8H), 0.85 (t, ^{3}J (^{1}H-^{1}H) = 6.0 Hz, $CH_2\underline{CH_3}$, 12H)
^{13}C NMR:	($CDCl_3$, 75 MHz) δ_C 133.5 (Arom), 132.8 (Arom), 131.5 (Arom), 128.9 (Arom), 48.9 ($\underline{CH_2}CH_3$), 14.8 ($CH_2\underline{CH_3}$)
^{31}P NMR:	($CDCl_3$, 161.98 MHz) δ_P 69.06 (dd, ^{1}J (^{107}Ag-^{31}P) = 248.1, ^{1}J (^{109}Ag-^{31}P) = 285.3Hz)
MS:	1022 (45 %, M - NO_3), 563 (56 %, L + Ag), 455 (47 %, L),
EA:	Calc: ($AgP_4N_5O_3C_{56}H_{60}$) C 62.11 %, H 5.58 %, N 6.47 % Found: C 60.08 %, H 5.54%, N 5.85 %
MP:	127 – 130 ^{o}C

4.4.4.3 Bis(bis(di(4-methoxyphenyl)phosphino)dimethylhydrazine)silver nitrate (46)

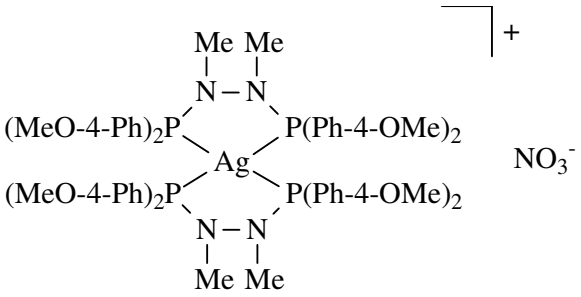

Reaction:

- **15**: 324 mg (0.59 mmol)
- **$AgNO_3$**: 50 mg (0.29 mmol)
- THF: 5 ml
- Yield: 79 %

Properties:

- Light yellow solid
- Decomposes slowly in air
- Hygroscopic
- Stored under argon in a Schlenk tube

Characterisation:

^{1}H NMR: ($CDCl_3$, 400 MHz) δ_H 7.21 (d, coupling not resolved, Arom, 16H), 6.70 (d, ^{3}J (^{1}H-^{1}H) = 8.4 Hz, Arom, 16H), 3.75 (O$\underline{CH}_3$, 24H), 2.54 (N$\underline{CH}_3$, 12H)

^{13}C NMR: Due to sample breakdown ^{13}C could not be done

^{31}P NMR: ($CDCl_3$, 162 MHz) δ_P 66.18 (dd, ^{1}J (^{107}Ag-^{31}P) = 246.9 Hz, ^{1}J (^{109}Ag-^{31}P) = 284.9Hz)

MS: 1206 (36 %, M - NO_3), 655 (34%, L + Ag), 245 (100%, $P(PhOMe)_2$)

EA: Calc: ($AgP_4N_5O_{11}C_{60}H_{68}$) C 56.88 %, H 5.41 %, N 5.53 %
Found: C 56.78%, H 5.51 %, N 4.84 %

MP: 90 - 93 ^{o}C

4.4.4.4 Bis(bis(di(4-methoxyphenyl)phosphino)diethylhydrazine)silver nitrate (47)

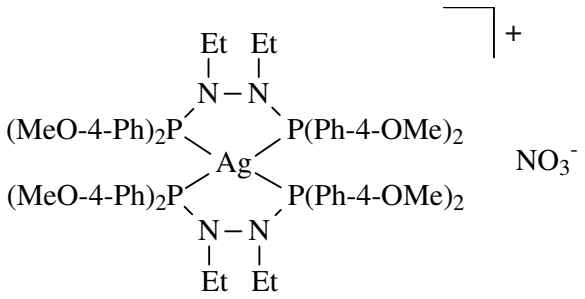

Reaction:

- **16**: 341 mg (0.59 mmol)
- **$AgNO_3$**: 50 mg (0.29 mmol)
- THF: 5 ml
- Yield: 83 %

Properties:

- Light yellow solid
- Decomposes slowly in air
- Hygroscopic
- Stored under argon in a Schlenk tube

Characterisation:

^{1}H NMR: ($CDCl_3$, 400 MHz) δ_H 7.53 (d, Arom, ^3J (^{1}H-^{1}H) = 8.8Hz, 16H), 6.99 (d, Arom, ^3J (^{1}H-^{1}H) = 8.8Hz, 16H), 3.78 (O$\underline{CH_3}$, 24H), 2.90 (bs, $\underline{CH_2}CH_3$, 8H), 0.85 (bs, $CH_2\underline{CH_3}$, 12H)

^{13}C NMR: ($CDCl_3$, 100.6 MHz) δ_C 161.8 (m, Arom), 132.8 (m, Arom), 113.2 (m, Arom), 52.6 (s, O$\underline{CH_3}$), 42.9 (m, $\underline{CH_2}CH_3$), 13.2 (m, $CH_2\underline{CH_3}$),

^{31}P NMR: ($CDCl_3$, 162 MHz) δ_P 67.54 (dd, ^1J (^{107}Ag-^{31}P) = 249.9, ^1J (^{109}Ag-^{31}P) = 285.3 Hz)

MS: 1261 (22 %, M - NO_3), 683 (20 %, L + Ag), 245 (100 %, $P(PhOMe)_2$)

EA: Calc: ($AgP_4N_5O_{11}C_{64}H_{76}$) C 58.10 %, H 5.79 %, N 5.29 %
Found: C 58.27 %, H 5.96 %, N 4.88 %

MP: 76 - 78 ^oC

4.4.4.5 Bis(bis(di(N,N-dimethyl-4-aminophenyl)phosphino)dimethylhydrazine)silver nitrate (48)

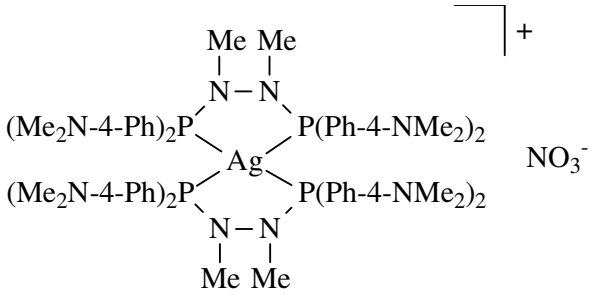

Reaction:

- **17**: 354 mg (0.59 mmol)
- **$AgNO_3$**: 50 mg (0.29 mmol)
- THF: 5 ml

The complex could not be fully characterised due to the breakdown of ligand during complexation

Characterisation:

^{31}P NMR: (*d*-DMSO, 161.98 MHz) δ_P 66.56 (dd, ^1J (^{107}Ag-^{31}P) = 246.4, ^1J (^{109}Ag-^{31}P) = 284.2 Hz)

4.4.4.6 Bis(bis(di(N,N-dimethyl-4-aminophenyl)phosphino)diethylhydrazine)silver nitrate (49)

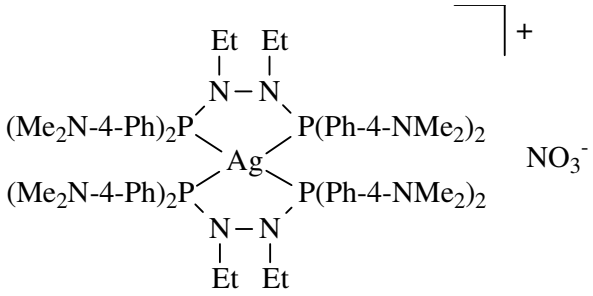

Reaction:

- **17**: 371 mg (0.59 mmol)
- **$AgNO_3$**: 50 mg (0.29 mmol)
- THF: 5 ml
- Yield: 76 %

Properties:

- Light brown solid
- Decomposes slowly in air
- Stored under argon in a Schlenk tube

Characterisation:

^{1}H NMR:	(*d*-DMSO, 400 MHz) δ_H 7.6 - 6.4 (various multiplets, Arom), 2.87 (NCH_3, 48H), 2.67 (m, CH_2CH_3, 8H), 0.88 (bs, CH_2CH_3, 12H)
^{13}C NMR:	Due to sample breakdown ^{13}C could not be done
^{31}P NMR:	(*d*-DMSO, 162 MHz) δ_P 67.60 (dd, ^1J (^{107}Ag-^{31}P) = 248.3, ^1J (^{109}Ag-^{31}P) = 286.1Hz)
MS:	1365 (50 %, M - NO_3), 735 (74 %, L + Ag), 271 (100 %, $P(PhNMe_2)_2$)
EA:	Calc: ($AgP_4N_{13}O_3C_{72}H_{100}$) C 60.58 %, H 7.06 %, N 12.76 % Found: C 59.25 %, H 6.86 %, N 12.24 %
MP:	125 - 127 ^{o}C

Chapter 5

Biological Experimental Procedures

5.1 GENERAL

Experimental reagents were prepared according to in-house publications.[185]

5.1.1 Experimental Conditions

Plastic tips and tubes were autoclaved and kept in closed containers in laminar flow cabinets. Only sterile, disposable plastic-ware was used. Laminar flow cabinets were kept clean and sterile by wiping with 70% alcohol on a regular basis.

5.1.2 Culture Medium

Roswell Park Memorial Institute medium (RPMI), Eagle's minimal essential medium (EMEM) and Dulbecco's minimal essential medium (DMEM) culture media were commercially obtained (Sigma-Aldrich) and supplemented with 1% penstrep mixture (10 000 U penicillin/ml and 10 000 µg streptomycin/ml) (Adcock-Ingram) and 10% Heat Inactivated Foetal Calf Serum (HI FCS) (Adcock-Ingram). DMEM culture medium used for cultivating MCF-7 cell line was further supplemented with 2% non-essential amino acids. Culture medium used for MCF-12 cell line was made up from a 1:1 mixture of DMEM and Ham's F12 medium and was supplemented with hydrocortisone (10 mg/ml), chlora toxin (1 mg/ml), insulin (20 mg/ml), 10% HI FCS and epidermal growth factor (100 mg/ml). All culture medium was stored at 4^{o}C.

[185] G. Joone, C.E. Medlen, *In-house publications*, Department of Pharmacology, University of Pretoria.

5.1.3 Heat Inactivated Foetal Calf Serum (HI FCS)

A defrosted sealed bottle, containing 100 ml foetal calf serum (Adcock-Ingram), was incubated at 56 ^{o}C for 45 minutes in a water bath. The FCS was mixed periodically during incubation by gently swirling the container. The container was, after incubation, immediately divided into 2 sterile 50 ml centrifuge tubes and stored frozen until needed.

5.1.4 White Cell Counting Fluid

1 ml of a 0.1 % aqueous solution of Crystal Violet (Merck) was added to a solution of 97 ml deionised water and 2 ml acetic acid. The resulting solution was stored at 4 ^{o}C.

5.1.5 Phosphate Buffered Saline (PBS)

FTA hemaglutination buffer (9.23 g) (The Scientific Group) was dissolved in 1 L of distilled water and the pH adjusted to 7.2 using either sodium hydroxide or hydrochloric acid.

5.1.6 MTT Stain Solution

3-(4,5-dimethylthiazol-2-yl)-2,5-diphenyl tetrazolium bromide (MTT) (250 mg) (Sigma-Aldrich) was dissolved in 50 ml PBS and filter sterilised through a filter with a pore size of 0.2 µm. The solution was stored at 4 ^{o}C in the dark.

5.1.7 Valinomycin

Frozen Valinomycin stock solution (50 µl, 1 mM) was diluted to 100 µM and 1 µM concentrations. The final concentrations in mitochondrial membrane potential experiments after addition of 0.2 ml of the stock solution to flow cytometer tubes were 10 µM and 0.1 µM, respectively.

5.1.8 JC-1

PBS (3900 µl) was added to 100 µl of a 1.5 mM frozen JC-1 [5,5',6,6'-tetrachloro-1,1',3,3'-tetraethylbenzimidazolylcarbocyanine iodide] stock solution and mixed very well to minimise separation before use.

5.1.9 Hepes Binding Buffer

Into 100 ml of de-ionised water was dissolved Hepes buffering agent [4-(2-hydroxyethyl)-1-piperazineethanesulphonic acid] (238.3 mg, 10 mM) (BD Bioscience), sodium chloride (876,6 mg, 150 mM), potassium chloride (37.3 mg, 5 mM), calcium chloride (26.5 mg, 1.8 mM) and magnesium chloride (9.5 mg, 1 mM). The pH was adjusted to 7.4 using either sodium hydroxide or hydrochloric acid and stored at 4 ^{o}C.

5.1.10 Propidium Iodide (PI)

Propidium iodide (2.5 g) was dissolved in 50 ml PBS. The solution was stored at 4 ^{o}C in the dark.

5.1.11 Ammonium Chloride Solution

Ammonium chloride (8.3 g), sodium bicarbonate (1 g) and EDTA [ethylenediamine-tetraaceticacid] (74 mg) (Sigma-Aldrich) were dissolved in distilled water (1 L). The solution was filter sterilised through a 0.2 µm pore size filter and stored at 4 ^{o}C in the dark.

5.1.12 Phytohaemaglutinine (PHA)

Sterile distilled water (5 ml) was added to the freeze dried content of a bottle of commercial PHA (BIOWEB) and mixed gently. 0.2 ml aliquots were dispensed into sterile tubes, which were then stored at -20 ^{o}C.

5.1.13 Heparin

Commercial Heparin (sodium salt) (90 mg) (Sigma-Aldrich) was dissolved in distilled water (30 ml), that was sterislised before use, and the solution was stored at 4 ^{o}C.

5.1.14 Cell Cultures

The following cell cultures were used:

Code	Description	ATCC code	Culture medium
HeLa	Human adenocarcinoma of the cervix	CCL-2	EMEM
CoLo 320 DM	Human colon cancer	CCL-220	RPMI
Jurkat	Human T-cell cancer	NRBM 0062	RPMI
A2780	Human ovarian cancer	EACC 93112519	RPMI
A2780cis	Human ovarian cancer (cisplatin resistant)	EACC 93112519 exposed to cisplatin	RPMI
MCF-7	Human breast cancer	HTB 22	DMEM
MCF-12A	Modified human non-cancerous breast cells	CRL 10782	DMEM

Table 5.1: Summary of the cell cultures used in biological studies. American Type Culture Collection (ATCC) codes are also provided.

5.2 INSTRUMENTATION

5.2.1 Microplate Reader

MTT assays were performed using a BIO-TEK Instruments, ELx800 UV Universal microplate reader.

5.2.2 Flowcytometer

Mitochondria and apoptosis assays were performed on a Beckman Coulter Cytomics FC 500 flowcytometer equipped with a 488nm argon laser.

5.3 BIOLOGICAL STUDIES

Procedures were carried out following in-house procedures.[185]

5.3.1 Maintenance of Cultures

Viable cells in appropriate media were kept in a culture flask at 37 ^{o}C in an atmosphere of 5 % CO_2 in air. The media were replaced 2 to 3 times a week. The lid of the culture flask was not tightened completely to allow for pH regulation by the inflow of CO_2.

5.3.2 Trypsination of Adherent Cell Lines

This applies to the following cell lines: HeLa, A2780, A2780cis, MCF-7 and MCF-12A. Cells were examined under an invert microscope to determine satisfactory growth (cells should not reach confluency) and to check for possible infection.

The medium was removed and washed with Trypsin/Versene solution (0.25% Trypsin and 0.05 % EDTA solution in Ca^{2+} and Mg^{2+} free Dulbecco buffer, commercially obtained) (approx. 5 ml) to remove all traces of culture medium as this inhibits the activity of Trypsin. Enough Trypsin/Versene (approx. 3 ml) was added to cover the cells on the bottom of the flask. The cells were incubated for approx. 10 minutes at 37 ^{o}C until the cells detached themselves from the bottom of the flask. The cells were aspirated into a centrifuge tube (15 ml) and culture medium was added to fill the tube. Culture medium was added as it contains proteins that prevent cell damage caused by Trypsin and EDTA. The tube was centrifuged for 5 minutes at 1000 rpm and supernatant liquid was discarded. The remaining cell pellet was resuspended in 1 ml of culture medium. The resuspended cells were used for cell population counting and with appropriate dilution were loaded onto a 96 well plate.

5.3.3 Lymphocyte Preparation

Heparinised blood (30 ml, 5 units/ml blood) from a healthy adult human volunteer was carefully loaded onto 15 ml Histopaque 1077. The suspension was centrifuged for 25 minutes at 1800 rpm. The top plasma layer was removed and the lymphocytes/monocyte layer was transferred to a sterile 50 ml tube. The 50 ml tube was filled with RPMI medium and centrifuged for 15 minutes at 1000 rpm to remove contaminating platelets. The supernatant fluid was discarded and the tube refilled with RPMI. The suspension was centrifuged for 10 minutes at 1000 rpm. The supernatant fluid was discarded and the tube filled with cold ammonium chloride solution. The suspension was left on ice for 10 minutes to lyse contaminating red cells. The tube was centrifuged for 10 minutes at 1000 rpm and the supernatant liquid discarded. The remaining pellet was resuspended in RPMI medium followed by centrifuging for 10 minutes at 1000 rpm. The supernatant liquid was discarded and the pellet resuspended in 1 ml RPMI with 10 % FCS. Cells were counted and diluted for use.

5.3.4 Counting of Cells

The resuspended pellet (50 µl) was added to white cell counting fluid (450 µl) and thoroughly mixed. A small amount of the suspension was put on a Haemocytometer and counted using a Reichert-Jung Microstar 110 microscope at a magnification of 10x. Final concentrations required for a 96 well plate were made up by dilution of the 1 ml resuspended cell pellet (Table 5.2).

Cell Line	Cell Concentration Needed
HeLa	1:4 dilution of 2.5 x 10^4
CoLo 320 DM	1:4 dilution of 2 x 10^4
Jurkat	1:4 dilution of 3 x 10^4
A2780	1:4 dilution of 2.5 x 10^4
A2780cis	1:4 dilution of 2.5 x 10^4
MCF-7	1:4 dilution of 2 x 10^4
MCF-12A	1:4 dilution of 2 x 10^4
Lymphocytes	2 x 10^6

Table 5.2: Cell concentrations for loading onto plates.

5.3.5 IC_{50} Toxicity Tests

This procedure applies to all cell lines except lymphocytes. Culture medium (80 µl) was dispensed into the 96 wells of the plate and left to warm to 37 ^oC in the incubation oven while cells were prepared. A cell suspension (100 µl) of the appropriate concentration was dispensed into wells and the plate was left to incubate for one hour at 37 ^oC in an atmosphere of 5 % CO_2. The drug solution (20 µl) or the culture medium (in the case of the control experiments) was dispensed into wells (triple experiments) and incubated for 7 days. Plates are incubated in a closed (not sealed) container with a kitchen towel soaked with sterile water at the bottom to minimise edge effect from evaporation of culture medium.

5.3.6 IC_{50} Drug Toxicity Testing for Lymphocytes

Culture medium (60 µl) was dispensed into the 96 wells of the plate and left to warm to 37 ^oC in the incubation oven while cells were prepared. 100 µl of cell suspension at the appropriate concentration were dispensed into wells and the plate was left to incubate for 1 hour at 37 ^oC in a 5 % CO_2 atmosphere. The drug solution (20 µl) or the culture medium (in the case of the control experiments) were dispensed into wells (triple experiments). After 5 minutes PHA (20 µl) was added to stimulate lymphocytes in one set of experiments, while culture medium (20 µl) was added to

the set of resting lymphocyte experiments. The plates were incubated for 3 days. Plates were incubated in a closed (not sealed) container with a kitchen towel soaked with sterile water at the bottom to minimise edge effect from evaporation of culture medium.

5.3.7 Drug Preparation

Stock solutions (10 mM) of the drugs were prepared by dissolving the drug in DMSO (1 ml). The stock solutions were dispensed in 50 µl aliquots into Eppendorf tubes and stored at -20 ^{o}C. Dilutions of the stock solutions were made directly before they were administered to stabilised cells in 96 well plates. Eight dilutions of the drugs in question were prepared from the stock solution by subsequent dilution in a ratio of 1:1 (see example below). The final percentage DMSO solvent per well was less than 0.5 %.

Example of stock dilutions for plate loading:

50 µl 10 mM stock solution
50 µl stock solution + 450 µl medium → 500 µl 1 mM drug solution
100 µl 1 mM solution + 100 µl medium → 200 µl 500 µM drug solution

1:1 dilutions (100 µl of previous solution + 100 µl medium)
500 µM = first drug dose → 20 µl per well to give a final conc. of 50.00 µM
250 µM = second drug dose → 20 µl per well to give a final conc. of 25.00 µM
125 µM = third drug dose → 20 µl per well to give a final conc. of 12.50 µM
62.5 µM = fourth drug dose → 20 µl per well to give a final conc. of 6.25 µM
31.3 µM = fifth drug dose → 20 µl per well to give a final conc. of 3.13 µM
15.6 µM = sixth drug dose → 20 µl per well to give a final conc. of 1.56 µM
7.8 µM = seventh drug dose → 20 µl per well to give a final conc. of 0.78 µM
3.9 µM = eighth drug dose → 20 µl per well to give a final conc. of 0.39 µM

5.3.8 MTT Assay

MTT stain solution (20 µl) was added to each well after the 7 day incubation period of the respective cells. The plate was re-incubated for another 3½ to 4 hours for viable cell staining. The plate was centrifuged for 10 minutes at 2000 rpm. The supernatant fluid was discarded without disturbing the pellet and the cells were washed with 150 µl PBS, followed by 10 minuntes centrifugation of the mixture at 2000 rpm. The supernatant liquid was discarded and the pellet left to dry overnight in the dark. The next morning 100 µl DMSO were added and the plates were placed on a shaker for approximately 2 hours to facilitate dissolution of the purple formazan crystals formed from MTT by viable cells. The absorbance of viable and proliferating cells was analysed with a 900 Micro-ELISA reader.

5.3.9 Determination of the Cell Membrane Potential of Mitochondria

Jurkat or lymphocyte cells (1.8 ml) at appropriate concentrations (Table 5.2) were incubated for 1 hour in flow cytometer tubes. To this was added the appropriate drug dilution (0.2 ml) for Jurkat cells and for lymphocyte cells (0.22 ml). All experiments were carried out in the same manner using a control sample (no addition of toxin) and multiples (1x, 2x, 5x, 10x) of the IC_{50} value of the drug as determined in previous toxicological experiments. For the lymphocyte experiment the cells were stimulated with PHA (0.2 ml) 5 minutes after dispension of the drug. The cells were left to incubate for 24 hours. Two tubes that were incubated without drug were treated with 0.1 mM (0.2 ml) and 10 mM (0.2 ml) Valinomycin (known to decrease mitochondrial membrane potential), respectively and incubated for 10 minutes. The tubes were centrifuged for 5 minutes at 1800 rpm. The obtained pellet was resuspended in the appropriate supplemented medium (900 µl) and JC-1 (100 µl) was added. The tubes were left in the dark for 20 minutes and then centrifuged for 5 minutes at 1800 rpm. The isolated pellet was washed with PBS (approximately 3 ml), the mixture was centrifuged for 5 minutes at 1800 rpm and the supernatant liquid was discarded. The obtained pellet was resuspended in PBS (1 ml) supplemented with 10 % FCS and analysed using the flowcytometer.

5.3.10 Apoptosis Test

Jurkat cells of the appropriate concentration (Table 5.2) were incubated for 1 hour in culture flasks (45 ml cell solution per 250 ml flask). All experiments were carried out in the same manner using a control sample (no addition of toxin) and multiples (1x, 2x) of the concentration related to the IC_{50} value of the drug as determined in previous toxicological experiments. The flasks were incubated for 48 hours and after 6, 24 and 48 hours 15 ml aliquots were removed from each flask for analyses.

Centrifuge tubes (15 ml) were filled with samples from the 250 ml culture flasks and centrifuged for 7 minutes at 800 rpm. The supernatant liquid was discarded and the remaining pellet was washed twice with PBS (2 ml) containing 1% FCS. It was then centrifuged again for 7 minutes at 800 rpm and the supernatant liquid was discarded. The isolated pellet was resuspended in Hepes binding buffer (1 ml) and two flow cytometer tubes were filled with 100 µl aliquots of each of the cell suspensions. One of the tubes was left unstained while PI (10 µl) and Annexin V-FITC (Fluorescence conjugated Annexin-V) (5 µl) was added to the second tube. The tubes were left for 15 minutes in the dark (Annexin-V is light sensitive). Hepes binding buffer (400 µl) was added to each tube and the suspended cells analysed using the flowcytometer.

5.3.11 Statistical Analysis

The results of the assays are expressed as the mean percentage (%) of ±SEM. The statistical program GRAPHPAD was used to determine the IC_{50} concentration of the drug treated groups.

Appendix A

Molecular Structures

Bis(diphenylphosphino)diethylhydrazine (14)

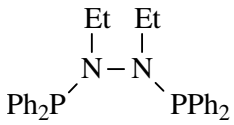

Table 1: Crystal data and structure refinement for **14**.

Empirical formula	$P_2N_2C_{28}H_{30}$	
Formula weight	456.48	
Temperature	173(2) K	
Wavelength	0.71073 Å	
Crystal system	Monoclinic	
Space group	$P2_1/c$	
Unit cell dimensions	a = 14.623(5) Å	$\alpha = 90°$
	b = 13.085(4) Å	$\beta = 108.2(6)°$
	c = 13.494(4) Å	$\gamma = 90°$
Volume	2453.1(13) $Å^3$	
Z	4	
Density (calculated)	1.236 Mg/m^3	
Absorption coefficient	0.196 mm^{-1}	
F(000)	968	
Crystal size	0.44 x 0.17 x 0.17 mm^3	
Theta range for data collection	1.47 to 26.00°	
Index ranges	-16<=h<=18, -12<=k<=16, -16<=l<=14	

Reflections collected	13465
Independent reflections	4813 [R(int) = 0.0490]
Completeness to theta = 26.00°	99.9 %
Absorption correction	Semi-empirical from equivalents
Max. and min. transmission	0.9675 and 0.9189
Refinement method	Full-matrix least-squares on F2
Data/restraints/parameters	4813/0/291
Goodness-of-fit on F2	1.014
Final R indices [I>2sigma(I)]	R1 = 0.0508, wR2 = 0.1188
R indices (all data)	R1 = 0.0860, wR2 = 0.1371
Largest diff. peak and hole	0.787 and -0.419 e.Å^{-3}

Table 2: Bond lengths [Å] and angles [°] for **14**.

N(1)-N(2)	1.427(3)	C(21)-C(22)	1.404(4)
N(1)-C(1)	1.471(3)	C(22)-C(23)	1.385(4)
N(1)-P(1)	1.710(2)	C(23)-C(24)	1.386(4)
N(2)-C(3)	1.466(3)	C(24)-C(25)	1.378(4)
N(2)-P(2)	1.692(2)	C(25)-C(26)	1.390(4)
P(1)-C(21)	1.832(3)	C(31)-C(36)	1.394(4)
P(1)-C(11)	1.846(3)	C(31)-C(32)	1.399(4)
P(2)-C(41)	1.835(3)	C(32)-C(33)	1.391(4)
P(2)-C(31)	1.847(3)	C(33)-C(34)	1.377(4)
C(1)-C(2)	1.510(4)	C(34)-C(35)	1.383(4)
C(3)-C(4)	1.511(4)	C(35)-C(36)	1.385(4)
C(11)-C(16)	1.394(4)	C(41)-C(42)	1.395(4)
C(11)-C(12)	1.394(4)	C(41)-C(46)	1.398(4)
C(12)-C(13)	1.388(4)	C(42)-C(43)	1.382(4)
C(13)-C(14)	1.375(4)	C(43)-C(44)	1.381(4)
C(14)-C(15)	1.381(4)	C(44)-C(45)	1.376(4)
C(15)-C(16)	1.383(4)	C(45)-C(46)	1.387(4)
C(21)-C(26)	1.396(4)		

N(2)-N(1)-C(1)	114.65(19)	C(26)-C(21)-P(1)	124.5(2)
N(2)-N(1)-P(1)	116.47(16)	C(22)-C(21)-P(1)	118.0(2)
C(1)-N(1)-P(1)	122.01(17)	C(23)-C(22)-C(21)	121.3(3)
N(1)-N(2)-C(3)	114.49(19)	C(22)-C(23)-C(24)	120.2(3)
N(1)-N(2)-P(2)	118.43(16)	C(25)-C(24)-C(23)	119.6(3)
C(3)-N(2)-P(2)	126.88(17)	C(24)-C(25)-C(26)	120.5(3)
N(1)-P(1)-C(21)	102.16(11)	C(25)-C(26)-C(21)	121.1(3)
N(1)-P(1)-C(11)	104.85(11)	C(36)-C(31)-C(32)	118.2(2)
C(21)-P(1)-C(11)	99.34(12)	C(36)-C(31)-P(2)	124.81(19)
N(2)-P(2)-C(41)	105.91(11)	C(32)-C(31)-P(2)	116.9(2)
N(2)-P(2)-C(31)	105.31(11)	C(33)-C(32)-C(31)	120.6(3)
C(41)-P(2)-C(31)	98.32(11)	C(34)-C(33)-C(32)	120.1(3)
N(1)-C(1)-C(2)	113.7(2)	C(33)-C(34)-C(35)	120.0(3)
N(2)-C(3)-C(4)	114.7(2)	C(34)-C(35)-C(36)	120.1(3)
C(16)-C(11)-C(12)	117.5(3)	C(35)-C(36)-C(31)	120.9(3)
C(16)-C(11)-P(1)	125.0(2)	C(42)-C(41)-C(46)	117.6(2)
C(12)-C(11)-P(1)	117.4(2)	C(42)-C(41)-P(2)	116.7(2)
C(13)-C(12)-C(11)	120.7(3)	C(46)-C(41)-P(2)	125.8(2)
C(14)-C(13)-C(12)	121.0(3)	C(43)-C(42)-C(41)	121.4(3)
C(13)-C(14)-C(15)	119.0(3)	C(44)-C(43)-C(42)	120.2(3)
C(14)-C(15)-C(16)	120.3(3)	C(45)-C(44)-C(43)	119.3(3)
C(15)-C(16)-C(11)	121.5(3)	C(44)-C(45)-C(46)	120.9(3)
C(26)-C(21)-C(22)	117.5(2)	C(45)-C(46)-C(41)	120.5(3)

Table 3: Torsion angles [°] for **14**.

C(1)-N(1)-N(2)-C(3)	-113.0(2)	C(1)-N(1)-P(1)-C(21)	79.0(2)
P(1)-N(1)-N(2)-C(3)	95.3(2)	N(2)-N(1)-P(1)-C(11)	125.12(18)
C(1)-N(1)-N(2)-P(2)	71.9(2)	C(1)-N(1)-P(1)-C(11)	-24.3(2)
P(1)-N(1)-N(2)-P(2)	-79.7(2)	N(1)-N(2)-P(2)-C(41)	-123.64(18)
N(2)-N(1)-P(1)-C(21)	-131.65(17)	C(3)-N(2)-P(2)-C(41)	62.0(2)

N(1)-N(2)-P(2)-C(31)	132.83(18)	C(24)-C(25)-C(26)-C(21)	-0.6(4)
C(3)-N(2)-P(2)-C(31)	-41.6(2)	C(22)-C(21)-C(26)-C(25)	1.9(4)
N(2)-N(1)-C(1)-C(2)	57.0(3)	P(1)-C(21)-C(26)-C(25)	179.7(2)
P(1)-N(1)-C(1)-C(2)	-153.1(2)	N(2)-P(2)-C(31)-C(36)	85.1(2)
N(1)-N(2)-C(3)-C(4)	-60.6(3)	C(41)-P(2)-C(31)-C(36)	-24.0(2)
P(2)-N(2)-C(3)-C(4)	113.9(2)	N(2)-P(2)-C(31)-C(32)	-98.2(2)
N(1)-P(1)-C(11)-C(16)	105.1(2)	C(41)-P(2)-C(31)-C(32)	152.7(2)
C(21)-P(1)-C(11)-C(16)	-0.2(3)	C(36)-C(31)-C(32)-C(33)	0.2(4)
N(1)-P(1)-C(11)-C(12)	-78.5(2)	P(2)-C(31)-C(32)-C(33)	-176.7(2)
C(21)-P(1)-C(11)-C(12)	176.1(2)	C(31)-C(32)-C(33)-C(34)	-0.7(4)
C(16)-C(11)-C(12)-C(13)	-0.5(4)	C(32)-C(33)-C(34)-C(35)	-0.1(4)
P(1)-C(11)-C(12)-C(13)	-177.1(3)	C(33)-C(34)-C(35)-C(36)	1.2(4)
C(11)-C(12)-C(13)-C(14)	1.0(5)	C(34)-C(35)-C(36)-C(31)	-1.7(4)
C(12)-C(13)-C(14)-C(15)	-0.2(5)	C(32)-C(31)-C(36)-C(35)	0.9(4)
C(13)-C(14)-C(15)-C(16)	-1.0(5)	P(2)-C(31)-C(36)-C(35)	177.6(2)
C(14)-C(15)-C(16)-C(11)	1.5(4)	N(2)-P(2)-C(41)-C(42)	176.14(19)
C(12)-C(11)-C(16)-C(15)	-0.7(4)	C(31)-P(2)-C(41)-C(42)	-75.2(2)
P(1)-C(11)-C(16)-C(15)	175.6(2)	N(2)-P(2)-C(41)-C(46)	-3.5(3)
N(1)-P(1)-C(21)-C(26)	0.9(2)	C(31)-P(2)-C(41)-C(46)	105.1(2)
C(11)-P(1)-C(21)-C(26)	108.4(2)	C(46)-C(41)-C(42)-C(43)	-1.9(4)
N(1)-P(1)-C(21)-C(22)	178.7(2)	P(2)-C(41)-C(42)-C(43)	178.4(2)
C(11)-P(1)-C(21)-C(22)	-73.8(2)	C(41)-C(42)-C(43)-C(44)	0.5(4)
C(26)-C(21)-C(22)-C(23)	-1.7(4)	C(42)-C(43)-C(44)-C(45)	1.0(4)
P(1)-C(21)-C(22)-C(23)	-179.7(2)	C(43)-C(44)-C(45)-C(46)	-1.0(4)
C(21)-C(22)-C(23)-C(24)	0.2(4)	C(44)-C(45)-C(46)-C(41)	-0.4(4)
C(22)-C(23)-C(24)-C(25)	1.2(4)	C(42)-C(41)-C(46)-C(45)	1.9(4)
C(23)-C(24)-C(25)-C(26)	-1.0(4)	P(2)-C(41)-C(46)-C(45)	-178.4(2)

Di(phenylphosphino)cyclotetramethyldihydrazine (52)

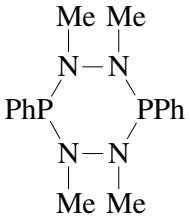

Table 4: Crystal data and structure refinement for **52**.

Empirical formula	$P_2N_4C_{16}H_{22}$	
Formula weight	332.32	
Temperature	193(2) K	
Wavelength	0.71073 Å	
Crystal system	Orthorhombic	
Space group	*Pbca*	
Unit cell dimensions	a = 13.2879(16) Å	α = 90°
	b = 7.5426(9) Å	β = 90°
	c = 17.125(2) Å	γ = 90°
Volume	1716.4(4) $Å^3$	
Z	4	
Density (calculated)	1.286 Mg/m^3	
Absorption coefficient	0.255 mm^{-1}	
F(000)	704	
Crystal size	0.38 x 0.27 x 0.26 mm^3	
Theta range for data collection	2.38 to 27.00°	
Index ranges	-15<=h<=16, -7<=k<=9, -21<=l<=21	
Reflections collected	10040	
Independent reflections	1873 [R(int) = 0.0313]	
Completeness to theta = 27.00°	100.0 %	
Absorption correction	None	
Max. and min. transmission	0.9366 and 0.9092	
Refinement method	Full-matrix least-squares on F^2	

Data/restraints/parameters	1873/0/100
Goodness-of-fit on F^2	1.080
Final R indices [I>2sigma(I)]	R1 = 0.0302, wR2 = 0.0888
R indices (all data)	R1 = 0.0370, wR2 = 0.0935
Largest diff. peak and hole	0.318 and -0.248 e.Å^{-3}

Table 5: Bond lengths [Å] and angles [°] for **52**.

C(1)-N(1)	1.4583(18)	C(14)-C(15)	1.389(2)
C(2)-N(2)	1.4605(17)	C(15)-C(16)	1.395(2)
C(11)-C(16)	1.398(2)	N(1)-N(2)$^{\#}$1	1.4321(17)
C(11)-C(12)	1.400(2)	N(1)-P(1)	1.6953(14)
C(11)-P(1)	1.8412(15)	N(2)-N(1)$^{\#}$1	1.4321(17)
C(12)-C(13)	1.393(2)	N(2)-P(1)	1.6984(12)
C(13)-C(14)	1.384(2)		

C(16)-C(11)-C(12)	118.12(13)	N(2)$^{\#}$1-N(1)-P(1)	120.94(9)
C(16)-C(11)-P(1)	121.12(11)	C(1)-N(1)-P(1)	121.23(10)
C(12)-C(11)-P(1)	119.90(11)	N(1)$^{\#}$1-N(2)-C(2)	114.43(11)
C(13)-C(12)-C(11)	121.04(14)	N(1)$^{\#}$1-N(2)-P(1)	120.04(9)
C(14)-C(13)-C(12)	120.08(14)	C(2)-N(2)-P(1)	119.18(10)
C(13)-C(14)-C(15)	119.73(14)	N(1)-P(1)-N(2)	106.49(6)
C(14)-C(15)-C(16)	120.24(14)	N(1)-P(1)-C(11)	101.67(6)
C(15)-C(16)-C(11)	120.72(14)	N(2)-P(1)-C(11)	100.84(6)
N(2)$^{\#}$1-N(1)-C(1)	114.56(12)		

Symmetry transformations used to generate equivalent atoms:

$^{\#}$1 -x,-y,-z.

Table 6: Torsion angles [°] for **52**.

C(16)-C(11)-C(12)-C(13)	-2.7(2)	N(2)#1-N(1)-P(1)-C(11)	-66.99(11)
P(1)-C(11)-C(12)-C(13)	-172.18(11)	C(1)-N(1)-P(1)-C(11)	134.55(11)
C(11)-C(12)-C(13)-C(14)	0.5(2)	N(1)#1-N(2)-P(1)-N(1)	-37.75(13)
C(12)-C(13)-C(14)-C(15)	1.3(2)	C(2)-N(2)-P(1)-N(1)	112.73(11)
C(13)-C(14)-C(15)-C(16)	-1.0(2)	N(1)#1-N(2)-P(1)-C(11)	68.00(11)
C(14)-C(15)-C(16)-C(11)	-1.3(2)	C(2)-N(2)-P(1)-C(11)	-141.52(11)
C(12)-C(11)-C(16)-C(15)	3.1(2)	C(16)-C(11)-P(1)-N(1)	148.76(12)
P(1)-C(11)-C(16)-C(15)	172.42(12)	C(12)-C(11)-P(1)-N(1)	-42.10(12)
N(2)#1-N(1)-P(1)-N(2)	38.17(13)	C(16)-C(11)-P(1)-N(2)	39.20(13)
C(1)-N(1)-P(1)-N(2)	-120.30(12)	C(12)-C(11)-P(1)-N(2)	-151.65(11)

Symmetry transformations used to generate equivalent atoms:

#1 -x,-y,-z.

Bis(diphenylphosphino)dimethylhydrazine di(gold chloride) (22)

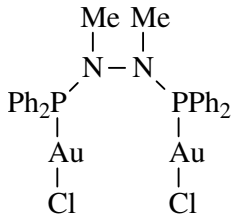

Table 7: Crystal data and structure refinement for **22**.

Empirical formula	$Au_2Cl_2P_2N_2C_{26}H_{26}$	
Formula weight	893.26	
Temperature	193(2) K	
Wavelength	0.71073 Å	
Crystal system	Tetragonal	
Space group	$P4_12_12$	
Unit cell dimensions	a = 10.6720(14) Å	α = 90°
	b = 10.6720(14) Å	β = 90°

	c = 23.439(4) Å γ = 90°
Volume	2669.5(7) $Å^3$
Z	4
Density (calculated)	2.223 Mg/m^3
Absorption coefficient	11.317 mm^{-1}
F(000)	1672
Crystal size	18 x 10 x 8 mm^3
Theta range for data collection	2.10 to 28.29°
Index ranges	-14<=h<=14, -11<=k<=14, -31<=l<=31
Reflections collected	25347
Independent reflections	3312 [R(int) = 0.0906]
Completeness to theta = 28.29°	99.9 %
Absorption correction	Integration
Max. and min. transmission	0.4566 and 0.2936
Refinement method	Full-matrix least-squares on F^2
Data/restraints/parameters	3312/0/154
Goodness-of-fit on F^2	0.975
Final R indices [I>2sigma(I)]	R1 = 0.0296, wR2 = 0.0531
R indices (all data)	R1 = 0.0467, wR2 = 0.0560
Absolute structure parameter	0.011(10)
Largest diff. peak and hole	1.443 and -0.767 $e.Å^{-3}$

Table 8: Bond lengths [Å] and angles [°] for **22**.

Au-P	2.2318(16)	C(21)-C(26)	1.394(9)
Au-Cl	2.2976(17)	C(11)-C(12)	1.394(8)
P-N	1.702(5)	C(11)-C(16)	1.402(9)
P-C(21)	1.805(6)	C(23)-C(24)	1.379(10)
P-C(11)	1.811(6)	C(23)-C(22)	1.388(8)
$N-N^{\#}1$	1.425(10)	C(16)-C(15)	1.386(9)
N-C(1)	1.455(8)	C(25)-C(26)	1.349(9)
C(21)-C(22)	1.393(8)	C(25)-C(24)	1.404(9)

C(15)-C(14)	1.372(9)	C(13)-C(14)	1.374(9)
C(13)-C(12)	1.373(9)		

P-Au-Cl	176.34(6)	C(12)-C(11)-C(16)	118.1(6)
N-P-C(21)	110.1(3)	C(12)-C(11)-P	120.4(5)
N-P-C(11)	103.8(3)	C(16)-C(11)-P	120.9(5)
C(21)-P-C(11)	106.0(3)	C(24)-C(23)-C(22)	119.1(6)
N-P-Au	108.89(18)	C(15)-C(16)-C(11)	119.9(6)
C(21)-P-Au	114.4(2)	C(26)-C(25)-C(24)	120.3(7)
C(11)-P-Au	113.1(2)	C(14)-C(15)-C(16)	120.8(6)
$N^{\#}1$-N-C(1)	115.9(4)	C(12)-C(13)-C(14)	120.5(6)
$N^{\#}1$-N-P	113.3(5)	C(23)-C(22)-C(21)	120.8(6)
C(1)-N-P	121.9(4)	C(13)-C(12)-C(11)	120.9(6)
C(22)-C(21)-C(26)	118.9(6)	C(23)-C(24)-C(25)	120.0(6)
C(22)-C(21)-P	118.2(5)	C(25)-C(26)-C(21)	120.8(6)
C(26)-C(21)-P	122.9(5)	C(15)-C(14)-C(13)	119.6(6)

Symmetry transformations used to generate equivalent atoms:

$^{\#}1$ -y+1,-x+1,-z+1/2.

Table 9: Torsion angles [°] for **22**.

C(21)-P-N-$N^{\#}1$	-89.2(4)	C(11)-P-C(21)-C(26)	42.7(6)
C(11)-P-N-$N^{\#}1$	157.7(3)	Au-P-C(21)-C(26)	168.0(5)
Au-P-N-$N^{\#}1$	37.0(4)	N-P-C(11)-C(12)	-42.6(6)
C(21)-P-N-C(1)	56.8(6)	C(21)-P-C(11)-C(12)	-158.7(5)
C(11)-P-N-C(1)	-56.3(6)	Au-P-C(11)-C(12)	75.2(5)
Au-P-N-C(1)	-177.0(5)	N-P-C(11)-C(16)	145.7(5)
N-P-C(21)-C(22)	110.1(5)	C(21)-P-C(11)-C(16)	29.7(6)
C(11)-P-C(21)-C(22)	-138.3(5)	Au-P-C(11)-C(16)	-96.5(5)
Au-P-C(21)-C(22)	-13.0(6)	C(12)-C(11)-C(16)-C(15)	-0.2(10)
N-P-C(21)-C(26)	-69.0(6)	P-C(11)-C(16)-C(15)	171.6(5)

C(11)-C(16)-C(15)-C(14)	0.9(10)	C(22)-C(23)-C(24)-C(25)	4.1(10)
C(24)-C(23)-C(22)-C(21)	-2.1(9)	C(26)-C(25)-C(24)-C(23)	-3.1(10)
C(26)-C(21)-C(22)-C(23)	-0.9(9)	C(24)-C(25)-C(26)-C(21)	0.0(10)
P-C(21)-C(22)-C(23)	180.0(5)	C(22)-C(21)-C(26)-C(25)	2.0(10)
C(14)-C(13)-C(12)-C(11)	-0.5(10)	P-C(21)-C(26)-C(25)	-179.0(5)
C(16)-C(11)-C(12)-C(13)	0.0(9)	C(16)-C(15)-C(14)-C(13)	-1.3(11)
P-C(11)-C(12)-C(13)	-171.8(5)	C(12)-C(13)-C(14)-C(15)	1.1(11)

Symmetry transformations used to generate equivalent atoms:

#1 -y+1,-x+1,-z+1/2.

Bis(diphenylphosphino)diethylhydrazine di(gold chloride) (23)

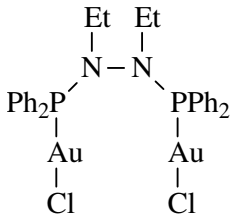

Table 10: Crystal data and structure refinement for **23**.

Empirical formula	$Au_2Cl_2P_2N_2O_2C_{36}H_{46}$	
Formula weight	1065.52	
Temperature	173(2) K	
Wavelength	0.71073 Å	
Crystal system	Orthorhombic	
Space group	*Pccn*	
Unit cell dimensions	a = 12.3275(18) Å	α = 90°
	b = 17.200(3) Å	β = 90°
	c = 18.173(3) Å	γ = 90°
Volume	3853.4(10) $Å^3$	
Z	4	
Density (calculated)	1.837 Mg/m^3	
Absorption coefficient	7.860 mm^{-1}	

F(000)	2056
Crystal size	0.48 x 0.23 x 0.14 mm^3
Theta range for data collection	2.03 to 27.00°
Index ranges	-11<=h<=15, -21<=k<=21, -22<=l<=23
Reflections collected	23024
Independent reflections	4199 [R(int) = 0.0450]
Completeness to theta = 27.00°	99.8 %
Absorption correction	Integration
Max. and min. transmission	0.3395 and 0.1191
Refinement method	Full-matrix least-squares on F^2
Data/restraints/parameters	4199/0/209
Goodness-of-fit on F_2	1.063
Final R indices [I>2sigma(I)]	R1 = 0.0256, wR2 = 0.0485
R indices (all data)	R1 = 0.0417, wR2 = 0.0518
Largest diff. peak and hole	0.523 and -1.219 e.$Å^{-3}$

Table 11: Bond lengths [Å] and angles [°] for **23**.

Au(1)-P(1)	2.2331(11)	C(14)-C(15)	1.361(6)
Au(1)-Cl(1)	2.3021(10)	C(15)-C(16)	1.394(6)
Au(1)-Au(1)$^{\#}$1	3.1310(5)	C(21)-C(22)	1.399(6)
N(1)-N(1)$^{\#}$1	1.416(6)	C(21)-C(26)	1.400(6)
N(1)-C(1)	1.481(5)	C(22)-C(23)	1.383(6)
N(1)-P(1)	1.679(3)	C(23)-C(24)	1.385(7)
P(1)-C(21)	1.810(4)	C(24)-C(25)	1.367(6)
P(1)-C(11)	1.820(4)	C(25)-C(26)	1.369(6)
C(1)-C(2)	1.526(6)	O(1)-C(31)	1.340(9)
C(11)-C(12)	1.386(6)	O(1)-C(34)	1.349(8)
C(11)-C(16)	1.397(5)	C(31)-C(32)	1.497(9)
C(12)-C(13)	1.388(6)	C(32)-C(33)	1.491(9)
C(13)-C(14)	1.377(6)	C(33)-C(34)	1.479(8)

P(1)-Au(1)-Cl(1)	179.22(4)	C(14)-C(13)-C(12)	120.6(4)
P(1)-Au(1)-Au(1)$^{\#}$1	86.37(3)	C(15)-C(14)-C(13)	120.0(4)
Cl(1)-Au(1)-Au(1)$^{\#}$1	94.01(3)	C(14)-C(15)-C(16)	120.4(4)
N(1)$^{\#}$1-N(1)-C(1)	117.4(3)	C(15)-C(16)-C(11)	120.0(4)
N(1)$^{\#}$1-N(1)-P(1)	118.4(3)	C(22)-C(21)-C(26)	118.0(4)
C(1)-N(1)-P(1)	123.1(2)	C(22)-C(21)-P(1)	122.5(3)
N(1)-P(1)-C(21)	104.36(17)	C(26)-C(21)-P(1)	119.5(3)
N(1)-P(1)-C(11)	108.90(18)	C(23)-C(22)-C(21)	119.7(4)
C(21)-P(1)-C(11)	103.71(18)	C(22)-C(23)-C(24)	120.6(5)
N(1)-P(1)-Au(1)	110.68(11)	C(25)-C(24)-C(23)	120.3(5)
C(21)-P(1)-Au(1)	113.12(13)	C(24)-C(25)-C(26)	119.6(5)
C(11)-P(1)-Au(1)	115.30(14)	C(25)-C(26)-C(21)	121.7(4)
N(1)-C(1)-C(2)	113.1(3)	C(31)-O(1)-C(34)	112.3(6)
C(12)-C(11)-C(16)	118.9(4)	O(1)-C(31)-C(32)	110.3(7)
C(12)-C(11)-P(1)	122.2(3)	C(33)-C(32)-C(31)	102.4(6)
C(16)-C(11)-P(1)	118.8(3)	C(34)-C(33)-C(32)	106.3(6)
C(11)-C(12)-C(13)	120.0(4)	O(1)-C(34)-C(33)	108.3(6)

Symmetry transformations used to generate equivalent atoms:

$^{\#}$1 -x+3/2,-y+1/2,z.

Table 12: Torsion angles [°] for **23**.

N(1)$^{\#}$1-N(1)-P(1)-C(21)	-155.3(2)	N(1)$^{\#}$1-N(1)-C(1)-C(2)	90.6(4)
C(1)-N(1)-P(1)-C(21)	37.0(3)	P(1)-N(1)-C(1)-C(2)	-101.6(4)
N(1)$^{\#}$1-N(1)-P(1)-C(11)	94.4(3)	N(1)-P(1)-C(11)-C(12)	11.5(4)
C(1)-N(1)-P(1)-C(11)	-73.3(3)	C(21)-P(1)-C(11)-C(12)	-99.2(4)
N(1)$^{\#}$1-N(1)-P(1)-Au(1)	-33.3(3)	Au(1)-P(1)-C(11)-C(12)	136.5(3)
C(1)-N(1)-P(1)-Au(1)	159.0(3)	N(1)-P(1)-C(11)-C(16)	-168.9(3)
Au(1)$^{\#}$1-Au(1)-P(1)-N(1)	-38.27(13)	C(21)-P(1)-C(11)-C(16)	80.4(3)
Au(1)$^{\#}$1-Au(1)-P(1)-C(21)	78.44(14)	Au(1)-P(1)-C(11)-C(16)	-43.8(4)
Au(1)$^{\#}$1-Au(1)-P(1)-C(11)	-162.42(14)	C(16)-C(11)-C(12)-C(13)	-1.2(6)

P(1)-C(11)-C(12)-C(13)	178.4(3)	C(26)-C(21)-C(22)-C(23)	-1.4(7)
C(11)-C(12)-C(13)-C(14)	-0.6(7)	P(1)-C(21)-C(22)-C(23)	177.8(4)
C(12)-C(13)-C(14)-C(15)	1.6(7)	C(21)-C(22)-C(23)-C(24)	0.5(8)
C(13)-C(14)-C(15)-C(16)	-0.8(7)	C(22)-C(23)-C(24)-C(25)	0.0(9)
C(14)-C(15)-C(16)-C(11)	-0.9(7)	C(23)-C(24)-C(25)-C(26)	0.5(8)
C(12)-C(11)-C(16)-C(15)	1.9(6)	C(24)-C(25)-C(26)-C(21)	-1.6(8)
P(1)-C(11)-C(16)-C(15)	-177.7(3)	C(22)-C(21)-C(26)-C(25)	2.0(7)
N(1)-P(1)-C(21)-C(22)	-95.7(4)	P(1)-C(21)-C(26)-C(25)	-177.3(4)
C(11)-P(1)-C(21)-C(22)	18.3(4)	C(34)-O(1)-C(31)-C(32)	-2.4(12)
Au(1)-P(1)-C(21)-C(22)	144.0(3)	O(1)-C(31)-C(32)-C(33)	5.2(11)
N(1)-P(1)-C(21)-C(26)	83.6(4)	C(31)-C(32)-C(33)-C(34)	-5.8(9)
C(11)-P(1)-C(21)-C(26)	-162.4(3)	C(31)-O(1)-C(34)-C(33)	-1.6(11)
Au(1)-P(1)-C(21)-C(26)	-36.8(4)	C(32)-C(33)-C(34)-O(1)	4.9(10)

Symmetry transformations used to generate equivalent atoms:

#1 -x+3/2,-y+1/2,z.

Bis(di(4-methoxyphenyl))dimethylhydrazine di(gold chloride) (24)

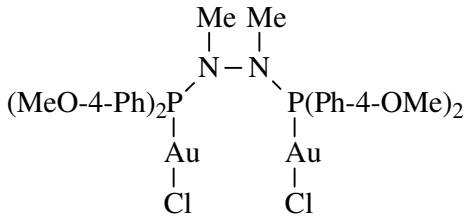

Table 13: Crystal data and structure refinement for **24**.

Empirical formula	$Au_2Cl_2P_2N_2O_6C_{38}H_{50}$
Formula weight	1157.57
Temperature	173(2) K
Wavelength	0.71073 Å
Crystal system	Monoclinic
Space group	*C2/c*

Unit cell dimensions	a = 23.208(5) Å	α = 90°
	b = 9.080(5) Å	β = 92.4(5)°
	c = 20.220(5) Å	γ = 90°
Volume	4257(3) $Å^3$	
Z	4	
Density (calculated)	1.806 Mg/m^3	
Absorption coefficient	7.129 mm^{-1}	
F(000)	2248	
Crystal size	0.58 x 0.45 x 0.10 mm^3	
Theta range for data collection	1.76 to 28.29°	
Index ranges	-30<=h<=30, -12<=k<=11, -25<=l<=26	
Reflections collected	33198	
Independent reflections	5264 [R(int) = 0.0400]	
Completeness to theta = 28.29°	99.6 %	
Absorption correction	Integration	
Max. and min. transmission	0.5670 and 0.0436	
Refinement method	Full-matrix least-squares on F^2	
Data/restraints/parameters	5264/0/235	
Goodness-of-fit on F^2	1.037	
Final R indices [I>2sigma(I)]	R1 = 0.0193, wR2 = 0.0460	
R indices (all data)	R1 = 0.0249, wR2 = 0.0486	
Largest diff. peak and hole	1.077 and -0.795 $e.Å^{-3}$	

Table 14: Bond lengths [Å] and angles [°] for **24**.

C(1)-N	1.460(3)	C(14)-C(15)	1.378(4)
C(11)-C(16)	1.382(4)	C(15)-C(16)	1.391(3)
C(11)-C(12)	1.395(4)	C(17)-O(1)	1.419(4)
C(11)-P	1.803(2)	C(21)-C(22)	1.382(4)
C(12)-C(13)	1.376(4)	C(21)-C(26)	1.391(4)
C(13)-C(14)	1.388(4)	C(21)-P	1.807(2)
C(14)-O(1)	1.362(3)	C(22)-C(23)	1.396(4)

C(23)-C(24)	1.380(4)	C(33)-C(34)	1.361(9)
C(24)-O(2)	1.365(3)	C(34)-O(3)	1.366(7)
C(24)-C(25)	1.393(4)	N-N$^{\#}$1	1.417(4)
C(25)-C(26)	1.378(4)	N-P	1.678(2)
C(27)-O(2)	1.430(4)	P-Au	2.2238(11)
C(31)-O(3)	1.371(6)	Cl-Au	2.2905(11)
C(31)-C(32)	1.495(7)	Au-Au$^{\#}$1	3.1222(7)
C(32)-C(33)	1.449(9)		

C(16)-C(11)-C(12)	118.8(2)	O(3)-C(31)-C(32)	105.7(5)
C(16)-C(11)-P	119.45(19)	C(33)-C(32)-C(31)	105.2(5)
C(12)-C(11)-P	121.61(19)	C(34)-C(33)-C(32)	104.1(6)
C(13)-C(12)-C(11)	120.4(3)	C(33)-C(34)-O(3)	113.0(6)
C(12)-C(13)-C(14)	120.1(3)	N$^{\#}$1-N-C(1)	116.05(18)
O(1)-C(14)-C(15)	124.4(3)	N$^{\#}$1-N-P	115.65(17)
O(1)-C(14)-C(13)	115.2(3)	C(1)-N-P	126.33(17)
C(15)-C(14)-C(13)	120.4(2)	C(14)-O(1)-C(17)	117.6(3)
C(14)-C(15)-C(16)	119.1(3)	C(24)-O(2)-C(27)	117.0(3)
C(11)-C(16)-C(15)	121.2(2)	C(34)-O(3)-C(31)	105.4(5)
C(22)-C(21)-C(26)	118.8(2)	N-P-C(11)	102.26(11)
C(22)-C(21)-P	119.4(2)	N-P-C(21)	109.71(12)
C(26)-C(21)-P	121.73(19)	C(11)-P-C(21)	104.57(11)
C(21)-C(22)-C(23)	121.0(3)	N-P-Au	110.83(8)
C(24)-C(23)-C(22)	119.2(3)	C(11)-P-Au	116.63(9)
O(2)-C(24)-C(23)	124.8(3)	C(21)-P-Au	112.20(9)
O(2)-C(24)-C(25)	114.8(3)	P-Au-Cl	175.68(3)
C(23)-C(24)-C(25)	120.4(2)	P-Au-Au$^{\#}$1	88.241(19)
C(26)-C(25)-C(24)	119.6(3)	Cl-Au-Au$^{\#}$1	94.74(2)
C(25)-C(26)-C(21)	120.9(2)		

Symmetry transformations used to generate equivalent atoms:

$^{\#}$1 -x+1,y,-z+1/2.

Table 15: Torsion angles [°] for **24**.

C(16)-C(11)-C(12)-C(13)	-1.9(4)	C(33)-C(34)-O(3)-C(31)	26.4(12)
P-C(11)-C(12)-C(13)	174.3(2)	C(32)-C(31)-O(3)-C(34)	-23.6(9)
C(11)-C(12)-C(13)-C(14)	1.0(5)	N$^{\#}$1-N-P-C(11)	-165.00(15)
C(12)-C(13)-C(14)-O(1)	-178.9(3)	C(1)-N-P-C(11)	31.7(3)
C(12)-C(13)-C(14)-C(15)	0.6(5)	N$^{\#}$1-N-P-C(21)	84.44(16)
O(1)-C(14)-C(15)-C(16)	178.3(3)	C(1)-N-P-C(21)	-78.9(3)
C(13)-C(14)-C(15)-C(16)	-1.3(5)	N$^{\#}$1-N-P-Au	-40.01(16)
C(12)-C(11)-C(16)-C(15)	1.3(4)	C(1)-N-P-Au	156.7(2)
P-C(11)-C(16)-C(15)	-175.0(2)	C(16)-C(11)-P-N	76.7(2)
C(14)-C(15)-C(16)-C(11)	0.3(4)	C(12)-C(11)-P-N	-99.5(2)
C(26)-C(21)-C(22)-C(23)	1.4(4)	C(16)-C(11)-P-C(21)	-168.9(2)
P-C(21)-C(22)-C(23)	-175.7(2)	C(12)-C(11)-P-C(21)	14.9(3)
C(21)-C(22)-C(23)-C(24)	-1.3(4)	C(16)-C(11)-P-Au	-44.4(2)
C(22)-C(23)-C(24)-O(2)	-179.7(3)	C(12)-C(11)-P-Au	139.4(2)
C(22)-C(23)-C(24)-C(25)	0.1(4)	C(22)-C(21)-P-N	-162.70(19)
O(2)-C(24)-C(25)-C(26)	-179.3(2)	C(26)-C(21)-P-N	20.2(2)
C(23)-C(24)-C(25)-C(26)	0.9(4)	C(22)-C(21)-P-C(11)	88.3(2)
C(24)-C(25)-C(26)-C(21)	-0.7(4)	C(26)-C(21)-P-C(11)	-88.8(2)
C(22)-C(21)-C(26)-C(25)	-0.5(4)	C(22)-C(21)-P-Au	-39.0(2)
P-C(21)-C(26)-C(25)	176.63(19)	C(26)-C(21)-P-Au	143.88(19)
O(3)-C(31)-C(32)-C(33)	14.1(8)	N-P-Au-Cl	101.1(3)
C(31)-C(32)-C(33)-C(34)	1.1(10)	C(11)-P-Au-Cl	-142.5(3)
C(32)-C(33)-C(34)-O(3)	-16.7(13)	C(21)-P-Au-Cl	-21.9(4)
C(15)-C(14)-O(1)-C(17)	-9.2(5)	N-P-Au-Au$^{\#}$1	-32.68(8)
C(13)-C(14)-O(1)-C(17)	170.4(3)	C(11)-P-Au-Au$^{\#}$1	83.74(9)
C(23)-C(24)-O(2)-C(27)	-5.4(5)	C(21)-P-Au-Au$^{\#}$1	-155.70(9)
C(25)-C(24)-O(2)-C(27)	174.8(3)		

Symmetry transformations used to generate equivalent atoms:

$^{\#}$1 -x+1,y,-z+1/2.

Bis(di(4-methoxyphenyl))diethylhydrazine di(gold chloride) (25)

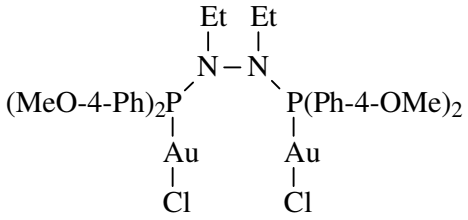

Table 16: Crystal data and structure refinement for **25**.

Empirical formula	$Au_2Cl_2P_2N_2O_6C_{40}H_{54}$	
Formula weight	1185.63	
Temperature	173(2) K	
Wavelength	0.71073 Å	
Crystal system	Monoclinic	
Space group	*C2/c*	
Unit cell dimensions	a = 23.638(5) Å	α = 90°
	b = 9.126(5) Å	β = 94.0(5)°
	c = 20.227(5) Å	γ = 90°
Volume	4353(3) $Å^3$	
Z	4	
Density (calculated)	1.809 Mg/m^3	
Absorption coefficient	6.975 mm^{-1}	
F(000)	2312	
Crystal size	0.36 x 0.20 x 0.07 mm^3	
Theta range for data collection	1.73 to 35.26°	
Index ranges	-38<=h<=36, -14<=k<=14, -32<=l<=32	
Reflections collected	52013	
Independent reflections	9147 [R(int) = 0.1649]	
Completeness to theta = 35.26°	93.5 %	
Absorption correction	None	
Refinement method	Full-matrix least-squares on F^2	
Data/restraints/parameters	9147/0/245	

Goodness-of-fit on F^2	1.003
Final R indices [I>2sigma(I)]	R1 = 0.0522, wR2 = 0.1322
R indices (all data)	R1 = 0.0638, wR2 = 0.1379
Largest diff. peak and hole	7.150 and -3.416 e.$Å^{-3}$

Table 17: Bond lengths [Å] and angles [°] for **25**.

C(1)-N(1)	1.474(5)	C(23)-C(24)	1.394(6)
C(1)-C(2)	1.527(6)	C(24)-O(2)	1.365(5)
C(11)-C(12)	1.395(5)	C(24)-C(25)	1.393(6)
C(11)-C(16)	1.400(5)	C(25)-C(26)	1.397(6)
C(11)-P(1)	1.813(4)	C(27)-O(2)	1.414(7)
C(12)-C(13)	1.392(6)	N(1)-N(1)$^{\#}$1	1.405(6)
C(13)-C(14)	1.395(6)	N(1)-P(1)	1.685(3)
C(14)-O(1)	1.347(5)	P(1)-Au(1)	2.2267(13)
C(14)-C(15)	1.393(6)	Cl(1)-Au(1)	2.2935(14)
C(15)-C(16)	1.387(6)	Au(1)-Au(1)$^{\#}$1	3.1408(7)
C(17)-O(1)	1.434(8)	O(3)-C(34)	1.426(8)
C(21)-C(26)	1.389(5)	O(3)-C(31)	1.626(11)
C(21)-C(22)	1.398(5)	C(34)-C(33)	1.487(13)
C(21)-P(1)	1.805(4)	C(33)-C(32)	1.377(16)
C(22)-C(23)	1.372(6)	C(31)-C(32)	1.430(18)

N(1)-C(1)-C(2)	113.7(3)	C(16)-C(15)-C(14)	120.2(4)
C(12)-C(11)-C(16)	119.0(4)	C(15)-C(16)-C(11)	120.5(4)
C(12)-C(11)-P(1)	119.3(3)	C(26)-C(21)-C(22)	118.4(4)
C(16)-C(11)-P(1)	121.7(3)	C(26)-C(21)-P(1)	119.5(3)
C(13)-C(12)-C(11)	120.7(4)	C(22)-C(21)-P(1)	121.9(3)
C(12)-C(13)-C(14)	119.8(4)	C(23)-C(22)-C(21)	121.0(4)
O(1)-C(14)-C(15)	115.3(4)	C(22)-C(23)-C(24)	120.1(4)
O(1)-C(14)-C(13)	124.8(4)	O(2)-C(24)-C(25)	124.0(4)
C(15)-C(14)-C(13)	119.8(4)	O(2)-C(24)-C(23)	115.8(4)

C(25)-C(24)-C(23)	120.2(4)	N(1)-P(1)-Au(1)	111.61(11)
C(24)-C(25)-C(26)	118.8(4)	C(21)-P(1)-Au(1)	115.65(11)
C(21)-C(26)-C(25)	121.4(4)	C(11)-P(1)-Au(1)	112.19(13)
N(1)$^{\#}$1-N(1)-C(1)	117.4(3)	P(1)-Au(1)-Cl(1)	175.99(4)
N(1)$^{\#}$1-N(1)-P(1)	117.5(2)	P(1)-Au(1)-Au(1)$^{\#}$1	87.78(3)
C(1)-N(1)-P(1)	123.2(2)	Cl(1)-Au(1)-Au(1)$^{\#}$1	95.56(3)
C(14)-O(1)-C(17)	116.6(4)	C(34)-O(3)-C(31)	97.3(5)
C(24)-O(2)-C(27)	118.1(4)	O(3)-C(34)-C(33)	114.5(6)
N(1)-P(1)-C(21)	102.36(16)	C(32)-C(33)-C(34)	106.3(9)
N(1)-P(1)-C(11)	109.44(17)	C(32)-C(31)-O(3)	107.5(8)
C(21)-P(1)-C(11)	104.93(17)	C(33)-C(32)-C(31)	109.9(11)

Symmetry transformations used to generate equivalent atoms:

$^{\#}$1 -x+1,y,-z+3/2.

Table 18: Torsion angles [°] for **25**.

C(16)-C(11)-C(12)-C(13)	-0.4(6)	C(23)-C(24)-C(25)-C(26)	1.5(7)
P(1)-C(11)-C(12)-C(13)	179.5(3)	C(22)-C(21)-C(26)-C(25)	-3.1(6)
C(11)-C(12)-C(13)-C(14)	1.2(7)	P(1)-C(21)-C(26)-C(25)	172.8(3)
C(12)-C(13)-C(14)-O(1)	178.8(4)	C(24)-C(25)-C(26)-C(21)	1.2(7)
C(12)-C(13)-C(14)-C(15)	-0.7(7)	C(2)-C(1)-N(1)-N(1)$^{\#}$1	-94.3(4)
O(1)-C(14)-C(15)-C(16)	179.8(4)	C(2)-C(1)-N(1)-P(1)	102.0(4)
C(13)-C(14)-C(15)-C(16)	-0.6(6)	C(15)-C(14)-O(1)-C(17)	-179.0(6)
C(14)-C(15)-C(16)-C(11)	1.4(6)	C(13)-C(14)-O(1)-C(17)	1.4(8)
C(12)-C(11)-C(16)-C(15)	-1.0(6)	C(25)-C(24)-O(2)-C(27)	11.0(8)
P(1)-C(11)-C(16)-C(15)	179.2(3)	C(23)-C(24)-O(2)-C(27)	-168.6(6)
C(26)-C(21)-C(22)-C(23)	2.3(7)	N(1)$^{\#}$1-N(1)-P(1)-C(21)	161.0(2)
P(1)-C(21)-C(22)-C(23)	-173.4(4)	C(1)-N(1)-P(1)-C(21)	-35.3(3)
C(21)-C(22)-C(23)-C(24)	0.3(8)	N(1)$^{\#}$1-N(1)-P(1)-C(11)	-88.1(3)
C(22)-C(23)-C(24)-O(2)	177.4(5)	C(1)-N(1)-P(1)-C(11)	75.6(3)
C(22)-C(23)-C(24)-C(25)	-2.2(8)	N(1)$^{\#}$1-N(1)-P(1)-Au(1)	36.7(3)
O(2)-C(24)-C(25)-C(26)	-178.1(5)	C(1)-N(1)-P(1)-Au(1)	-159.6(3)

C(26)-C(21)-P(1)-N(1)	-80.2(3)	N(1)-P(1)-Au(1)-Cl(1)	-111.8(6)
C(22)-C(21)-P(1)-N(1)	95.5(4)	C(21)-P(1)-Au(1)-Cl(1)	131.7(6)
C(26)-C(21)-P(1)-C(11)	165.5(3)	C(11)-P(1)-Au(1)-Cl(1)	11.4(6)
C(22)-C(21)-P(1)-C(11)	-18.8(4)	N(1)-P(1)-Au(1)-Au(1)$^{\#}$1	34.73(12)
C(26)-C(21)-P(1)-Au(1)	41.3(4)	C(21)-P(1)-Au(1)-Au(1)$^{\#}$1	-81.73(14)
C(22)-C(21)-P(1)-Au(1)	-143.0(3)	C(11)-P(1)-Au(1)-Au(1)$^{\#}$1	157.97(13)
C(12)-C(11)-P(1)-N(1)	163.0(3)	C(31)-O(3)-C(34)-C(33)	15.6(11)
C(16)-C(11)-P(1)-N(1)	-17.1(4)	O(3)-C(34)-C(33)-C(32)	-5.6(17)
C(12)-C(11)-P(1)-C(21)	-87.8(3)	C(34)-O(3)-C(31)-C(32)	-20.6(12)
C(16)-C(11)-P(1)-C(21)	92.1(3)	C(34)-C(33)-C(32)-C(31)	-9.5(19)
C(12)-C(11)-P(1)-Au(1)	38.5(3)	O(3)-C(31)-C(32)-C(33)	19.4(18)
C(16)-C(11)-P(1)-Au(1)	-141.6(3)		

Symmetry transformations used to generate equivalent atoms:

$^{\#}$1 -x+1,y,-z+3/2.

Bis(di(N,N-dimetyl-4-aminophenyl))diethylhydrazine di(gold chloride) (27)

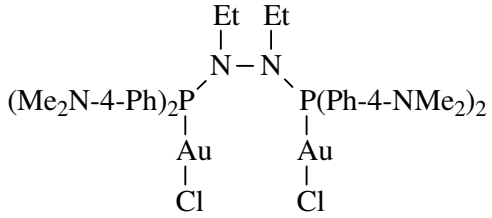

Table 19: Crystal data and structure refinement for **27**.

Empirical formula	$Au_2Cl_2P_2N_4C_{30}H_{30}$	
Formula weight	973.35	
Temperature	173(2) K	
Wavelength	0.71073 Å	
Crystal system	Monoclinic	
Space group	$P2_1/c$	
Unit cell dimensions	a = 13.9122(13) Å	α = 90°
	b = 14.9533(15) Å	β = 96.9(6)°

	c = 23.806(2) Å γ = 90°
Volume	4916.7(8) $Å^3$
Z	6
Density (calculated)	1.972 Mg/m^3
Absorption coefficient	9.228 mm^{-1}
F(000)	2760
Crystal size	0.16 x 0.08 x 0.04 mm^3
Theta range for data collection	1.47 to 28.00°
Index ranges	-16<=h<=18, -19<=k<=19, -31<=l<=31
Reflections collected	41431
Independent reflections	11865 [R(int) = 0.3658]
Completeness to theta = 28.00°	100.0 %
Absorption correction	Integration
Max. and min. transmission	0.7091 and 0.3199
Refinement method	Full-matrix least-squares on F^2
Data/restraints/parameters	11865/0/449
Goodness-of-fit on F^2	0.921
Final R indices [I>2sigma(I)]	R1 = 0.0845, wR2 = 0.1890
R indices (all data)	R1 = 0.2862, wR2 = 0.2727
Largest diff. peak and hole	2.503 and -2.498 $e.Å^{-3}$

Table 20: Bond lengths [Å] and angles [°] for **27**.

C(1)-N(1)	1.46(2)	C(14)-N(3)	1.37(3)
C(1)-C(2)	1.52(3)	C(14)-C(15)	1.39(3)
C(3)-N(2)	1.43(3)	C(15)-C(16)	1.39(3)
C(3)-C(4)	1.51(3)	C(17)-N(3)	1.47(3)
C(11)-C(12)	1.39(3)	C(18)-N(3)	1.44(3)
C(11)-C(16)	1.40(3)	C(21)-C(22)	1.42(3)
C(11)-P(1)	1.82(2)	C(21)-C(26)	1.40(3)
C(12)-C(13)	1.37(3)	C(21)-P(1)	1.76(2)
C(13)-C(14)	1.42(3)	C(22)-C(23)	1.41(3)

C(23)-C(24)	1.38(3)	C(42)-C(43)	1.35(3)
C(24)-N(4)	1.38(3)	C(43)-C(44)	1.38(3)
C(24)-C(25)	1.39(3)	C(44)-N(6)	1.35(3)
C(25)-C(26)	1.38(3)	C(44)-C(45)	1.44(3)
C(27)-N(4)	1.40(3)	C(45)-C(46)	1.42(3)
C(28)-N(4)	1.44(3)	C(47)-N(6)	1.45(3)
C(31)-C(36)	1.40(3)	C(48)-N(6)	1.51(3)
C(31)-C(32)	1.42(3)	C(98)-C(99)	1.78(11)
C(31)-P(2)	1.814(19)	C(98)-Cl(98)	1.84(5)
C(32)-C(33)	1.42(3)	C(99)-Cl(99)	1.59(10)
C(33)-C(34)	1.41(3)	C(99)-Cl(98)	2.14(10)
C(34)-N(5)	1.37(3)	N(1)-N(2)	1.43(2)
C(34)-C(35)	1.44(3)	N(1)-P(1)	1.683(17)
C(35)-C(36)	1.35(3)	N(2)-P(2)	1.667(18)
C(37)-N(5)	1.47(3)	P(1)-Au(1)	2.238(5)
C(38)-N(5)	1.40(4)	P(2)-Au(2)	2.239(6)
C(41)-C(46)	1.38(3)	Cl(1)-Au(1)	2.313(5)
C(41)-C(42)	1.44(3)	Cl(2)-Au(2)	2.313(7)
C(41)-P(2)	1.79(2)	Au(1)-Au(2)	3.1860(13)

N(1)-C(1)-C(2)	111.8(18)	C(22)-C(21)-P(1)	120.6(15)
N(2)-C(3)-C(4)	116(2)	C(26)-C(21)-P(1)	124.7(18)
C(12)-C(11)-C(16)	116.7(19)	C(21)-C(22)-C(23)	123(2)
C(12)-C(11)-P(1)	123.3(15)	C(24)-C(23)-C(22)	120(2)
C(16)-C(11)-P(1)	119.8(15)	N(4)-C(24)-C(25)	119(2)
C(13)-C(12)-C(11)	123.1(19)	N(4)-C(24)-C(23)	122(3)
C(12)-C(13)-C(14)	119.3(19)	C(25)-C(24)-C(23)	118(2)
N(3)-C(14)-C(15)	121.7(19)	C(24)-C(25)-C(26)	121(2)
N(3)-C(14)-C(13)	119.8(19)	C(25)-C(26)-C(21)	123(2)
C(15)-C(14)-C(13)	118.5(19)	C(36)-C(31)-C(32)	116.8(18)
C(16)-C(15)-C(14)	120.4(18)	C(36)-C(31)-P(2)	120.3(15)
C(15)-C(16)-C(11)	122.0(18)	C(32)-C(31)-P(2)	122.9(14)
C(22)-C(21)-C(26)	114.5(19)	C(31)-C(32)-C(33)	123(2)

C(34)-C(33)-C(32)	118(2)	C(24)-N(4)-C(27)	124(2)
N(5)-C(34)-C(33)	120(2)	C(24)-N(4)-C(28)	118(2)
N(5)-C(34)-C(35)	122(2)	C(27)-N(4)-C(28)	118(2)
C(33)-C(34)-C(35)	118(2)	C(34)-N(5)-C(38)	120(2)
C(36)-C(35)-C(34)	121(2)	C(34)-N(5)-C(37)	121(2)
C(35)-C(36)-C(31)	123(2)	C(38)-N(5)-C(37)	118(2)
C(46)-C(41)-C(42)	114.2(18)	C(44)-N(6)-C(47)	120.2(19)
C(46)-C(41)-P(2)	124.2(15)	C(44)-N(6)-C(48)	120.7(19)
C(42)-C(41)-P(2)	121.6(15)	C(47)-N(6)-C(48)	119.0(18)
C(43)-C(42)-C(41)	123.1(19)	N(1)-P(1)-C(21)	105.1(9)
C(42)-C(43)-C(44)	122.4(19)	N(1)-P(1)-C(11)	108.3(9)
N(6)-C(44)-C(43)	122.5(18)	C(21)-P(1)-C(11)	104.2(10)
N(6)-C(44)-C(45)	120(2)	N(1)-P(1)-Au(1)	111.4(6)
C(43)-C(44)-C(45)	117.6(19)	C(21)-P(1)-Au(1)	113.6(7)
C(46)-C(45)-C(44)	118(2)	C(11)-P(1)-Au(1)	113.6(6)
C(41)-C(46)-C(45)	125(2)	N(2)-P(2)-C(41)	107.6(9)
C(99)-C(98)-Cl(98)	72(4)	N(2)-P(2)-C(31)	110.0(9)
C(98)-C(99)-Cl(99)	143(8)	C(41)-P(2)-C(31)	102.8(9)
C(98)-C(99)-Cl(98)	55(3)	N(2)-P(2)-Au(2)	113.4(7)
Cl(99)-C(99)-Cl(98)	106(6)	C(41)-P(2)-Au(2)	111.9(7)
N(2)-N(1)-C(1)	116.6(16)	C(31)-P(2)-Au(2)	110.6(6)
N(2)-N(1)-P(1)	119.2(12)	C(98)-Cl(98)-C(99)	53(3)
C(1)-N(1)-P(1)	123.2(14)	P(1)-Au(1)-Cl(1)	176.6(2)
N(1)-N(2)-C(3)	119.0(16)	P(1)-Au(1)-Au(2)	86.16(14)
N(1)-N(2)-P(2)	117.7(13)	Cl(1)-Au(1)-Au(2)	97.14(16)
C(3)-N(2)-P(2)	122.7(15)	P(2)-Au(2)-Cl(2)	175.9(3)
C(14)-N(3)-C(18)	121.0(19)	P(2)-Au(2)-Au(1)	85.13(14)
C(14)-N(3)-C(17)	119.1(18)	Cl(2)-Au(2)-Au(1)	99.0(2)
C(18)-N(3)-C(17)	117.0(19)		

Table 21: Torsion angles [°] for **27**.

C(16)-C(11)-C(12)-C(13)	0(3)	P(2)-C(41)-C(42)-C(43)	-175.5(17)
P(1)-C(11)-C(12)-C(13)	175.1(16)	C(41)-C(42)-C(43)-C(44)	-3(3)
C(11)-C(12)-C(13)-C(14)	2(3)	C(42)-C(43)-C(44)-N(6)	-179(2)
C(12)-C(13)-C(14)-N(3)	176.2(18)	C(42)-C(43)-C(44)-C(45)	0(3)
C(12)-C(13)-C(14)-C(15)	-2(3)	N(6)-C(44)-C(45)-C(46)	180(2)
N(3)-C(14)-C(15)-C(16)	-177.7(18)	C(43)-C(44)-C(45)-C(46)	1(3)
C(13)-C(14)-C(15)-C(16)	0(3)	C(42)-C(41)-C(46)-C(45)	-5(3)
C(14)-C(15)-C(16)-C(11)	2(3)	P(2)-C(41)-C(46)-C(45)	176.4(18)
C(12)-C(11)-C(16)-C(15)	-2(3)	C(44)-C(45)-C(46)-C(41)	2(4)
P(1)-C(11)-C(16)-C(15)	-176.9(15)	Cl(98)-C(98)-C(99)-Cl(99)	-69(12)
C(26)-C(21)-C(22)-C(23)	0(3)	C(2)-C(1)-N(1)-N(2)	-90(2)
P(1)-C(21)-C(22)-C(23)	175.4(16)	C(2)-C(1)-N(1)-P(1)	101(2)
C(21)-C(22)-C(23)-C(24)	-1(3)	C(1)-N(1)-N(2)-C(3)	-77(2)
C(22)-C(23)-C(24)-N(4)	178(2)	P(1)-N(1)-N(2)-C(3)	92(2)
C(22)-C(23)-C(24)-C(25)	3(3)	C(1)-N(1)-N(2)-P(2)	94.3(18)
N(4)-C(24)-C(25)-C(26)	180(2)	P(1)-N(1)-N(2)-P(2)	-96.4(15)
C(23)-C(24)-C(25)-C(26)	-5(4)	C(4)-C(3)-N(2)-N(1)	-87(2)
C(24)-C(25)-C(26)-C(21)	4(4)	C(4)-C(3)-N(2)-P(2)	103(2)
C(22)-C(21)-C(26)-C(25)	-2(3)	C(15)-C(14)-N(3)-C(18)	-159(2)
P(1)-C(21)-C(26)-C(25)	-176.9(19)	C(13)-C(14)-N(3)-C(18)	22(3)
C(36)-C(31)-C(32)-C(33)	4(3)	C(15)-C(14)-N(3)-C(17)	1(3)
P(2)-C(31)-C(32)-C(33)	-173.5(16)	C(13)-C(14)-N(3)-C(17)	-177(2)
C(31)-C(32)-C(33)-C(34)	-3(3)	C(25)-C(24)-N(4)-C(27)	-1(4)
C(32)-C(33)-C(34)-N(5)	-178(2)	C(23)-C(24)-N(4)-C(27)	-177(2)
C(32)-C(33)-C(34)-C(35)	-1(3)	C(25)-C(24)-N(4)-C(28)	-176(2)
N(5)-C(34)-C(35)-C(36)	-179(2)	C(23)-C(24)-N(4)-C(28)	8(4)
C(33)-C(34)-C(35)-C(36)	4(4)	C(33)-C(34)-N(5)-C(38)	-169(3)
C(34)-C(35)-C(36)-C(31)	-2(4)	C(35)-C(34)-N(5)-C(38)	15(4)
C(32)-C(31)-C(36)-C(35)	-2(3)	C(33)-C(34)-N(5)-C(37)	-1(4)
P(2)-C(31)-C(36)-C(35)	176.1(19)	C(35)-C(34)-N(5)-C(37)	-178(2)
C(46)-C(41)-C(42)-C(43)	6(3)	C(43)-C(44)-N(6)-C(47)	-7(4)

C(45)-C(44)-N(6)-C(47)	175(2)	C(42)-C(41)-P(2)-N(2)	-92.7(18)
C(43)-C(44)-N(6)-C(48)	170(3)	C(46)-C(41)-P(2)-C(31)	-30(2)
C(45)-C(44)-N(6)-C(48)	-8(4)	C(42)-C(41)-P(2)-C(31)	151.1(17)
N(2)-N(1)-P(1)-C(21)	155.7(14)	C(46)-C(41)-P(2)-Au(2)	-148.8(17)
C(1)-N(1)-P(1)-C(21)	-35.8(19)	C(42)-C(41)-P(2)-Au(2)	32.5(19)
N(2)-N(1)-P(1)-C(11)	-93.4(15)	C(36)-C(31)-P(2)-N(2)	164.7(17)
C(1)-N(1)-P(1)-C(11)	75.1(18)	C(32)-C(31)-P(2)-N(2)	-17.8(19)
N(2)-N(1)-P(1)-Au(1)	32.3(15)	C(36)-C(31)-P(2)-C(41)	-81.0(19)
C(1)-N(1)-P(1)-Au(1)	-159.2(14)	C(32)-C(31)-P(2)-C(41)	96.5(18)
C(22)-C(21)-P(1)-N(1)	-83.3(18)	C(36)-C(31)-P(2)-Au(2)	38.6(19)
C(26)-C(21)-P(1)-N(1)	91.6(19)	C(32)-C(31)-P(2)-Au(2)	-143.9(15)
C(22)-C(21)-P(1)-C(11)	162.8(16)	Cl(99)-C(99)-Cl(98)-C(98)	144(8)
C(26)-C(21)-P(1)-C(11)	-22(2)	N(1)-P(1)-Au(1)-Cl(1)	-154(3)
C(22)-C(21)-P(1)-Au(1)	38.7(19)	C(21)-P(1)-Au(1)-Cl(1)	88(4)
C(26)-C(21)-P(1)-Au(1)	-146.4(16)	C(11)-P(1)-Au(1)-Cl(1)	-31(4)
C(12)-C(11)-P(1)-N(1)	-15(2)	N(1)-P(1)-Au(1)-Au(2)	38.9(7)
C(16)-C(11)-P(1)-N(1)	159.3(15)	C(21)-P(1)-Au(1)-Au(2)	-79.5(8)
C(12)-C(11)-P(1)-C(21)	96.0(18)	C(11)-P(1)-Au(1)-Au(2)	161.6(8)
C(16)-C(11)-P(1)-C(21)	-89.2(17)	N(2)-P(2)-Au(2)-Cl(2)	-148(3)
C(12)-C(11)-P(1)-Au(1)	-139.8(15)	C(41)-P(2)-Au(2)-Cl(2)	90(3)
C(16)-C(11)-P(1)-Au(1)	34.9(18)	C(31)-P(2)-Au(2)-Cl(2)	-23(3)
N(1)-N(2)-P(2)-C(41)	156.1(13)	N(2)-P(2)-Au(2)-Au(1)	38.3(7)
C(3)-N(2)-P(2)-C(41)	-32.9(19)	C(41)-P(2)-Au(2)-Au(1)	-83.7(7)
N(1)-N(2)-P(2)-C(31)	-92.6(14)	C(31)-P(2)-Au(2)-Au(1)	162.4(7)
C(3)-N(2)-P(2)-C(31)	78.4(18)	P(1)-Au(1)-Au(2)-P(2)	-65.7(2)
N(1)-N(2)-P(2)-Au(2)	31.8(15)	Cl(1)-Au(1)-Au(2)-P(2)	115.1(2)
C(3)-N(2)-P(2)-Au(2)	-157.2(15)	P(1)-Au(1)-Au(2)-Cl(2)	114.8(2)
C(46)-C(41)-P(2)-N(2)	86.0(19)	Cl(1)-Au(1)-Au(2)-Cl(2)	-64.5(2)

Bis(bis(di(N,N-dimetyl-4-aminophenyl))diethylhydrazine)gold trinitrate (35)

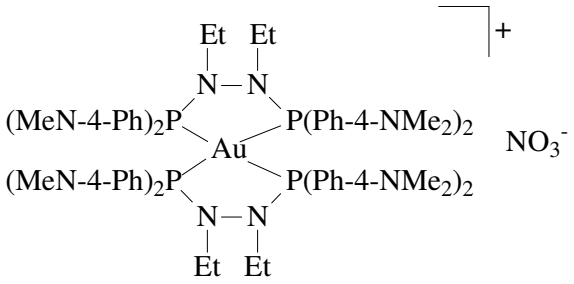

Table 22: Crystal data and structure refinement for **35**.

Empirical formula	$AuP_4N_{14}O_6C_{86}H_{100}$	
Formula weight	1746.65	
Temperature	173(2) K	
Wavelength	0.71073 Å	
Crystal system	Orthorhombic	
Space group	*Pban*	
Unit cell dimensions	a = 15.8970(8) Å	α = 90°
	b = 16.3239(8) Å	β = 90°
	c = 15.4379(8) Å	γ = 90°
Volume	4006.2(3) $Å^3$	
Z	2	
Density (calculated)	1.448 Mg/m^3	
Absorption coefficient	1.992 mm^{-1}	
F(000)	1802	
Crystal size	0.37 x 0.27 x 0.03 mm^3	
Theta range for data collection	1.79 to 28.00°	
Index ranges	-21<=h<=21, -21<=k<=20, -18<=l<=20	
Reflections collected	39748	
Independent reflections	4849 [R(int) = 0.1031]	
Completeness to theta = 28.00°	100.0 %	
Absorption correction	Integration	
Max. and min. transmission	0.9427 and 0.5260	

Refinement method	Full-matrix least-squares on F^2
Data/restraints/parameters	4849/0/254
Goodness-of-fit on F^2	0.979
Final R indices [I>2sigma(I)]	R1 = 0.0320, wR2 = 0.0754
R indices (all data)	R1 = 0.0613, wR2 = 0.0850
Largest diff. peak and hole	0.940 and -0.833 e.Å^{-3}

Table 23: Bond lengths [Å] and angles [°] for **35**.

C(1)-N(1)	1.460(4)	C(24)-C(25)	1.408(5)
C(1)-C(2)	1.518(5)	C(25)-C(26)	1.368(5)
C(11)-C(16)	1.394(5)	C(27)-N(3)	1.437(5)
C(11)-C(12)	1.403(5)	C(28)-N(3)	1.466(5)
C(11)-P(1)	1.766(3)	N(1)-N(1)$^{\#}$1	1.429(6)
C(12)-C(13)	1.372(5)	N(1)-P(1)	1.683(3)
C(13)-C(14)	1.403(5)	N(4)-O(1)	1.208(7)
C(14)-N(2)	1.369(5)	N(4)-O(2)$^{\#}$2	1.264(5)
C(14)-C(15)	1.408(5)	N(4)-O(2)	1.264(5)
C(15)-C(16)	1.370(5)	N(5)-O(4)$^{\#}$3	1.163(11)
C(17)-N(2)	1.462(6)	N(5)-O(4)	1.163(11)
C(18)-N(2)	1.423(5)	N(5)-O(3)	1.32(3)
C(21)-C(22)	1.393(5)	N(6)-O(5)$^{\#}$4	1.69(2)
C(21)-C(26)	1.399(5)	N(6)-O(5)	1.69(2)
C(21)-P(1)	1.774(3)	P(1)-Au(1)	2.3865(8)
C(22)-C(23)	1.379(5)	Au(1)-P(1)$^{\#}$5	2.3865(8)
C(23)-C(24)	1.412(5)	Au(1)-P(1)$^{\#}$1	2.3865(8)
C(24)-N(3)	1.358(5)	Au(1)-P(1)$^{\#}$6	2.3865(8)

N(1)-C(1)-C(2)	112.2(3)	C(12)-C(11)-P(1)	120.6(3)
C(16)-C(11)-C(12)	117.2(3)	C(13)-C(12)-C(11)	121.7(3)
C(16)-C(11)-P(1)	121.7(3)	C(12)-C(13)-C(14)	120.8(4)

N(2)-C(14)-C(13)	121.1(4)	C(24)-N(3)-C(28)	120.8(4)
N(2)-C(14)-C(15)	121.2(4)	C(27)-N(3)-C(28)	118.2(3)
C(13)-C(14)-C(15)	117.7(3)	O(1)-N(4)-O(2)#2	120.4(3)
C(16)-C(15)-C(14)	120.8(3)	O(1)-N(4)-O(2)	120.4(3)
C(15)-C(16)-C(11)	121.9(4)	O(2)#2-N(4)-O(2)	119.1(6)
C(22)-C(21)-C(26)	118.1(3)	O(4)#3-N(5)-O(4)	125(2)
C(22)-C(21)-P(1)	121.8(3)	O(4)#3-N(5)-O(3)	117.7(12)
C(26)-C(21)-P(1)	119.7(3)	O(4)-N(5)-O(3)	117.7(12)
C(23)-C(22)-C(21)	121.6(3)	O(5)#4-N(6)-O(5)	148(3)
C(22)-C(23)-C(24)	120.3(4)	N(1)-P(1)-C(11)	112.43(16)
N(3)-C(24)-C(25)	121.5(3)	N(1)-P(1)-C(21)	105.21(15)
N(3)-C(24)-C(23)	120.9(4)	C(11)-P(1)-C(21)	110.85(17)
C(25)-C(24)-C(23)	117.6(3)	N(1)-P(1)-Au(1)	100.37(11)
C(26)-C(25)-C(24)	121.4(3)	C(11)-P(1)-Au(1)	114.92(12)
C(25)-C(26)-C(21)	121.0(4)	C(21)-P(1)-Au(1)	112.25(13)
N(1)#1-N(1)-C(1)	117.9(2)	P(1)#5-Au(1)-P(1)#1	172.54(4)
N(1)#1-N(1)-P(1)	111.02(17)	P(1)#5-Au(1)-P(1)#6	83.50(4)
C(1)-N(1)-P(1)	128.8(3)	P(1)#1-Au(1)-P(1)#6	96.99(4)
C(14)-N(2)-C(18)	123.0(4)	P(1)#5-Au(1)-P(1)	96.99(4)
C(14)-N(2)-C(17)	119.5(4)	P(1)#1-Au(1)-P(1)	83.50(4)
C(18)-N(2)-C(17)	117.5(4)	P(1)#6-Au(1)-P(1)	172.54(4)
C(24)-N(3)-C(27)	121.0(3)		

Symmetry transformations used to generate equivalent atoms:

#1 -x+1/2,y,-z+1;

#2 x,-y+1/2,-z+1;

#3 -x+3/2,y,-z;

#4 x,-y+1/2,-z;

#5 -x+1/2,-y+3/2,z;

#6 x,-y+3/2,-z+1.

Table 24: Torsion angles [°] for **35**.

C(16)-C(11)-C(12)-C(13)	2.2(6)	C(23)-C(24)-N(3)-C(28)	179.6(4)
P(1)-C(11)-C(12)-C(13)	174.1(3)	N(1)$^{\#}$1-N(1)-P(1)-C(11)	-74.8(3)
C(11)-C(12)-C(13)-C(14)	-0.5(7)	C(1)-N(1)-P(1)-C(11)	87.3(3)
C(12)-C(13)-C(14)-N(2)	178.0(4)	N(1)$^{\#}$1-N(1)-P(1)-C(21)	164.5(3)
C(12)-C(13)-C(14)-C(15)	-1.9(6)	C(1)-N(1)-P(1)-C(21)	-33.4(3)
N(2)-C(14)-C(15)-C(16)	-177.2(4)	N(1)$^{\#}$1-N(1)-P(1)-Au(1)	47.8(3)
C(13)-C(14)-C(15)-C(16)	2.8(6)	C(1)-N(1)-P(1)-Au(1)	-150.1(3)
C(14)-C(15)-C(16)-C(11)	-1.1(6)	C(16)-C(11)-P(1)-N(1)	92.9(3)
C(12)-C(11)-C(16)-C(15)	-1.3(6)	C(12)-C(11)-P(1)-N(1)	-78.7(4)
P(1)-C(11)-C(16)-C(15)	-173.2(3)	C(16)-C(11)-P(1)-C(21)	-149.7(3)
C(26)-C(21)-C(22)-C(23)	2.5(6)	C(12)-C(11)-P(1)-C(21)	38.7(4)
P(1)-C(21)-C(22)-C(23)	175.7(3)	C(16)-C(11)-P(1)-Au(1)	-21.1(4)
C(21)-C(22)-C(23)-C(24)	0.0(6)	C(12)-C(11)-P(1)-Au(1)	167.3(3)
C(22)-C(23)-C(24)-N(3)	179.1(4)	C(22)-C(21)-P(1)-N(1)	146.3(3)
C(22)-C(23)-C(24)-C(25)	-1.7(6)	C(26)-C(21)-P(1)-N(1)	-40.6(3)
N(3)-C(24)-C(25)-C(26)	-179.9(4)	C(22)-C(21)-P(1)-C(11)	24.5(4)
C(23)-C(24)-C(25)-C(26)	0.9(6)	C(26)-C(21)-P(1)-C(11)	-162.4(3)
C(24)-C(25)-C(26)-C(21)	1.7(6)	C(22)-C(21)-P(1)-Au(1)	-105.5(3)
C(22)-C(21)-C(26)-C(25)	-3.3(6)	C(26)-C(21)-P(1)-Au(1)	67.6(3)
P(1)-C(21)-C(26)-C(25)	-176.6(3)	N(1)-P(1)-Au(1)-P(1)$^{\#}$5	173.54(11)
C(2)-C(1)-N(1)-N(1)$^{\#}$1	-64.3(5)	C(11)-P(1)-Au(1)-P(1)$^{\#}$5	-65.61(14)
C(2)-C(1)-N(1)-P(1)	134.6(3)	C(21)-P(1)-Au(1)-P(1)$^{\#}$5	62.26(13)
C(13)-C(14)-N(2)-C(18)	177.7(4)	N(1)-P(1)-Au(1)-P(1)$^{\#}$1	-13.95(10)
C(15)-C(14)-N(2)-C(18)	-2.4(7)	C(11)-P(1)-Au(1)-P(1)$^{\#}$1	106.89(14)
C(13)-C(14)-N(2)-C(17)	-5.1(7)	C(21)-P(1)-Au(1)-P(1)$^{\#}$1	-125.24(13)
C(15)-C(14)-N(2)-C(17)	174.9(4)	N(1)-P(1)-Au(1)-P(1)$^{\#}$6	80.24(10)
C(25)-C(24)-N(3)-C(27)	-177.9(4)	C(11)-P(1)-Au(1)-P(1)$^{\#}$6	-158.92(14)
C(23)-C(24)-N(3)-C(27)	1.3(7)	C(21)-P(1)-Au(1)-P(1)$^{\#}$6	-31.05(13)
C(25)-C(24)-N(3)-C(28)	0.4(6)		

Symmetry transformations used to generate equivalent atoms:

#1 -x+1/2,y,-z+1;

#2 x,-y+1/2,-z+1;

#3 -x+3/2,y,-z;

#4 x,-y+1/2,-z;

#5 -x+1/2,-y+3/2,z;

#6 x,-y+3/2,-z+1.

Bis(diphenylphosphino)diethylhydrazine di(silver nitrate) (39)

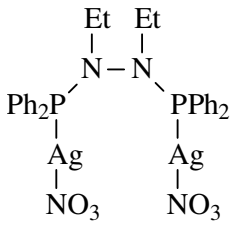

Table 25: Crystal data and structure refinement for **39**.

Empirical formula	$Ag_2P_2N_4O_6C_{28}H_{30}$	
Formula weight	796.24	
Temperature	193(2) K	
Wavelength	0.71073 Å	
Crystal system	Orthorhombic	
Space group	*Pna*2_1	
Unit cell dimensions	a = 16.3320(10) Å	α = 90°
	b = 20.6486(13) Å	β = 90°
	c = 9.0164(5) Å	γ = 90°
Volume	3040.6(3) $Å^3$	
Z	4	
Density (calculated)	1.739 Mg/m^3	
Absorption coefficient	1.441 mm^{-1}	
F(000)	1592	
Crystal size	0.22 x 0.08 x 0.07 mm^3	

Theta range for data collection	1.59 to 30.48°
Index ranges	-20<=h<=23, -10<=k<=29, -12<=l<=12
Reflections collected	13103
Independent reflections	8801 [R(int) = 0.0508]
Completeness to theta = 30.48°	99.5 %
Absorption correction	Integration
Max. and min. transmission	0.9069 and 0.7877
Refinement method	Full-matrix least-squares on F^2
Data/restraints/parameters	8801/1/379
Goodness-of-fit on F^2	1.011
Final R indices [I>2sigma(I)]	R1 = 0.0472, wR2 = 0.1134
R indices (all data)	R1 = 0.0825, wR2 = 0.1620
Absolute structure parameter	0.52(4)
Largest diff. peak and hole	0.590 and -0.731 e.$Å^{-3}$

Table 26: Bond lengths [Å] and angles [°] for **39**.

C(1)-C(2)	1.464(13)	C(23)-C(24)	1.348(12)
C(1)-N(1)	1.488(9)	C(24)-C(25)	1.376(11)
C(3)-N(2)	1.464(9)	C(25)-C(26)	1.394(11)
C(3)-C(4)	1.570(11)	C(31)-C(32)	1.393(10)
C(11)-C(16)	1.375(11)	C(31)-C(36)	1.425(9)
C(11)-C(12)	1.408(10)	C(31)-P(2)	1.810(7)
C(11)-P(1)	1.807(8)	C(32)-C(33)	1.390(10)
C(12)-C(13)	1.410(12)	C(33)-C(34)	1.415(11)
C(13)-C(14)	1.366(13)	C(34)-C(35)	1.371(14)
C(14)-C(15)	1.412(14)	C(35)-C(36)	1.362(11)
C(15)-C(16)	1.357(14)	C(41)-C(42)	1.407(11)
C(21)-C(22)	1.364(10)	C(41)-C(46)	1.409(10)
C(21)-C(26)	1.392(10)	C(41)-P(2)	1.840(7)
C(21)-P(1)	1.837(7)	C(42)-C(43)	1.381(11)
C(22)-C(23)	1.416(11)	C(43)-C(44)	1.388(12)
C(22)-H(22)	0.9300	C(44)-C(45)	1.388(13)

C(45)-C(46)	1.364(11)	O(1)-Ag(2)#1	2.592(5)
N(1)-N(2)	1.406(8)	O(2)-Ag(2)#2	2.314(5)
N(1)-P(1)	1.699(6)	O(2)-Ag(1)#1	2.553(5)
N(2)-P(2)	1.705(6)	O(4)-Ag(1)#3	2.506(5)
N(3)-O(3)	1.198(8)	O(4)-Ag(2)	2.548(5)
N(3)-O(2)	1.260(7)	P(1)-Ag(1)	2.3340(18)
N(3)-O(1)	1.287(8)	P(2)-Ag(2)	2.3491(18)
N(4)-O(6)	1.226(9)	Ag(1)-O(4)#1	2.506(5)
N(4)-O(5)	1.247(8)	Ag(1)-O(2)#3	2.553(5)
N(4)-O(4)	1.275(9)	Ag(2)-O(2)#4	2.314(5)
O(1)-Ag(1)	2.302(5)	Ag(2)-O(1)#3	2.592(5)

C(2)-C(1)-N(1)	118.5(8)	C(33)-C(32)-C(31)	119.6(7)
N(2)-C(3)-C(4)	113.4(6)	C(32)-C(33)-C(34)	120.9(8)
C(16)-C(11)-C(12)	116.1(7)	C(35)-C(34)-C(33)	118.3(8)
C(16)-C(11)-P(1)	125.8(6)	C(36)-C(35)-C(34)	122.2(8)
C(12)-C(11)-P(1)	118.1(5)	C(35)-C(36)-C(31)	120.0(8)
C(11)-C(12)-C(13)	121.4(7)	C(42)-C(41)-C(46)	117.4(6)
C(14)-C(13)-C(12)	120.2(8)	C(42)-C(41)-P(2)	118.6(5)
C(13)-C(14)-C(15)	118.1(8)	C(46)-C(41)-P(2)	123.9(5)
C(16)-C(15)-C(14)	120.8(8)	C(43)-C(42)-C(41)	120.6(7)
C(15)-C(16)-C(11)	123.2(9)	C(42)-C(43)-C(44)	119.6(8)
C(22)-C(21)-C(26)	118.8(7)	C(43)-C(44)-C(45)	121.3(7)
C(22)-C(21)-P(1)	123.8(5)	C(46)-C(45)-C(44)	118.4(7)
C(26)-C(21)-P(1)	117.4(6)	C(45)-C(46)-C(41)	122.6(7)
C(21)-C(22)-C(23)	120.1(7)	N(2)-N(1)-C(1)	118.9(6)
C(24)-C(23)-C(22)	120.0(7)	N(2)-N(1)-P(1)	117.7(4)
C(23)-C(24)-C(25)	121.2(7)	C(1)-N(1)-P(1)	123.3(5)
C(24)-C(25)-C(26)	118.8(7)	N(1)-N(2)-C(3)	115.8(5)
C(25)-C(26)-C(21)	121.0(7)	N(1)-N(2)-P(2)	116.9(4)
C(32)-C(31)-C(36)	118.8(7)	C(3)-N(2)-P(2)	122.2(4)
C(32)-C(31)-P(2)	121.6(5)	O(3)-N(3)-O(2)	122.6(6)
C(36)-C(31)-P(2)	118.6(5)	O(3)-N(3)-O(1)	121.6(6)

O(2)-N(3)-O(1)	115.8(6)	N(2)-P(2)-C(31)	104.0(3)
O(6)-N(4)-O(5)	120.8(7)	N(2)-P(2)-C(41)	111.0(3)
O(6)-N(4)-O(4)	122.2(7)	C(31)-P(2)-C(41)	101.3(3)
O(5)-N(4)-O(4)	116.9(6)	N(2)-P(2)-Ag(2)	118.8(2)
N(3)-O(1)-Ag(1)	114.6(4)	C(31)-P(2)-Ag(2)	106.6(2)
N(3)-O(1)-Ag(2)$^{\#}$1	132.6(4)	C(41)-P(2)-Ag(2)	113.1(2)
Ag(1)-O(1)-Ag(2)$^{\#}$1	97.92(18)	O(1)-Ag(1)-P(1)	164.67(13)
N(3)-O(2)-Ag(2)$^{\#}$2	116.2(4)	O(1)-Ag(1)-O(4)$^{\#}$1	71.71(19)
N(3)-O(2)-Ag(1)#1	143.5(4)	P(1)-Ag(1)-O(4)$^{\#}$1	116.32(14)
Ag(2)$^{\#}$2-O(2)-Ag(1)$^{\#}$1	98.70(18)	O(1)-Ag(1)-O(2)$^{\#}$3	67.25(18)
N(4)-O(4)-Ag(1)$^{\#}$3	116.8(5)	P(1)-Ag(1)-O(2)$^{\#}$3	126.75(13)
N(4)-O(4)-Ag(2)	101.5(4)	O(4)$^{\#}$1-Ag(1)-O(2)$^{\#}$3	72.65(17)
Ag(1)$^{\#}$3-O(4)-Ag(2)	93.96(17)	O(2)$^{\#}$4-Ag(2)-P(2)	154.16(13)
N(1)-P(1)-C(11)	104.8(3)	O(2)$^{\#}$4-Ag(2)-O(4)	75.93(19)
N(1)-P(1)-C(21)	108.9(3)	P(2)-Ag(2)-O(4)	118.77(12)
C(11)-P(1)-C(21)	102.0(3)	O(2)$^{\#}$4-Ag(2)-O(1)$^{\#}$3	66.38(17)
N(1)-P(1)-Ag(1)	114.0(2)	P(2)-Ag(2)-O(1)$^{\#}$3	137.65(12)
C(11)-P(1)-Ag(1)	113.7(2)	O(4)-Ag(2)-O(1)$^{\#}$3	66.56(16)
C(21)-P(1)-Ag(1)	112.5(2)		

Symmetry transformations used to generate equivalent atoms:

$^{\#}$1 -x,-y,z+1/2;

$^{\#}$2 x,y,z+1;

$^{\#}$3 -x,-y,z-1/2;

$^{\#}$4 x,y,z-1.

Table 27: Torsion angles [°] for **39**.

C(16)-C(11)-C(12)-C(13)	5.2(12)	C(14)-C(15)-C(16)-C(11)	0(2)
P(1)-C(11)-C(12)-C(13)	-174.2(7)	C(12)-C(11)-C(16)-C(15)	-2.3(16)
C(11)-C(12)-C(13)-C(14)	-5.6(14)	P(1)-C(11)-C(16)-C(15)	177.1(10)
C(12)-C(13)-C(14)-C(15)	2.8(17)	C(26)-C(21)-C(22)-C(23)	-4.1(12)
C(13)-C(14)-C(15)-C(16)	0(2)	P(1)-C(21)-C(22)-C(23)	177.9(7)

C(21)-C(22)-C(23)-C(24)	3.9(14)	O(3)-N(3)-O(2)-Ag(2)$^{\#}$2	-7.7(9)
C(22)-C(23)-C(24)-C(25)	-0.9(14)	O(1)-N(3)-O(2)-Ag(2)$^{\#}$2	170.7(4)
C(23)-C(24)-C(25)-C(26)	-1.8(13)	O(3)-N(3)-O(2)-Ag(1)$^{\#}$1	-169.2(6)
C(24)-C(25)-C(26)-C(21)	1.5(13)	O(1)-N(3)-O(2)-Ag(1)$^{\#}$1	9.2(11)
C(22)-C(21)-C(26)-C(25)	1.4(12)	O(6)-N(4)-O(4)-Ag(1)$^{\#}$3	-67.3(9)
P(1)-C(21)-C(26)-C(25)	179.6(6)	O(5)-N(4)-O(4)-Ag(1)$^{\#}$3	114.0(6)
C(36)-C(31)-C(32)-C(33)	3.7(11)	O(6)-N(4)-O(4)-Ag(2)	-167.7(8)
P(2)-C(31)-C(32)-C(33)	172.0(6)	O(5)-N(4)-O(4)-Ag(2)	13.5(7)
C(31)-C(32)-C(33)-C(34)	-3.0(13)	N(2)-N(1)-P(1)-C(11)	-141.3(5)
C(32)-C(33)-C(34)-C(35)	2.6(13)	C(1)-N(1)-P(1)-C(11)	42.3(7)
C(33)-C(34)-C(35)-C(36)	-3.1(14)	N(2)-N(1)-P(1)-C(21)	110.2(5)
C(34)-C(35)-C(36)-C(31)	4.0(13)	C(1)-N(1)-P(1)-C(21)	-66.2(7)
C(32)-C(31)-C(36)-C(35)	-4.2(11)	N(2)-N(1)-P(1)-Ag(1)	-16.4(5)
P(2)-C(31)-C(36)-C(35)	-172.8(6)	C(1)-N(1)-P(1)-Ag(1)	167.2(6)
C(46)-C(41)-C(42)-C(43)	1.3(10)	C(16)-C(11)-P(1)-N(1)	-89.0(8)
P(2)-C(41)-C(42)-C(43)	-175.9(5)	C(12)-C(11)-P(1)-N(1)	90.4(6)
C(41)-C(42)-C(43)-C(44)	-2.8(11)	C(16)-C(11)-P(1)-C(21)	24.5(9)
C(42)-C(43)-C(44)-C(45)	4.2(12)	C(12)-C(11)-P(1)-C(21)	-156.1(6)
C(43)-C(44)-C(45)-C(46)	-4.0(12)	C(16)-C(11)-P(1)-Ag(1)	145.9(8)
C(44)-C(45)-C(46)-C(41)	2.5(11)	C(12)-C(11)-P(1)-Ag(1)	-34.8(7)
C(42)-C(41)-C(46)-C(45)	-1.1(10)	C(22)-C(21)-P(1)-N(1)	10.2(7)
P(2)-C(41)-C(46)-C(45)	175.9(6)	C(26)-C(21)-P(1)-N(1)	-167.9(6)
C(2)-C(1)-N(1)-N(2)	82.7(10)	C(22)-C(21)-P(1)-C(11)	-100.2(7)
C(2)-C(1)-N(1)-P(1)	-100.9(9)	C(26)-C(21)-P(1)-C(11)	81.7(6)
C(1)-N(1)-N(2)-C(3)	71.4(8)	C(22)-C(21)-P(1)-Ag(1)	137.6(6)
P(1)-N(1)-N(2)-C(3)	-105.2(6)	C(26)-C(21)-P(1)-Ag(1)	-40.5(6)
C(1)-N(1)-N(2)-P(2)	-83.9(7)	N(1)-N(2)-P(2)-C(31)	-150.4(5)
P(1)-N(1)-N(2)-P(2)	99.5(5)	C(3)-N(2)-P(2)-C(31)	56.0(6)
C(4)-C(3)-N(2)-N(1)	68.1(8)	N(1)-N(2)-P(2)-C(41)	101.4(5)
C(4)-C(3)-N(2)-P(2)	-138.0(6)	C(3)-N(2)-P(2)-C(41)	-52.2(7)
O(3)-N(3)-O(1)-Ag(1)	-16.4(8)	N(1)-N(2)-P(2)-Ag(2)	-32.2(5)
O(2)-N(3)-O(1)-Ag(1)	165.2(5)	C(3)-N(2)-P(2)-Ag(2)	174.2(5)
O(3)-N(3)-O(1)-Ag(2)$^{\#}$1	-145.2(6)	C(32)-C(31)-P(2)-N(2)	29.7(7)
O(2)-N(3)-O(1)-Ag(2)$^{\#}$1	36.4(9)	C(36)-C(31)-P(2)-N(2)	-162.0(5)

C(32)-C(31)-P(2)-C(41)	144.9(6)	C(11)-P(1)-Ag(1)-O(4)#1	-60.5(3)
C(36)-C(31)-P(2)-C(41)	-46.8(6)	C(21)-P(1)-Ag(1)-O(4)#1	54.7(3)
C(32)-C(31)-P(2)-Ag(2)	-96.6(6)	N(1)-P(1)-Ag(1)-O(2)#3	-93.2(3)
C(36)-C(31)-P(2)-Ag(2)	71.7(6)	C(11)-P(1)-Ag(1)-O(2)#3	26.9(3)
C(42)-C(41)-P(2)-N(2)	-118.9(5)	C(21)-P(1)-Ag(1)-O(2)#3	142.1(3)
C(46)-C(41)-P(2)-N(2)	64.1(6)	N(2)-P(2)-Ag(2)-O(2)#4	91.3(4)
C(42)-C(41)-P(2)-C(31)	131.2(5)	C(31)-P(2)-Ag(2)-O(2)#4	-151.9(4)
C(46)-C(41)-P(2)-C(31)	-45.8(6)	C(41)-P(2)-Ag(2)-O(2)#4	-41.4(4)
C(42)-C(41)-P(2)-Ag(2)	17.5(6)	N(2)-P(2)-Ag(2)-O(4)	-148.9(3)
C(46)-C(41)-P(2)-Ag(2)	-159.5(5)	C(31)-P(2)-Ag(2)-O(4)	-32.1(3)
N(3)-O(1)-Ag(1)-P(1)	20.2(9)	C(41)-P(2)-Ag(2)-O(4)	78.4(3)
Ag(2)#1-O(1)-Ag(1)-P(1)	164.8(4)	N(2)-P(2)-Ag(2)-O(1)#3	-63.0(3)
N(3)-O(1)-Ag(1)-O(4)#1	-103.9(5)	C(31)-P(2)-Ag(2)-O(1)#3	53.9(3)
Ag(2)#1-O(1)-Ag(1)-O(4)#1	40.70(17)	C(41)-P(2)-Ag(2)-O(1)#3	164.3(3)
N(3)-O(1)-Ag(1)-O(2)#3	177.8(5)	N(4)-O(4)-Ag(2)-O(2)#4	85.6(5)
Ag(2)#1-O(1)-Ag(1)-O(2)#3	-37.65(16)	Ag(1)#3-O(4)-Ag(2)-O(2)#4	-32.80(18)
N(1)-P(1)-Ag(1)-O(1)	60.7(6)	N(4)-O(4)-Ag(2)-P(2)	-71.5(5)
C(11)-P(1)-Ag(1)-O(1)	-179.2(6)	Ag(1)#3-O(4)-Ag(2)-P(2)	170.15(9)
C(21)-P(1)-Ag(1)-O(1)	-63.9(6)	N(4)-O(4)-Ag(2)-O(1)#3	155.6(5)
N(1)-P(1)-Ag(1)-O(4)#1	179.4(3)	Ag(1)#3-O(4)-Ag(2)-O(1)#3	37.23(16)

Symmetry transformations used to generate equivalent atoms:

#1 -x,-y,z+1/2;

#2 x,y,z+1;

#3 -x,-y,z-1/2;

#4 x,y,z-1.

Bis(bis(diphenylphosphino)diethylhydrazine)silver nitrate (45)

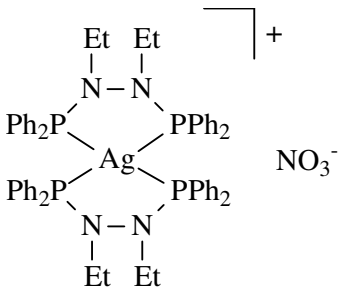

Table 28: Crystal data and structure refinement for **45**.

Empirical formula	$AgP_4N_5O_4C_{60}H_{65}$	
Formula weight	1151.92	
Temperature	193(2) K	
Wavelength	0.71073 Å	
Crystal system	Triclinic	
Space group	P_{-1}	
Unit cell dimensions	a = 11.912(5) Å	α = 81.1(5)°
	b = 14.954(5) Å	β = 85.4 (5)°
	c = 15.795(5) Å	γ = 84.2 (5)°
Volume	2759.5(17) $Å^3$	
Z	2	
Density (calculated)	1.386 Mg/m^3	
Absorption coefficient	0.533 mm^{-1}	
F(000)	1198	
Crystal size	0.42 x 0.07 x 0.02 mm^3	
Theta range for data collection	1.31 to 28.37°	
Index ranges	-15<=h<=15, -19<=k<=19, -20<=l<=20	
Reflections collected	27916	
Independent reflections	13642 [R(int) = 0.1465]	
Completeness to theta = 28.37°	98.8 %	
Absorption correction	None	
Refinement method	Full-matrix least-squares on F^2	

Data/restraints/parameters	13642/0/667
Goodness-of-fit on F^2	1.423
Final R indices [I>2sigma(I)]	R1 = 0.1825, wR2 = 0.4667
R indices (all data)	R1 = 0.2927, wR2 = 0.5069
Largest diff. peak and hole	5.731 and -1.801 e.$Å^{-3}$

Table 29: Bond lengths [Å] and angles [°] for **45**.

C(1)-C(2)	1.51(3)	C(31)-P(2)	1.821(16)
C(1)-N(1)	1.49(2)	C(32)-C(33)	1.33(3)
C(3)-N(2)	1.433(19)	C(33)-C(34)	1.42(3)
C(3)-C(4)	1.51(2)	C(34)-C(35)	1.37(3)
C(5)-N(3)	1.468(19)	C(35)-C(36)	1.43(2)
C(5)-C(6)	1.49(3)	C(41)-C(46)	1.39(2)
C(7)-N(4)	1.44(2)	C(41)-C(42)	1.42(2)
C(7)-C(8)	1.67(3)	C(41)-P(2)	1.798(16)
C(11)-C(12)	1.38(3)	C(42)-C(43)	1.39(2)
C(11)-C(16)	1.41(3)	C(43)-C(44)	1.39(3)
C(11)-P(1)	1.82(2)	C(44)-C(45)	1.39(3)
C(12)-C(13)	1.36(3)	C(45)-C(46)	1.42(3)
C(13)-C(14)	1.44(3)	C(51)-C(56)	1.36(2)
C(14)-C(15)	1.43(3)	C(51)-C(52)	1.39(2)
C(15)-C(16)	1.33(3)	C(51)-P(3)	1.836(17)
C(21)-C(26)	1.38(3)	C(52)-C(53)	1.36(2)
C(21)-C(22)	1.40(2)	C(53)-C(54)	1.41(3)
C(21)-P(1)	1.792(18)	C(54)-C(55)	1.34(3)
C(22)-C(23)	1.40(3)	C(55)-C(56)	1.43(3)
C(23)-C(24)	1.47(3)	C(61)-C(66)	1.40(2)
C(24)-C(25)	1.31(4)	C(61)-C(62)	1.38(2)
C(25)-C(26)	1.37(3)	C(61)-P(3)	1.798(16)
C(31)-C(32)	1.41(2)	C(62)-C(63)	1.37(2)
C(31)-C(36)	1.43(2)	C(63)-C(64)	1.37(3)

C(64)-C(65)	1.40(3)	N(2)-P(2)	1.684(13)
C(65)-C(66)	1.43(2)	N(3)-N(4)	1.42(2)
C(71)-C(72)	1.37(3)	N(3)-P(3)	1.696(13)
C(71)-C(76)	1.40(3)	N(4)-P(4)	1.739(17)
C(71)-P(4)	1.814(19)	N(5)-O(2)	1.18(3)
C(72)-C(73)	1.38(3)	N(5)-O(3)	1.19(3)
C(73)-C(74)	1.37(3)	N(5)-O(1)	1.21(4)
C(74)-C(75)	1.32(3)	P(1)-Ag(1)	2.531(5)
C(75)-C(76)	1.38(3)	P(2)-Ag(1)	2.526(4)
C(81)-C(82)	1.39(3)	P(3)-Ag(1)	2.513(4)
C(81)-C(86)	1.38(3)	P(4)-Ag(1)	2.528(4)
C(81)-P(4)	1.788(18)	C(8)-C(7)1	1.67(3)
C(82)-C(83)	1.47(3)	O(4)-C(91)	1.32(6)
C(83)-C(84)	1.31(3)	O(4)-C(94)	1.53(6)
C(84)-C(85)	1.36(3)	C(91)-C(92)	1.32(6)
CC(85)-C(86)	1.32(3)	C(94)-C(93)	1.46(6)
N(1)-N(2)	1.474(18)	C(93)-C(92)	1.54(6)
N(1)-P(1)	1.729(15)		

C(2)-C(1)-N(1)	115.3(19)	C(23)-C(22)-C(21)	124(2)
N(2)-C(3)-C(4)	116.7(14)	C(22)-C(23)-C(24)	113(2)
N(3)-C(5)-C(6)	116.6(15)	C(25)-C(24)-C(23)	122(2)
N(4)-C(7)-C(8)	99.5(19)	C(24)-C(25)-C(26)	122(3)
C(12)-C(11)-C(16)	118.4(19)	C(25)-C(26)-C(21)	121(2)
C(12)-C(11)-P(1)	119.2(15)	C(32)-C(31)-C(36)	118.4(15)
C(16)-C(11)-P(1)	122.4(15)	C(32)-C(31)-P(2)	119.8(12)
C(11)-C(12)-C(13)	123(2)	C(36)-C(31)-P(2)	121.7(13)
C(12)-C(13)-C(14)	118(2)	C(33)-C(32)-C(31)	121.1(17)
C(15)-C(14)-C(13)	118.1(19)	C(32)-C(33)-C(34)	121.6(18)
C(16)-C(15)-C(14)	121(2)	C(35)-C(34)-C(33)	120.2(17)
C(15)-C(16)-C(11)	121(2)	C(34)-C(35)-C(36)	118.9(17)
C(26)-C(21)-C(22)	117.2(17)	C(35)-C(36)-C(31)	119.7(17)
C(26)-C(21)-P(1)	123.9(15)	C(46)-C(41)-C(42)	117.6(16)
C(22)-C(21)-P(1)	118.9(14)	C(46)-C(41)-P(2)	120.3(13)

C(42)-C(41)-P(2)	121.2(12)	C(84)-C(83)-C(82)	118(2)
C(43)-C(42)-C(41)	121.6(16)	C(83)-C(84)-C(85)	122(3)
C(42)-C(43)-C(44)	120.4(18)	C(86)-C(85)-C(84)	121(3)
C(43)-C(44)-C(45)	118.7(18)	C(85)-C(86)-C(81)	122(2)
C(46)-C(45)-C(44)	121(2)	N(2)-N(1)-C(1)	108.1(13)
C(41)-C(46)-C(45)	120.4(19)	N(2)-N(1)-P(1)	106.5(10)
C(56)-C(51)-C(52)	118.2(16)	C(1)-N(1)-P(1)	114.2(11)
C(56)-C(51)-P(3)	116.6(13)	C(3)-N(2)-N(1)	112.5(12)
C(52)-C(51)-P(3)	124.7(13)	C(3)-N(2)-P(2)	125.5(11)
C(53)-C(52)-C(51)	122.1(18)	N(1)-N(2)-P(2)	120.1(9)
C(52)-C(53)-C(54)	120.2(17)	N(4)-N(3)-C(5)	114.1(12)
C(55)-C(54)-C(53)	118.2(18)	N(4)-N(3)-P(3)	120.0(10)
C(54)-C(55)-C(56)	121.4(18)	C(5)-N(3)-P(3)	123.3(12)
C(51)-C(56)-C(55)	119.5(18)	N(3)-N(4)-C(7)	116.8(16)
C(66)-C(61)-C(62)	117.8(15)	N(3)-N(4)-P(4)	108.3(10)
C(66)-C(61)-P(3)	123.4(13)	C(7)-N(4)-P(4)	113.1(12)
C(62)-C(61)-P(3)	118.5(12)	O(2)-N(5)-O(3)	109(4)
C(63)-C(62)-C(61)	122.9(17)	O(2)-N(5)-O(1)	121(4)
C(64)-C(63)-C(62)	120.0(18)	O(3)-N(5)-O(1)	129(3)
C(63)-C(64)-C(65)	120.2(16)	N(1)-P(1)-C(21)	102.7(8)
C(64)-C(65)-C(66)	118.8(16)	N(1)-P(1)-C(11)	101.5(7)
C(61)-C(66)-C(65)	120.3(16)	C(21)-P(1)-C(11)	103.7(8)
C(72)-C(71)-C(76)	118.5(18)	N(1)-P(1)-Ag(1)	101.0(5)
C(72)-C(71)-P(4)	123.8(15)	C(21)-P(1)-Ag(1)	129.6(6)
C(76)-C(71)-P(4)	117.7(13)	C(11)-P(1)-Ag(1)	114.2(6)
C(71)-C(72)-C(73)	121(2)	N(2)-P(2)-C(41)	104.9(7)
C(74)-C(73)-C(72)	120.1(19)	N(2)-P(2)-C(31)	107.4(7)
C(75)-C(74)-C(73)	117.8(18)	C(41)-P(2)-C(31)	103.3(7)
C(74)-C(75)-C(76)	125.3(19)	N(2)-P(2)-Ag(1)	102.7(4)
C(75)-C(76)-C(71)	116.8(17)	C(41)-P(2)-Ag(1)	111.1(5)
C(82)-C(81)-C(86)	117.6(18)	C(31)-P(2)-Ag(1)	125.8(5)
C(82)-C(81)-P(4)	122.8(18)	N(3)-P(3)-C(61)	104.1(7)
C(86)-C(81)-P(4)	119.6(15)	N(3)-P(3)-C(51)	107.3(7)
C(81)-C(82)-C(83)	119(2)	C(61)-P(3)-C(51)	102.6(7)

N(3)-P(3)-Ag(1)	102.5(5)	P(3)-Ag(1)-P(4)	79.35(14)
C(61)-P(3)-Ag(1)	109.7(5)	P(2)-Ag(1)-P(4)	128.83(15)
C(51)-P(3)-Ag(1)	128.5(6)	P(3)-Ag(1)-P(1)	125.94(15)
N(4)-P(4)-C(81)	101.7(8)	P(2)-Ag(1)-P(1)	79.22(14)
N(4)-P(4)-C(71)	104.0(8)	P(4)-Ag(1)-P(1)	121.34(16)
C(81)-P(4)-C(71)	106.0(9)	C(91)-O(4)-C(94)	103(5)
N(4)-P(4)-Ag(1)	99.3(5)	O(4)-C(91)-C(92)	112(6)
C(81)-P(4)-Ag(1)	114.9(7)	C(93)-C(94)-O(4)	101(5)
C(71)-P(4)-Ag(1)	127.1(6)	C(94)-C(93)-C(92)	104(5)
P(3)-Ag(1)-P(2)	129.03(15)	C(93)-C(92)-C(91)	104(6)

Table 30: Torsion angles [°] for **45**.

C(16)-C(11)-C(12)-C(13)	0(3)	C(31)-C(32)-C(33)-C(34)	-4(3)
P(1)-C(11)-C(12)-C(13)	179.5(17)	C(32)-C(33)-C(34)-C(35)	2(3)
C(11)-C(12)-C(13)-C(14)	0(3)	C(33)-C(34)-C(35)-C(36)	0(3)
C(12)-C(13)-C(14)-C(15)	-1(3)	C(34)-C(35)-C(36)-C(31)	-1(3)
C(13)-C(14)-C(15)-C(16)	1(3)	C(32)-C(31)-C(36)-C(35)	0(2)
C(14)-C(15)-C(16)-C(11)	-2(3)	P(2)-C(31)-C(36)-C(35)	176.5(14)
C(12)-C(11)-C(16)-C(15)	1(3)	C(46)-C(41)-C(42)-C(43)	-3(2)
P(1)-C(11)-C(16)-C(15)	-178.8(16)	P(2)-C(41)-C(42)-C(43)	-172.1(12)
C(26)-C(21)-C(22)-C(23)	7(3)	C(41)-C(42)-C(43)-C(44)	2(2)
P(1)-C(21)-C(22)-C(23)	-173.7(18)	C(42)-C(43)-C(44)-C(45)	0(3)
C(21)-C(22)-C(23)-C(24)	-4(3)	C(43)-C(44)-C(45)-C(46)	-1(3)
C(22)-C(23)-C(24)-C(25)	-2(4)	C(42)-C(41)-C(46)-C(45)	2(2)
C(23)-C(24)-C(25)-C(26)	5(5)	P(2)-C(41)-C(46)-C(45)	171.4(14)
C(24)-C(25)-C(26)-C(21)	-2(5)	C(44)-C(45)-C(46)-C(41)	0(3)
C(22)-C(21)-C(26)-C(25)	-4(4)	C(56)-C(51)-C(52)-C(53)	3(3)
P(1)-C(21)-C(26)-C(25)	177(2)	P(3)-C(51)-C(52)-C(53)	175.1(16)
C(36)-C(31)-C(32)-C(33)	3(3)	C(51)-C(52)-C(53)-C(54)	2(3)
P(2)-C(31)-C(32)-C(33)	-174.1(15)	C(52)-C(53)-C(54)-C(55)	-5(3)

C(53)-C(54)-C(55)-C(56)	3(3)	C(1)-N(1)-N(2)-P(2)	62.7(15)
C(52)-C(51)-C(56)-C(55)	-4(3)	P(1)-N(1)-N(2)-P(2)	-60.4(12)
P(3)-C(51)-C(56)-C(55)	-177.3(15)	C(6)-C(5)-N(3)-N(4)	64(2)
C(54)-C(55)-C(56)-C(51)	1(3)	C(6)-C(5)-N(3)-P(3)	-97.2(18)
C(66)-C(61)-C(62)-C(63)	1(2)	C(5)-N(3)-N(4)-C(7)	-93.3(18)
P(3)-C(61)-C(62)-C(63)	174.2(14)	P(3)-N(3)-N(4)-C(7)	69.0(18)
C(61)-C(62)-C(63)-C(64)	-2(3)	C(5)-N(3)-N(4)-P(4)	137.7(12)
C(62)-C(63)-C(64)-C(65)	1(3)	P(3)-N(3)-N(4)-P(4)	-60.0(14)
C(63)-C(64)-C(65)-C(66)	1(3)	C(8)#1-C(7)-N(4)-N(3)	130.2(14)
C(62)-C(61)-C(66)-C(65)	1(2)	C(8)#1-C(7)-N(4)-P(4)	-103.1(13)
P(3)-C(61)-C(66)-C(65)	-171.9(13)	N(2)-N(1)-P(1)-C(21)	-169.7(10)
C(64)-C(65)-C(66)-C(61)	-2(3)	C(1)-N(1)-P(1)-C(21)	71.1(13)
C(76)-C(71)-C(72)-C(73)	-1(5)	N(2)-N(1)-P(1)-C(11)	-62.6(11)
P(4)-C(71)-C(72)-C(73)	-179(3)	C(1)-N(1)-P(1)-C(11)	178.2(12)
C(71)-C(72)-C(73)-C(74)	-1(6)	N(2)-N(1)-P(1)-Ag(1)	55.2(9)
C(72)-C(73)-C(74)-C(75)	2(5)	C(1)-N(1)-P(1)-Ag(1)	-64.1(12)
C(73)-C(74)-C(75)-C(76)	-1(4)	C(26)-C(21)-P(1)-N(1)	46(2)
C(74)-C(75)-C(76)-C(71)	0(4)	C(22)-C(21)-P(1)-N(1)	-133.6(15)
C(72)-C(71)-C(76)-C(75)	1(3)	C(26)-C(21)-P(1)-C(11)	-60(2)
P(4)-C(71)-C(76)-C(75)	179.7(15)	C(22)-C(21)-P(1)-C(11)	121.1(15)
C(86)-C(81)-C(82)-C(83)	1(3)	C(26)-C(21)-P(1)-Ag(1)	161.8(15)
P(4)-C(81)-C(82)-C(83)	-179.7(15)	C(22)-C(21)-P(1)-Ag(1)	-17.5(19)
C(81)-C(82)-C(83)-C(84)	0(3)	C(12)-C(11)-P(1)-N(1)	144.8(15)
C(82)-C(83)-C(84)-C(85)	-1(4)	C(16)-C(11)-P(1)-N(1)	-35.4(17)
C(83)-C(84)-C(85)-C(86)	2(5)	C(12)-C(11)-P(1)-C(21)	-108.9(16)
C(84)-C(85)-C(86)-C(81)	-2(4)	C(16)-C(11)-P(1)-C(21)	70.9(17)
C(82)-C(81)-C(86)-C(85)	0(3)	C(12)-C(11)-P(1)-Ag(1)	37.1(17)
P(4)-C(81)-C(86)-C(85)	-179(2)	C(16)-C(11)-P(1)-Ag(1)	-143.2(14)
C(2)-C(1)-N(1)-N(2)	155.7(16)	C(3)-N(2)-P(2)-C(41)	-51.5(14)
C(2)-C(1)-N(1)-P(1)	-85.9(18)	N(1)-N(2)-P(2)-C(41)	145.0(11)
C(4)-C(3)-N(2)-N(1)	56(2)	C(3)-N(2)-P(2)-C(31)	57.9(14)
C(4)-C(3)-N(2)-P(2)	-108.5(18)	N(1)-N(2)-P(2)-C(31)	-105.5(12)
C(1)-N(1)-N(2)-C(3)	-102.7(15)	C(3)-N(2)-P(2)-Ag(1)	-167.7(12)
P(1)-N(1)-N(2)-C(3)	134.1(11)	N(1)-N(2)-P(2)-Ag(1)	28.9(12)

C(46)-C(41)-P(2)-N(2)	160.4(12)	N(3)-N(4)-P(4)-Ag(1)	56.4(10)
C(42)-C(41)-P(2)-N(2)	-30.5(14)	C(7)-N(4)-P(4)-Ag(1)	-74.7(15)
C(46)-C(41)-P(2)-C(31)	48.0(14)	C(82)-C(81)-P(4)-N(4)	-39.0(17)
C(42)-C(41)-P(2)-C(31)	-142.9(13)	C(86)-C(81)-P(4)-N(4)	140.4(15)
C(46)-C(41)-P(2)-Ag(1)	-89.4(12)	C(82)-C(81)-P(4)-C(71)	69.4(17)
C(42)-C(41)-P(2)-Ag(1)	79.7(12)	C(86)-C(81)-P(4)-C(71)	-111.2(16)
C(32)-C(31)-P(2)-N(2)	101.4(14)	C(82)-C(81)-P(4)-Ag(1)	-145.1(14)
C(36)-C(31)-P(2)-N(2)	-75.5(14)	C(86)-C(81)-P(4)-Ag(1)	34.3(17)
C(32)-C(31)-P(2)-C(41)	-148.1(13)	C(72)-C(71)-P(4)-N(4)	67(3)
C(36)-C(31)-P(2)-C(41)	35.1(15)	C(76)-C(71)-P(4)-N(4)	-111.8(16)
C(32)-C(31)-P(2)-Ag(1)	-19.3(16)	C(72)-C(71)-P(4)-C(81)	-40(3)
C(36)-C(31)-P(2)-Ag(1)	163.9(11)	C(76)-C(71)-P(4)-C(81)	141.4(17)
N(4)-N(3)-P(3)-C(61)	141.0(13)	C(72)-C(71)-P(4)-Ag(1)	-180(2)
C(5)-N(3)-P(3)-C(61)	-58.4(15)	C(76)-C(71)-P(4)-Ag(1)	2(2)
N(4)-N(3)-P(3)-C(51)	-110.7(14)	N(3)-P(3)-Ag(1)-P(2)	-124.4(5)
C(5)-N(3)-P(3)-C(51)	49.9(15)	C(61)-P(3)-Ag(1)-P(2)	125.5(5)
N(4)-N(3)-P(3)-Ag(1)	26.7(13)	C(51)-P(3)-Ag(1)-P(2)	0.0(7)
C(5)-N(3)-P(3)-Ag(1)	-172.7(12)	N(3)-P(3)-Ag(1)-P(4)	7.6(5)
C(66)-C(61)-P(3)-N(3)	-22.1(15)	C(61)-P(3)-Ag(1)-P(4)	-102.5(6)
C(62)-C(61)-P(3)-N(3)	165.0(12)	C(51)-P(3)-Ag(1)-P(4)	132.0(7)
C(66)-C(61)-P(3)-C(51)	-133.8(14)	N(3)-P(3)-Ag(1)-P(1)	128.7(5)
C(62)-C(61)-P(3)-C(51)	53.3(14)	C(61)-P(3)-Ag(1)-P(1)	18.6(6)
C(66)-C(61)-P(3)-Ag(1)	87.0(13)	C(51)-P(3)-Ag(1)-P(1)	-106.9(7)
C(62)-C(61)-P(3)-Ag(1)	-85.9(13)	N(2)-P(2)-Ag(1)-P(3)	-122.3(5)
C(56)-C(51)-P(3)-N(3)	89.9(15)	C(41)-P(2)-Ag(1)-P(3)	126.1(6)
C(52)-C(51)-P(3)-N(3)	-82.4(17)	C(31)-P(2)-Ag(1)-P(3)	0.4(7)
C(56)-C(51)-P(3)-C(61)	-160.8(15)	N(2)-P(2)-Ag(1)-P(4)	127.4(5)
C(52)-C(51)-P(3)-C(61)	26.9(18)	C(41)-P(2)-Ag(1)-P(4)	15.8(6)
C(56)-C(51)-P(3)-Ag(1)	-32.6(18)	C(31)-P(2)-Ag(1)-P(4)	-109.9(7)
C(52)-C(51)-P(3)-Ag(1)	155.1(14)	N(2)-P(2)-Ag(1)-P(1)	5.6(5)
N(3)-N(4)-P(4)-C(81)	-61.6(12)	C(41)-P(2)-Ag(1)-P(1)	-106.0(6)
C(7)-N(4)-P(4)-C(81)	167.4(15)	C(31)-P(2)-Ag(1)-P(1)	128.3(7)
N(3)-N(4)-P(4)-C(71)	-171.5(11)	N(4)-P(4)-Ag(1)-P(3)	-31.2(5)
C(7)-N(4)-P(4)-C(71)	57.4(16)	C(81)-P(4)-Ag(1)-P(3)	76.4(7)

C(71)-P(4)-Ag(1)-P(3)	-146.7(9)	C(21)-P(1)-Ag(1)-P(2)	-147.5(8)
N(4)-P(4)-Ag(1)-P(2)	101.0(5)	C(11)-P(1)-Ag(1)-P(2)	77.3(6)
C(81)-P(4)-Ag(1)-P(2)	-151.5(7)	N(1)-P(1)-Ag(1)-P(4)	-159.9(5)
C(71)-P(4)-Ag(1)-P(2)	-14.5(9)	C(21)-P(1)-Ag(1)-P(4)	83.3(8)
N(4)-P(4)-Ag(1)-P(1)	-157.0(5)	C(11)-P(1)-Ag(1)-P(4)	-51.8(7)
C(81)-P(4)-Ag(1)-P(1)	-49.4(7)	C(94)-O(4)-C(91)-C(92)	-41(6)
C(71)-P(4)-Ag(1)-P(1)	87.5(9)	C(91)-O(4)-C(94)-C(93)	36(6)
N(1)-P(1)-Ag(1)-P(3)	100.1(5)	O(4)-C(94)-C(93)-C(92)	-20(6)
C(21)-P(1)-Ag(1)-P(3)	-16.7(8)	C(94)-C(93)-C(92)-C(91)	-2(7)
C(11)-P(1)-Ag(1)-P(3)	-151.8(6)	O(4)-C(91)-C(92)-C(93)	28(7)
N(1)-P(1)-Ag(1)-P(2)	-30.8(5)		

Appendix B

IC_{50} Determination

Initial Activity Screening

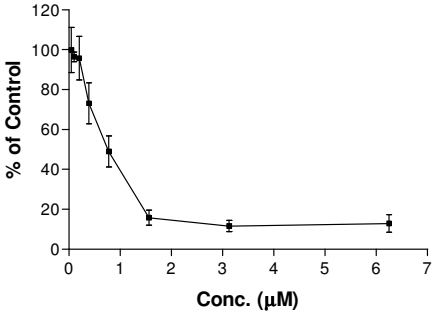

Graph 3.1: Effect of **37** on growth of HeLa.

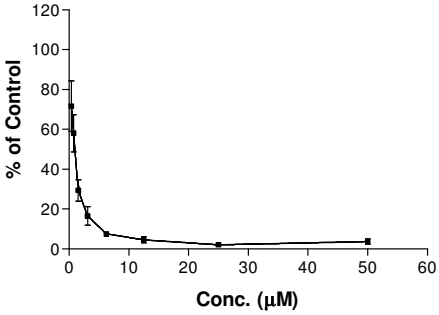

Graph 3.3: Effect of **24** on growth of HeLa.

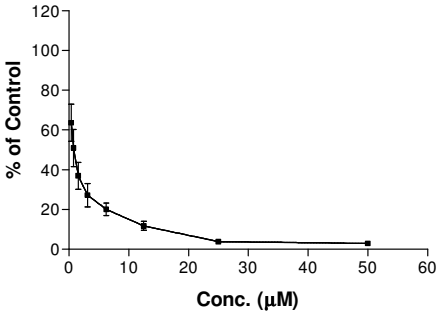

Graph 3.2: Effect of **23** on growth of HeLa.

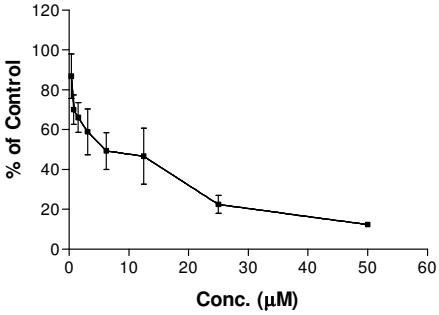

Graph 3.4: Effect of **25** on growth of HeLa.

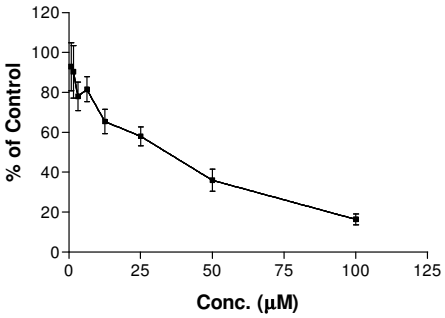

Graph 3.5: Effect of **27** on growth of HeLa.

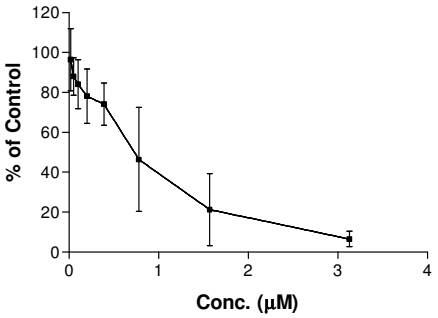

Graph 3.8: Effect of **30** on growth of HeLa.

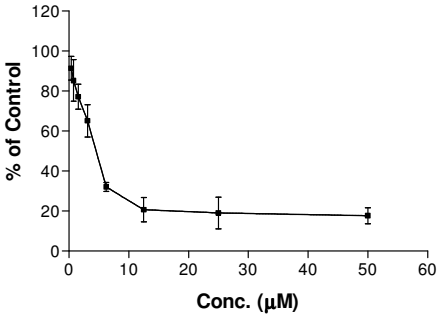

Graph 3.6: Effect of **28** on growth of HeLa.

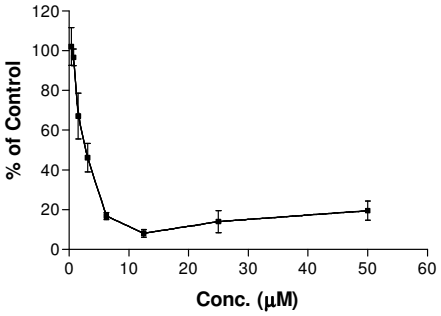

Graph 3.9: Effect of **31** on growth of HeLa.

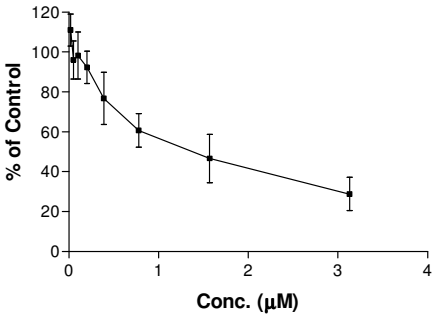

Graph 3.7: Effect of **29** on growth of HeLa.

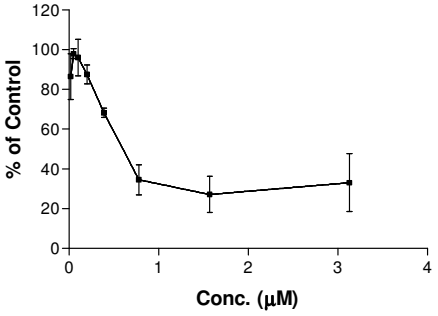

Graph 3.10: Effect of **43** on growth of HeLa.

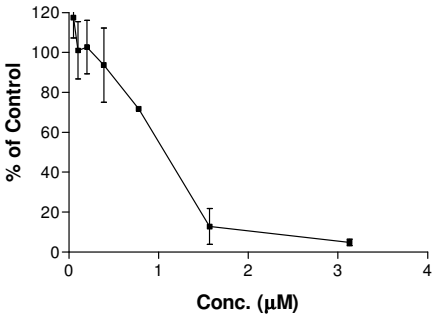

Graph 3.11: Effect of **45** on growth of HeLa.

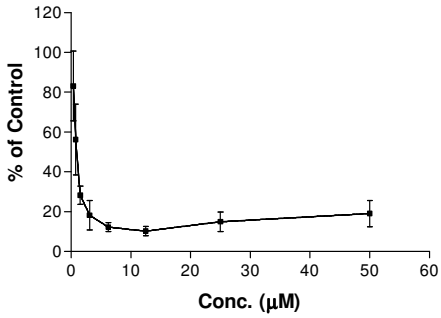

Graph 3.13: Effect of **47** on growth of HeLa.

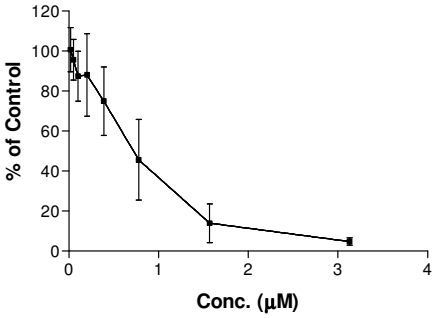

Graph 3.12: Effect of **46** on growth of HeLa.

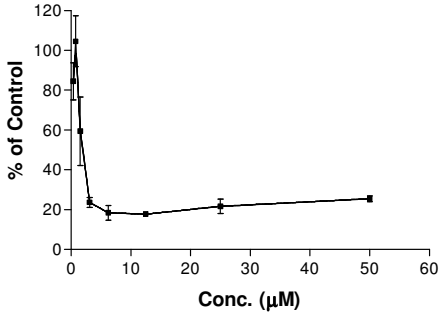

Graph 3.14: Effect of **49** on growth of Hela.

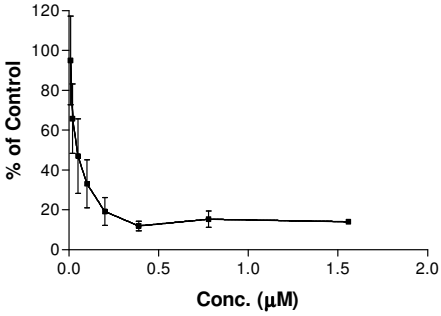

Graph 3.15: Effect of **37** on growth of Jurkat.

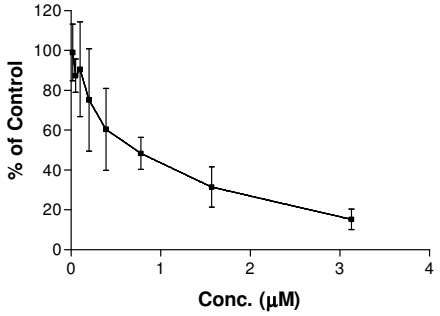

Graph 3.16: Effect of **23** on growth of Jurkat.

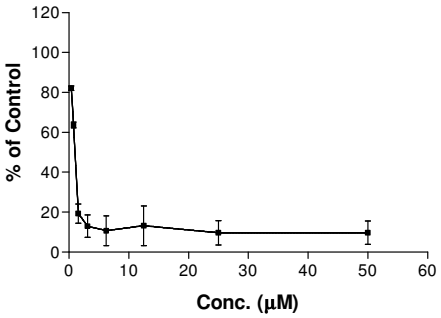

Graph 3.17: Effect of **24** on growth of Jurkat.

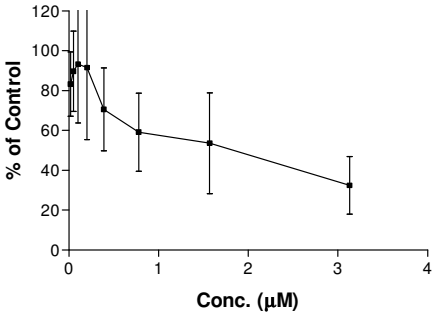

Graph 3.18: Effect of **25** on growth of Jurkat.

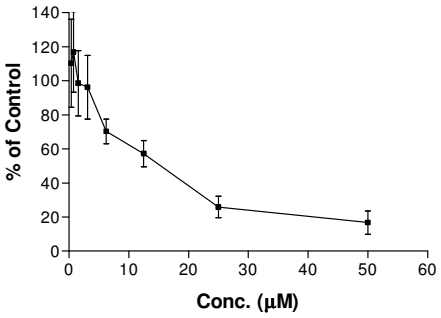

Graph 3.19: Effect of **27** on growth of Jurkat.

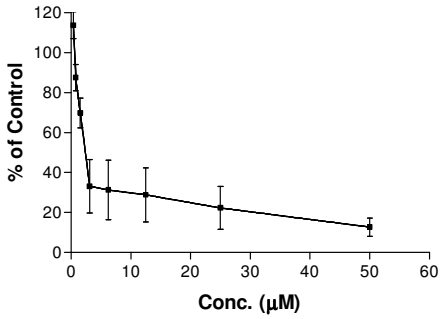

Graph 3.20: Effect of **28** on growth of Jurkat.

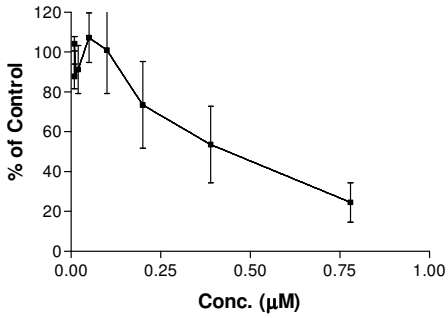

Graph 3.21: Effect of **29** on growth of Jurkat.

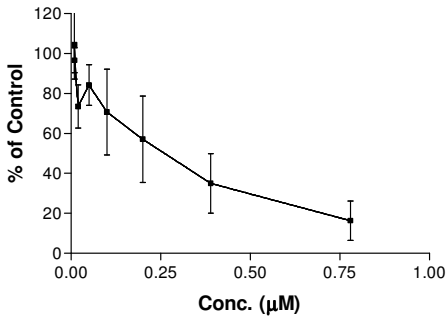

Graph 3.22: Effect of **30** on growth of Jurkat.

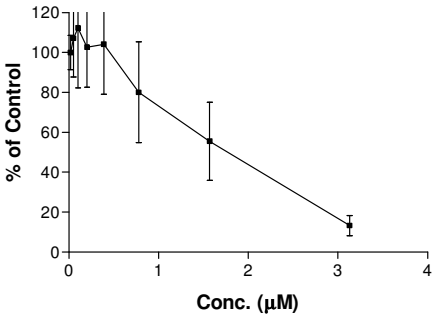

Graph 3.23: Effect of **31** on growth of Jurkat.

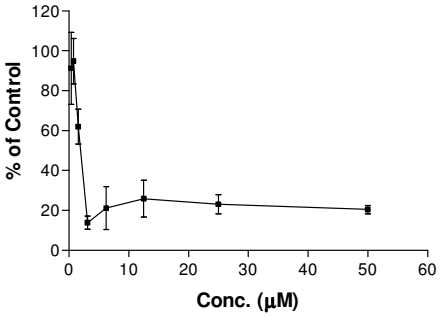

Graph 3.24: Effect of **43** on growth of Jurkat.

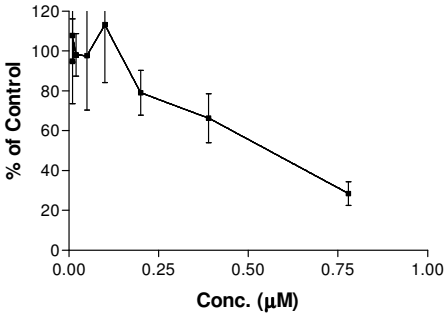

Graph 3.25: Effect of **45** on growth of Jurkat.

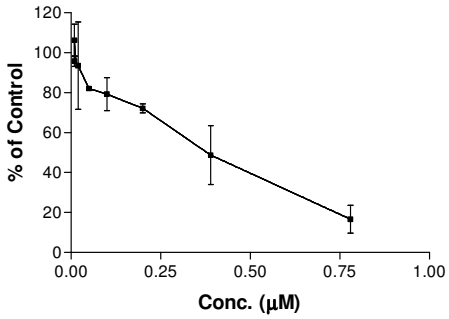

Graph 3.26: Effect of **46** on growth of Jurkat.

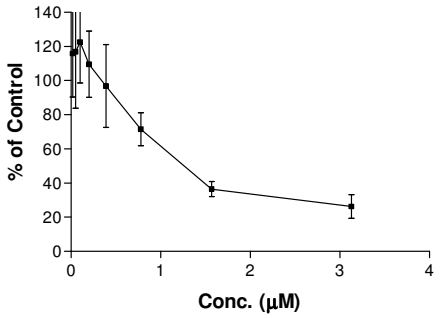

Graph 3.27: Effect of **47** on growth of Jurkat.

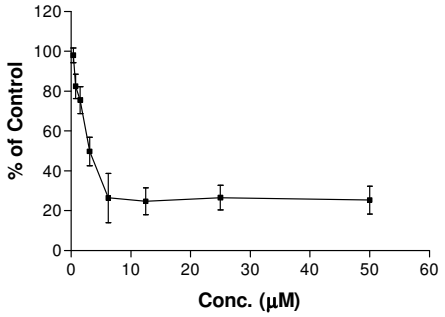

Graph 3.28: Effect of **49** on growth of Jurkat.

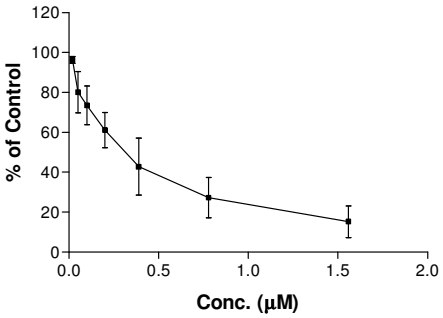

Graph 3.29: Effect of **37**on growth of resting Lymphocytes.

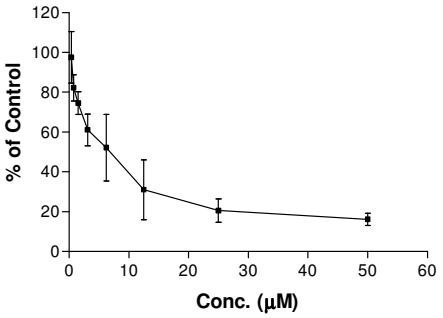

Graph 3.32: Effect of **25** on growth of resting Lymphocytes.

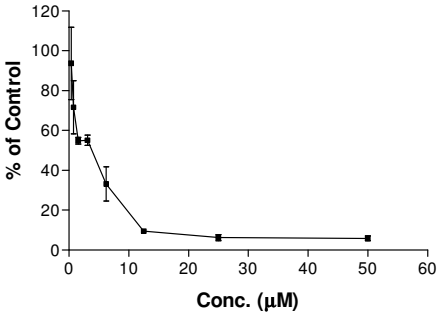

Graph 3.30: Effect of **23** on growth of resting Lymphocytes.

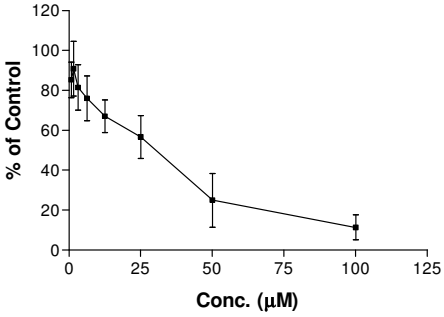

Graph 3.33: Effect of **27** on growth of resting Lymphocytes.

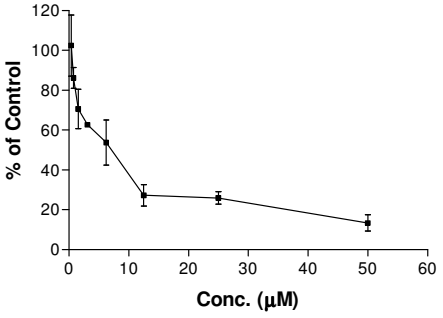

Graph 3.31: Effect of **24** on growth of resting Lymphocytes.

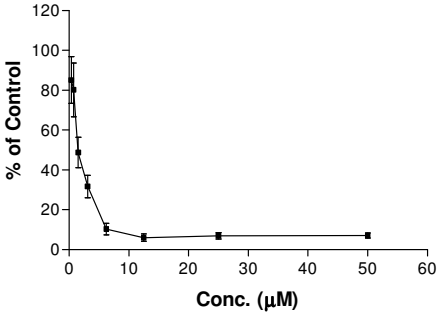

Graph 3.34: Effect of **28** on growth of resting Lymphocytes.

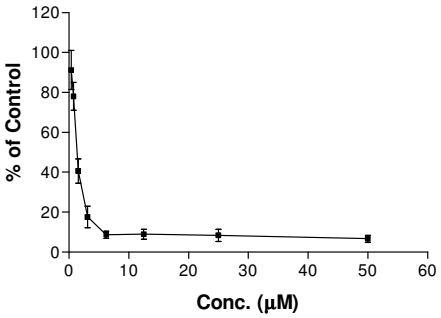

Graph 3.35: Effect of **29** on growth of resting Lymphocytes.

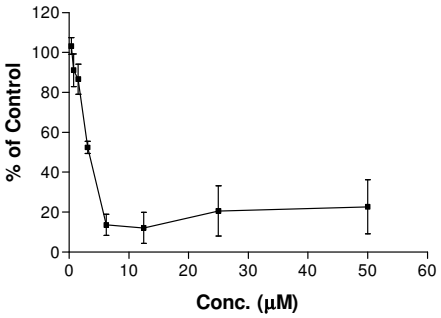

Graph 3.38: Effect of **43** on growth of resting Lymphocytes.

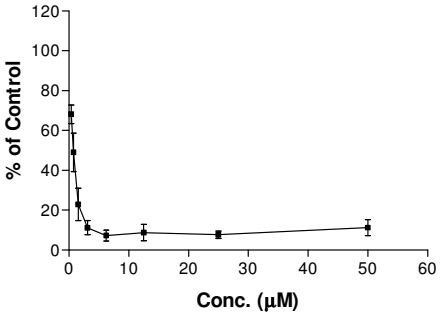

Graph 3.36: Effect of **30** on growth of resting Lymphocytes.

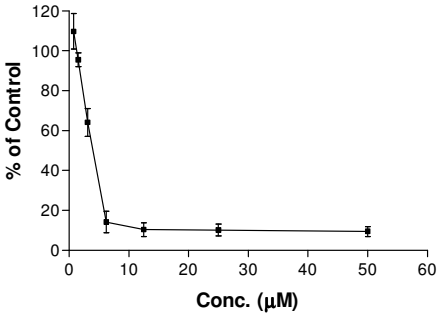

Graph 3.39: Effect of **45** on growth of resting Lymphocytes.

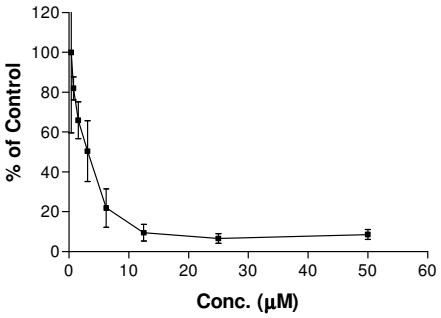

Graph 3.37: Effect of **31** on growth of resting Lymphocytes.

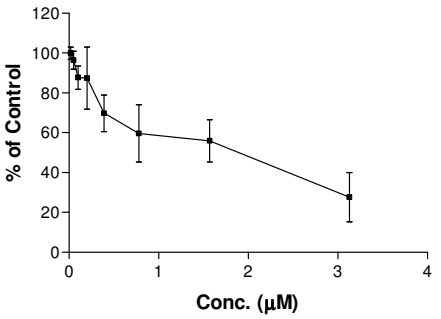

Graph 3.40: Effect of **46** on growth of resting Lymphocytes.

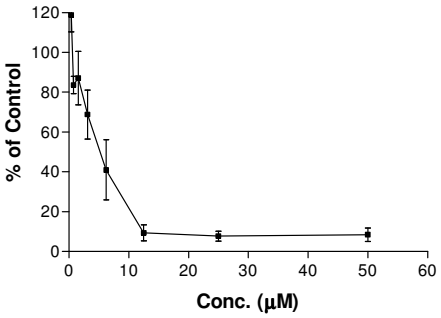

Graph 3.41: Effect of **47** on growth of resting Lymphocytes.

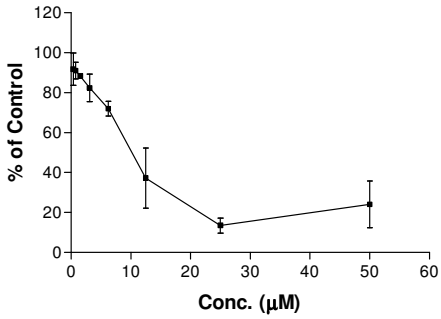

Graph 3.42: Effect of **49** on growth of resting Lymphocytes.

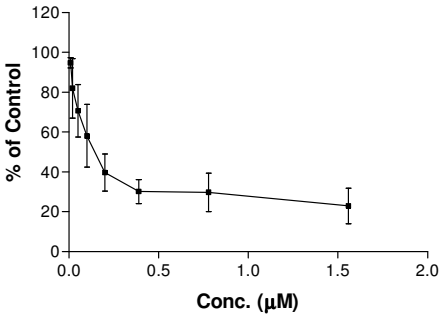

Graph 3.43: Effect of **37**on growth of stimulated Lymphocytes.

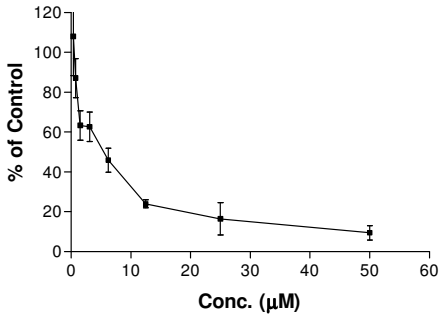

Graph 3.45: Effect of **24** on growth of stimulated Lymphocytes.

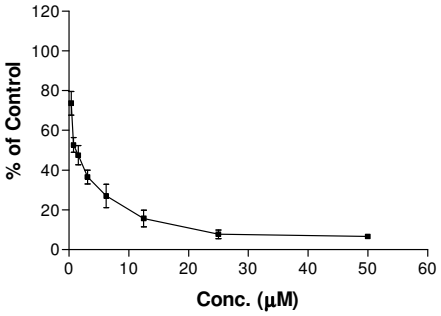

Graph 3.44: Effect of **23** on growth of stimulated Lymphocytes.

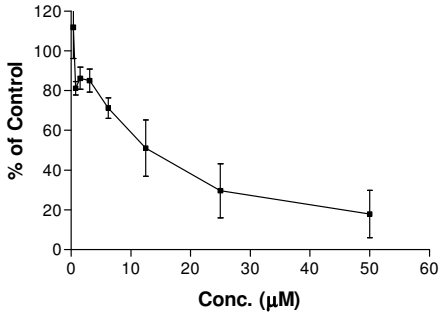

Graph 3.46: Effect of **25** on growth of stimulated Lymphocytes.

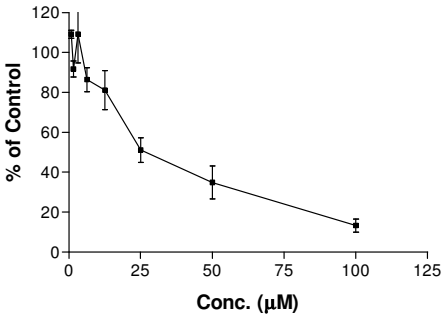

Graph 3.47: Effect of **27** on growth of stimulated Lymphocytes.

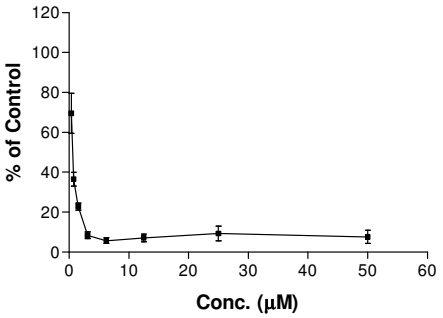

Graph 3.50: Effect of **30** on growth of stimulated Lymphocytes.

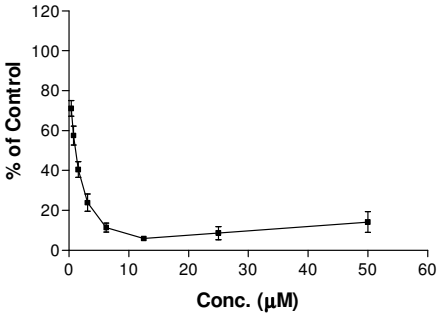

Graph 3.48: Effect of **28** on growth of stimulated Lymphocytes.

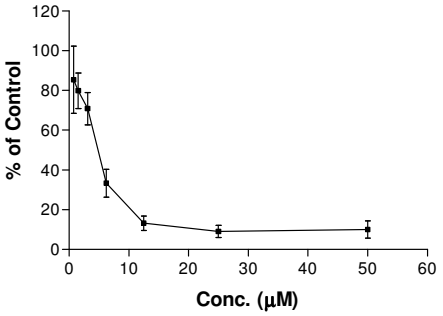

Graph 3.51: Effect of **31** on growth of stimulated Lymphocytes.

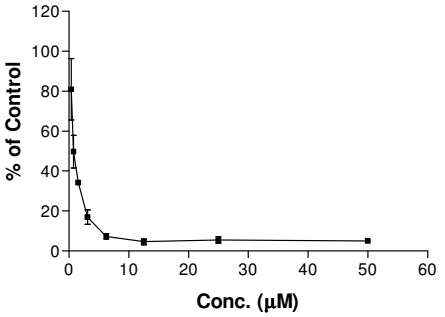

Graph 3.49: Effect of **29** on growth of stimulated Lymphocytes.

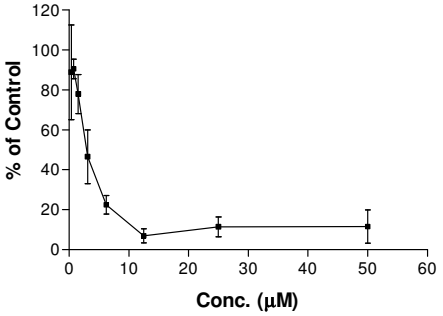

Graph 3.52: Effect of **43** on growth of stimulated Lymphocytes.

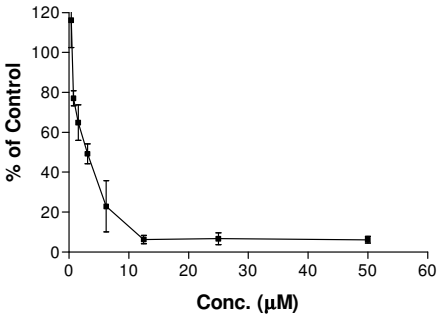

Graph 3.53: Effect of **45** on growth of stimulated Lymphocytes.

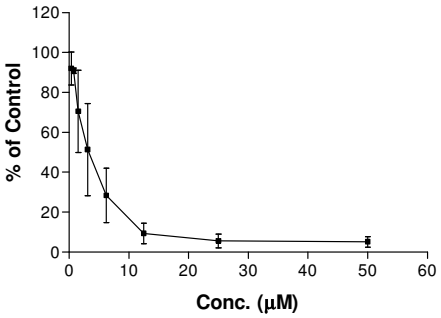

Graph 3.55: Effect of **47** on growth of stimulated Lymphocytes.

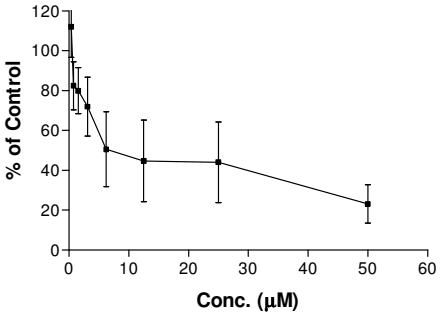

Graph 3.54: Effect of **46** on growth of stimulated Lymphocytes.

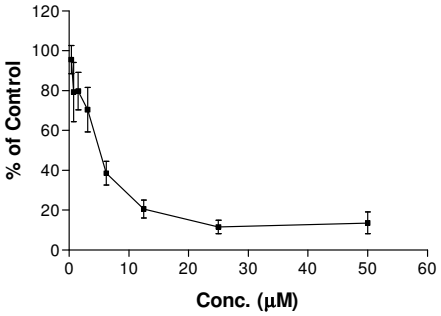

Graph 3.56: Effect of **49** on growth of stimulated Lymphocytes.

Activity Screening

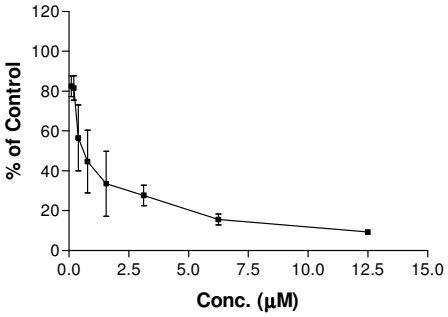

Graph 3.57: Effect of **37**on growth of Colo 320 DM.

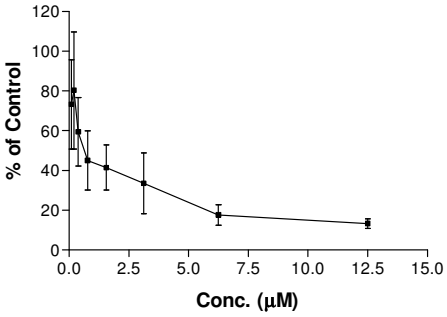

Graph 3.58: Effect of **24** on growth of Colo 320 DM.

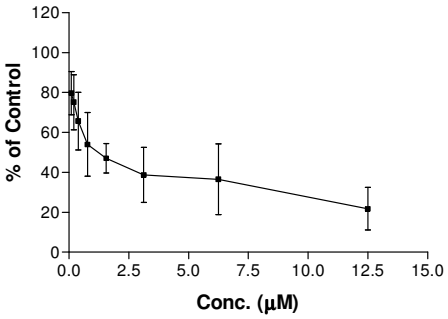

Graph 3.59: Effect of **25** on growth of Colo 320 DM.

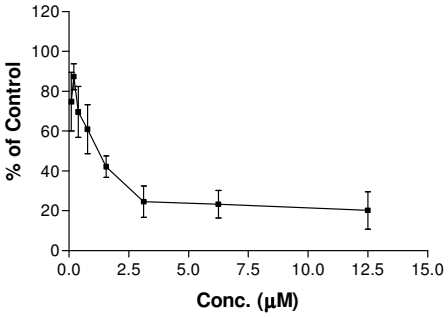

Graph 3.60: Effect of **45** on growth of Colo 320 DM.

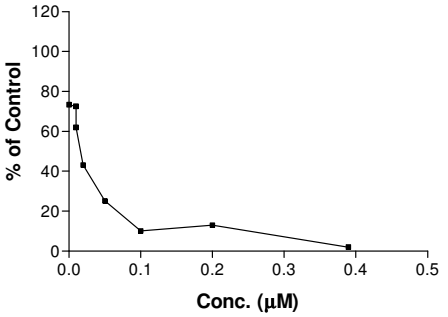

Graph 3.63: Effect of **37** on growth of A2780.

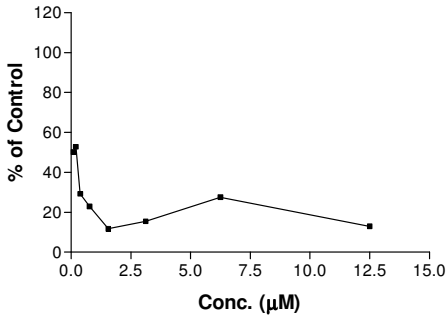

Graph 3.61: Effect of **46** on growth of Colo 320 DM.

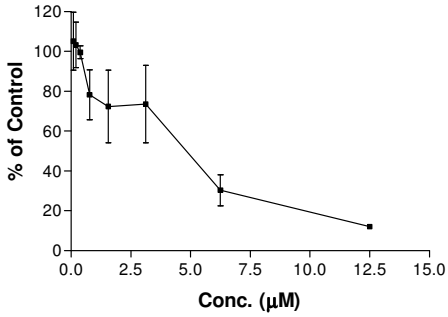

Graph 3.62: Effect of **49** on growth of Colo 320 DM.

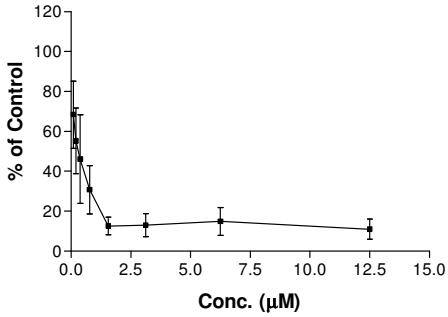

Graph 3.64: Effect of **24** on growth of A2780.

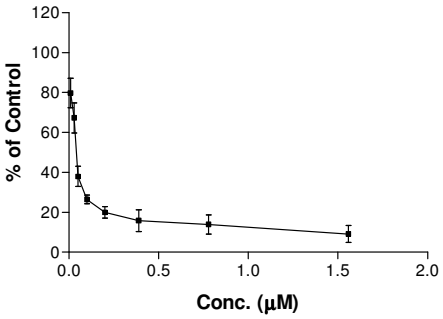

Graph 3.65: Effect of **25** on growth of A2780.

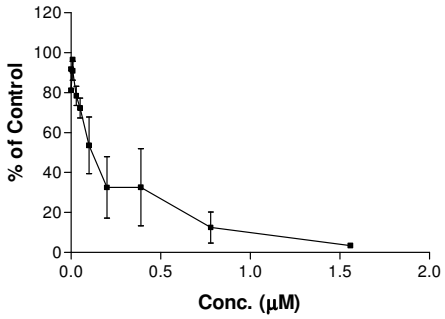

Graph 3.67: Effect of **46** on growth of A2780.

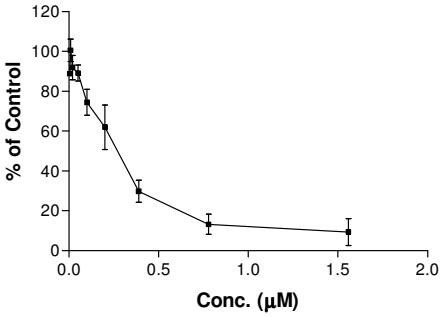

Graph 3.66: Effect of **45** on growth of A2780.

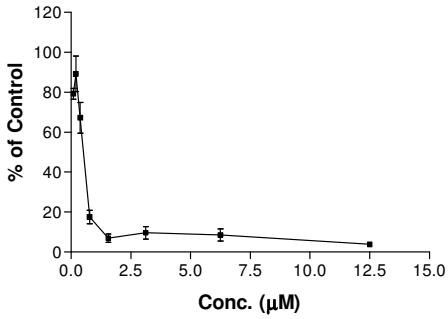

Graph 3.68: Effect of **49** on growth of A2780.

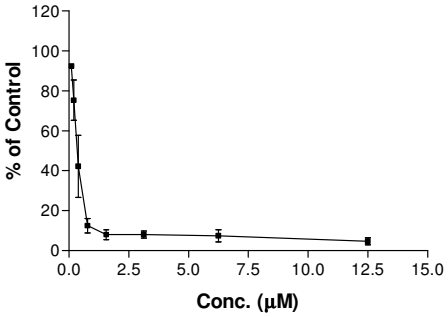

Graph 3.69: Effect of **37**on growth of A2780cis.

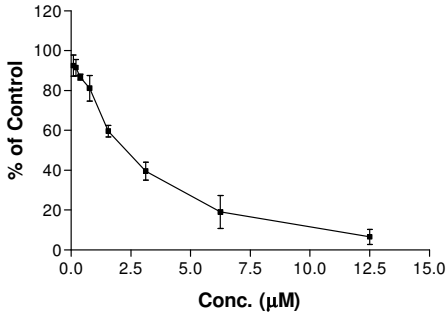

Graph 3.70: Effect of **24** on growth of A2780cis.

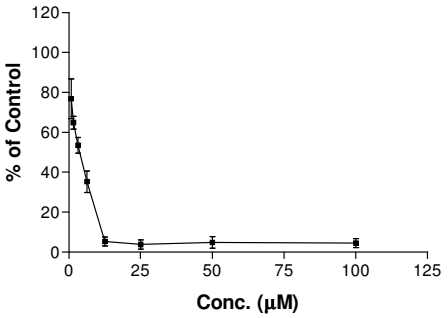

Graph 3.71: Effect of **25** on growth of A2780cis.

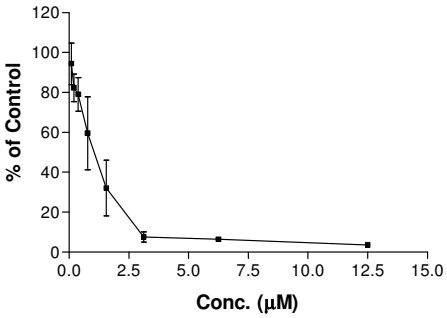

Graph 3.73: Effect of **46** on growth of A2780cis.

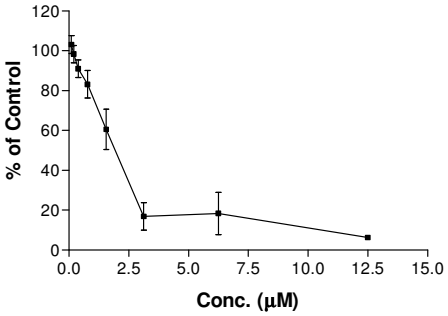

Graph 3.72: Effect of **45** on growth of A2780cis.

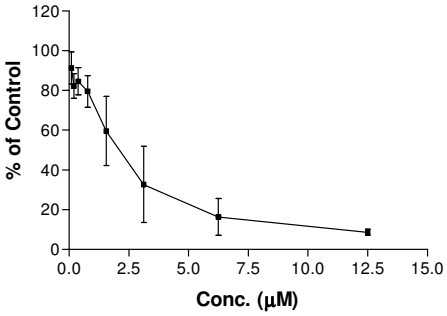

Graph 3.74: Effect of **49** on growth of A2780cis.

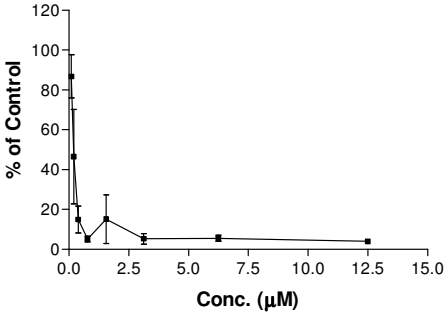

Graph 3.75: Effect of **37**on growth of MCF-7.

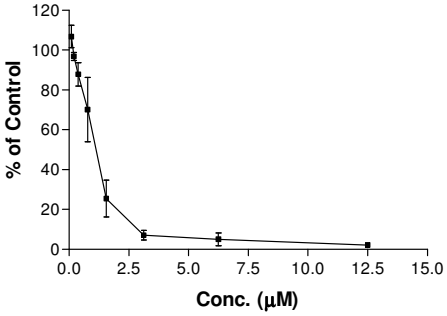

Graph 3.76: Effect of **24** on growth of MCF-7.

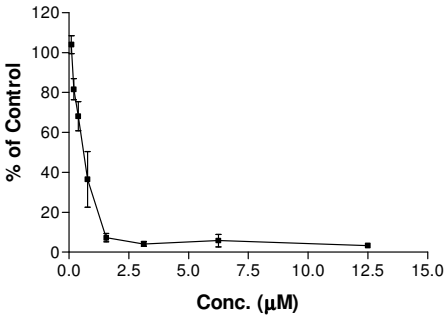

Graph 3.77: Effect of **25** on growth of MCF-7.

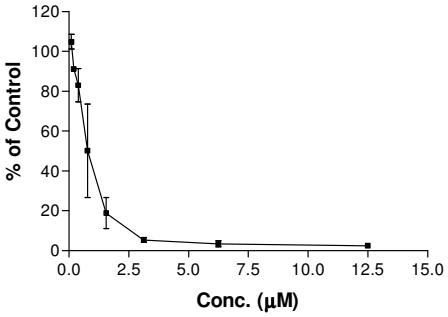

Graph 3.78 Effect of **45** on growth of MCF-7.

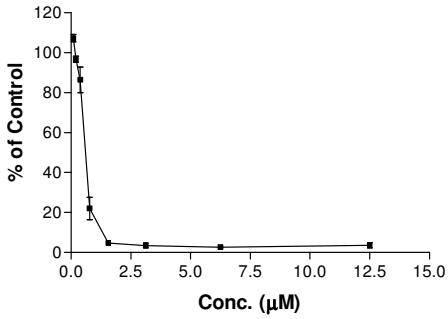

Graph 3.79: Effect of **46** on growth of MCF-7.

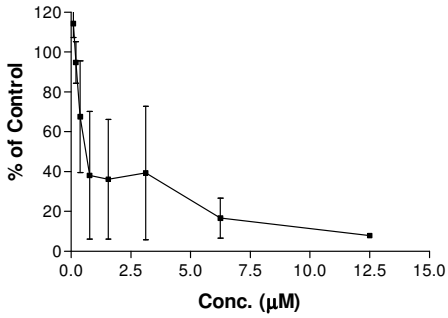

Graph 3.80: Effect of **49** on growth of MCF-7.

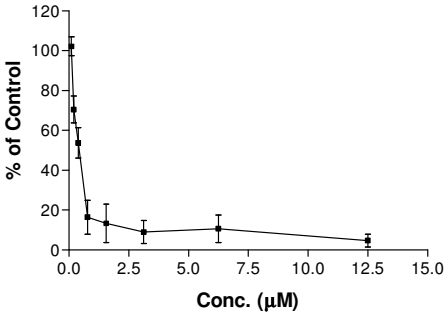

Graph 3.81: Effect of **37** on growth of MCF-12A.

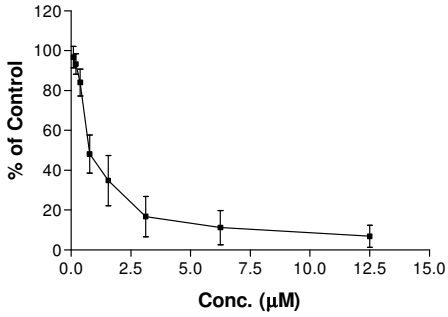

Graph 3.82: Effect of **24** on growth of MCF-12A.

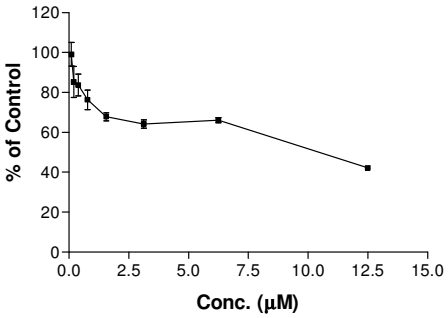

Graph 3.83: Effect of **25** on growth of MCF-12A.

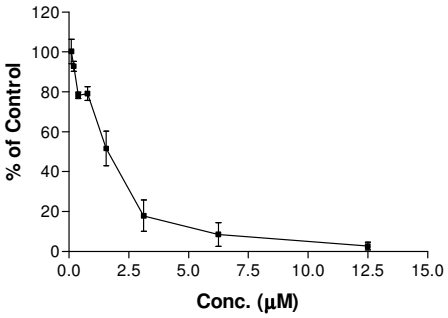

Graph 3.84: Effect of **45** on growth of MCF-12A.

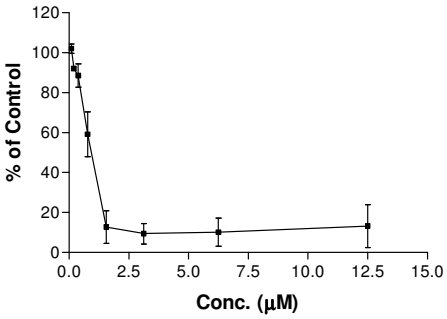

Graph 3.85: Effect of **46** on growth of MCF-12A.

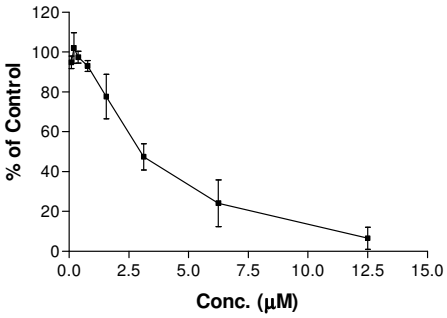

Graph 3.86: Effect of **49** on growth of MCF-12A.

Appendix C

Apoptosis and Necrosis Assay Flowcytometry Results

6 Hour Results

Contol Samples (1 x IC_{50} Concentration)

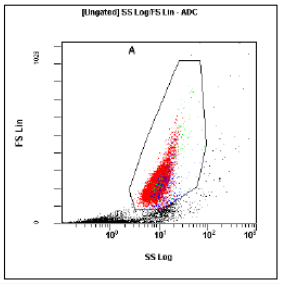

[Ungated] SS Log/FS Lin

Region	Number	%Total	%Gated	X-Mean	Y-Mean
ALL	58977	100.00	100.00	7.23	153
A	40187	68.14	68.14	9.28	218

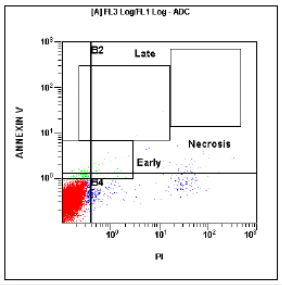

[A] FL3 Log/FL1 Log

Region	Number	%Total	%Gated	X-Mean	Y-Mean
ALL	40187	68.14	100.00	0.397	0.365
B3	39476	66.93	98.23	0.144	0.352
B4	542	0.92	1.35	12.6	0.66
Early	270	0.46	0.67	0.418	1.32
B2	106	0.18	0.26	32.2	2.73
B1	63	0.11	0.16	0.277	1.46
Late	4	0.01	0.01	8.09	19.2
Necrosis	0	0.00	0.00	0	0

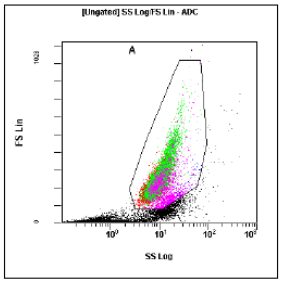

[Ungated] SS Log/FS Lin

Region	Number	%Total	%Gated	X-Mean	Y-Mean
ALL	68379	100.00	100.00	8.58	174
A	50276	73.53	73.53	9.93	228

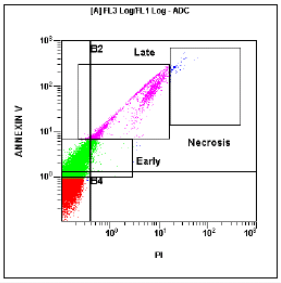

[A] FL3 Log/FL1 Log

Region	Number	%Total	%Gated	X-Mean	Y-Mean
ALL	50276	73.53	100.00	0.643	7.93
B3	31294	45.77	62.24	0.146	0.699
Early	20674	30.23	41.12	0.22	2.09
B1	13604	19.89	27.06	0.229	2.38
B2	5373	7.86	10.69	4.59	64.1
Late	4489	6.56	8.93	4.75	68.3
Necrosis	122	0.18	0.24	23.7	278
B4	5	0.01	0.01	0.675	1.01

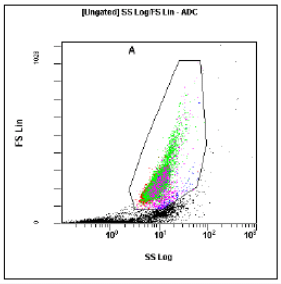

[Ungated] SS Log/FS Lin

Region	Number	%Total	%Gated	X-Mean	Y-Mean
ALL	54207	100.00	100.00	6.91	138
A	32416	59.80	59.80	9.76	221

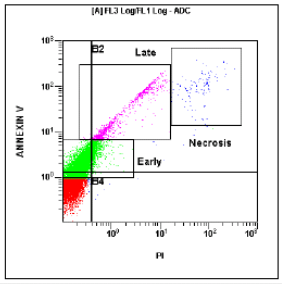

[A] FL3 Log/FL1 Log

Region	Number	%Total	%Gated	X-Mean	Y-Mean
ALL	32416	59.80	100.00	1.05	4.79
B3	17350	32.01	53.52	0.16	0.745
Early	16971	31.31	52.35	0.261	2.21
B1	10750	19.83	33.16	0.248	2.3
B2	4249	7.84	13.11	6.7	27.7
Late	2136	3.94	6.59	2.73	38.4
Necrosis	257	0.47	0.79	82.3	108
B4	67	0.12	0.21	0.577	0.917

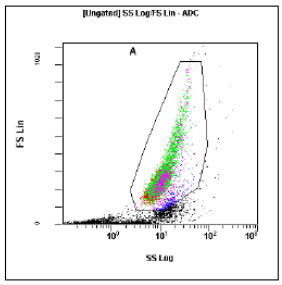

[Ungated] SS Log/FS Lin

Region	Number	%Total	%Gated	X-Mean	Y-Mean
ALL	39680	100.00	100.00	8.26	162
A	24129	60.81	60.81	11.4	255

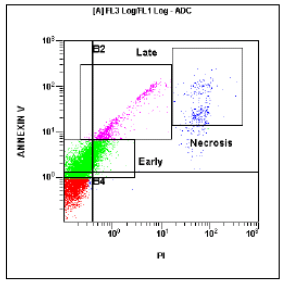

[A] FL3 Log/FL1 Log

Region	Number	%Total	%Gated	X-Mean	Y-Mean
ALL	24129	60.81	100.00	2.24	4.76
Early	13684	34.49	56.71	0.297	2.43
B3	10671	26.89	44.22	0.165	0.756
B1	8083	20.37	33.50	0.254	2.36
B2	5304	13.37	21.98	9.46	16.5
Late	1937	4.88	8.03	2.03	25.4
Necrosis	537	1.35	2.23	68.9	49.7
B4	71	0.18	0.29	0.951	0.977

*Compound **37** (Ref) Samples (1 x IC_{50} Concentration)*

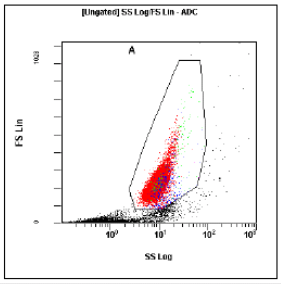

[Ungated] SS Log/FS Lin

Region	Number	%Total	%Gated	X-Mean	Y-Mean
ALL	58977	100.00	100.00	7.23	153
A	40187	68.14	68.14	9.28	218

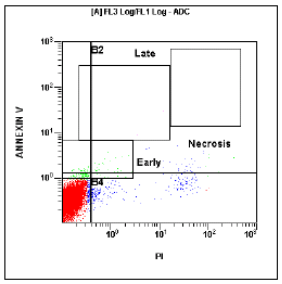

[A] FL3 Log/FL1 Log

Region	Number	%Total	%Gated	X-Mean	Y-Mean
ALL	40187	68.14	100.00	0.397	0.365
B3	39476	66.93	98.23	0.144	0.352
B4	542	0.92	1.35	12.6	0.66
Early	270	0.46	0.67	0.418	1.32
B2	106	0.18	0.26	32.2	2.73
B1	63	0.11	0.16	0.277	1.46
Late	4	0.01	0.01	8.09	19.2
Necrosis	0	0.00	0.00	0	0

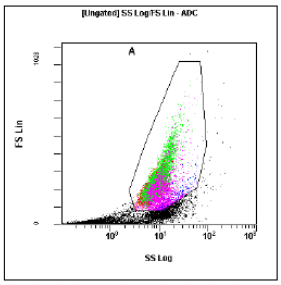

[Ungated] SS Log/FS Lin

Region	Number	%Total	%Gated	X-Mean	Y-Mean
ALL	65000	100.00	100.00	7.53	152
A	43653	67.16	67.16	9.19	215

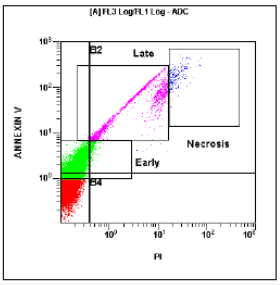

[A] FL3 Log/FL1 Log

Region	Number	%Total	%Gated	X-Mean	Y-Mean
ALL	43653	67.16	100.00	1.01	10.9
B3	24756	38.09	56.71	0.145	0.711
Early	18923	29.11	43.35	0.219	2.11
B1	12705	19.55	29.10	0.227	2.38
B2	6188	9.52	14.18	6.05	68.9
Late	5119	7.88	11.73	5.33	68.1
Necrosis	386	0.59	0.88	25.4	194
B4	4	0.01	0.01	1.92	0.984

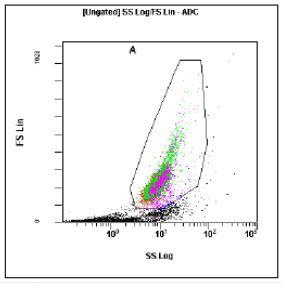

[Ungated] SS Log/FS Lin

Region	Number	%Total	%Gated	X-Mean	Y-Mean
ALL	40795	100.00	100.00	6.8	140
A	24943	61.14	61.14	9.5	220

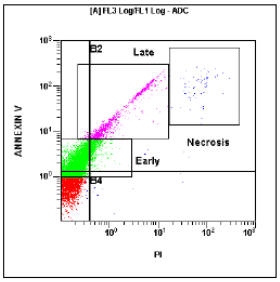

[A] FL3 Log/FL1 Log

Region	Number	%Total	%Gated	X-Mean	Y-Mean
ALL	24943	61.14	100.00	0.9	5.66
Early	14395	35.29	57.71	0.251	2.4
B3	10982	26.92	44.03	0.152	0.762
B1	9837	24.11	39.44	0.236	2.48
B2	4084	10.01	16.37	4.5	26.5
Late	2425	5.94	9.72	2.27	34.1
Necrosis	155	0.38	0.62	76.6	123
B4	40	0.10	0.16	2.15	0.85

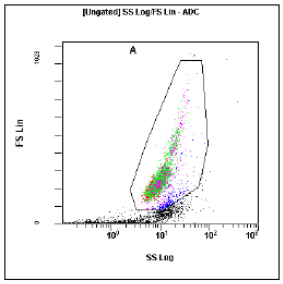

[Ungated] SS Log/FS Lin

Region	Number	%Total	%Gated	X-Mean	Y-Mean
ALL	16409	100.00	100.00	7.72	135
A	8308	50.63	50.63	11.4	248

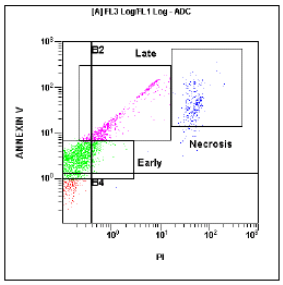

[A] FL3 Log/FL1 Log

Region	Number	%Total	%Gated	X-Mean	Y-Mean
ALL	8308	50.63	100.00	3.78	11.3
Early	4741	28.89	57.07	0.196	2.69
B1	3798	23.15	45.71	0.183	2.97
B3	2371	14.45	28.54	0.115	0.791
B2	2134	13.01	25.69	14.3	37.7
Late	1405	8.56	16.91	2.36	35.3
Necrosis	470	2.86	5.66	52.3	61.3
B4	5	0.03	0.06	1.08	0.854

*Compound **25** Samples (1 x IC_{50} Concentration)*

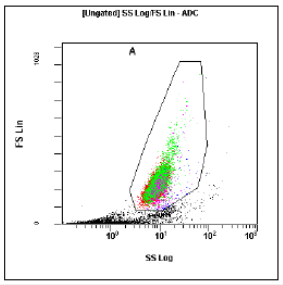

[Ungated] SS Log/FS Lin

Region	Number	%Total	%Gated	X-Mean	Y-Mean
ALL	50508	100.00	100.00	6.71	150
A	33880	67.08	67.08	8.94	218

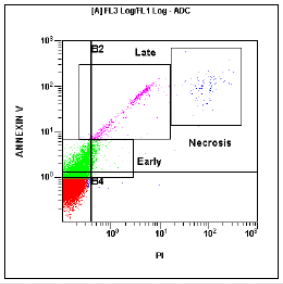

[A] FL3 Log/FL1 Log

Region	Number	%Total	%Gated	X-Mean	Y-Mean
ALL	33880	67.08	100.00	0.718	2.96
B3	25816	51.11	76.20	0.161	0.699
Early	11281	22.34	33.30	0.238	1.83
B1	6212	12.30	18.34	0.242	2.14
B2	1806	3.58	5.33	10.3	38.1
Late	1048	2.07	3.09	3.02	46.1
Necrosis	152	0.30	0.45	99.5	119
B4	46	0.09	0.14	0.968	0.817

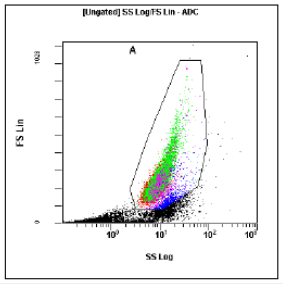

[Ungated] SS Log/FS Lin

Region	Number	%Total	%Gated	X-Mean	Y-Mean
ALL	65130	100.00	100.00	7.51	148
A	40335	61.93	61.93	9.87	225

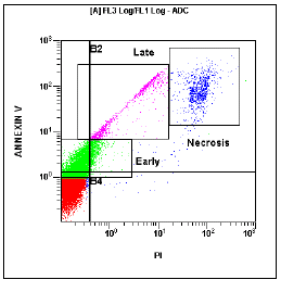

[A] FL3 Log/FL1 Log

Region	Number	%Total	%Gated	X-Mean	Y-Mean
ALL	40335	61.93	100.00	3.66	8.59
B3	25453	39.08	63.10	0.167	0.68
Early	15754	24.19	39.06	0.27	2.09
B1	9158	14.06	22.70	0.258	2.23
B2	5635	8.65	13.97	25	54.8
Late	2128	3.27	5.28	3.84	58.2
Necrosis	1688	2.59	4.18	76	105
B4	89	0.14	0.22	2.29	0.865

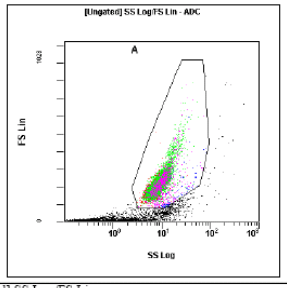

[Ungated] SS Log/FS Lin

Region	Number	%Total	%Gated	X-Mean	Y-Mean
ALL	37122	100.00	100.00	6.43	130
A	21499	57.91	57.91	9.24	215

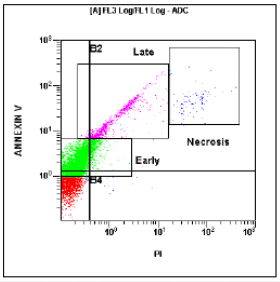

[A] FL3 Log/FL1 Log

Region	Number	%Total	%Gated	X-Mean	Y-Mean
ALL	21499	57.91	100.00	0.981	4.21
Early	13278	35.77	61.76	0.246	2.41
B1	9394	25.31	43.70	0.229	2.5
B3	8794	23.69	40.90	0.149	0.78
B2	3275	8.82	15.23	5.37	18.3
Late	1795	4.84	8.35	1.72	22.5
Necrosis	194	0.52	0.90	66.7	63.5
B4	36	0.10	0.17	1.11	0.876

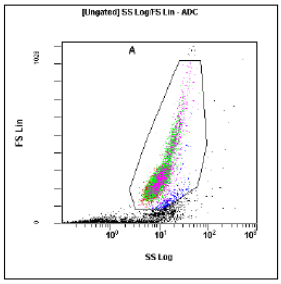

[Ungated] SS Log/FS Lin					
Region	Number	%Total	%Gated	X-Mean	Y-Mean
ALL	28585	100.00	100.00	7.79	149
A	15402	53.88	53.88	11.4	260

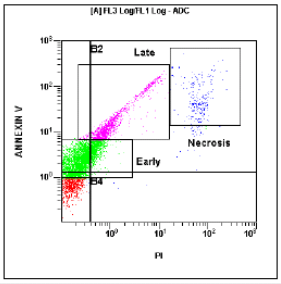

[A] FL3 Log/FL1 Log					
Region	Number	%Total	%Gated	X-Mean	Y-Mean
ALL	15402	53.88	100.00	2.93	8.52
Early	9397	32.87	61.01	0.276	2.73
B1	6237	21.82	40.49	0.23	2.68
B2	4836	16.92	31.40	8.88	23
B3	4306	15.06	27.96	0.149	0.806
Late	2653	9.28	17.23	1.84	26.3
Necrosis	450	1.57	2.92	74.4	74.8
B4	23	0.08	0.15	1.16	1.02

*Compound **46** Samples (1 x IC_{50} Concentration)*

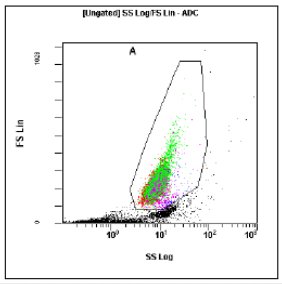

[Ungated] SS Log/FS Lin					
Region	Number	%Total	%Gated	X-Mean	Y-Mean
ALL	46954	100.00	100.00	6.68	146
A	30418	64.78	64.78	8.71	217

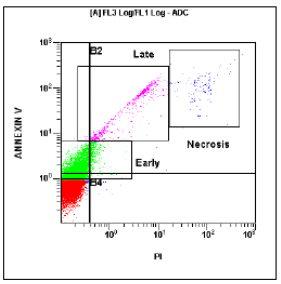

[A] FL3 Log/FL1 Log					
Region	Number	%Total	%Gated	X-Mean	Y-Mean
ALL	30418	64.78	100.00	0.986	4.03
B3	21443	45.67	70.49	0.159	0.711
Early	11769	25.06	38.69	0.239	1.88
B1	6751	14.38	22.19	0.24	2.14
B2	2172	4.63	7.14	11.5	42.7
Late	1205	2.57	3.96	3.62	52.1
Necrosis	223	0.47	0.73	86.8	119
B4	52	0.11	0.17	0.912	0.929

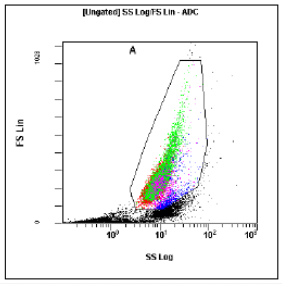

[Ungated] SS Log/FS Lin					
Region	Number	%Total	%Gated	X-Mean	Y-Mean
ALL	60249	100.00	100.00	8.37	165
A	41275	68.51	68.51	9.96	229

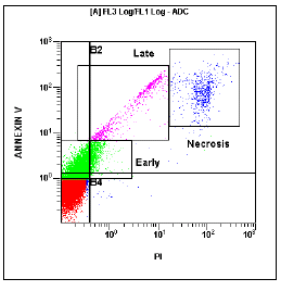

[A] FL3 Log/FL1 Log					
Region	Number	%Total	%Gated	X-Mean	Y-Mean
ALL	41275	68.51	100.00	3.57	7.39
B3	28209	46.82	68.34	0.172	0.648
Early	14097	23.40	34.15	0.287	2.05
B1	7460	12.38	18.07	0.263	2.16
B2	5431	9.01	13.16	25.9	49.8
Late	1886	3.13	4.57	4.31	60.3
Necrosis	1432	2.38	3.47	89.7	104
B4	175	0.29	0.42	0.779	0.936

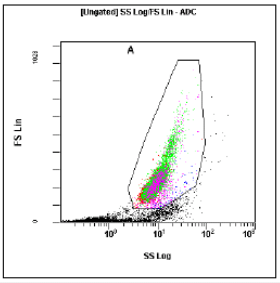

[Ungated] SS Log/FS Lin

Region	Number	%Total	%Gated	X-Mean	Y-Mean
ALL	45862	100.00	100.00	6.94	144
A	28777	62.75	62.75	9.5	221

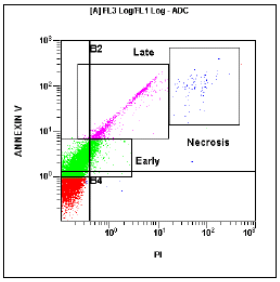

[A] FL3 Log/FL1 Log

Region	Number	%Total	%Gated	X-Mean	Y-Mean
ALL	28777	62.75	100.00	0.858	5.12
Early	15672	34.17	54.46	0.254	2.32
B3	14302	31.18	49.70	0.154	0.739
B1	10416	22.71	36.20	0.242	2.42
B2	4029	8.79	14.00	4.95	27.7
Late	2261	4.93	7.86	2.42	36.3
Necrosis	203	0.44	0.71	64	110
B4	30	0.07	0.10	0.715	0.936

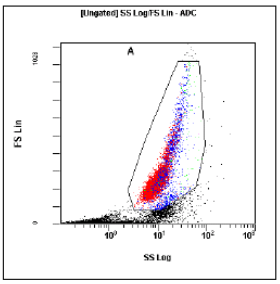

[Ungated] SS Log/FS Lin

Region	Number	%Total	%Gated	X-Mean	Y-Mean
ALL	39861	100.00	100.00	7.52	144
A	21052	52.81	52.81	11.4	256

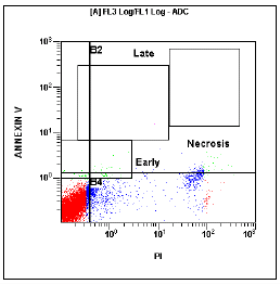

[A] FL3 Log/FL1 Log

Region	Number	%Total	%Gated	X-Mean	Y-Mean
ALL	21052	52.81	100.00	2.85	0.306
B3	18636	46.75	88.52	0.174	0.251
B4	2187	5.49	10.39	19.8	0.63
B2	219	0.55	1.04	61.8	1.74
Early	158	0.40	0.75	0.693	1.26
B1	10	0.03	0.05	0.218	1.43
Necrosis	0	0.00	0.00	0	0
Late	1	0.00	0.00	8.63	15.6

Control Samples (2 x IC_{50} Concentration)

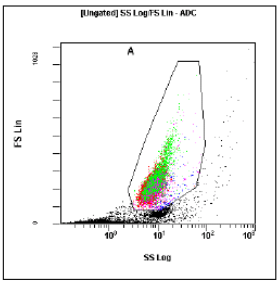

[Ungated] SS Log/FS Lin

Region	Number	%Total	%Gated	X-Mean	Y-Mean
ALL	50192	100.00	100.00	7.19	152
A	34210	68.16	68.16	8.22	214

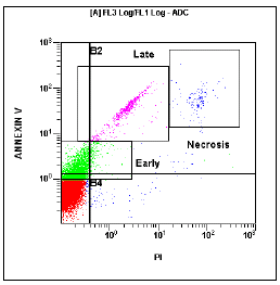

[A] FL3 Log/FL1 Log

Region	Number	%Total	%Gated	X-Mean	Y-Mean
ALL	34210	68.16	100.00	0.902	2.7
B3	28160	56.10	82.32	0.15	0.606
Early	7601	15.14	22.22	0.232	1.79
B1	3968	7.91	11.60	0.234	2.14
B2	1951	3.89	5.70	13	34.3
Late	1261	2.51	3.69	2.62	37.7
Necrosis	271	0.54	0.79	73	65.5
B4	131	0.26	0.38	2.92	0.594

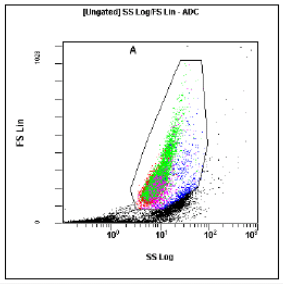

[Ungated] SS Log/FS Lin

Region	Number	%Total	%Gated	X-Mean	Y-Mean
ALL	63647	100.00	100.00	7.96	149
A	38849	61.04	61.04	9.41	227

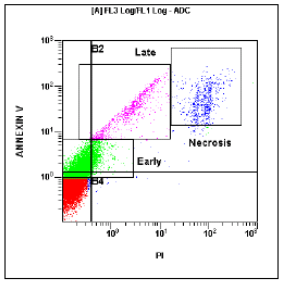

[A] FL3 Log/FL1 Log

Region	Number	%Total	%Gated	X-Mean	Y-Mean
ALL	38849	61.04	100.00	3.84	5.38
B3	25086	39.41	64.57	0.168	0.694
Early	15251	23.96	39.26	0.271	1.95
B1	8488	13.34	21.85	0.256	2.1
B2	5153	8.10	13.26	27.7	33.7
Late	1821	2.86	4.69	3.45	41
Necrosis	1474	2.32	3.79	87.6	62.1
B4	122	0.19	0.31	0.82	0.956

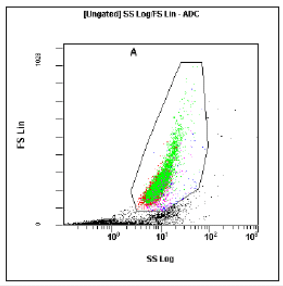

[Ungated] SS Log/FS Lin

Region	Number	%Total	%Gated	X-Mean	Y-Mean
ALL	38026	100.00	100.00	6.93	149
A	24178	63.58	63.58	9.52	227

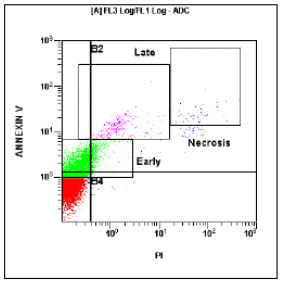

[A] FL3 Log/FL1 Log

Region	Number	%Total	%Gated	X-Mean	Y-Mean
ALL	24178	63.58	100.00	0.699	1.61
B3	16435	43.22	67.98	0.154	0.693
Early	10249	26.95	42.39	0.244	1.92
B1	6067	15.95	25.09	0.233	2.12
B2	1624	4.27	6.72	7.9	9.08
Late	607	1.60	2.51	1.9	13.8
Necrosis	105	0.28	0.43	73.1	25.2
B4	52	0.14	0.22	2.34	0.979

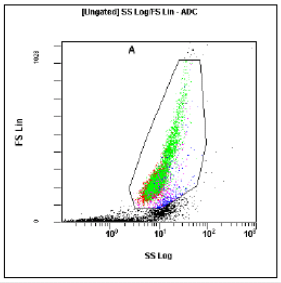

[Ungated] SS Log/FS Lin

Region	Number	%Total	%Gated	X-Mean	Y-Mean
ALL	33008	100.00	100.00	7.37	148
A	18663	56.54	56.54	10.5	246

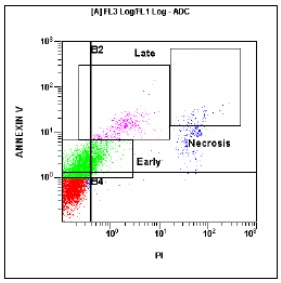

[A] FL3 Log/FL1 Log

Region	Number	%Total	%Gated	X-Mean	Y-Mean
ALL	18663	56.54	100.00	2.2	2.2
B3	11504	34.85	61.64	0.16	0.664
Early	7840	23.75	42.01	0.305	2.09
B1	4032	12.22	21.60	0.244	2.16
B2	2979	9.03	15.96	12.6	8.24
Late	732	2.22	3.92	2.41	16.2
Necrosis	157	0.48	0.84	67.5	26.3
B4	148	0.45	0.79	3.85	0.981

*Compound **37** (Ref) Samples (2 x IC_{50} Concentration)*

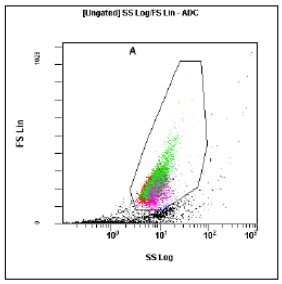

[Ungated] SS Log/FS Lin

Region	Number	%Total	%Gated	X-Mean	Y-Mean
ALL	35120	100.00	100.00	6.93	154
A	24479	69.70	69.70	7.99	213

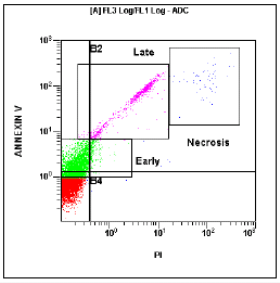

[A] FL3 Log/FL1 Log

Region	Number	%Total	%Gated	X-Mean	Y-Mean
ALL	24479	69.70	100.00	0.9	6.04
B3	16467	46.89	67.27	0.144	0.723
Early	9743	27.74	39.80	0.211	1.9
B1	5913	16.84	24.16	0.216	2.23
B2	2081	5.93	8.50	8.83	59
Late	1610	4.58	6.58	4.14	64.2
Necrosis	111	0.32	0.45	103	163
B4	18	0.05	0.07	0.598	0.893

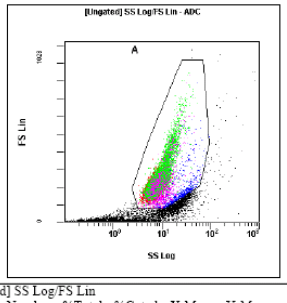

[Ungated] SS Log/FS Lin

Region	Number	%Total	%Gated	X-Mean	Y-Mean
ALL	54033	100.00	100.00	8.87	164
A	36580	67.70	67.70	9.41	227

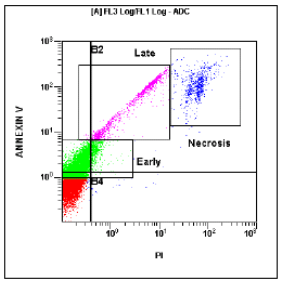

[A] FL3 Log/FL1 Log

Region	Number	%Total	%Gated	X-Mean	Y-Mean
ALL	36580	67.70	100.00	3.11	12.1
B3	19541	36.16	53.42	0.153	0.738
Early	17374	32.15	47.50	0.245	2.12
B1	11158	20.65	30.50	0.239	2.28
B2	5832	10.79	15.94	18.5	69.1
Late	2914	5.39	7.97	4.44	70.1
Necrosis	1485	2.75	4.06	63.2	130
B4	49	0.09	0.13	1.45	0.904

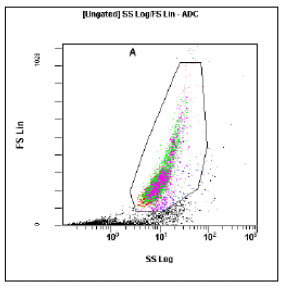

[Ungated] SS Log/FS Lin

Region	Number	%Total	%Gated	X-Mean	Y-Mean
ALL	31427	100.00	100.00	7.44	159
A	20177	64.20	64.20	9.91	238

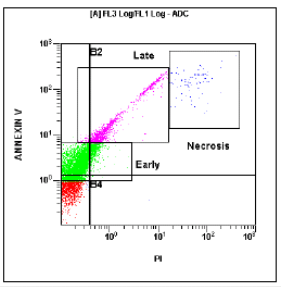

[A] FL3 Log/FL1 Log

Region	Number	%Total	%Gated	X-Mean	Y-Mean
ALL	20177	64.20	100.00	1.01	7.96
Early	12590	40.06	62.40	0.244	2.64
B1	9123	29.03	45.21	0.225	2.72
B3	6717	21.37	33.29	0.142	0.788
B2	4320	13.75	21.41	4.02	30.2
Late	2852	9.07	14.13	2.16	34.3
Necrosis	161	0.51	0.80	65.4	164
B4	17	0.05	0.08	0.965	0.959

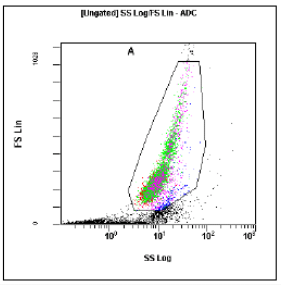

[Ungated] SS Log/FS Lin

Region	Number	%Total	%Gated	X-Mean	Y-Mean
ALL	28983	100.00	100.00	7.85	161
A	16554	57.12	57.12	11.1	263

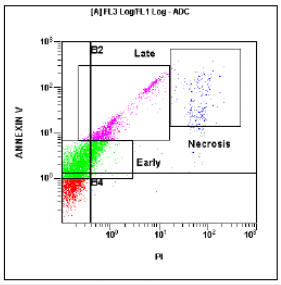

[A] FL3 Log/FL1 Log

Region	Number	%Total	%Gated	X-Mean	Y-Mean
ALL	16554	57.12	100.00	2.55	8.04
Early	9475	32.69	57.24	0.278	2.61
B1	6071	20.95	36.67	0.229	2.55
B3	6002	20.71	36.26	0.146	0.759
B2	4441	15.32	26.83	8.99	25.5
Late	2245	7.75	13.56	2.37	33.2
Necrosis	423	1.46	2.56	69.2	73.1
B4	40	0.14	0.24	0.898	1

*Compound **25** Samples (2 x IC_{50} Concentration)*

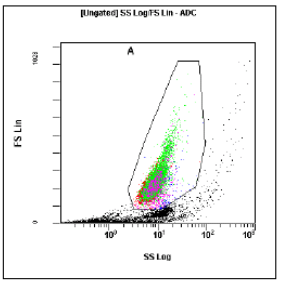

[Ungated] SS Log/FS Lin

Region	Number	%Total	%Gated	X-Mean	Y-Mean
ALL	50099	100.00	100.00	7.82	151
A	32569	65.01	65.01	8.48	221

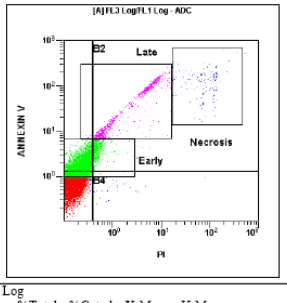

[A] FL3 Log/FL1 Log

Region	Number	%Total	%Gated	X-Mean	Y-Mean
ALL	32569	65.01	100.00	1.08	4.92
B3	20190	40.30	61.99	0.16	0.744
Early	15269	30.48	46.88	0.245	1.99
B1	9355	18.67	28.72	0.242	2.2
B2	2945	5.88	9.04	9.98	42.3
Late	1621	3.24	4.98	3.38	51.5
Necrosis	242	0.48	0.74	90.2	149
B4	79	0.16	0.24	2.26	0.809

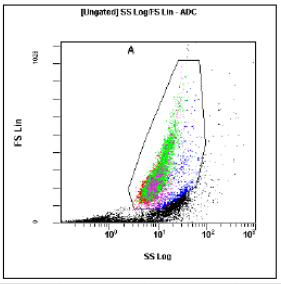

[Ungated] SS Log/FS Lin

Region	Number	%Total	%Gated	X-Mean	Y-Mean
ALL	57512	100.00	100.00	8.7	159
A	36352	63.21	63.21	9.72	234

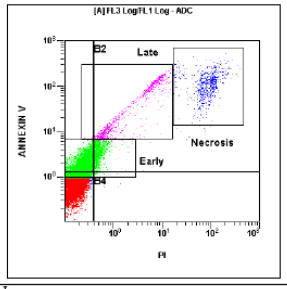

[A] FL3 Log/FL1 Log

Region	Number	%Total	%Gated	X-Mean	Y-Mean
ALL	36352	63.21	100.00	4.03	8.7
B3	21245	36.94	58.44	0.169	0.716
Early	16500	28.69	45.39	0.28	2.1
B1	9477	16.48	26.07	0.259	2.17
B2	5529	9.61	15.21	25.4	50.7
Late	1844	3.21	5.07	3.59	52.3
Necrosis	1407	2.45	3.87	92.9	124
B4	101	0.18	0.28	0.766	0.98

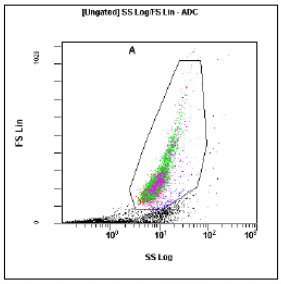

[Ungated] SS Log/FS Lin

Region	Number	%Total	%Gated	X-Mean	Y-Mean
ALL	27486	100.00	100.00	6.81	146
A	16568	60.28	60.28	9.56	231

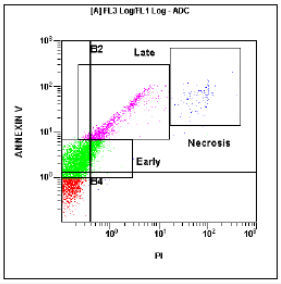

[A] FL3 Log/FL1 Log

Region	Number	%Total	%Gated	X-Mean	Y-Mean
ALL	16568	60.28	100.00	1.14	5.14
Early	10610	38.60	64.04	0.24	2.64
B1	7744	28.17	46.74	0.216	2.71
B3	5533	20.13	33.40	0.14	0.786
B2	3276	11.92	19.77	5.02	18.3
Late	1961	7.13	11.84	1.69	22.2
Necrosis	167	0.61	1.01	73.6	67.6
B4	15	0.05	0.09	0.845	0.984

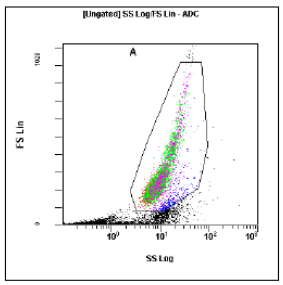

[Ungated] SS Log/FS Lin

Region	Number	%Total	%Gated	X-Mean	Y-Mean
ALL	29451	100.00	100.00	7.37	143
A	15325	52.04	52.04	10.9	256

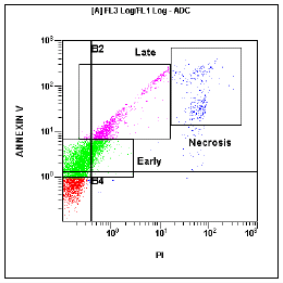

[A] FL3 Log/FL1 Log

Region	Number	%Total	%Gated	X-Mean	Y-Mean
ALL	15325	52.04	100.00	3.23	10.7
Early	8844	30.03	57.71	0.28	2.68
B1	5722	19.43	37.34	0.231	2.61
B3	5130	17.42	33.47	0.149	0.78
B2	4446	15.10	29.01	10.7	32.5
Late	2205	7.49	14.39	2.43	35.9
Necrosis	567	1.93	3.70	64.5	103
B4	27	0.09	0.18	1.98	0.955

*Compound **46** Samples (2 x IC_{50} Concentration)*

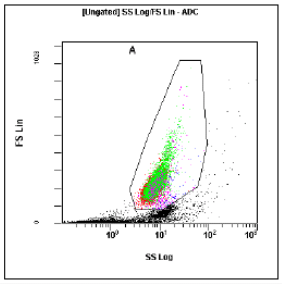

[Ungated] SS Log/FS Lin

Region	Number	%Total	%Gated	X-Mean	Y-Mean
ALL	40179	100.00	100.00	7.11	140
A	24435	60.82	60.82	8.39	218

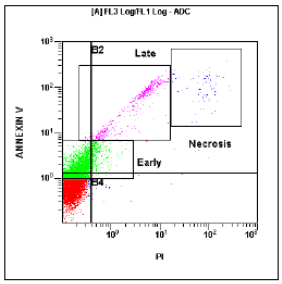

[A] FL3 Log/FL1 Log

Region	Number	%Total	%Gated	X-Mean	Y-Mean
ALL	24435	60.82	100.00	1.12	4.54
B3	17079	42.51	69.90	0.158	0.695
Early	9324	23.21	38.16	0.249	1.91
B1	5197	12.93	21.27	0.234	2.14
B2	2079	5.17	8.51	11.2	42.3
Late	1112	2.77	4.55	3.99	56.1
Necrosis	183	0.46	0.75	96.4	123
B4	80	0.20	0.33	1.4	0.908

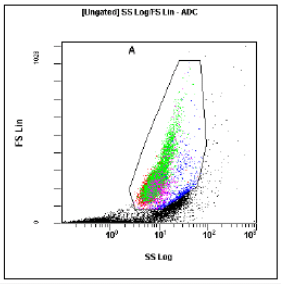

[Ungated] SS Log/FS Lin

Region	Number	%Total	%Gated	X-Mean	Y-Mean
ALL	54888	100.00	100.00	8.28	152
A	34162	62.24	62.24	9.39	228

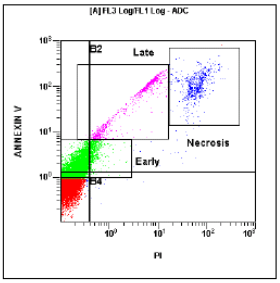

[A] FL3 Log/FL1 Log

Region	Number	%Total	%Gated	X-Mean	Y-Mean
ALL	34162	62.24	100.00	3.04	9.66
B3	20756	37.82	60.76	0.157	0.712
Early	14648	26.69	42.88	0.253	2.04
B1	8796	16.03	25.75	0.244	2.2
B2	4544	8.28	13.30	21.6	65.1
Late	1815	3.31	5.31	4.43	68.1
Necrosis	1329	2.42	3.89	66.7	125
B4	66	0.12	0.19	0.996	0.936

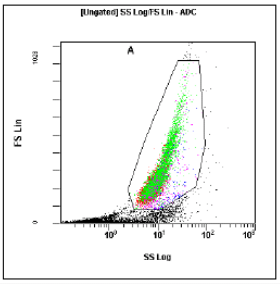

[Ungated] SS Log/FS Lin

Region	Number	%Total	%Gated	X-Mean	Y-Mean
ALL	49786	100.00	100.00	7.01	153
A	30587	61.44	61.44	9.83	239

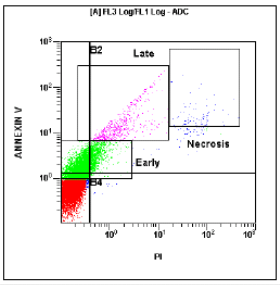

[A] FL3 Log/FL1 Log

Region	Number	%Total	%Gated	X-Mean	Y-Mean
ALL	30587	61.44	100.00	0.866	2
B3	20077	40.33	65.64	0.172	0.663
Early	12791	25.69	41.82	0.304	2.1
B1	6721	13.50	21.97	0.262	2.12
B2	3665	7.36	11.98	5.78	9.12
Late	1078	2.17	3.52	2.1	18.3
Necrosis	149	0.30	0.49	76.9	29.7
B4	124	0.25	0.41	0.547	0.975

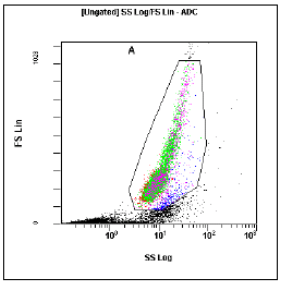

[Ungated] SS Log/FS Lin

Region	Number	%Total	%Gated	X-Mean	Y-Mean
ALL	34806	100.00	100.00	7.59	154
A	19084	54.83	54.83	11.1	261

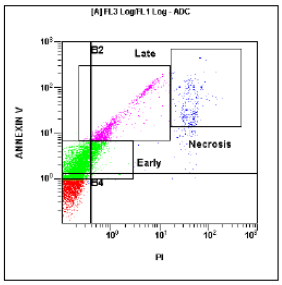

[A] FL3 Log/FL1 Log

Region	Number	%Total	%Gated	X-Mean	Y-Mean
ALL	19084	54.83	100.00	2.06	6.78
Early	10854	31.18	56.87	0.267	2.57
B3	7473	21.47	39.16	0.148	0.759
B1	7089	20.37	37.15	0.236	2.55
B2	4504	12.94	23.60	8.09	23.4
Late	2161	6.21	11.32	2.03	28.7
Necrosis	547	1.57	2.87	48.2	64.5
B4	18	0.05	0.09	6.69	1.02

24 Hour Results

Contol Samples (1 x IC_{50} Concentration)

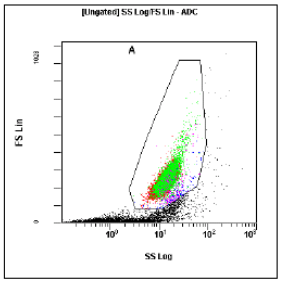

[Ungated] SS Log/FS Lin

Region	Number	%Total	%Gated	X-Mean	Y-Mean
ALL	70061	100.00	100.00	9.3	140
A	39664	56.61	56.61	14.2	237

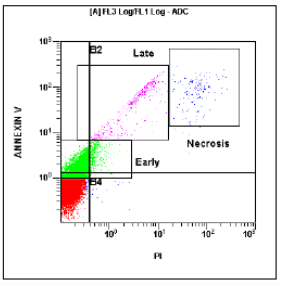

[A] FL3 Log/FL1 Log

Region	Number	%Total	%Gated	X-Mean	Y-Mean
ALL	39664	56.61	100.00	0.806	2.8
B3	30100	42.96	75.89	0.164	0.664
Early	13501	19.27	34.04	0.251	1.76
B1	7439	10.62	18.76	0.248	1.97
B2	2021	2.88	5.10	12.4	37.8
Late	807	1.15	2.03	3.89	52.9
Necrosis	292	0.42	0.74	70.6	102
B4	104	0.15	0.26	0.836	0.892

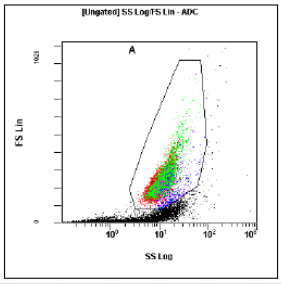

[Ungated] SS Log/FS Lin

Region	Number	%Total	%Gated	X-Mean	Y-Mean
ALL	87128	100.00	100.00	6.82	111
A	40665	46.67	46.67	10.9	222

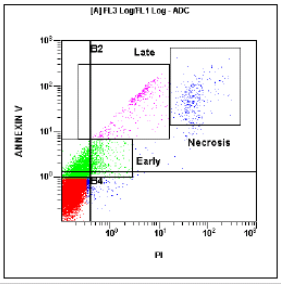

[A] FL3 Log/FL1 Log

Region	Number	%Total	%Gated	X-Mean	Y-Mean
ALL	40665	46.67	100.00	1.27	2.66
B3	33927	38.94	83.43	0.172	0.537
Early	7959	9.13	19.57	0.318	1.77
B1	3590	4.12	8.83	0.267	1.93
B2	2667	3.06	6.56	16.7	31
Late	736	0.84	1.81	4.4	51.3
Necrosis	598	0.69	1.47	62.2	67.8
B4	481	0.55	1.18	0.816	0.845

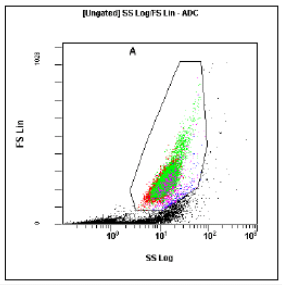

[Ungated] SS Log/FS Lin

Region	Number	%Total	%Gated	X-Mean	Y-Mean
ALL	95104	100.00	100.00	9.04	149
A	58621	61.64	61.64	12.9	233

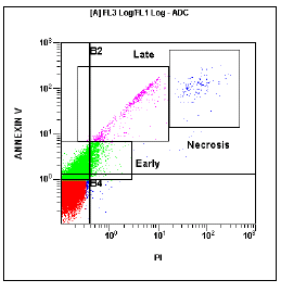

[A] FL3 Log/FL1 Log

Region	Number	%Total	%Gated	X-Mean	Y-Mean
ALL	58621	61.64	100.00	0.611	2.51
B3	45524	47.87	77.66	0.174	0.64
Early	17922	18.84	30.57	0.269	1.87
B1	9602	10.10	16.38	0.262	2.06
B2	3293	3.46	5.62	7.68	29.8
Late	1319	1.39	2.25	3.25	46.4
Necrosis	282	0.30	0.48	67	109
B4	202	0.21	0.34	0.542	0.9

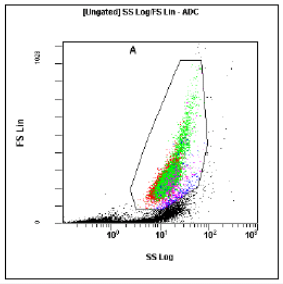

[Ungated] SS Log/FS Lin

Region	Number	%Total	%Gated	X-Mean	Y-Mean
ALL	82025	100.00	100.00	8.96	129
A	41730	50.87	50.87	14.3	240

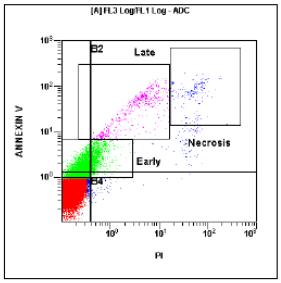

[A] FL3 Log/FL1 Log

Region	Number	%Total	%Gated	X-Mean	Y-Mean
ALL	41730	50.87	100.00	0.946	2.69
B3	32260	39.33	77.31	0.18	0.586
Early	11329	13.81	27.15	0.323	1.9
B1	5201	6.34	12.46	0.278	1.96
B2	3836	4.68	9.19	8.3	21.6
Late	1198	1.46	2.87	4.35	42
B4	433	0.53	1.04	0.871	0.929
Necrosis	321	0.39	0.77	56.3	77.3

*Compound **37** (Ref) Samples (1 x IC_{50} Concentration)*

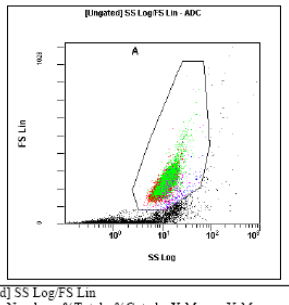

[Ungated] SS Log/FS Lin

Region	Number	%Total	%Gated	X-Mean	Y-Mean
ALL	57035	100.00	100.00	7.89	129
A	31459	55.16	55.16	11.7	224

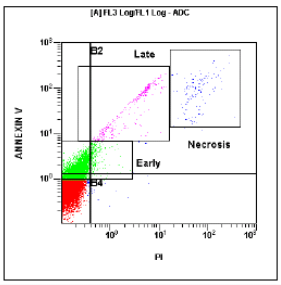

[A] FL3 Log/FL1 Log

Region	Number	%Total	%Gated	X-Mean	Y-Mean
ALL	31459	55.16	100.00	0.838	2.79
B3	24564	43.07	78.08	0.154	0.644
Early	9824	17.22	31.23	0.233	1.75
B1	5476	9.60	17.41	0.237	2
B2	1354	2.37	4.30	15.7	45
Late	617	1.08	1.96	3.73	55
Necrosis	230	0.40	0.73	77.6	106
B4	65	0.11	0.21	0.83	0.842

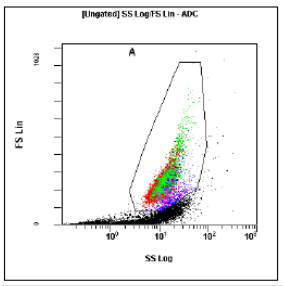

[Ungated] SS Log/FS Lin

Region	Number	%Total	%Gated	X-Mean	Y-Mean
ALL	87289	100.00	100.00	6.98	95.9
A	33636	38.53	38.53	12.7	226

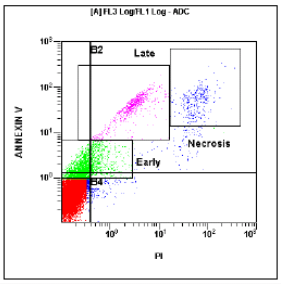

[A] FL3 Log/FL1 Log

Region	Number	%Total	%Gated	X-Mean	Y-Mean
ALL	33636	38.53	100.00	1.89	3.47
B3	27151	31.10	80.72	0.175	0.487
Early	5702	6.53	16.95	0.364	1.88
B2	3455	3.96	10.27	16.7	28.5
B1	2363	2.71	7.03	0.275	2.02
Late	1388	1.59	4.13	3.51	40.6
B4	667	0.76	1.98	0.792	0.851
Necrosis	639	0.73	1.90	66.3	58

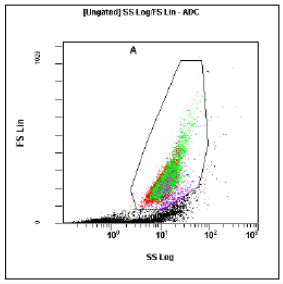

[Ungated] SS Log/FS Lin

Region	Number	%Total	%Gated	X-Mean	Y-Mean
ALL	97362	100.00	100.00	8.61	143
A	60370	62.01	62.01	12.2	224

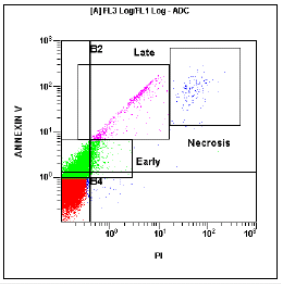

[A] FL3 Log/FL1 Log

Region	Number	%Total	%Gated	X-Mean	Y-Mean
ALL	60370	62.01	100.00	0.555	2.32
B3	47338	48.62	78.41	0.171	0.636
Early	18168	18.66	30.09	0.264	1.83
B1	9753	10.02	16.16	0.258	2.04
B2	3105	3.19	5.14	7.34	29
Late	1297	1.33	2.15	3.1	45.7
Necrosis	267	0.27	0.44	62.4	94.1
B4	174	0.18	0.29	0.687	0.904

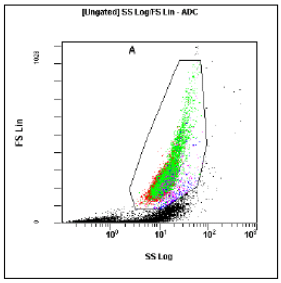

[Ungated] SS Log/FS Lin

Region	Number	%Total	%Gated	X-Mean	Y-Mean
ALL	80197	100.00	100.00	8.86	136
A	43593	54.36	54.36	13.3	238

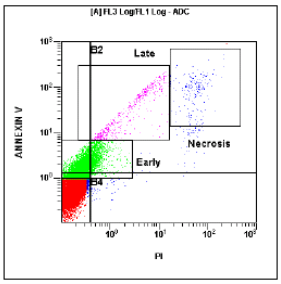

[A] FL3 Log/FL1 Log

Region	Number	%Total	%Gated	X-Mean	Y-Mean
ALL	43593	54.36	100.00	0.943	2.98
B3	32423	40.43	74.38	0.176	0.614
Early	13916	17.35	31.92	0.312	1.95
B1	6750	8.42	15.48	0.271	2.03
B2	3991	4.98	9.16	8.31	24
Late	1036	1.29	2.38	3.59	44
B4	429	0.53	0.98	0.84	0.924
Necrosis	343	0.43	0.79	63.8	113

*Compound **25** Samples (1 x IC_{50} Concentration)*

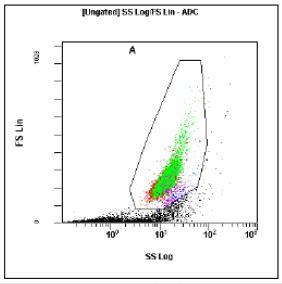

[Ungated] SS Log/FS Lin

Region	Number	%Total	%Gated	X-Mean	Y-Mean
ALL	60586	100.00	100.00	8.66	132
A	32349	53.39	53.39	13.9	237

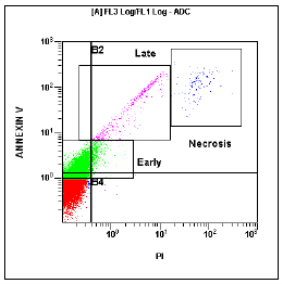

[A] FL3 Log/FL1 Log

Region	Number	%Total	%Gated	X-Mean	Y-Mean
ALL	32349	53.39	100.00	0.693	3.17
B3	22842	37.70	70.61	0.158	0.689
Early	12968	21.40	40.09	0.242	1.83
B1	7673	12.66	23.72	0.24	2.03
B2	1779	2.94	5.50	9.52	40
Late	752	1.24	2.32	3.71	56.7
Necrosis	190	0.31	0.59	67.9	132
B4	55	0.09	0.17	0.7	0.885

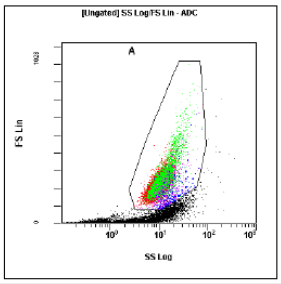

[Ungated] SS Log/FS Lin

Region	Number	%Total	%Gated	X-Mean	Y-Mean
ALL	84636	100.00	100.00	6.88	110
A	39607	46.80	46.80	11	221

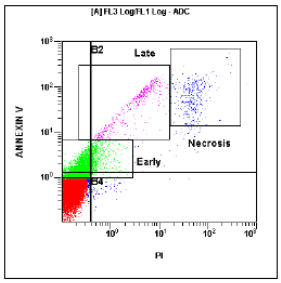

[A] FL3 Log/FL1 Log

Region	Number	%Total	%Gated	X-Mean	Y-Mean
ALL	39607	46.80	100.00	1.38	3.69
B3	31507	37.23	79.55	0.17	0.578
Early	9538	11.27	24.08	0.3	1.82
B1	4649	5.49	11.74	0.266	1.98
B2	3075	3.63	7.76	15.5	38.4
Late	998	1.18	2.52	4.47	57.4
Necrosis	726	0.86	1.83	54.8	77.6
B4	376	0.44	0.95	0.872	0.868

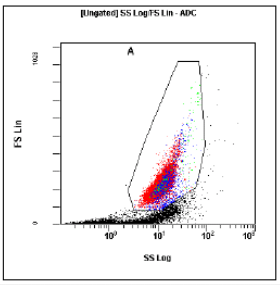

[Ungated] SS Log/FS Lin

Region	Number	%Total	%Gated	X-Mean	Y-Mean
ALL	94806	100.00	100.00	8.17	139
A	58391	61.59	61.59	11.4	217

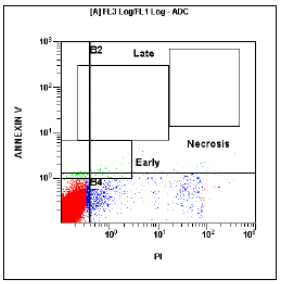

[A] FL3 Log/FL1 Log

Region	Number	%Total	%Gated	X-Mean	Y-Mean
ALL	58391	61.59	100.00	0.614	0.264
B3	56700	59.81	97.10	0.164	0.252
B4	1534	1.62	2.63	15.8	0.545
Early	323	0.34	0.55	0.702	1.28
B2	124	0.13	0.21	18.4	1.93
B1	33	0.03	0.06	0.284	1.41
Necrosis	0	0.00	0.00	0	0
Late	0	0.00	0.00	0	0

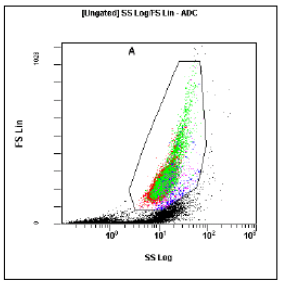

[Ungated] SS Log/FS Lin

Region	Number	%Total	%Gated	X-Mean	Y-Mean
ALL	83303	100.00	100.00	8.72	132
A	43663	52.41	52.41	13.3	239

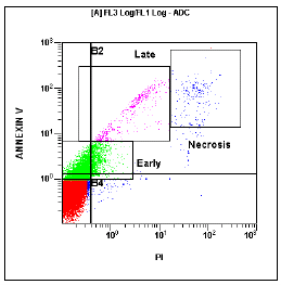

[A] FL3 Log/FL1 Log

Region	Number	%Total	%Gated	X-Mean	Y-Mean
ALL	43663	52.41	100.00	0.954	2.54
B3	33996	40.81	77.86	0.18	0.582
Early	11823	14.19	27.08	0.32	1.93
B1	5546	6.66	12.70	0.275	2.02
B2	3626	4.35	8.30	9.24	22
Late	916	1.10	2.10	3.66	43.1
B4	495	0.59	1.13	0.978	0.893
Necrosis	396	0.48	0.91	60.9	80.6

*Compound **46** Samples (1 x IC_{50} Concentration)*

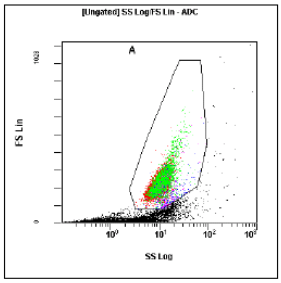

[Ungated] SS Log/FS Lin

Region	Number	%Total	%Gated	X-Mean	Y-Mean
ALL	73428	100.00	100.00	6.54	113
A	36123	49.20	49.20	10.4	217

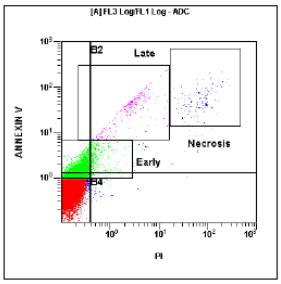

[A] FL3 Log/FL1 Log

Region	Number	%Total	%Gated	X-Mean	Y-Mean
ALL	36123	49.20	100.00	0.816	1.77
B3	30414	41.42	84.20	0.164	0.585
Early	8213	11.19	22.74	0.271	1.69
B1	4033	5.49	11.16	0.256	1.92
B2	1517	2.07	4.20	15.3	25.2
Late	534	0.73	1.48	3.24	38.5
Necrosis	261	0.36	0.72	72.3	58.1
B4	159	0.22	0.44	1.19	0.904

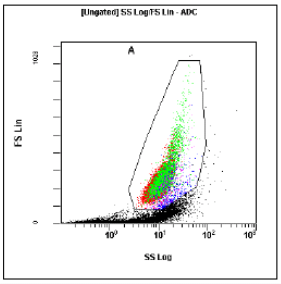

[Ungated] SS Log/FS Lin

Region	Number	%Total	%Gated	X-Mean	Y-Mean
ALL	95744	100.00	100.00	6.76	113
A	44862	46.86	46.86	10.9	227

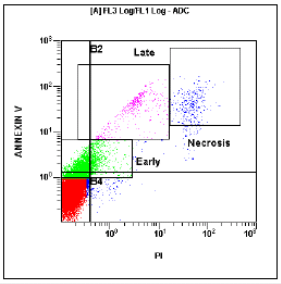

[A] FL3 Log/FL1 Log

Region	Number	%Total	%Gated	X-Mean	Y-Mean
ALL	44862	46.86	100.00	1.13	2.09
B3	38070	39.76	84.86	0.17	0.522
Early	7951	8.30	17.72	0.323	1.75
B1	3437	3.59	7.66	0.271	1.93
B2	2811	2.94	6.27	15.2	23.7
Late	807	0.84	1.80	4.08	38.9
Necrosis	631	0.66	1.41	52.4	48.6
B4	544	0.57	1.21	0.794	0.85

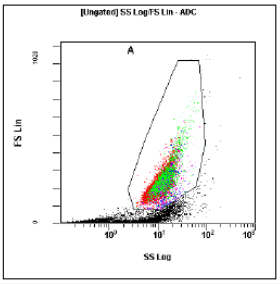

[Ungated] SS Log/FS Lin

Region	Number	%Total	%Gated	X-Mean	Y-Mean
ALL	95706	100.00	100.00	8.21	139
A	59054	61.70	61.70	11.5	217

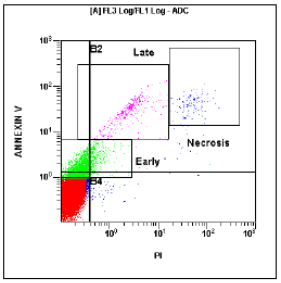

[A] FL3 Log/FL1 Log

Region	Number	%Total	%Gated	X-Mean	Y-Mean
ALL	59054	61.70	100.00	0.561	1.27
B3	53427	55.82	90.47	0.172	0.49
Early	7418	7.75	12.56	0.291	1.71
B1	3349	3.50	5.67	0.267	1.93
B2	1970	2.06	3.34	11.6	21.4
Late	776	0.81	1.31	3.06	31.8
Necrosis	312	0.33	0.53	56	46.9
B4	308	0.32	0.52	0.969	0.822

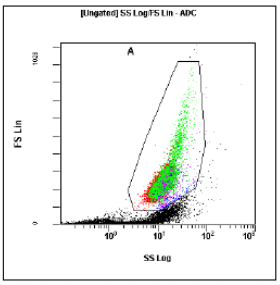

[Ungated] SS Log/FS Lin

Region	Number	%Total	%Gated	X-Mean	Y-Mean
ALL	76302	100.00	100.00	8.65	131
A	40229	52.72	52.72	13.1	236

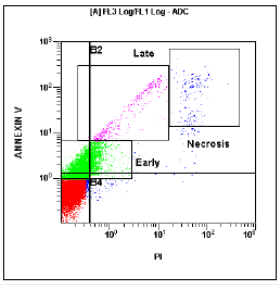

[A] FL3 Log/FL1 Log

Region	Number	%Total	%Gated	X-Mean	Y-Mean
ALL	40229	52.72	100.00	0.922	2.88
B3	29395	38.52	73.07	0.18	0.632
Early	13438	17.61	33.40	0.315	1.96
B1	6576	8.62	16.35	0.272	2.03
B2	3792	4.97	9.43	7.8	22
Late	926	1.21	2.30	3.66	44.9
B4	466	0.61	1.16	0.94	0.913
Necrosis	350	0.46	0.87	57	95.6

Control Samples (2 x IC_{50} Concentration)

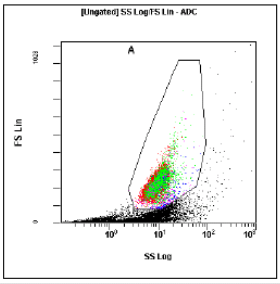

[Ungated] SS Log/FS Lin

Region	Number	%Total	%Gated	X-Mean	Y-Mean
ALL	81475	100.00	100.00	6.52	108
A	39107	48.00	48.00	9.04	210

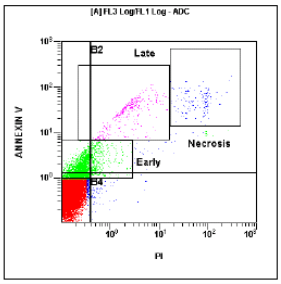

[A] FL3 Log/FL1 Log

Region	Number	%Total	%Gated	X-Mean	Y-Mean
ALL	39107	48.00	100.00	0.909	1.69
B3	33995	41.72	86.93	0.165	0.489
Early	6195	7.60	15.84	0.302	1.77
B1	2865	3.52	7.33	0.261	1.99
B2	1836	2.25	4.69	15.8	23.6
Late	702	0.86	1.80	3.39	34.5
B4	411	0.50	1.05	0.642	0.825
Necrosis	295	0.36	0.75	76.4	55.4

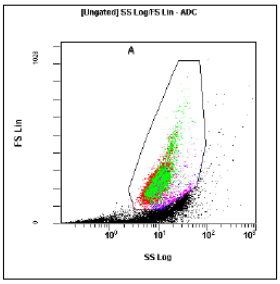

[Ungated] SS Log/FS Lin

Region	Number	%Total	%Gated	X-Mean	Y-Mean
ALL	94976	100.00	100.00	6.7	105
A	40873	43.04	43.04	9.77	219

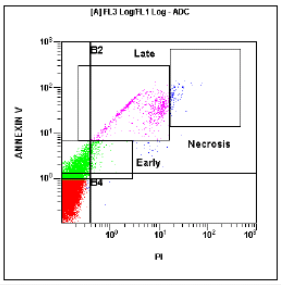

[A] FL3 Log/FL1 Log

Region	Number	%Total	%Gated	X-Mean	Y-Mean
ALL	40873	43.04	100.00	0.5	2.41
B3	34026	35.83	83.25	0.141	0.526
Early	8265	8.70	20.22	0.224	1.8
B1	4690	4.94	11.47	0.231	2.08
B2	2142	2.26	5.24	6.79	33.1
Late	1544	1.63	3.78	6.3	36
Necrosis	195	0.21	0.48	22.5	70.7
B4	15	0.02	0.04	1.52	0.917

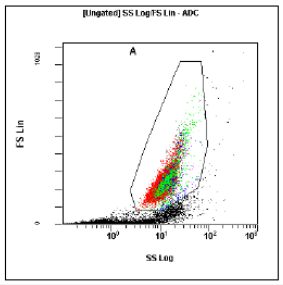

[Ungated] SS Log/FS Lin

Region	Number	%Total	%Gated	X-Mean	Y-Mean
ALL	100000	100.00	100.00	8.52	146
A	62550	62.55	62.55	11.9	226

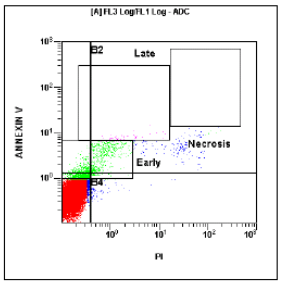

[A] FL3 Log/FL1 Log

Region	Number	%Total	%Gated	X-Mean	Y-Mean
ALL	62550	62.55	100.00	0.471	0.542
B3	60167	60.17	96.19	0.173	0.436
Early	2967	2.97	4.74	0.452	1.98
B2	1389	1.39	2.22	13.4	4.56
B1	589	0.59	0.94	0.277	1.68
B4	405	0.41	0.65	0.754	0.882
Late	103	0.10	0.16	3.22	8.29
Necrosis	3	0.00	0.00	116	17.9

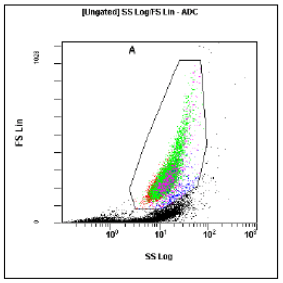

[Ungated] SS Log/FS Lin

Region	Number	%Total	%Gated	X-Mean	Y-Mean
ALL	82079	100.00	100.00	8.53	123
A	39614	48.26	48.26	13.8	239

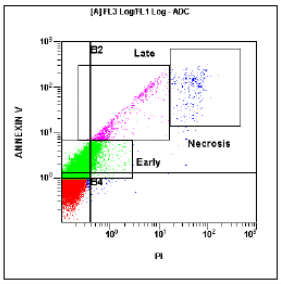

[A] FL3 Log/FL1 Log

Region	Number	%Total	%Gated	X-Mean	Y-Mean
ALL	39614	48.26	100.00	1.06	4.37
Early	21580	26.29	54.48	0.295	2.15
B3	21422	26.10	54.08	0.178	0.763
B1	12542	15.28	31.66	0.264	2.16
B2	5440	6.63	13.73	6.38	23.8
Late	1610	1.96	4.06	2.69	34.7
Necrosis	520	0.63	1.31	52.1	117
B4	210	0.26	0.53	0.718	0.952

*Compound **37** (Ref) Samples (2 x IC_{50} Concentration)*

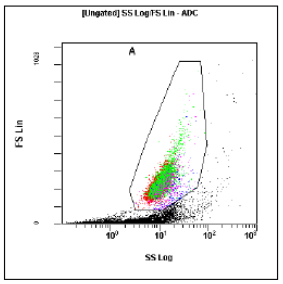

[Ungated] SS Log/FS Lin

Region	Number	%Total	%Gated	X-Mean	Y-Mean
ALL	67216	100.00	100.00	7.32	118
A	33340	49.60	49.60	10.9	225

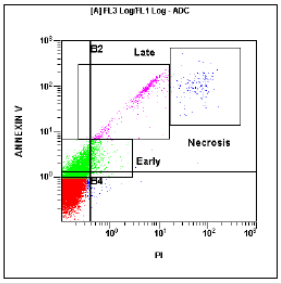

[A] FL3 Log/FL1 Log

Region	Number	%Total	%Gated	X-Mean	Y-Mean
ALL	33340	49.60	100.00	0.96	4.29
B3	25748	38.31	77.23	0.161	0.62
Early	9684	14.41	29.05	0.26	1.81
B1	5192	7.72	15.57	0.249	2.04
B2	2207	3.28	6.62	12	52.6
Late	1081	1.61	3.24	4.74	71
Necrosis	305	0.45	0.91	67.3	121
B4	193	0.29	0.58	0.649	0.859

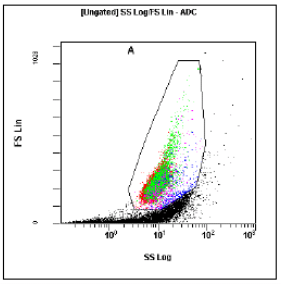

[Ungated] SS Log/FS Lin

Region	Number	%Total	%Gated	X-Mean	Y-Mean
ALL	80350	100.00	100.00	7.11	110
A	36604	45.56	45.56	9.66	219

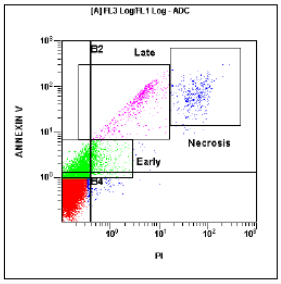

[A] FL3 Log/FL1 Log

Region	Number	%Total	%Gated	X-Mean	Y-Mean
ALL	36604	45.56	100.00	1.68	4.28
B3	28671	35.68	78.33	0.165	0.557
Early	8632	10.74	23.58	0.314	1.84
B1	4071	5.07	11.12	0.26	2.02
B2	3361	4.18	9.18	16.5	39.2
Late	1238	1.54	3.38	4.39	53.1
Necrosis	791	0.98	2.16	60.8	78.2
B4	501	0.62	1.37	0.696	0.885

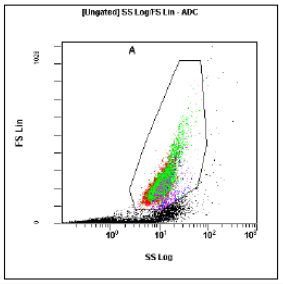

[Ungated] SS Log/FS Lin

Region	Number	%Total	%Gated	X-Mean	Y-Mean
ALL	91635	100.00	100.00	8.05	143
A	59398	64.82	64.82	10.8	214

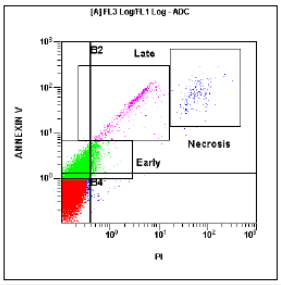

[A] FL3 Log/FL1 Log

Region	Number	%Total	%Gated	X-Mean	Y-Mean
ALL	59398	64.82	100.00	0.646	2.17
B3	48858	53.32	82.26	0.168	0.584
Early	14517	15.84	24.44	0.264	1.78
B1	7659	8.36	12.89	0.259	1.99
B2	2708	2.96	4.56	10.4	31.3
Late	1130	1.23	1.90	3.33	45.6
Necrosis	348	0.38	0.59	66.1	83.5
B4	173	0.19	0.29	0.648	0.906

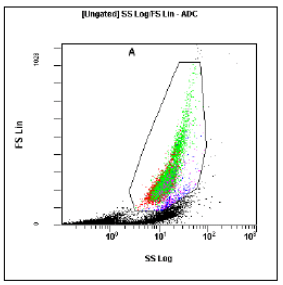

[Ungated] SS Log/FS Lin

Region	Number	%Total	%Gated	X-Mean	Y-Mean
ALL	67540	100.00	100.00	8.2	125
A	32780	48.53	48.53	13.5	238

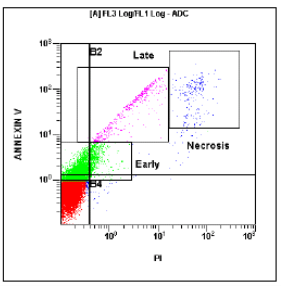

[A] FL3 Log/FL1 Log

Region	Number	%Total	%Gated	X-Mean	Y-Mean
ALL	32780	48.53	100.00	1.21	3.8
B3	24897	36.86	75.95	0.168	0.621
Early	9846	14.58	30.04	0.284	1.85
B1	5028	7.44	15.34	0.262	2
B2	2720	4.03	8.30	12.5	36.3
Late	932	1.38	2.84	3.87	52
Necrosis	465	0.69	1.42	59	98.6
B4	135	0.20	0.41	0.959	0.93

*Compound **25** Samples (2 x IC_{50} Concentration)*

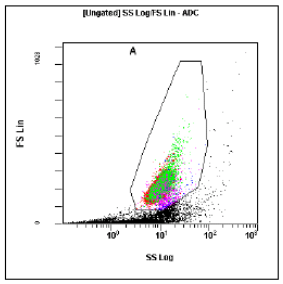

[Ungated] SS Log/FS Lin

Region	Number	%Total	%Gated	X-Mean	Y-Mean
ALL	65275	100.00	100.00	7.23	108
A	32196	49.32	49.32	10.3	205

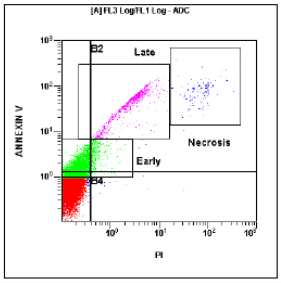

[A] FL3 Log/FL1 Log

Region	Number	%Total	%Gated	X-Mean	Y-Mean
ALL	32196	49.32	100.00	1.04	4.34
B3	24017	36.79	74.60	0.161	0.603
Early	9361	14.34	29.08	0.263	1.86
B1	5095	7.81	15.82	0.25	2.05
B2	2949	4.52	9.16	9.58	38.9
Late	1781	2.73	5.53	3.23	49
Necrosis	296	0.45	0.92	73	82.1
B4	135	0.21	0.42	0.943	0.959

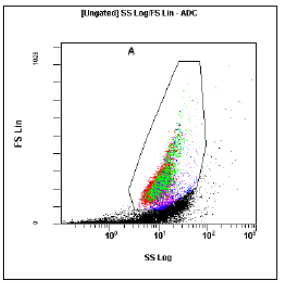

[Ungated] SS Log/FS Lin

Region	Number	%Total	%Gated	X-Mean	Y-Mean
ALL	87647	100.00	100.00	7.37	106
A	39400	44.95	44.95	10.5	213

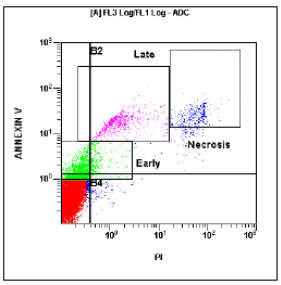

[A] FL3 Log/FL1 Log

Region	Number	%Total	%Gated	X-Mean	Y-Mean
ALL	39400	44.95	100.00	1.56	1.8
B3	33589	38.32	85.25	0.165	0.486
Early	5444	6.21	13.82	0.31	1.68
B2	2995	3.42	7.60	18.3	16.6
B1	2295	2.62	5.82	0.264	1.96
Late	1422	1.62	3.61	2.21	19.3
Necrosis	690	0.79	1.75	61.9	27
B4	521	0.59	1.32	0.755	0.802

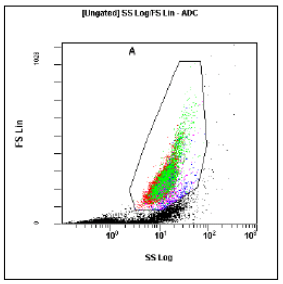

[Ungated] SS Log/FS Lin

Region	Number	%Total	%Gated	X-Mean	Y-Mean
ALL	98114	100.00	100.00	8.41	142
A	59676	60.82	60.82	11.8	224

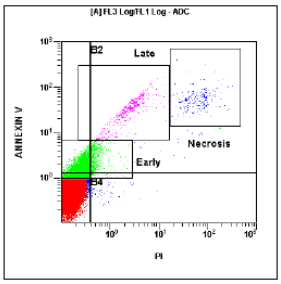

[A] FL3 Log/FL1 Log

Region	Number	%Total	%Gated	X-Mean	Y-Mean
ALL	59676	60.82	100.00	0.74	1.81
B3	51160	52.14	85.73	0.173	0.532
Early	11029	11.24	18.48	0.285	1.76
B1	5310	5.41	8.90	0.266	1.97
B2	2813	2.87	4.71	11.9	24.9
Late	1152	1.17	1.93	3.09	35.7
Necrosis	410	0.42	0.69	67.9	60.5
B4	393	0.40	0.66	0.686	0.844

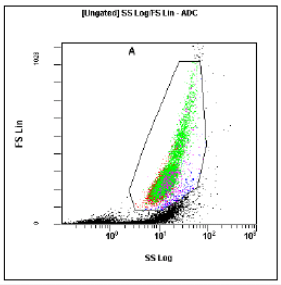

[Ungated] SS Log/FS Lin

Region	Number	%Total	%Gated	X-Mean	Y-Mean
ALL	72131	100.00	100.00	8.78	128
A	34789	48.23	48.23	14.3	248

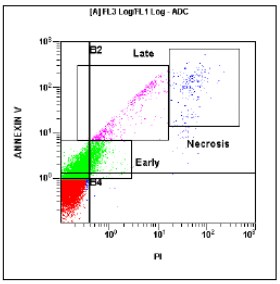

[A] FL3 Log/FL1 Log

Region	Number	%Total	%Gated	X-Mean	Y-Mean
ALL	34789	48.23	100.00	0.973	3.86
B3	23247	32.23	66.82	0.172	0.662
Early	14026	19.45	40.32	0.301	2.05
B1	7436	10.31	21.37	0.266	2.07
B2	3948	5.47	11.35	7.03	26.2
Late	1093	1.52	3.14	3.19	41.6
Necrosis	393	0.54	1.13	52.1	124
B4	158	0.22	0.45	0.77	0.984

*Compound **46** Samples (2 x IC_{50} Concentration)*

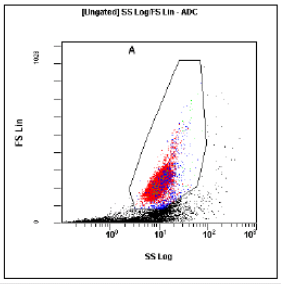

[Ungated] SS Log/FS Lin

Region	Number	%Total	%Gated	X-Mean	Y-Mean
ALL	74150	100.00	100.00	6.31	108
A	34628	46.70	46.70	9.96	217

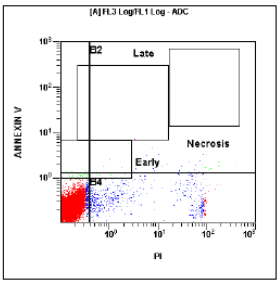

[A] FL3 Log/FL1 Log

Region	Number	%Total	%Gated	X-Mean	Y-Mean
ALL	34628	46.70	100.00	1.25	0.259
B3	33218	44.80	95.93	0.158	0.246
B4	1301	1.75	3.76	26.6	0.43
Early	147	0.20	0.42	0.583	1.33
B2	86	0.12	0.25	42.4	2.39
B1	23	0.03	0.07	0.233	1.38
Necrosis	0	0.00	0.00	0	0
Late	3	0.00	0.01	4.64	8.25

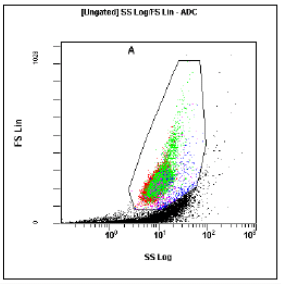

[Ungated] SS Log/FS Lin

Region	Number	%Total	%Gated	X-Mean	Y-Mean
ALL	85166	100.00	100.00	7.33	115
A	40133	47.12	47.12	9.89	224

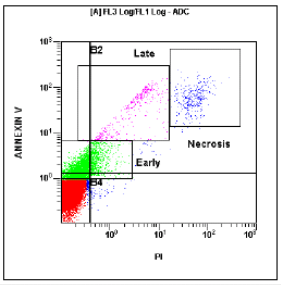

[A] FL3 Log/FL1 Log

Region	Number	%Total	%Gated	X-Mean	Y-Mean
ALL	40133	47.12	100.00	1.25	2.82
B3	31850	37.40	79.36	0.169	0.576
Early	10074	11.83	25.10	0.313	1.82
B1	4652	5.46	11.59	0.264	1.96
B2	3116	3.66	7.76	13.9	27.4
Late	784	0.92	1.95	3.94	43.2
Necrosis	666	0.78	1.66	57.9	68.4
B4	515	0.60	1.28	0.656	0.905

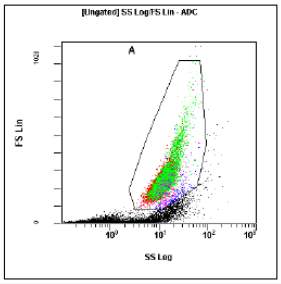

[Ungated] SS Log/FS Lin

Region	Number	%Total	%Gated	X-Mean	Y-Mean
ALL	89053	100.00	100.00	8.43	137
A	50614	56.84	56.84	12.6	232

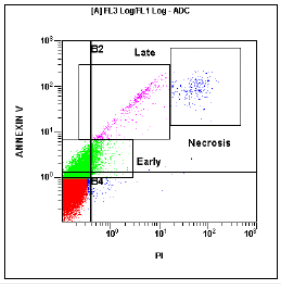

[A] FL3 Log/FL1 Log

Region	Number	%Total	%Gated	X-Mean	Y-Mean
ALL	50614	56.84	100.00	0.702	2.53
B3	39577	44.44	78.19	0.175	0.612
Early	14937	16.77	29.51	0.285	1.85
B1	7553	8.48	14.92	0.267	2.02
B2	3190	3.58	6.30	8.25	27.8
Late	984	1.10	1.94	3.54	46.5
Necrosis	362	0.41	0.72	59.6	101
B4	294	0.33	0.58	1	0.885

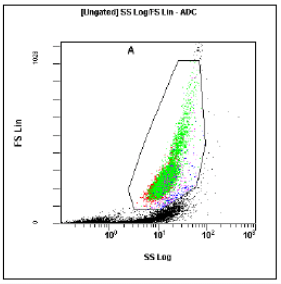

[Ungated] SS Log/FS Lin

Region	Number	%Total	%Gated	X-Mean	Y-Mean
ALL	72287	100.00	100.00	8.09	118
A	32518	44.98	44.98	14.2	245

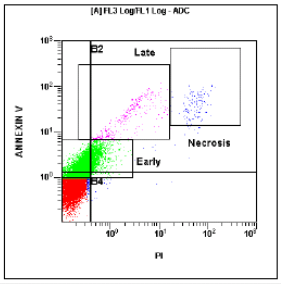

[A] FL3 Log/FL1 Log

Region	Number	%Total	%Gated	X-Mean	Y-Mean
ALL	32518	44.98	100.00	0.849	2.16
B3	20793	28.76	63.94	0.187	0.708
Early	15088	20.87	46.40	0.314	1.97
B1	7724	10.69	23.75	0.273	2.01
B2	3757	5.20	11.55	5.71	10.5
Late	651	0.90	2.00	3.06	26.4
Necrosis	306	0.42	0.94	53.9	42.9
B4	244	0.34	0.75	0.686	0.992

48 Hour Results

Contol Samples (1 x IC_{50} Concentration)

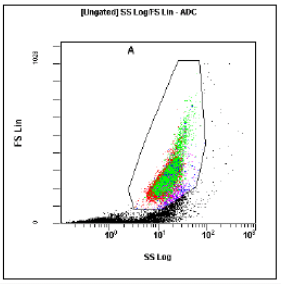

[Ungated] SS Log/FS Lin

Region	Number	%Total	%Gated	X-Mean	Y-Mean
ALL	100000	100.00	100.00	8.97	131
A	51649	51.65	51.65	15.1	244

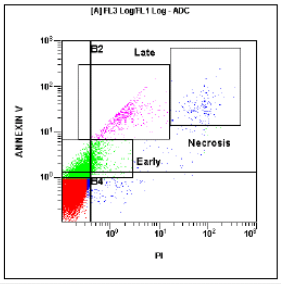

[A] FL3 Log/FL1 Log

Region	Number	%Total	%Gated	X-Mean	Y-Mean
ALL	51649	51.65	100.00	0.844	1.5
B3	44210	44.21	85.60	0.189	0.592
Early	10509	10.51	20.35	0.306	1.61
B1	4217	4.22	8.16	0.284	1.81
B2	2737	2.74	5.30	12.2	15.8
Late	1002	1.00	1.94	2.42	25.3
B4	485	0.48	0.94	1.17	0.841
Necrosis	327	0.33	0.63	77.9	41.3

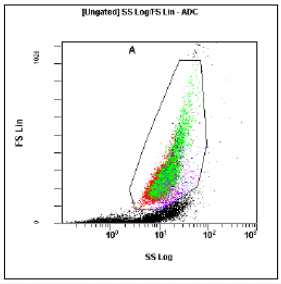

[Ungated] SS Log/FS Lin

Region	Number	%Total	%Gated	X-Mean	Y-Mean
ALL	100000	100.00	100.00	7.26	114
A	43485	43.48	43.48	12.9	244

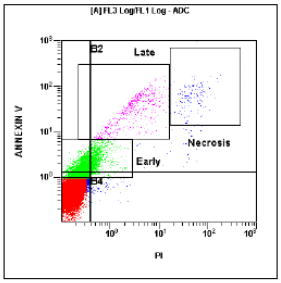

[A] FL3 Log/FL1 Log

Region	Number	%Total	%Gated	X-Mean	Y-Mean
ALL	43485	43.48	100.00	0.722	2.22
B3	35288	35.29	81.15	0.187	0.57
Early	10454	10.45	24.04	0.332	1.79
B1	4301	4.30	9.89	0.288	1.88
B2	3467	3.47	7.97	6.72	19.6
Late	1055	1.05	2.43	3.85	37.6
B4	429	0.43	0.99	0.625	0.913
Necrosis	313	0.31	0.72	52.1	67.3

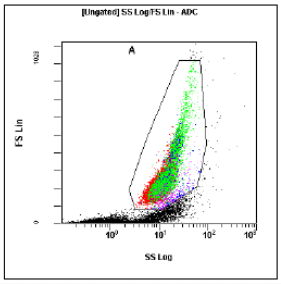

[Ungated] SS Log/FS Lin

Region	Number	%Total	%Gated	X-Mean	Y-Mean
ALL	100000	100.00	100.00	7.97	135
A	55256	55.26	55.26	12.1	234

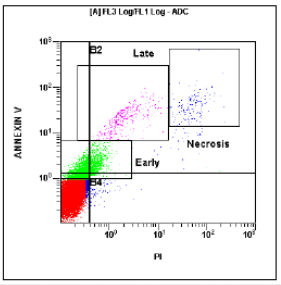

[A] FL3 Log/FL1 Log

Region	Number	%Total	%Gated	X-Mean	Y-Mean
ALL	55256	55.26	100.00	0.631	1.26
B3	48280	48.28	87.38	0.199	0.538
Early	9324	9.32	16.87	0.349	1.6
B2	3141	3.14	5.68	7.6	11.9
B1	3010	3.01	5.45	0.298	1.76
B4	825	0.82	1.49	0.549	0.951
Late	789	0.79	1.43	2.76	24.2
Necrosis	289	0.29	0.52	60	45.4

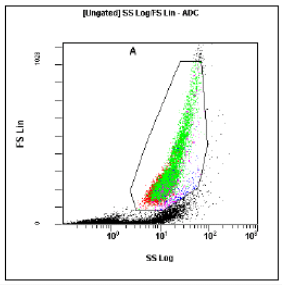

[Ungated] SS Log/FS Lin

Region	Number	%Total	%Gated	X-Mean	Y-Mean
ALL	82868	100.00	100.00	8.12	121
A	37395	45.13	45.13	14.3	248

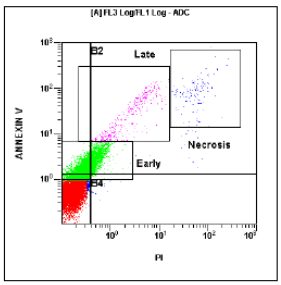

[A] FL3 Log/FL1 Log

Region	Number	%Total	%Gated	X-Mean	Y-Mean
ALL	37395	45.13	100.00	0.758	2.47
B3	26329	31.77	70.41	0.186	0.639
Early	14260	17.21	38.13	0.338	1.99
B1	6251	7.54	16.72	0.286	1.89
B2	4640	5.60	12.41	4.65	13.7
Late	738	0.89	1.97	3.24	35.4
Necrosis	251	0.30	0.67	62	95.2
B4	175	0.21	0.47	0.501	1.02

*Compound **37** (Ref) Samples (1 x IC_{50} Concentration)*

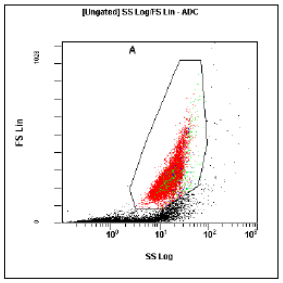

[Ungated] SS Log/FS Lin

Region	Number	%Total	%Gated	X-Mean	Y-Mean
ALL	100000	100.00	100.00	10	145
A	57902	57.90	57.90	15.3	242

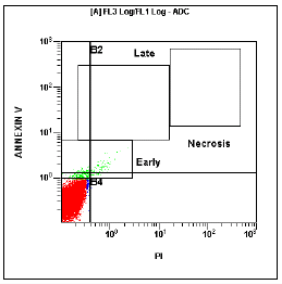

[A] FL3 Log/FL1 Log

Region	Number	%Total	%Gated	X-Mean	Y-Mean
ALL	57902	57.90	100.00	0.156	0.355
B3	57464	57.46	99.24	0.153	0.346
Early	683	0.68	1.18	0.433	1.38
B2	186	0.19	0.32	0.753	1.95
B4	155	0.16	0.27	0.466	1.01
B1	97	0.10	0.17	0.285	1.44
Necrosis	0	0.00	0.00	0	0
Late	0	0.00	0.00	0	0

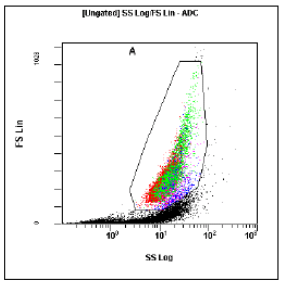

[Ungated] SS Log/FS Lin

Region	Number	%Total	%Gated	X-Mean	Y-Mean
ALL	100000	100.00	100.00	7.77	101
A	37371	37.37	37.37	15	246

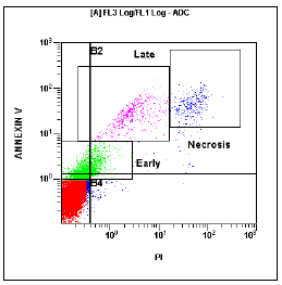

[A] FL3 Log/FL1 Log

Region	Number	%Total	%Gated	X-Mean	Y-Mean
ALL	37371	37.37	100.00	1.32	2.36
B3	31656	31.66	84.71	0.19	0.509
Early	5929	5.93	15.87	0.357	1.67
B2	3147	3.15	8.42	13.4	21.6
B1	1947	1.95	5.21	0.291	1.83
Late	1070	1.07	2.86	3.7	30.2
Necrosis	655	0.66	1.75	53.1	48.6
B4	621	0.62	1.66	0.821	0.927

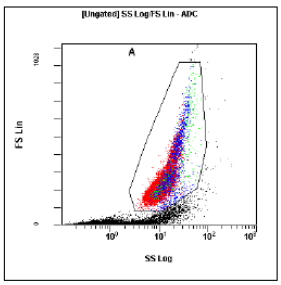

[Ungated] SS Log/FS Lin

Region	Number	%Total	%Gated	X-Mean	Y-Mean
ALL	100000	100.00	100.00	7.84	132
A	53629	53.63	53.63	12.3	234

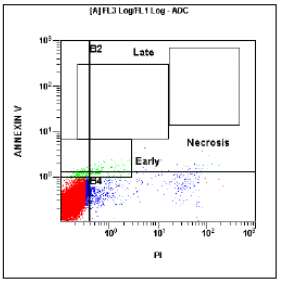

[A] FL3 Log/FL1 Log

Region	Number	%Total	%Gated	X-Mean	Y-Mean
ALL	53629	53.63	100.00	0.498	0.349
B3	51305	51.31	95.67	0.189	0.326
B4	2001	2.00	3.73	6.41	0.715
Early	844	0.84	1.57	0.532	1.23
B2	254	0.25	0.47	16.4	1.83
B1	69	0.07	0.13	0.29	1.41
Necrosis	0	0.00	0.00	0	0
Late	1	0.00	0.00	4.48	7.41

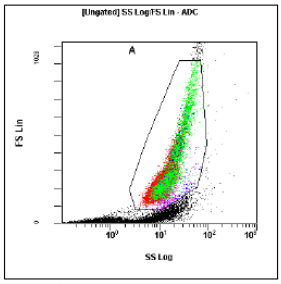

[Ungated] SS Log/FS Lin

Region	Number	%Total	%Gated	X-Mean	Y-Mean
ALL	100000	100.00	100.00	8.61	131
A	47261	47.26	47.26	14.2	252

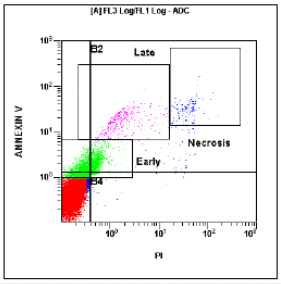

[A] FL3 Log/FL1 Log

Region	Number	%Total	%Gated	X-Mean	Y-Mean
ALL	47261	47.26	100.00	0.544	1.15
B3	40673	40.67	86.06	0.18	0.491
Early	8403	8.40	17.78	0.355	1.67
B2	3332	3.33	7.05	5.13	8.72
B1	2762	2.76	5.84	0.294	1.78
Late	772	0.77	1.63	2.66	19.5
B4	494	0.49	1.05	0.99	1.03
Necrosis	251	0.25	0.53	43.5	32.9

*Compound **25** Samples (1 x IC_{50} Concentration)*

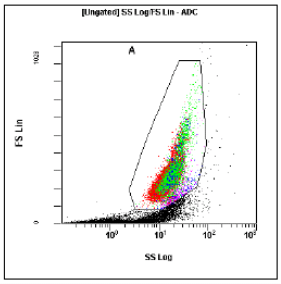

[Ungated] SS Log/FS Lin

Region	Number	%Total	%Gated	X-Mean	Y-Mean
ALL	100000	100.00	100.00	10	144
A	55678	55.68	55.68	15.5	248

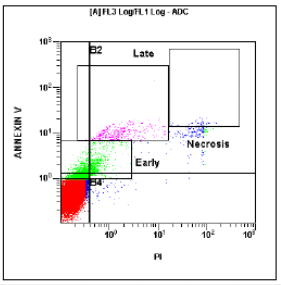

[A] FL3 Log/FL1 Log

Region	Number	%Total	%Gated	X-Mean	Y-Mean
ALL	55678	55.68	100.00	0.868	0.816
B3	51219	51.22	91.99	0.189	0.509
Early	5542	5.54	9.95	0.364	1.56
B2	2425	2.42	4.36	15.5	6.75
B1	1433	1.43	2.57	0.3	1.72
Late	776	0.78	1.39	2.15	10.5
B4	601	0.60	1.08	0.82	0.958
Necrosis	95	0.10	0.17	80.4	16

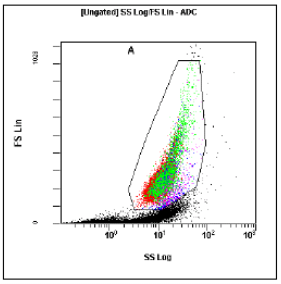

[Ungated] SS Log/FS Lin

Region	Number	%Total	%Gated	X-Mean	Y-Mean
ALL	100000	100.00	100.00	7.35	118
A	45474	45.47	45.47	12.5	242

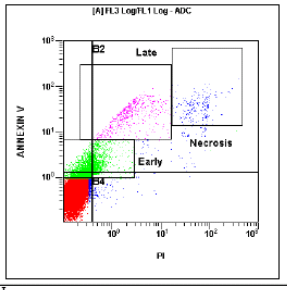

[A] FL3 Log/FL1 Log

Region	Number	%Total	%Gated	X-Mean	Y-Mean
ALL	45474	45.47	100.00	0.993	1.68
B3	38867	38.87	85.47	0.187	0.51
Early	7512	7.51	16.52	0.361	1.75
B2	3275	3.27	7.20	11.1	15.5
B1	2618	2.62	5.76	0.289	1.9
Late	1074	1.07	2.36	3.28	26.9
B4	714	0.71	1.57	0.876	0.899
Necrosis	397	0.40	0.87	65.4	41.5

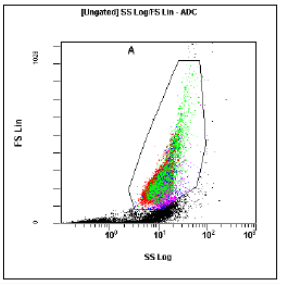

[Ungated] SS Log/FS Lin

Region	Number	%Total	%Gated	X-Mean	Y-Mean
ALL	100000	100.00	100.00	8.06	141
A	60849	60.85	60.85	11.1	222

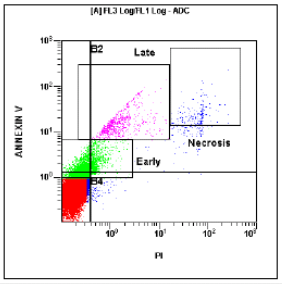

[A] FL3 Log/FL1 Log

Region	Number	%Total	%Gated	X-Mean	Y-Mean
ALL	60849	60.85	100.00	0.819	1.33
B3	52806	52.81	86.78	0.194	0.538
Early	9534	9.53	15.67	0.333	1.68
B2	3868	3.87	6.36	9.84	11.8
B1	3515	3.52	5.78	0.287	1.86
Late	1610	1.61	2.65	2.06	17.9
B4	660	0.66	1.08	0.786	0.912
Necrosis	374	0.37	0.61	66.2	28.1

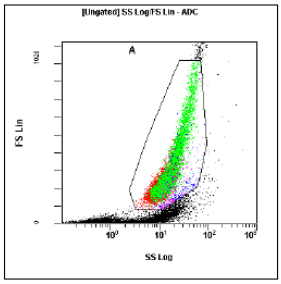

[Ungated] SS Log/FS Lin

Region	Number	%Total	%Gated	X-Mean	Y-Mean
ALL	100000	100.00	100.00	9.02	130
A	45169	45.17	45.17	15	257

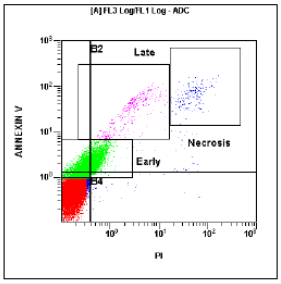

[A] FL3 Log/FL1 Log

Region	Number	%Total	%Gated	X-Mean	Y-Mean
ALL	45169	45.17	100.00	0.801	2.12
B3	34012	34.01	75.30	0.19	0.576
Early	13913	13.91	30.80	0.369	1.92
B2	5531	5.53	12.25	5.02	12
B1	5171	5.17	11.45	0.292	1.85
Late	772	0.77	1.71	3.49	35.6
B4	455	0.46	1.01	0.976	1.01
Necrosis	370	0.37	0.82	53.6	71

*Compound **46** Samples (1 x IC_{50} Concentration)*

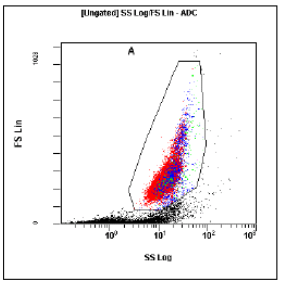

[Ungated] SS Log/FS Lin

Region	Number	%Total	%Gated	X-Mean	Y-Mean
ALL	100000	100.00	100.00	9.01	145
A	56989	56.99	56.99	14	247

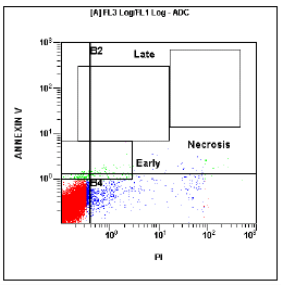

[A] FL3 Log/FL1 Log

Region	Number	%Total	%Gated	X-Mean	Y-Mean
ALL	56989	56.99	100.00	0.449	0.32
B3	55317	55.32	97.07	0.18	0.305
B4	1437	1.44	2.52	7.95	0.611
Early	471	0.47	0.83	0.582	1.25
B2	173	0.17	0.30	24.3	2.17
B1	62	0.06	0.11	0.296	1.39
Necrosis	0	0.00	0.00	0	0
Late	3	0.00	0.01	4.87	13.3

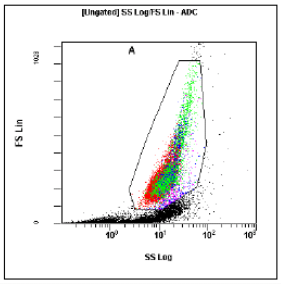

[Ungated] SS Log/FS Lin

Region	Number	%Total	%Gated	X-Mean	Y-Mean
ALL	100000	100.00	100.00	7.63	116
A	42752	42.75	42.75	13.6	251

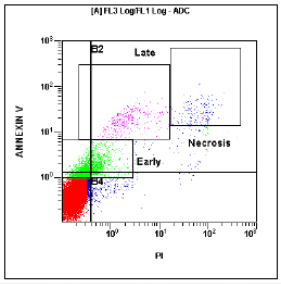

[A] FL3 Log/FL1 Log

Region	Number	%Total	%Gated	X-Mean	Y-Mean
ALL	42752	42.75	100.00	1.05	1.17
B3	37109	37.11	86.80	0.194	0.461
Early	5499	5.50	12.86	0.416	1.65
B2	2767	2.77	6.47	13	10.4
B1	1486	1.49	3.48	0.296	1.81
B4	1390	1.39	3.25	1.08	0.877
Late	731	0.73	1.71	3.28	19.3
Necrosis	325	0.33	0.76	71	30.8

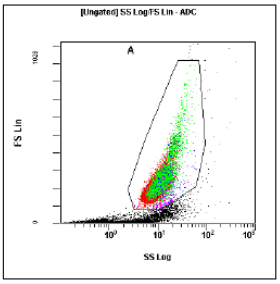

[Ungated] SS Log/FS Lin

Region	Number	%Total	%Gated	X-Mean	Y-Mean
ALL	100000	100.00	100.00	7.84	145
A	62392	62.39	62.39	10.9	226

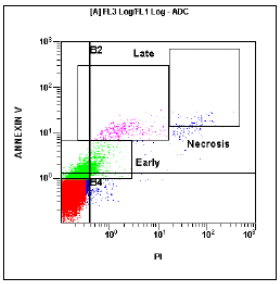

[A] FL3 Log/FL1 Log

Region	Number	%Total	%Gated	X-Mean	Y-Mean
ALL	62392	62.39	100.00	0.504	0.847
B3	56603	56.60	90.72	0.194	0.569
Early	9034	9.03	14.48	0.326	1.47
B1	2674	2.67	4.29	0.288	1.64
B2	2407	2.41	3.86	8.01	6.49
B4	708	0.71	1.13	0.613	0.874
Late	688	0.69	1.10	2.73	11.8
Necrosis	131	0.13	0.21	72	19.1

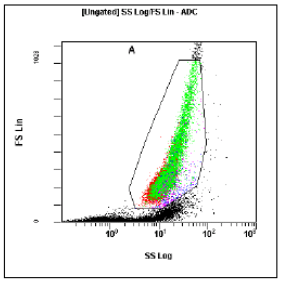

[Ungated] SS Log/FS Lin

Region	Number	%Total	%Gated	X-Mean	Y-Mean
ALL	100000	100.00	100.00	8.62	129
A	44560	44.56	44.56	14.9	261

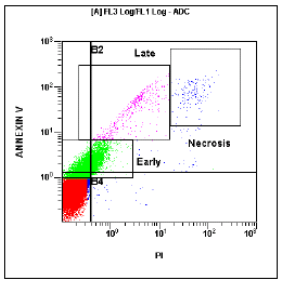

[A] FL3 Log/FL1 Log

Region	Number	%Total	%Gated	X-Mean	Y-Mean
ALL	44560	44.56	100.00	0.74	2.25
B3	32776	32.78	73.55	0.192	0.588
Early	14691	14.69	32.97	0.366	1.95
B2	5693	5.69	12.78	4.34	12.3
B1	5620	5.62	12.61	0.292	1.87
Late	851	0.85	1.91	3.55	37.4
B4	471	0.47	1.06	0.714	0.994
Necrosis	309	0.31	0.69	54.6	80.6

Control Samples (2 x IC_{50} Concentration)

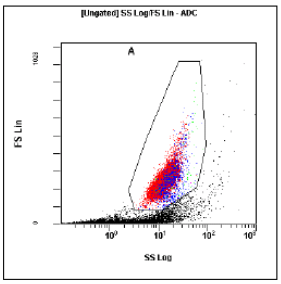

[Ungated] SS Log/FS Lin

Region	Number	%Total	%Gated	X-Mean	Y-Mean
ALL	66369	100.00	100.00	9.09	130
A	34313	51.70	51.70	13.6	239

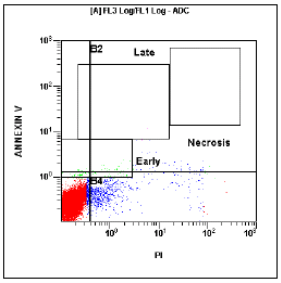

[A] FL3 Log/FL1 Log

Region	Number	%Total	%Gated	X-Mean	Y-Mean
ALL	34313	51.70	100.00	0.529	0.309
B3	32719	49.30	95.35	0.17	0.289
B4	1421	2.14	4.14	6.74	0.549
Early	192	0.29	0.56	0.931	1.29
B2	154	0.23	0.45	19.4	2.35
B1	19	0.03	0.06	0.27	1.37
Late	5	0.01	0.01	5.85	10.2
Necrosis	0	0.00	0.00	0	0

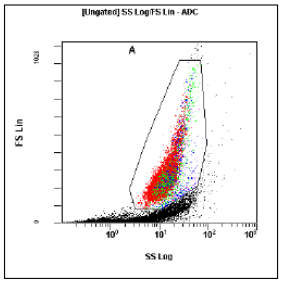

[Ungated] SS Log/FS Lin

Region	Number	%Total	%Gated	X-Mean	Y-Mean
ALL	100000	100.00	100.00	8.64	133
A	50090	50.09	50.09	13	246

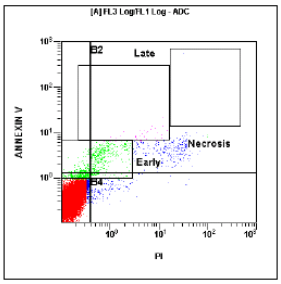

[A] FL3 Log/FL1 Log

Region	Number	%Total	%Gated	X-Mean	Y-Mean
ALL	50090	50.09	100.00	0.434	0.488
B3	47852	47.85	95.53	0.163	0.36
Early	1885	1.89	3.76	0.558	2.18
B2	1391	1.39	2.78	9.55	4.49
B4	536	0.54	1.07	1.05	0.817
B1	311	0.31	0.62	0.287	1.75
Late	64	0.06	0.13	5.24	8.64
Necrosis	1	0.00	0.00	32.7	581

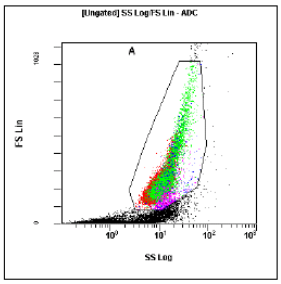

[Ungated] SS Log/FS Lin

Region	Number	%Total	%Gated	X-Mean	Y-Mean
ALL	100000	100.00	100.00	8.04	136
A	55256	55.26	55.26	11.9	232

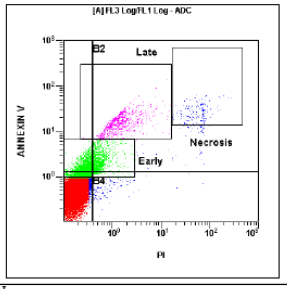

[A] FL3 Log/FL1 Log

Region	Number	%Total	%Gated	X-Mean	Y-Mean
ALL	55256	55.26	100.00	0.831	1.41
B3	46338	46.34	83.86	0.194	0.542
Early	10333	10.33	18.70	0.36	1.71
B2	4527	4.53	8.19	7.78	10.1
B1	3451	3.45	6.25	0.291	1.87
Late	1579	1.58	2.86	1.9	17.5
B4	940	0.94	1.70	0.748	0.936
Necrosis	353	0.35	0.64	66	30.3

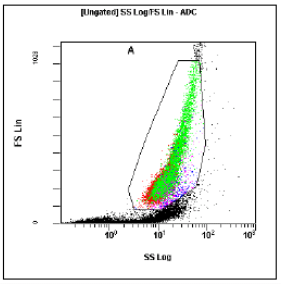

[Ungated] SS Log/FS Lin

Region	Number	%Total	%Gated	X-Mean	Y-Mean
ALL	100000	100.00	100.00	9.36	129
A	44692	44.69	44.69	15.6	256

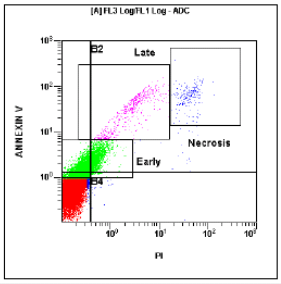

[A] FL3 Log/FL1 Log

Region	Number	%Total	%Gated	X-Mean	Y-Mean
ALL	44692	44.69	100.00	0.753	2.4
B3	33023	33.02	73.89	0.184	0.586
Early	14506	14.51	32.46	0.353	1.94
B1	5852	5.85	13.09	0.291	1.88
B2	5492	5.49	12.29	4.67	13.9
Late	999	1.00	2.24	3.39	36.7
Necrosis	400	0.40	0.90	46.5	69.1
B4	325	0.33	0.73	0.687	1.02

*Compound **37** (Ref) Samples (2 x IC_{50} Concentration)*

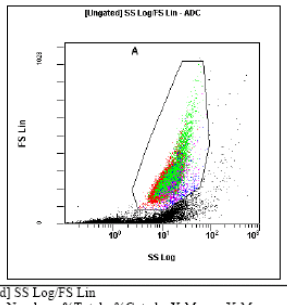

[Ungated] SS Log/FS Lin

Region	Number	%Total	%Gated	X-Mean	Y-Mean
ALL	100000	100.00	100.00	9.58	134
A	52773	52.77	52.77	14.2	241

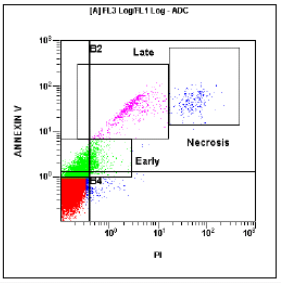

[A] FL3 Log/FL1 Log

Region	Number	%Total	%Gated	X-Mean	Y-Mean
ALL	52773	52.77	100.00	0.804	1.99
B3	44604	44.60	84.52	0.178	0.568
Early	10372	10.37	19.65	0.3	1.64
B1	4441	4.44	8.42	0.273	1.86
B2	3099	3.10	5.87	10.6	22.9
Late	1305	1.30	2.47	3.38	33.6
B4	629	0.63	1.19	0.749	0.856
Necrosis	453	0.45	0.86	59.4	51.4

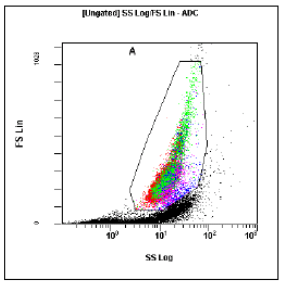

[Ungated] SS Log/FS Lin

Region	Number	%Total	%Gated	X-Mean	Y-Mean
ALL	100000	100.00	100.00	9.73	131
A	48716	48.72	48.72	14.2	247

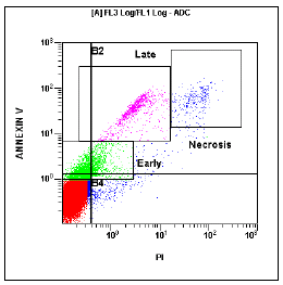

[A] FL3 Log/FL1 Log

Region	Number	%Total	%Gated	X-Mean	Y-Mean
ALL	48716	48.72	100.00	1.13	2.87
B3	40633	40.63	83.41	0.186	0.484
Early	7015	7.01	14.40	0.376	1.7
B2	4305	4.30	8.84	10.6	26.7
B1	2429	2.43	4.99	0.286	1.83
Late	1996	2.00	4.10	3.93	38.3
B4	1349	1.35	2.77	0.865	0.832
Necrosis	549	0.55	1.13	59.6	60.8

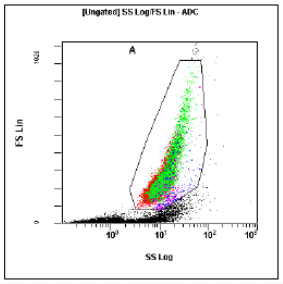

[Ungated] SS Log/FS Lin

Region	Number	%Total	%Gated	X-Mean	Y-Mean
ALL	100000	100.00	100.00	7.55	136
A	57201	57.20	57.20	11.2	229

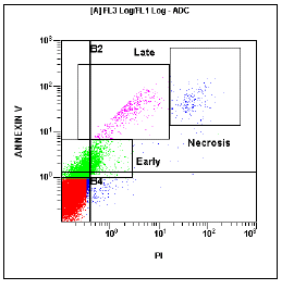

[A] FL3 Log/FL1 Log

Region	Number	%Total	%Gated	X-Mean	Y-Mean
ALL	57201	57.20	100.00	0.603	1.52
B3	48807	48.81	85.33	0.186	0.528
Early	10935	10.94	19.12	0.334	1.7
B1	4252	4.25	7.43	0.287	1.84
B2	3459	3.46	6.05	6.86	15.3
Late	956	0.96	1.67	3.09	31.5
B4	683	0.68	1.19	0.732	0.879
Necrosis	313	0.31	0.55	55.8	53.6

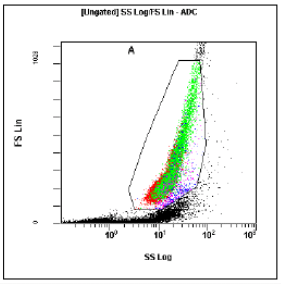

[Ungated] SS Log/FS Lin

Region	Number	%Total	%Gated	X-Mean	Y-Mean
ALL	100000	100.00	100.00	8.49	109
A	35311	35.31	35.31	17	267

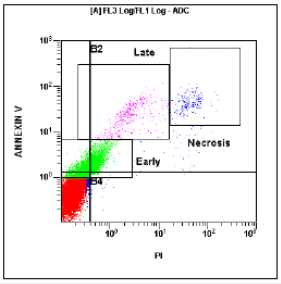

[A] FL3 Log/FL1 Log

Region	Number	%Total	%Gated	X-Mean	Y-Mean
ALL	35311	35.31	100.00	1.03	2.19
B3	26583	26.58	75.28	0.192	0.547
Early	10143	10.14	28.72	0.399	1.88
B2	5139	5.14	14.55	5.83	11.1
B1	3050	3.05	8.64	0.303	1.78
Late	835	0.83	2.36	3.56	27.2
B4	539	0.54	1.53	0.653	1.04
Necrosis	480	0.48	1.36	46.6	48.6

*Compound **25** Samples (2 x IC_{50} Concentration)*

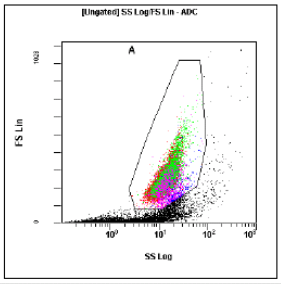

[Ungated] SS Log/FS Lin

Region	Number	%Total	%Gated	X-Mean	Y-Mean
ALL	100000	100.00	100.00	9.67	143
A	57598	57.60	57.60	13.5	237

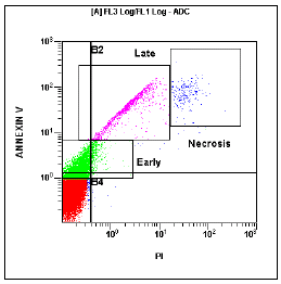

[A] FL3 Log/FL1 Log

Region	Number	%Total	%Gated	X-Mean	Y-Mean
ALL	57598	57.60	100.00	0.632	3.66
B3	47142	47.14	81.85	0.164	0.552
Early	11755	11.76	20.41	0.252	1.76
B1	6343	6.34	11.01	0.254	2.01
B2	4022	4.02	6.98	6.71	42.7
Late	2852	2.85	4.95	3.25	47.9
Necrosis	416	0.42	0.72	39.6	77.8
B4	91	0.09	0.16	0.62	0.827

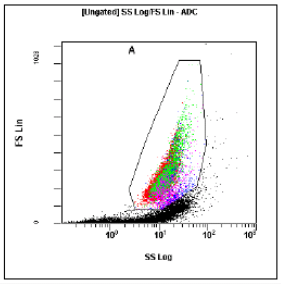

[Ungated] SS Log/FS Lin

Region	Number	%Total	%Gated	X-Mean	Y-Mean
ALL	100000	100.00	100.00	9.47	142
A	55791	55.79	55.79	12.8	239

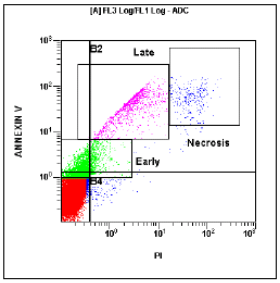

[A] FL3 Log/FL1 Log

Region	Number	%Total	%Gated	X-Mean	Y-Mean
ALL	55791	55.79	100.00	0.905	3.18
B3	47515	47.52	85.17	0.179	0.504
Early	8327	8.33	14.93	0.304	1.71
B2	4169	4.17	7.47	9.75	35
B1	3623	3.62	6.49	0.274	1.93
Late	2548	2.55	4.57	3.51	42.2
Necrosis	523	0.52	0.94	54.8	66.3
B4	484	0.48	0.87	0.726	0.83

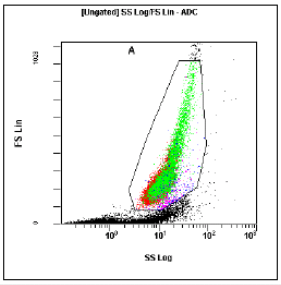

[Ungated] SS Log/FS Lin

Region	Number	%Total	%Gated	X-Mean	Y-Mean
ALL	100000	100.00	100.00	7.67	129
A	50987	50.99	50.99	12.1	235

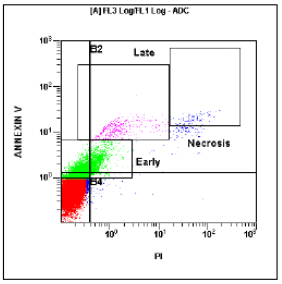

[A] FL3 Log/FL1 Log

Region	Number	%Total	%Gated	X-Mean	Y-Mean
ALL	50987	50.99	100.00	0.634	1.09
B3	42612	42.61	83.57	0.191	0.599
Early	11927	11.93	23.39	0.337	1.62
B1	4166	4.17	8.17	0.288	1.72
B2	3696	3.70	7.25	6.12	6.03
Late	728	0.73	1.43	2.44	13.4
B4	513	0.51	1.01	0.74	0.965
Necrosis	231	0.23	0.45	57.1	20.2

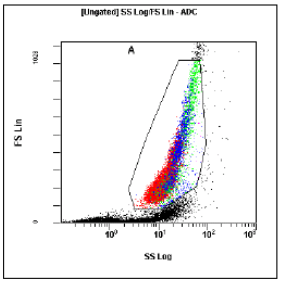

[Ungated] SS Log/FS Lin

Region	Number	%Total	%Gated	X-Mean	Y-Mean
ALL	100000	100.00	100.00	9	125
A	42076	42.08	42.08	15.7	259

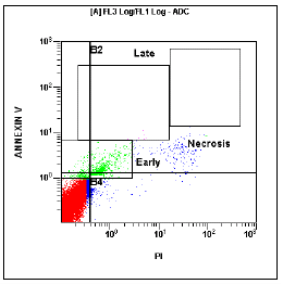

[A] FL3 Log/FL1 Log

Region	Number	%Total	%Gated	X-Mean	Y-Mean
ALL	42076	42.08	100.00	0.612	0.485
B3	37633	37.63	89.44	0.192	0.348
Early	2854	2.85	6.78	0.636	1.56
B4	2605	2.61	6.19	0.766	0.912
B2	1664	1.66	3.95	9.9	2.78
B1	174	0.17	0.41	0.288	1.83
Late	12	0.01	0.03	3.73	7.96
Necrosis	0	0.00	0.00	0	0

*Compound **46** Samples (2 x IC_{50} Concentration)*

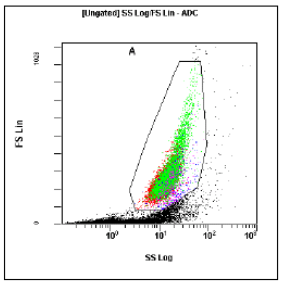

[Ungated] SS Log/FS Lin

Region	Number	%Total	%Gated	X-Mean	Y-Mean
ALL	100000	100.00	100.00	9.32	143
A	55134	55.13	55.13	14.2	248

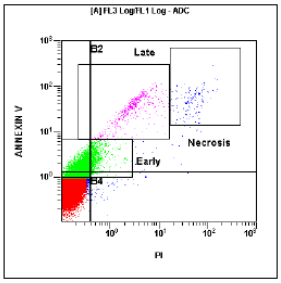

[A] FL3 Log/FL1 Log

Region	Number	%Total	%Gated	X-Mean	Y-Mean
ALL	55134	55.13	100.00	0.563	1.84
B3	44141	44.14	80.06	0.178	0.625
Early	15370	15.37	27.88	0.288	1.73
B1	7502	7.50	13.61	0.269	1.91
B2	3157	3.16	5.73	6.61	18.8
Late	1038	1.04	1.88	3.51	36.2
B4	334	0.33	0.61	0.863	0.896
Necrosis	302	0.30	0.55	50.6	54

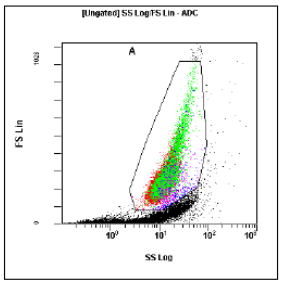

[Ungated] SS Log/FS Lin

Region	Number	%Total	%Gated	X-Mean	Y-Mean
ALL	100000	100.00	100.00	9.6	143
A	53452	53.45	53.45	13.4	249

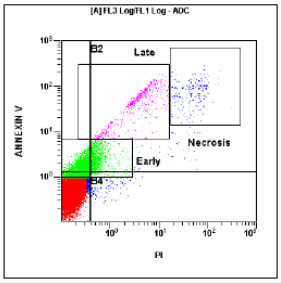

[A] FL3 Log/FL1 Log

Region	Number	%Total	%Gated	X-Mean	Y-Mean
ALL	53452	53.45	100.00	0.74	2.56
B3	43075	43.08	80.59	0.183	0.562
Early	12651	12.65	23.67	0.335	1.8
B1	5482	5.48	10.26	0.279	1.91
B2	4165	4.17	7.79	7.1	24.3
Late	1250	1.25	2.34	4.52	49.9
B4	730	0.73	1.37	0.78	0.874
Necrosis	398	0.40	0.74	51.6	79.7

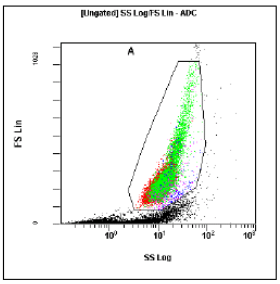

[Ungated] SS Log/FS Lin

Region	Number	%Total	%Gated	X-Mean	Y-Mean
ALL	100000	100.00	100.00	7.97	126
A	50209	50.21	50.21	12.9	236

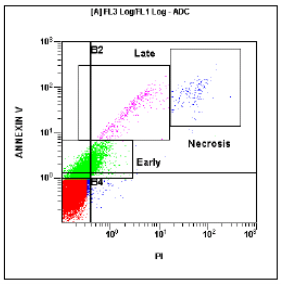

[A] FL3 Log/FL1 Log

Region	Number	%Total	%Gated	X-Mean	Y-Mean
ALL	50209	50.21	100.00	0.641	1.97
B3	39439	39.44	78.55	0.192	0.588
Early	14197	14.20	28.28	0.342	1.84
B1	5819	5.82	11.59	0.291	1.86
B2	4414	4.41	8.79	5.12	14.6
Late	773	0.77	1.54	3.43	38.2
B4	537	0.54	1.07	0.59	0.935
Necrosis	309	0.31	0.62	57	81.6

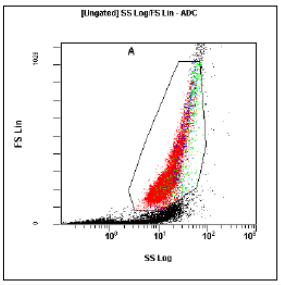

[Ungated] SS Log/FS Lin

Region	Number	%Total	%Gated	X-Mean	Y-Mean
ALL	100000	100.00	100.00	8	105
A	33468	33.47	33.47	16.4	264

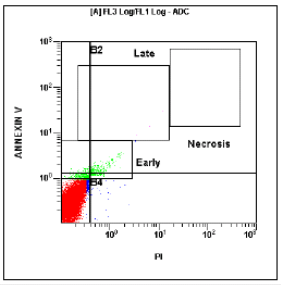

[A] FL3 Log/FL1 Log

Region	Number	%Total	%Gated	X-Mean	Y-Mean
ALL	33468	33.47	100.00	0.177	0.369
B3	32441	32.44	96.93	0.164	0.335
Early	1343	1.34	4.01	0.457	1.33
B4	533	0.53	1.59	0.503	0.987
B2	369	0.37	1.10	0.854	2.1
B1	125	0.13	0.37	0.306	1.45
Necrosis	1	0.00	0.00	21	49.4
Late	3	0.00	0.01	7.29	18.1